

“Iron-catalyzed Hydrogenations of Olefins”

Dissertation

zur Erlangung des Doktorgrades der Naturwissenschaften

Dr. rer. nat.

an der Fakultät für Chemie und Pharmazie
der Universität Regensburg



vorgelegt von

Tim Nicolas Gieshoff

aus Siegburg

Regensburg 2016

The experimental part of this work was carried out between November 2013 and October 2016 at the University of Regensburg, Institute of Organic Chemistry under the supervision of Prof. Dr. Axel Jacobi von Wangelin.

The thesis was submitted: November 8th, 2016

Date of the defense: December 15th, 2016

Board of examiners:

Prof. Dr. Achim Göpferich (chairman)

Prof. Dr. Axel Jacobi von Wangelin (1st referee)

Prof. Dr. Olga García Mancheño (2nd referee)

Prof. Dr. Frank-Michael Matysik (examiner)

Table of contents

1	Introduction	1
2	C=C Hydrogenations with iron group metal catalysts	3
2.1	Introduction	4
2.2	Iron	6
2.2.1	Introduction	6
2.2.2	Pincer complexes	7
2.2.3	Others	14
2.3	Cobalt	16
2.3.1	Introduction	16
2.3.1	Pincer complexes	17
2.3.2	Others	24
2.4	Nickel	30
2.4.1	Introduction	30
2.4.2	Pincer complexes	30
2.5	References	34
3	Stereoselective iron-catalyzed alkyne hydrogenation in ionic liquids	37
3.1	Introduction	38
3.2	Reaction conditions and substrate scope	39
3.3	Z-selective hydrogenation in absence of ionic liquids	44
3.4	Summary	46
3.5	Experimental	47
3.5.1	General	47
3.5.2	General hydrogenation procedures	48
3.5.3	Mechanistic experimental details	49
3.5.4	Synthesis of starting material	52
3.5.5	Hydrogenation products	59

3.6	References.....	66
4	Iron-catalyzed olefin hydrogenation at 1 bar H ₂ with a FeCl ₃ -LiAlH ₄ catalyst	67
4.1	Introduction.....	68
4.2	Reaction conditions and substrate scope	68
4.3	Mechanistic studies	73
4.4	Conclusions.....	77
4.5	Experimental.....	78
4.5.1	General.....	78
4.5.1	General hydrogenation procedures.....	79
4.5.2	Mechanistic experimental details	80
4.5.3	Synthesis of starting material	89
4.5.4	Hydrogenation products	107
4.5.5	[Li(thf) ₂ {Fe(tmeda)} ₂ (μ-AlH ₅)(μ-Al ₂ H ₉) (4)	124
4.6	References.....	126
5	Iron-catalyzed hydrogenation of sterically hindered alkenes	129
5.1	Introduction.....	130
5.2	Results and discussion	131
5.3	Mechanistic experiments	138
5.4	Hydrogenation with similar chiral catalysts	146
5.5	Conclusions.....	149
5.6	Experimental.....	151
5.6.1	General.....	151
5.6.2	Hydrogenation procedures	153
5.6.3	Mechanistic experimental details	154
5.6.4	Synthesis of starting material	167
5.6.5	Hydrogenation products	179
5.6.6	Hydrogenation with chiral iron-complexes	190
5.7	References.....	198
6	Iron-catalyzed isomerizations and cyclotrimerizations	201

6.1	Introduction	202
6.2	Results and Discussion	202
6.3	Conclusion	205
6.4	Experimental.....	206
6.4.1	General.....	206
6.4.2	General procedure for isomerization of alkenes.....	206
6.4.3	General procedure for [2+2+2]-cyclotrimerization of alkynes.....	207
6.4.4	Synthesis of starting material	207
6.4.5	Products of [2+2+2]-cycloisomerization.....	208
6.5	References	211
7	Synthesis and characterization of a low-valent tetranuclear iron cluster	213
7.1	Introduction	214
7.2	Results and Discussion	215
7.3	Conclusion	217
7.4	Experimental.....	218
7.4.1	General.....	218
7.4.2	Synthesis and characterization of [FeN(SiMe ₃) ₂] ₄ (toluene).....	218
7.5	References	221
8	Appendix	223
8.1	List of abbreviations	223
8.2	Summary.....	224
8.3	Zusammenfassung	225
8.4	Acknowledgements.....	227
8.5	Curriculum Vitae	228
8.6	Eidesstattliche Erklärung	230

1 Introduction

The hydrogenation of unsaturated compounds is without doubt one of the most important transformation in large industrial processes (ammonia-synthesis, gas-to-liquid) as well as in the synthesis of fine chemicals.¹ Over the last decades, homogeneous noble complexes based on Pd, Rh, Ru and Ir were preferably used in the synthesis of pharmaceuticals (levodopa, (*S*)-naproxene), flavors or other fine chemicals.² Whereas high productivity in combination with excellent selectivity were observed in many examples, the low abundance and high prices of these metals prompted the search for cheaper catalysts. In addition, catalyst recycling often is costly due to its homogeneous nature.

In recent years, the development of alternative iron-based catalysts for olefin hydrogenation was gaining more and more interest as evidenced by an increasing amount of reports. A part of these protocols make use of simple iron precursors which are activated by common main group reductants such as Grignard reagents or aluminium and boron hydrides or organyls. Under these conditions, iron nanoparticles can be formed. The concept of nanoparticle catalysts aims to combine higher stability and facile separation of heterogeneous catalysts with high dispersion and activity of homogeneous catalysts. Until now, these iron-based protocols cannot compete with precious metal catalysts due to lower activity, selectivity and stability.³

The aim of this work is directed to the development of iron-based hydrogenation catalysts with the focus on simple systems derived from easily accessible iron-precursors and activation agents. By careful choice of the preparation method and reactants, problems of former similar protocols (activity, stability, selectivity) should be addressed. To that end, ionic liquids were contemplated as suitable stabilizing agent for nanoparticles, which have been shown to enable easy catalyst recycling.⁴

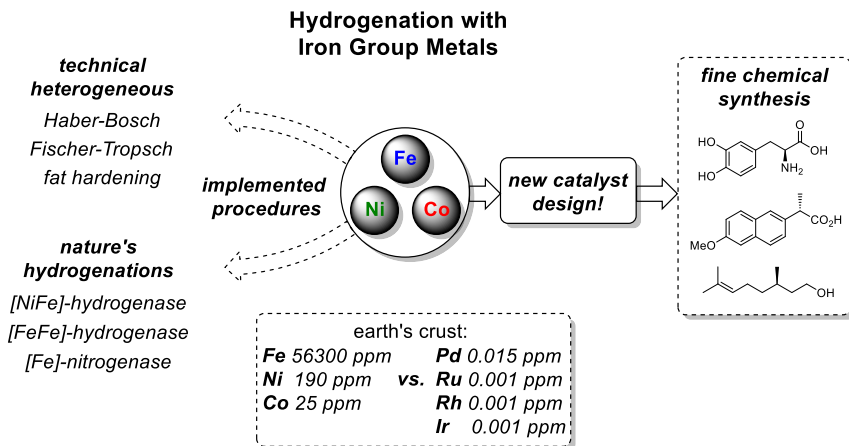
¹ J. G. de Vries, C. J. Elsevier (Ed.) *The handbook of homogeneous hydrogenation*, WILEY-VCH, Weinheim, **2006**.

² a) W. S. Knowles, *J. Chem. Educ.* **1986**, 63, 222; b) T. Ohta, H. Takaya, M. Kitamura, K. Nagai, R. Noyori, *J. Org. Chem.* **1987**, 52, 3174; c) G. Heydrich, G. Gralla, K. Ebel, W. Krause, N. Kashani-Shirazi, WO2009033870 A1, **2009**.

³ For recent examples, see: a) D. J. Frank, L. Guet, A. Kaslin, E. Murphy, S. P. Thomas, *RSC Adv* **2013**, 3, 25698; b) A. Welther, M. Bauer, M. Mayer, A. Jacobi von Wangelin, *ChemCatChem* **2012**, 4, 1088; c) C. Rangheard, C. de Julián Fernández, P.-H. Phua, J. Hoorn, L. Lefort, J. G. de Vries, *Dalton Trans* **2010**, 39, 8464; d) N. Guo, M.-Y. Hu, Y. Feng, S.-F. Zhu, *Org. Chem. Front.* **2015**, 2, 692.

⁴ See chapter 3.

2 C=C Hydrogenations with iron group metal catalystsⁱ



In the last decade, the field of homogeneous base-metal catalyzed C=C hydrogenations flourished due to the development of well-defined base-metal complexes in hydrogenation reactions. Through rational ligand design, new dihydrogen activation mechanisms were enabled with iron group metal complexes and applied in the hydrogenation of alkenes and alkynes. This chapter aims to summarize the latest advances in homogeneous C=C hydrogenation catalysis based on iron, cobalt and nickel.

ⁱ This chapter will be published as “C=C Hydrogenations with iron group metals”, T. N. Gieshoff, A. Jacobi von Wangelin in “Non-Noble Metal Catalysis: Molecular Approaches and Reactions”, R. J. M. Klein Gebbink, M. Moret (eds.), *Wiley-VCH*, 2017. Copyright Wiley-VCH Verlag GmbH & Co. KGaA. Reproduced with permission. Schemes, tables and text may differ from published version

2.1 Introduction

Metal-catalyzed hydrogenations of C=C bonds are key operations in many organic synthesis endeavours and the technical manufacture of chemicals. Heterogeneous catalysts dominate industrial hydrogenation processes with numerous examples in all areas of applications such as the petrochemical valorization of alkene and arene cracking products or the large-scale hydrogenation of vegetable oils.^[1] Molecular catalysts in homogeneous phase are often employed where the desired reaction requires especially high selectivity, e.g. enantioselectivity, which can be induced by rational ligand design and rationalized through a deeper mechanistic understanding. Important examples of technical C=C hydrogenations are the synthesis of the anti-parkinson drug levodopa, the anti-inflammatory drug naproxen or the flavor citronellol prior to its conversion to (-)-menthol (Figure 2-1).^[2]

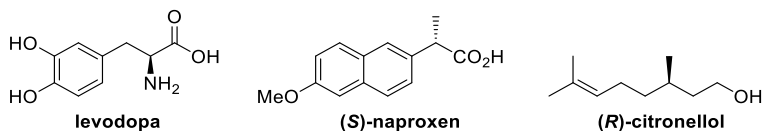


Figure 2-1. Technical products from homogeneous C=C hydrogenations.

Various molecular sources of hydrogen atoms and metal-centered activation and delivery mechanisms are known in the literature.^[3] Gaseous dihydrogen, H₂, is the most widely available, cleanest and most versatile source of hydrogen, especially on larger scales.^[1a] This chapter focuses on C=C hydrogenations with gaseous dihydrogen in the presence of molecular iron group metal catalysts.

Most developments of active hydrogenation catalysts in homogeneous phase involve the increasingly rare noble metals rhodium, iridium, ruthenium, palladium, and platinum.^[4] Applications of these catalysts to various syntheses of organic molecules have documented their high activities, high selectivities, wide substrate scopes, and high functional group compatibilities.^[4] Furthermore, the mode of action of such processes is rather well understood since the advent of modern spectroscopic and theoretical tools. However, modern economic and environmental constraints have recently prompted the search for alternative metal catalysts. The high abundance and accessibility, low costs and low toxicities make iron group metals (iron, cobalt, nickel) an especially attractive class of hydrogenation catalysts which have received only very little attention in the past decades.^[5] Further stimulus to study such catalysts comes from the facts that many of the largest technical hydrogenations (Haber-Bosch process, Fischer-Tropsch or gas-to-liquid (GTL) processes, plant oil hydrogenation to margarine, adiponitrile reduction) and many biological hydrogenations are catalyzed by iron group metals. Figure 2-2 illustrates the active sites of natural hydrogenase enzymes which reversibly oxidize dihydrogen.^[6]

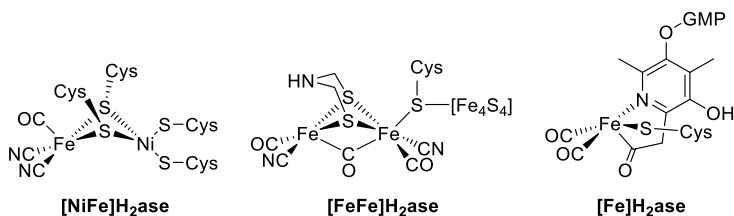


Figure 2-2. Active sites of different hydrogenases. Cysteine (Cys), guanosyl-5'-monophosphate (GMP).

The field of hydrogenations catalyzed by base metals has rapidly developed in the past decade with many new molecular catalysts reported in the literature (Figure 2-3.)^[7] Especially C=C hydrogenation methods with tridentate pincer complexes have been highly successful. The following chapters provide an overview of the most important developments in the field.

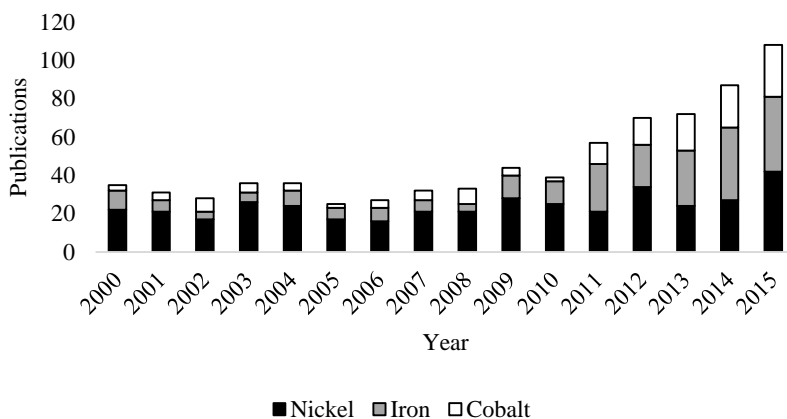


Figure 2-3. Publications per year for the search terms “nickel”, “cobalt” or “iron” and “hydrogenation”^[7]

2.2 Iron

2.2.1 Introduction

Iron-catalyzed hydrogenations of alkenes and alkynes have been known for many decades. Heterogeneous iron catalysts like Raney[®]-iron or Urushibara-iron were reported to partially hydrogenate alkynes at high temperatures.^[8] Ziegler-type hydrogenation catalysts were developed immediately following the observation of the famous “nickel effect” in Ziegler-Natta polymerizations in the 1960’s. Ziegler-type iron catalysts based on the reaction of an iron(III) salt with a triorganoaluminium compound (AlR_3) were successfully applied to hydrogenations of largely unfunctionalized alkenes at ambient hydrogen pressures and temperatures.^[9] Various theories were postulated to describe the true nature of this type of bimetallic catalyst but a generalization is difficult due to the vast number of different catalyst compositions, conditions of preparations, and observed catalytic activities.^[10]

In the last decade, an increasing amount of conceptually similar bimetallic catalysts formed from simple iron salt precursors and simple main group metal reductants have been reported to be active in hydrogenations of various alkenes and alkynes. These protocols mainly aimed at the *in situ* preparation of active catalyst mixtures that operate in the absence of a complex or expensive ligand. Common reducing agents include Grignard reagents and group 13 hydrides (Figure 2-4).^[11] In many cases, spectroscopic and kinetic studies were indicative of the formation of iron nanoparticles which act as the active catalysts. Good activities were mostly observed for the hydrogenation of alkenes and alkynes at ambient conditions. However, the presence of a fairly basic or nucleophilic reductant limits the application of such *in situ* prepared catalysts to substrates that are void of acidic and highly electrophilic substituents.

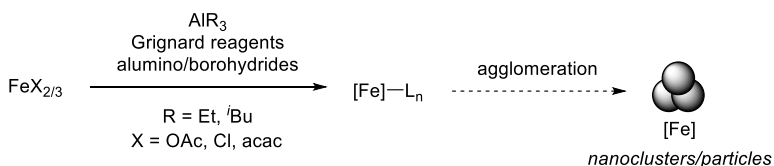


Figure 2-4. Generation of Ziegler-type hydrogenation catalysts and similar bimetallic catalysts

Metal nanoparticle catalysis is a hybrid concept that combines the best of two worlds: the higher stability and facile downstream separation of heterogeneous catalysts and the high dispersion, high modularity, high activity, and easier mechanistic investigations of homogeneous catalysts.^[12] Only very few applications of well-defined iron nanoparticles to the hydrogenation of alkenes and alkynes were reported. Monodisperse iron nanoparticles of 1.5 ± 0.2 nm were synthesized by decomposition of $\{\text{Fe}[\text{N}(\text{Si}(\text{CH}_3)_3)_2]_2\}_2$

at 3 bar of H_2 at 150 °C and extensively characterized. At elevated pressure of H_2 (10 bar), mono- and di-substituted alkenes and alkynes were hydrogenated in excellent yields.^[13] Highly selective amine-linked polystyrene-supported iron nanoparticles were synthesized by thermal decomposition of $Fe(CO)_5$ to give an active catalyst for hydrogenations operated in flow reactors.^[14] Chemically derived graphene-supported iron nanoparticles were synthesized and applied to alkene hydrogenations.^[15]

The early use of molecular iron catalysts in hydrogenations is mainly associated with iron carbonyl derivatives which were intensively studied in the 1960s. Iron pentacarbonyl was reported to convert methyl linoleate to methyl stearate under high temperature conditions.^[16] Later, UV irradiation was shown to enhance the catalyst activity, most likely through the more facile dissociation of CO ligands to give the active low-valent species $Fe(CO)_3$.^[17] It is important to note, that under thermal and UV treatment, iron carbonyls can form several homogeneous species but also iron nanoparticles, so that an unambiguous distinction between homogeneous and heterogeneous mechanisms is difficult.^[14,15] Several hydrogenation protocols employing well-defined molecular iron catalysts were developed in the late decades of the 20th century but satisfyingly high catalyst stabilities and reactivities were only observed with the introduction of *P*- and *N*-based pincer ligands.

2.2.2 Pincer complexes

Peters *et al.* reported the synthesis of a series of cationic alkyliron(II) *P,P,P* pincer complexes synthesized from the reaction of an iron(II)chloride pincer complex with the corresponding alkyllithium or Grignard reagents (Figure 2-5).^[18]

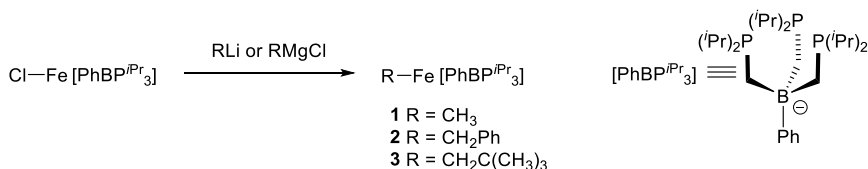


Figure 2-5. Synthesis of iron(II)-alkyl *P,P,P* pincer complexes

These first generation catalysts showed moderate activities in the hydrogenation of largely non-functionalized substrates such as styrene, 1-hexene, ethylene, cyclooctene and 2-pentyne. Catalyst **2** was slightly more active, yet the turnover frequencies were between 1.6 to 24 mol substrate per mol catalyst and hour. Competitive oligomerizations and polymerizations were observed in the hydrogenation of terminal alkynes. While catalyst activity and substrate scope were rather limited, the underlying reaction mechanism was thoroughly studied. Several plausible intermediates of a catalytic hydrogenation cycle could be isolated upon trapping with phosphine ligands. A trihydridoiron(IV) complex **4** was formed upon oxidative addition of dihydrogen. The reversibility of the H_2 activation

was proven by conversion of **4** to the monohydridoiron(II) complex **5** in the absence of dihydrogen (Figure 2-6).

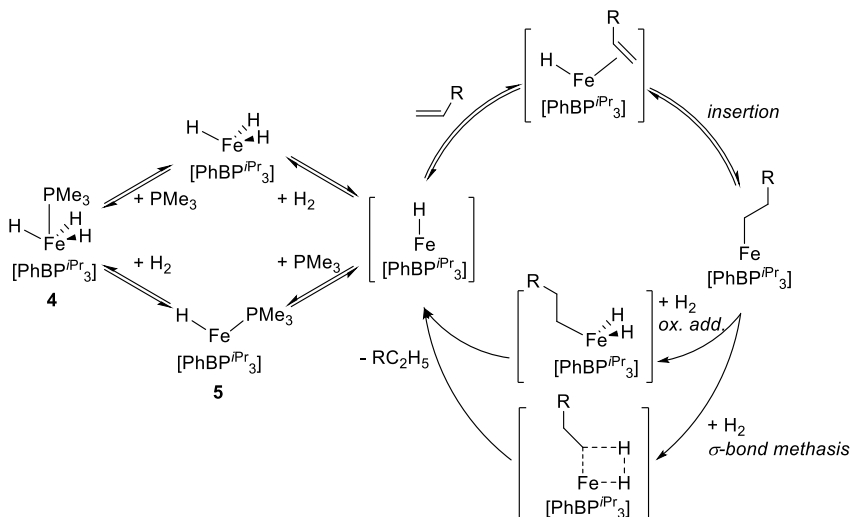


Figure 2-6. Mechanism for hydrogenation proposed by Peters *et al.*

Based on these results, the authors proposed the key role of an iron(II/IV) redox process. The determination of reaction orders in substrate, iron catalyst, and H_2 suggest that the oxidative addition of dihydrogen at the alkyliron species is the rate-determining step.

Budzelaar *et al.* introduced bis(imino)pyridine iron(II) complexes to the field of alkene hydrogenations. These complexes were activated according to a Ziegler protocol with tris(isobutyl)aluminum. Excellent activities in the hydrogenation of 1-octene were observed.^[19] Shortly after, Chirik and coworkers prepared the bis(imino)pyridine *N,N,N*-pincer iron complex **7** by reduction of the corresponding iron(II) halide complexes **6** with sodium amalgam or sodium triethylborohydride which effected ligand reduction rather than iron center reduction (Figure 2-7).^[20] Catalyst **7** contains a dianionic diradical form of the ligand which coordinates the iron(II) center as supported by Mössbauer spectroscopy and computational studies (Figure 2-7).^[21]

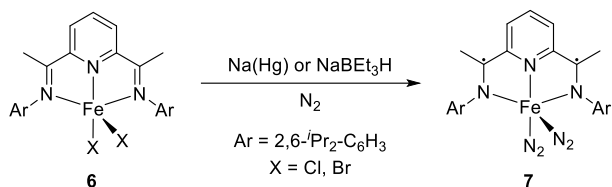


Figure 2-7. Synthesis of bis(imino)pyridine iron complex **7**

The active catalyst is generated upon dissociation of the labile dinitrogen ligands which gives a tri-coordinated iron complex similar to $\text{Fe}(\text{CO})_3$. The coordination of an olefin is followed by oxidative addition of dihydrogen. Reductive elimination gives the desired hydrogenation product and regenerates the active catalyst (Figure 2-8).

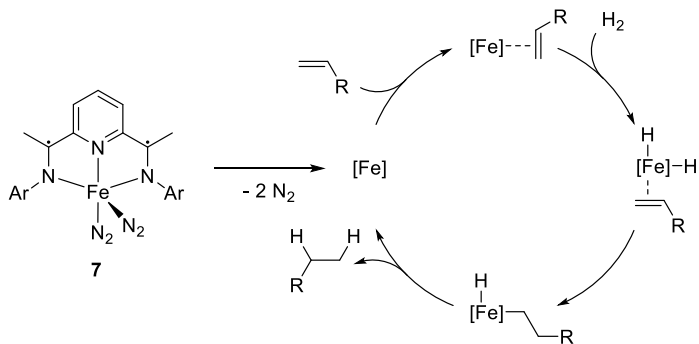


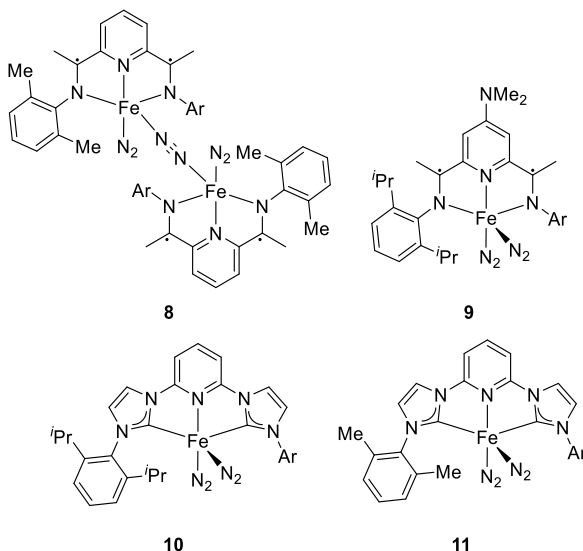
Figure 2-8. Mechanistic proposal of alkene hydrogenation with **7** according to Chirik *et al.*

The catalyst **7** exhibited excellent activities in the hydrogenation of a diverse set of alkenes and exceeds the productivity (turnover frequency, TOF) of some common precious metal catalysts (Table 2-1).^[20] Largely non-functionalized mono- and di-substituted alkenes, styrenes, and oxygen- and nitrogen-containing alkenes were cleanly hydrogenated under mild conditions. Non-productive carbonyl and primary amine coordination to the catalyst compete with the olefin coordination so that hydrogenation rates decrease in the presence of such functional groups.^[22]

Table 2-1. Comparison of **7** with various precious metal catalysts in the hydrogenation of 1-hexene.

Entry	Catalyst	Time /min	TOF /h ⁻¹
1	7	12	1814
2	10% Pd/C	12	366
3	(PPh ₃) ₃ RhCl	12	10
4	[(cod)Ir(PCy ₃)py]PF ₆	12	75

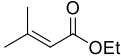
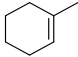
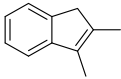
The high activity of the complex prompted the synthesis of a small library of similar complexes by the same group (Figure 2-9). By decreasing steric bulk of the *N*-aryl substituents (**8**) and the introduction of an electron-donating group in the *para*-position of the pyridine (**9**), the catalytic activities in the hydrogenation of ethyl 3,3-dimethylacrylate was greatly improved.^[23]

**Figure 2-9.** Modified bis(imino)pyridine and bis(*NHC*)pyridine iron complexes by Chirik *et al.*

Largely non-functionalized and sterically hindered tri- and tetra-substituted alkenes could be cleanly converted. Substitution of the imine moieties by strongly σ -donating *N*-heterocyclic carbenes further increased the electron density on the metal.^[24] The

resultant *C,N,C*-pincer ligands showed only little redox activity so that the corresponding bis(dinitrogen) iron complexes **10** and **11** contained iron(0) centers, which was supported by Mössbauer spectroscopy, X-ray absorption spectroscopy and DFT calculations.^[25] The latter complex (**11**) was a competent catalyst for the hydrogenation of 2,3-dimethylindene (Table 2-2) and thus represented one of the most active molecular iron catalysts reported at that time.^[23b,26]

Table 2-2. Comparison of complexes **7-11** in the hydrogenation of sterically hindered substrates

Entry	Substrate	% Conv (reaction time) with catalyst				
		7	8	9	10	11
1		65 (24 h)	>95 (7 h)	>95 (1 h)	>95 (1 h)	35 (1 h)
2		0 (24 h)	2 (24 h)	3 (24 h)	20 (24 h)	>95 (12 h)
3		3 (48 h)	<1 (48 h)	3 (48 h)	4 (48 h)	68 (48 h)

In 2013, Milstein and coworkers developed the new acridine-based *P,N,P* pincer iron complex **12**.^[27] Synthesis was accomplished by reaction of iron(II) bromide with the bis(phosphine) ligand and subsequent reduction with sodium borohydride in acetonitrile (Figure 2-10). The resultant complex can be viewed as the nitrogen analogue of a Xantphos iron complex.

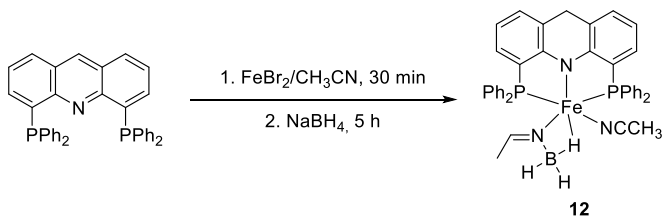
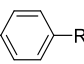


Figure 2-10. Synthesis of *P,N,P* pincer iron complex **12** by Milstein *et al.*

Complex **12** was employed in the semi-hydrogenations of alkynes to alkenes which generally bear the challenge of chemoselectivity and stereoselectivity. (*E*)-alkenes were selectively formed at elevated H₂ pressure and elevated temperature (Table 2-3). The

reaction conditions tolerated nitriles, ketones and esters. Over-reduction to the alkanes was observed only in few examples.

Table 2-3. Selected examples of the (*E*)-selective hydrogenation with **12**

$\text{R}^1\text{---}\text{C}\equiv\text{C}\text{---}\text{R}^2 \xrightarrow[4\text{-}10\text{ bar H}_2, 90\text{ }^\circ\text{C}]{0.6\text{-}4\text{ mol\% } \mathbf{12}} \text{R}^1\text{---}\text{CH}=\text{CH}\text{---}\text{R}^2$				
Entry	Substrate	R	% Yield (alkane)	<i>E</i> : <i>Z</i>
1		H	99	-
2	Ph—C≡C—R	Ph	99	100:0
3		SiMe ₃	76 (24)	99:1
4		C(O)Me	99	64:36
5	Ph—C≡C—  —R	CO ₂ Et	89 (11)	99:1
6		CN	94	99:1

The authors rationalize the observed high (*E*)-selectivity with an isomerization of the initially formed (*Z*)-alkene under reaction conditions. Experiments in absence of dihydrogen proved that **12** quantitatively converted (*Z*)-stilbene to (*E*)-stilbene. The initial formation of (*Z*)-stilbene under hydrogenation conditions was observed at lower temperatures.

The *P,N,P*-pincer iron complex **13** with a saturated backbone was shown to be active in the dehydrogenation of methanol and the hydrogenation of unactivated esters. The mechanism operates under basic conditions via reversible addition of H₂ to the bifunctional Fe-N moiety.^[28] The deprotonated complex **14** was also applied to hydrogenations and dehydrogenations of *N*-heterocycles (Table 2-4) and hydrogenations of styrenes at mild conditions (Table 2-5) by Jones *et al.*^[29] Isolation of a dihydridoiron(II) complex was achieved upon borane trapping (**16**) which indicates the key role of **15** as catalytic intermediate of this hydrogenation mechanism (Figure 2-11). Consistently, *N*-methylation of the ligand resulted in complete inhibition of hydrogenation activity. DFT calculations supported the notion of a step-wise mechanism with initial Fe-centered hydride transfer to the alkene followed by proton transfer from the amine. Such mechanistic scenario should facilitate hydrogenations of polar double bond systems. Indeed, experiments with catalyst **14** demonstrated its high activity in the hydrogenation of functionalized electron-deficient styrenes and inertness towards 1-hexene.

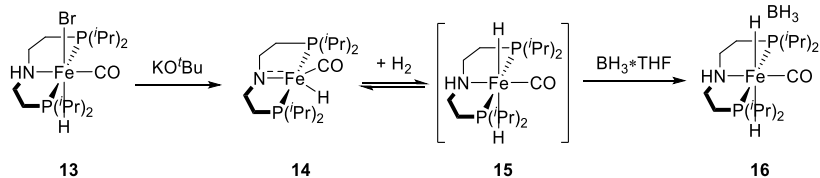


Figure 2-11. Aliphatic *P,N,P* complex **13** and possible key intermediates in hydrogenations

Table 2-4. Selected examples of the hydrogenation of *N*-heterocycles with **13**

$ \begin{array}{ccc} \text{R}^1\text{-} \text{[Quinoline]} \text{-R}^2 & \xrightarrow[5-10 \text{ bar H}_2, 80^\circ\text{C}, 24 \text{ h}]{3 \text{ mol\% } \mathbf{13}, 10 \text{ mol\% KO}^t\text{Bu}} & \text{R}^1\text{-} \text{[Saturated Quinoline]} \text{-R}^2 \end{array} $		
Entry	Substrate	% Yield
1		66
2		92
3		60

Table 2-5. Selected examples of the hydrogenation of styrenes with **14**

$ \begin{array}{ccc} \text{R-} \text{[Styrene]} & \xrightarrow[1 \text{ bar H}_2, 23^\circ\text{C}]{5 \text{ mol\% } \mathbf{14}} & \text{R-} \text{[Ethylbenzene]} \end{array} $				
Entry	Substrate	R	Time / h	% Yield
1		H	24	100
2		OMe	168	100
3		CO ₂ Me	0.7	100

2.2.3 Others

Arene ferrates were studied in catalytic alkene hydrogenations by Jacobi von Wangelin and Wolf. The monoanionic bis(anthracene) ferrate (**17**) showed good activity for styrenes. However, the cobaltate derivative was much more active and tolerated various functional groups.^[30] Such homoleptic arene complexes were first prepared by Ellis *et al.* by reduction of the metal(II) bromides with potassium/anthracene and can be viewed as homogenous sources of metal species in the oxidation state -I (Figure 2-12).^[31] Mechanistic studies were mostly performed with the cobaltate which underwent rapid π -ligand exchange with various alkenes as initiating step under hydrogenation conditions.

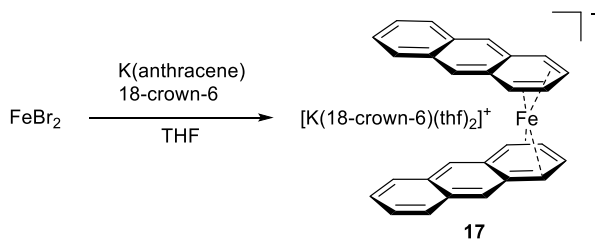


Figure 2-12. Synthesis of potassium bis(anthracene)ferrate **17**

In addition, the same group prepared a library of homoleptic and heteroleptic arene/alkene metalates and compared their activity in the hydrogenation of alkenes (Table 2-6).^[32] In this series, iron complexes, which were initially reported by Jonas (**18**) and Wolf (**19**) were studied in alkene hydrogenation (Figure 2-13).^[33]

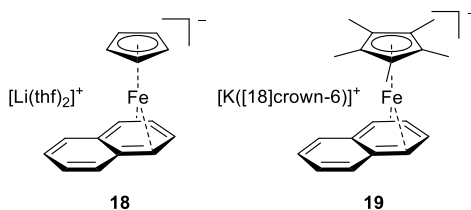


Figure 2-13. Cyclopentadienyl iron complexes **18** and **19**

Table 2-6. Comparative hydrogenation with iron complexes **17**, **18** and **19**

<div><div><div><div><div></div><div>R</div></div><div><div></div><div></div></div></div><div><div></div><div></div></div><div><div></div><div></div></div></div><div>5 mol% [Fe] 2 bar H₂, 20 °C, 24 h</div><div><div><div></div><div>R</div></div><div><div></div><div></div></div></div><div><div></div><div></div></div></div>
--

2.3 Cobalt

2.3.1 Introduction

Cobalt-based hydrogenation catalysts were developed mostly parallel to their iron counterparts when probing the activities of the less expensive first row transition metals in comparison with the established noble metal systems. Heterogeneous Raney®-cobalt was reported to hydrogenate styrene already in 1958 but its activity is far inferior to Raney®-nickel. However, superior selectivity was observed in hydrogenations of nitriles and oximes.^[34] With the advent of Ziegler-Natta polymerization catalysis, various combinations of simple cobalt salt precursors with triorganoaluminium additives were applied to catalytic hydrogenations of simple alkenes such as 1-hexene and cyclohexene.^[9] The differences in catalyst precursors, additives, conditions, and preparation methods have so far prevented a unified proposal of the operating catalyst species.^[10] Recently, Finke and coworkers demonstrated that active cobalt clusters are formed from a cobalt(II)neodecanoate/ Et_3Al catalyst system by careful choice of poisoning tests as well as analysis by mass spectrometry, X-ray absorption fine structure, transmission electron microscopy.^[35]

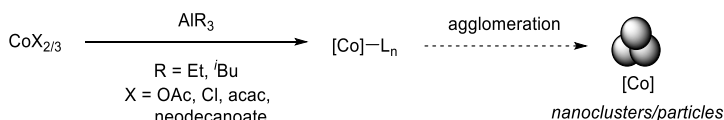


Figure 2-14. Generation of cobalt-based Ziegler-type hydrogenation catalysts

While defined cobalt nanoparticles were prepared by various methods and their surface, size, and composition was carefully analyzed, extended catalytic studies into hydrogenation reactions remained scarce until the very recent past. Beller and coworkers prepared $\text{Co}_3\text{O}_4/\text{Co}$ core/shell nanoparticles featuring nitrogen-doped graphene layers on alumina by pyrolysis of cobalt(II) acetate/phenantroline and applied them in the hydrogenation of *N*-heteroarenes.^[36] Cobalt nanoparticles on charcoal were synthesized by thermal treatment of dicobalt octacarbonyl which were also shown to be active in the hydrogenation of alkenes.^[37]

Several cobalt-catalyzed C=C hydrogenation protocols were developed with homogeneous cobalt carbonyl complexes following the seminal discovery of the hydroformylation of olefins with syngas (CO/H_2).^[38] Improvements in selectivity and activity were achieved by introducing monodentate phosphine ligands in the late 1970's which enabled clean hydrogenations of alkynes and alkenes.^[39] Later, the use of bidentate ligands and their applications to stereoselective hydrogenations of functionalized olefins were reported.^[40] The majority of recent reports emphasized tridentate amine/pyridine-based pincer ligand motifs.

6.1.1 Pincer complexes

Concurrent with the development of bis(imino)pyridine iron catalysts, the related cobalt complexes were initially studied in olefin polymerization reactions and shortly after also in olefin hydrogenations, both under Ziegler conditions in the presence of triisobutylaluminum as activator.^[19,41] The structurally defined alkylcobalt complex **22** was synthesized by sequential alkylation of bis(imino)pyridinecobalt(II) dichloride (**20**) with methyllithium/MAO and trimethylsilylmethyl lithium (Figure 2-15).^[42] Strong redox-participation of the ligand accounts for the formulation of **22** as a low-spin Co(II) center with a ligand-centered radical anion.^[43]

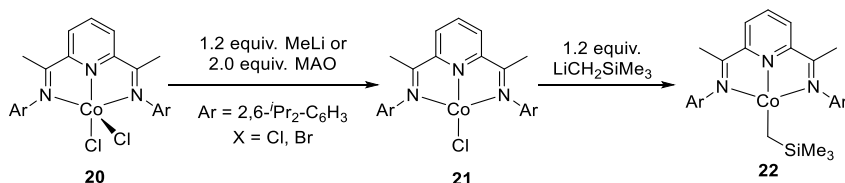


Figure 2-15. Synthesis of alkyl bis(imino)pyridine cobalt **20**

Under reaction conditions, complex **22** effects dihydrogen activation upon release of tetramethylsilane. The resultant monohydridocobalt intermediate was identified by ¹H- and ¹³C-NMR and is believed to be the catalytically active species in hydrogenations of terminal and internal di-substituted alkenes (Figure 2-16).

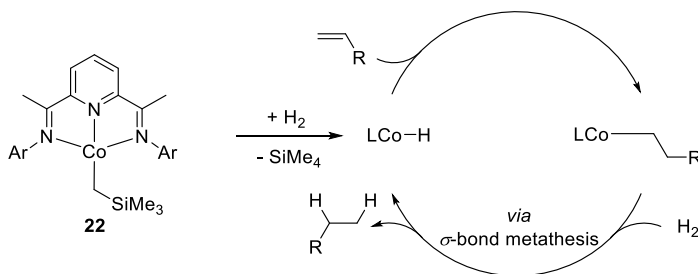


Figure 2-16. Mechanistic proposal of catalytic hydrogenation with **22**

According to DFT calculations, dihydrogen splitting does not operate by an oxidative addition event but through σ -bond metathesis which is the rate-limiting step. A chiral version of complex **22** was prepared by replacing one aryl group with a chiral *sec*-alkylamine moiety. Initially developed for oligomerization reactions by Bianchini *et al.*, the chiral bis(imino)pyridine(methyl)cobalt(I) complex (*S*)-**25** was prepared from (*S*)-**23** (Figure 2-17).^[44]

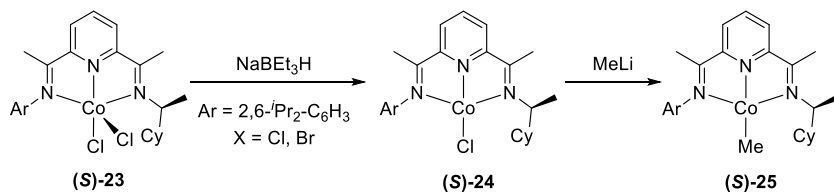


Figure 2-17. Synthesis of chiral bis(imino)pyridine methyl cobalt (*S*)-25

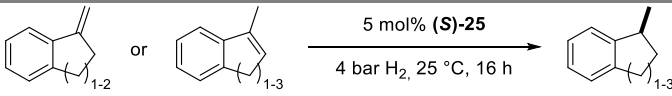
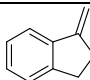
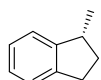
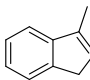

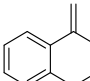
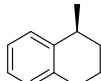
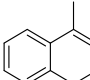
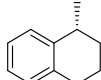
Complex (*S*)-25 was successfully applied to the hydrogenation of prochiral alkenes; notably no further directing groups were required to achieve high enantiomeric excess. In general, the stereoselective hydrogenation of such minimally functionalized is a challenging task due to the lack of chelating coordination modes, the absence of directing groups, and the lack of a strong stereochemical bias through bulky substituents. Higher enantiomeric excess values were observed for electron-rich styrenes which was explained by their lower reactivity and higher selectivity (Table 2-7).

Table 2-7. Selected examples of the hydrogenation of prochiral styrenes with (*S*)-25

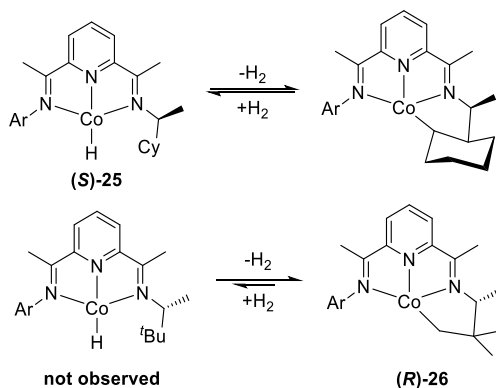
$\text{Ph-CH=CH-R} \xrightarrow[4 \text{ bar H}_2, 23^\circ\text{C, 24 h}]{5 \text{ mol\% (S)-25}} \text{Ph-CH}_2\text{-CH}_2\text{-R}$				
Entry	Substrate	R	% Yield	% ee
1		<i>i</i> Pr	87	90
2		Cy	70	80
3		NMe ₂	>98	96
4		F	>98	78

The origin of enantioselectivity in the hydrogenation of benzannulated exocyclic and endocyclic cycloalkenes was rationalized in a comprehensive report. The authors documented that the 1,2-alkene addition is the enantiodetermining and rate-limiting step. Isomerization of the starting material is competitive if the alkylcobalt complex populates a conformation that can undergo syn-β-hydride elimination (Table 2-8).^[45]

Table 2-8. Enantioselective hydrogenation of *exo*- and endocyclic alkenes with (*S*)-**25**

			
Entry	Substrate	Product	% Yield (ee)
1			84 (74)
2			88 (89)
3			87 (53)
4			96 (93)

Careful choice of the chiral moiety was necessary to suppress dehydrogenative CH insertion of the ligand side chains to give a cobaltacycle. Cyclometalation of (*S*)-**25** is reversible under hydrogenation conditions, whereas the *tert*-butyl homologue gave almost exclusively the inactive form (*R*)-**26** which underwent very slow conversion to the active hydridocobalt complex (Figure 2-18).

**Figure 2-18.** Competing cyclometalation of active cobalt hydride intermediates

In 2016, a related ligand design was embedded within the chiral oxazoline iminopyridine cobalt complex **27** by Lu and coworkers (Figure 2-19).^[46] In contrast to the earlier works by Budzelaar and Chirik, pre-catalyst activation was achieved *in situ* by the addition of sodium triethylborohydride. Application in the stereoselective hydrogenation of 1,1-diphenylethenes revealed a higher hydrogenation activity with higher enantiomeric excess under mild conditions compared to (*S*)-**25** in some examples, making this ligand an interesting modulation of the typical bis(imino)pyridines for further investigations.

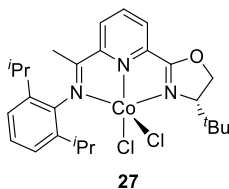


Figure 2-19. Oxazoline iminopyridine complex **27**

Table 2-9. Selected examples of the hydrogenation of 1,1-diarylethenes with **27**

Entry	Substrate	R	% Yield	% ee
1		F	>99	60
2		Cl	>99	90
3		Me	>99	80

In analogy to their observations in iron-catalyzed hydrogenations, the Chirik group has modified the bis(imino)pyridine ligand by replacing the imines with strongly σ -donating *N*-heterocyclic carbenes to enhance the electron density at the metal center (Figure 2-20).^[47]

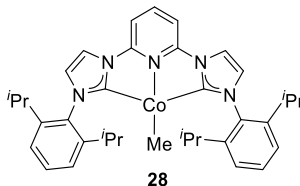


Figure 2-20. Bis(arylimidazol-2-ylidene)pyridine cobalt methyl **28**

Again, this ligand modification resulted in increased reactivity compared to its bis(imino)pyridine analogue. Therefore, **28** constitutes one of the most active base metal hydrogenation pre-catalysts for sterically hindered alkenes.

Table 2-10. Hydrogenation of sterically hindered alkenes with **28**

$ \begin{array}{c} \text{R}^3 \\ \diagup \quad \diagdown \\ \text{R}^1 \text{C} = \text{C} \text{R}^4 \\ \diagdown \quad \diagup \\ \text{R}^2 \end{array} \xrightarrow[4 \text{ bar H}_2, 22^\circ\text{C}]{5 \text{ mol\% } \mathbf{28}} \begin{array}{c} \text{R}^3 \\ \\ \text{R}^1 \text{CH} - \text{CH} \text{R}^4 \\ \\ \text{R}^2 \end{array} $		
Entry	Substrate	% Yield
1		>95 (1 h)
2		>95 (5 h)
3		15 (24 h)

Upon dihydrogen addition, **28** readily forms the hydride complex **29** which most likely is the active catalyst under hydrogenation conditions. Interestingly, **29** undergoes hydrogen migration from cobalt to the electrophilic 4-pyridyl position which has not been observed with the analogous iron complex **11** (Figure 2-21). A combined computational and spectroscopic study favors the presence of a pyridine-centered radical ligand which is responsible for the observed H atom migration and the redox-noninnocence of the *C,N,C*-pincer ligand.

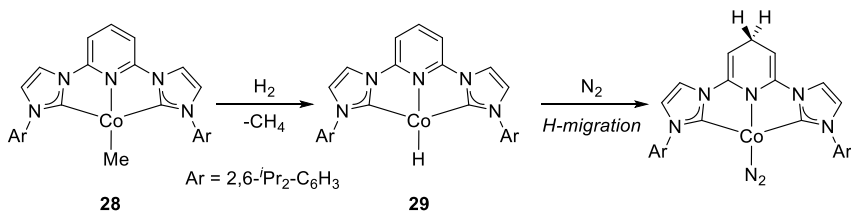


Figure 2-21. Reactivity of **28** with dihydrogen and sequential H-atom migration

In 2012, Hanson and coworkers applied cobalt pre-catalysts containing aliphatic *P,N,P*-pincer ligands to olefin and carbonyl hydrogenation reactions.^[48] Through the activation with the strong Brookhart acid $\text{H}[\text{BAR}^{\text{F}}_4](\text{Et}_2\text{O})_2$, the inactive precursor **30** was converted to the cationic hydrogenation catalyst **31** (Figure 2-22).

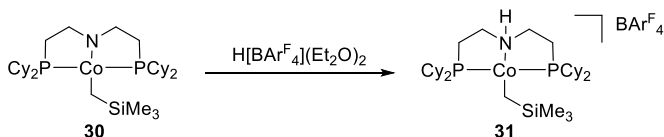


Figure 2-22. Formation of cationic pincer catalyst **31** by deprotonation of **30**

Similar to the alkylcobalt complex **22**, **31** formed an active hydridocobalt species under hydrogenation conditions upon release of tetramethylsilane (Figure 2-23) as evidenced by crossover and trapping experiments.

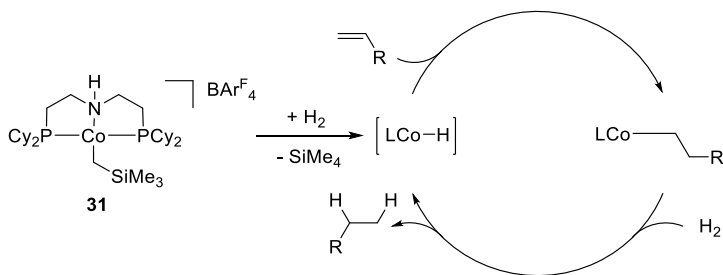


Figure 2-23. Proposed catalytic cycle with **31**

Hydrogenations of a wide scope of alkenes, imines, and ketones were performed with *in situ* generated **31**. The base-free operation enabled the tolerance of a various functional groups (e.g. carboxylic acids and ketones). The presence of alcohol functions or water did not effect the catalytic activity which attests to the high stability of **31**. Similar to catalysis by the analogous iron complex **14**, a bifunctional mechanism with amine participation was excluded due to the similar activity of the *N*-methylated complex. In accordance with

this assumption, **31** was also a competent catalyst in the hydrogenation of non-polar C=C bonds whereas **14** failed to hydrogenate 1-hexene. **31** showed high chemoselectivity in hydrogenations of less hindered C=C bonds and in the presence of carbonyl groups (Table 2-11). Elevated temperature also enabled the clean hydrogenation of carbonyl compounds.

Table 2-11. Selected examples of various alkene hydrogenation with pre-catalyst **30**

$ \begin{array}{c} \text{R}^1\text{CH=CH}\text{R}^2 \xrightarrow[1 \text{ bar H}_2, 25 \text{ }^\circ\text{C}]{\begin{array}{c} 2 \text{ mol\% } \mathbf{30} \\ 2 \text{ mol\% H[BArF}_4\text{]}(\text{Et}_2\text{O})_2 \end{array}} \text{R}^1\text{CH}_2\text{CH}_2\text{R}^2 \end{array} $				
Entry	Substrate	Product	Time / h	% Yield
1			40	80
2			24	99
3			24 (60 °C)	99
4			42	99

In 2014, Peters and coworkers applied new *P,B,P*-pincer cobalt complexes to hydrogenation reactions.^[49] The bis(phosphino)boranecobalt(I) complex **32** was synthesized by complexation of cobalt(II) bromide and sequential reduction with Na/Hg. Importantly, **32** is capable of activating two equivalents of dihydrogen in a reversible fashion to form the dihydridoboratocobalt dihydride **33**. Under mild hydrogenation conditions, simple olefins such as 1-octene and styrene were hydrogenated with turnover frequencies of 1000 h⁻¹ but the complex failed to convert internal olefins (i.e. cyclooctene, norbornene).

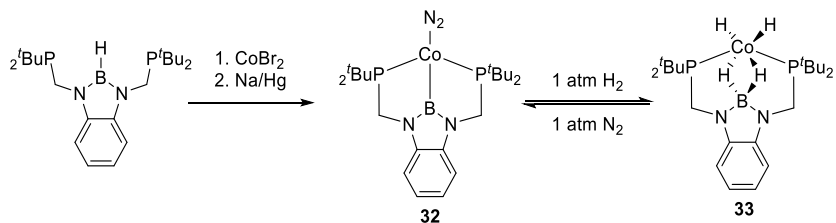


Figure 2-24. Synthesis and reversible hydrogen addition of *P,B,P* pincer complex **32**

6.1.2 Others

A different ligand design of the pre-catalyst was used by Wolf and Jacobi von Wangelin in their application of the heteroatom-free bis(anthracene)cobaltate complexes (**34**) to hydrogenation reactions of alkenes, alkynes, and carbonyls.^[30] The complex was first reported by Ellis and Brennessel in 2002 and constitutes a convenient metal (-I) source that contains labile hydrocarbon ligands.^[50]

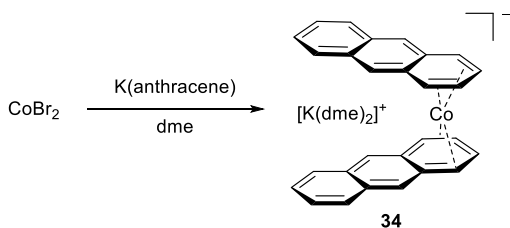


Figure 2-25. Synthesis of potassium bis(anthracene) cobaltate **34**

According to the authors, the catalyst is stabilized by the presence of various π -coordinating compounds which, under hydrogenation conditions, are the corresponding substrates (e.g. olefins). NMR studies documented the fast ligand exchange of anthracene by styrene, cod, and other simple alkenes. Longer reaction times and elevated pressure also led to the hydrogenation of the anthracene ligand. The absence of π -acidic ligands resulted in particle formation and catalyst deactivation, although the resultant nanoparticles are still moderately effective catalysts for the hydrogenation of simple alkenes and styrenes. Catalyst **34** was applied to a wide scope of alkenes (1–4 bar H_2 , r.t.), ketones and imines (10 bar H_2 , 60°C) and showed comparable activity to the cobalt catalyst **31**.

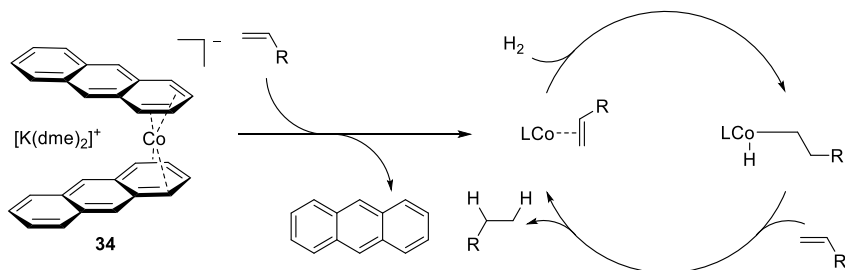


Figure 2-26. Proposed mechanism for catalytic hydrogenation with **34**

In an extended study, the same groups synthesized a library of heteroleptic bis(arene) and bis(alkene)cobaltate complexes (Figure 2-27). Despite only small stereoelectronic differences between these complexes, the nature of the π -hydrocarbon ligand drastically influenced catalytic reactivity (Table 2-12). The authors observe a decreasing reactivity for complexes with more strongly coordinating alkene substrates (**37**, **38**).

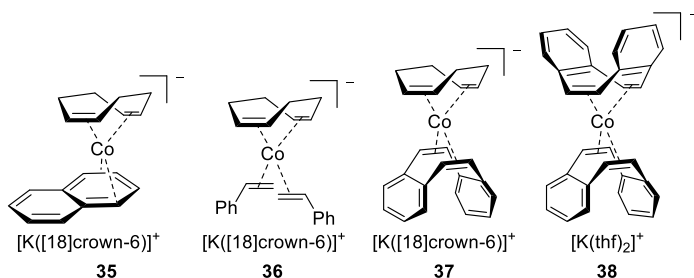


Figure 2-27. Selected examples of heteroleptic arene/alkene cobaltate complexes **35-38**

Table 2-12. Comparative hydrogenation of alkenes with **34-38**

		5 mol% [Co]				
		$\text{R}-\text{CH}=\text{CH}_2 \xrightarrow[2 \text{ bar H}_2, 20^\circ\text{C}, 24 \text{ h}]{}$				
Entry	Substrate	% Yield with [Co]				
		34	35	36	37	38
1		94	99	72	36	0
2		58	93	85	71	0

A structurally unique complex class was reported by Stryker and coworkers in 2013.^[51] By reaction of cobalt(II) chloride with a sterically demanding lithium phosphoranamide and sequential reduction with sodium amalgam, the tetrameric cobalt(I) cluster **39** was formed. The square-planar complex can be viewed as a simple ligand-supported mimetic of metallic surface arrays. The authors reported the good activity of **39** in the hydrogenation of allylbenzene and diphenylacetylene using only 0.5 mol% of catalyst.

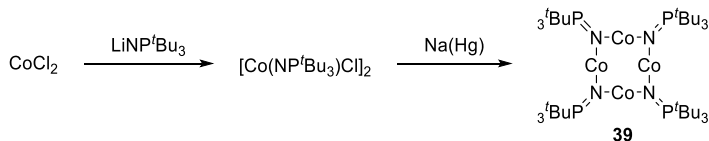
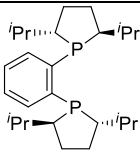
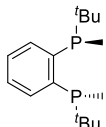
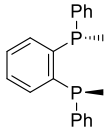


Figure 2-28. Synthesis of tetrameric cobalt complex **39**.

In a landmark publication, Chirik and coworkers reported the use of chiral bidentate bis(phosphine)cobalt catalysts in highly stereoselective hydrogenations of largely unfunctionalized alkenes and dehydroamino acids.^[52] Remarkably, the authors were able to identify very potent catalysts by high-throughput screening, which allowed the fast comparison of a vast number of chiral bidentate phosphine ligands in cobalt-catalyzed enantioselective alkene hydrogenations (Table 2-13).

Table 2-13. Selected bis(phosphine) ligands in enantioselective cobalt-catalyzed hydrogenation

Entry	Bis(phosphine)	% Yield	% ee (major isomer)
1	 (<i>R,R</i>)-QuinoxP	93.2	96.4 (<i>R</i>)

2	 <i>i</i> Pr-DuPhos	92.3	94.2 (<i>S</i>)
3	 (<i>R,R</i>)-BenzP	>99	93.4 (<i>R</i>)
4	 (<i>S,S</i>)-1,2-(MePhP) ₂ C ₆ H ₄	>99	77.0 (<i>S</i>)

After identification of *i*Pr-DuPhos as suitable ligand, complex **40** was isolated and applied in the hydrogenation of enamides (Figure 2-29) with excellent yield and moderate to good enantioselectivity.

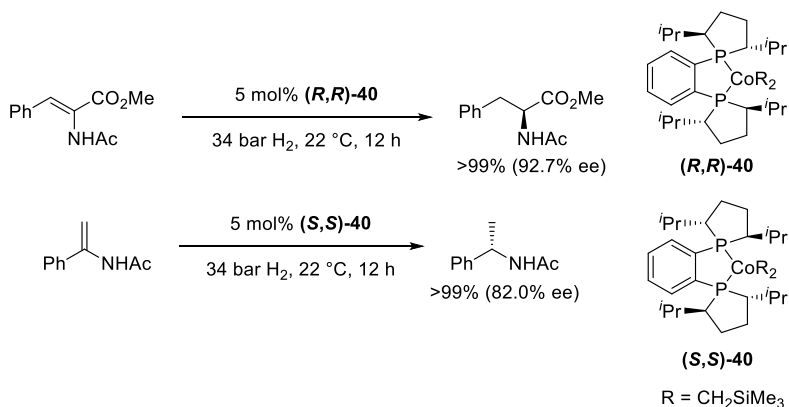


Figure 2-29. Enantioselective alkene hydrogenation with **40**

Soon after, the same group prepared related non-chiral bis(phosphine)cobalt(II) dialkyl complexes (Figure 2-30) which proved very active in alkene hydrogenations.^[53]

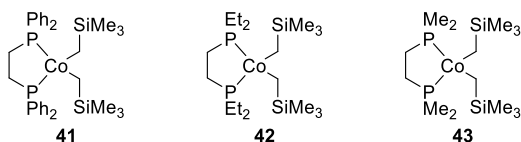


Figure 2-30. Bisphosphine cobalt(II) dialkyl cobalt (II) complexes **41**, **42** and **43**

Complex **42** effectively catalyzed the hydrogenation of terminal and di-substituted C=C bonds. Notably, the authors reported a catalyst activation in the presence of hydroxyl moieties which enabled the hydrogenation of tri-substituted alkenes under mild conditions (Table 2-14). Notably, the authors reported a catalyst activation in the presence of hydroxyl moieties which enabled the hydrogenation of tri-substituted alkenes under mild conditions. This activation effect is intramolecular in nature, an intermolecular activation by addition of alcohol was unsuccessful.

Table 2-14. Selected examples of the hydrogenation of oxygen-containing alkenes with **42**

$ \begin{array}{c} \text{R}^1 \text{---} \text{C}(\text{R}^2) = \text{C}(\text{R}^3) \xrightarrow[4 \text{ bar H}_2, 25^\circ \text{C}]{5 \text{ mol\% } \mathbf{42}} \text{R}^1 \text{---} \text{CH}_2 \text{---} \text{CH}(\text{R}^3) \text{---} \text{R}^2 \end{array} $				
Entry	Substrate	Product	Time / h	% Yield
1			14	<5
2			14	97
3			14	85
4			4	>99

Under hydrogenation conditions, the authors proposed hydrogenolysis of both alkyl moieties and formation of a dihydridocobalt(II) complex. Insertion of olefin gives a monohydridocobalt(II) alkyl complex which could reductively eliminate the resulting alkane upon generation of a cobalt(0) complex (Figure 2-31). The latter was supported by trapping a cyclooctadienecobalt(0) complex upon reaction of **42** with cyclooctadiene under dihydrogen atmosphere.

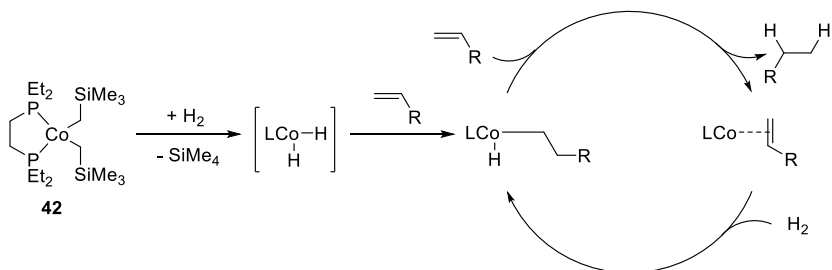


Figure 2-31. Proposed olefin hydrogenation with pre-catalyst **42**

2.4 Nickel

2.4.1 Introduction

Heterogeneous nickel catalysts in various forms are very well established for C=C hydrogenation reactions. Most prominent are applications of Raney®-nickel catalysts which were developed in already in 1926.^[54] The high catalyst activities at room temperature led to numerous implementation in industrial processes and organic synthesis programmes. The broad range of catalyzed reactions includes hydrogenation of C=C bonds, nitriles, nitro compounds, and other unsaturated functional groups. Similar activities were often achieved with the non-pyrophoric Urushibara-nickel catalysts (mostly Fe/Zn).^[55] Reports of olefin hydrogenations with Ziegler-type Ni/Al catalysts followed in the 1960's.^[10] Today, Raney®-nickel catalysts display the widest scope in hydrogenation reactions. However, the heterogeneous nature, rather undefined composition and surface properties, and the high reactivity with many functional groups have stimulated significant efforts toward the design of homogeneous catalysts that allow facile control over activity, selectivity, and physical properties through rational ligand design. Still only very few powerful homogeneous nickel-catalyzed C=C hydrogenations have been reported, despite the decades experience with the related Reppe and Wilke chemistry.^[56] Early examples include the hydrogenation of methyl linoleate with bis(triphenylphosphine)nickel(II) halides in 1967.^[57] Bidentate bis(phosphine) nickel(II) complexes were studied in the hydrogenation of 1-octene in 1998.^[58] The more recent applications of homogeneous nickel catalysts to hydrogenation reactions are summarized below.

2.4.2 Pincer complexes

One of the rare examples in homogeneous nickel hydrogenation chemistry was reported by Sanchez and coworkers in 2004. A set of aminosalen-type *O,N,N* pincer nickel(II) complexes were evaluated under hydrogenation conditions (Figure 2-32).^[59]

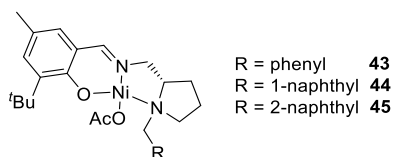
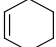
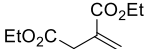
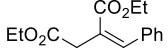


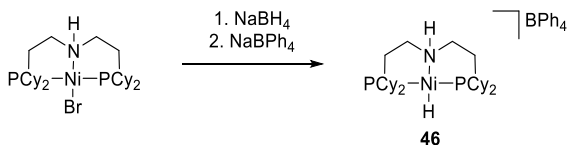
Figure 2-32. Salen-type nickel(II) complexes **43**, **44** and **45**

The chiral, air-stable complexes were active in hydrogenations of alkenes and imines (Table 2-15). No stereoselectivity was induced in reactions of prochiral alkenes. In a comparative study, the authors showed similar activities of **43-45** with the analogous palladium complexes in terms of turnover frequencies.

Table 2-15. Selected examples of the hydrogenation of alkenes with **43**

$ \begin{array}{c} \text{R}^3 \\ \diagup \quad \diagdown \\ \text{R}^1 \text{C} = \text{C} \text{R}^4 \\ \diagdown \quad \diagup \\ \text{R}^2 \end{array} \xrightarrow[4 \text{ bar H}_2, 40^\circ \text{C}]{0.1 \text{ mol\% } \mathbf{43}} \begin{array}{c} \text{R}^3 \\ \\ \text{R}^1 \text{CH} - \text{CH} \text{R}^4 \\ \\ \text{R}^2 \end{array} $		
Entry	Substrate	TOF/h ⁻¹
1		4020
2		2400
3		220

Parallel to their work on cobalt catalysts, Hanson *et al.* prepared the *P,N,P*-nickel(II) hydride complex **46** by reduction of the corresponding nickel(II) bromide complex and sequential protonation.^[60]

**Figure 2-33.** Synthesis of *P,N,P*-nickel(II) hydride (**46**)

The catalytic activity in the hydrogenation of terminal alkenes at 4 bar H₂, 80 °C was only moderate. A bifunctional mechanism that would involve alkane generation by an intramolecular protonation of the alkylnickel intermediates by the NH function (as observed with iron complex **14**), was excluded based on the observation that no methane was released from thermal treatment of the catalytically equally active methylnickel(II) complex **47** (Figure 2-34). The authors proposed a purely metal-centered mechanism via reversible alkene 1,2-insertion into the Ni-H bond, dihydrogen addition, and reductive elimination.

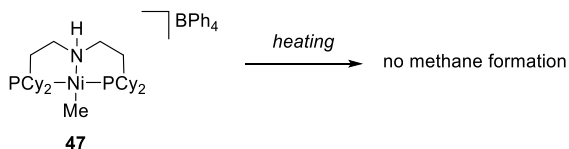


Figure 2-34. Stability of *P,N,P* nickel(II) methyl complex **47**

In 2012, Peters and coworkers reported the synthesis and comprehensive study of *P,B,P*-pincer nickel(II) complexes.^[61] The boryl bis(phosphine)nickel **48** reversibly added dihydrogen to give the square-planar borohydronickel(II) hydride **49** (Figure 2-35). The heterolysis of H₂ occurs at the nickel-boron bond where nickel acts as a Lewis base which formally accepts a proton. The Lewis acidic boryl ligand stabilizes the formal dihydronickel complex **49**, allowing reversible hydrogen activation at room temperature. Complex **48** was successfully applied to hydrogenations of styrene at mild conditions with a turnover frequency of about 20 h⁻¹.

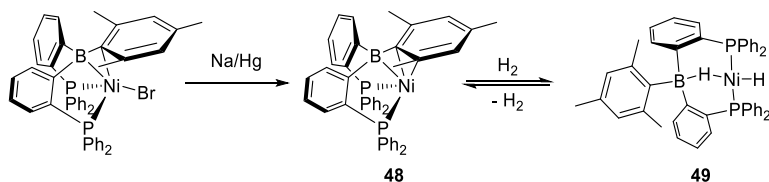


Figure 2-35. Synthesis of borylnickel complex **48** and reversible addition of dihydrogen

Two years later, the same group reported the *P,B,P*-nickel(I) hydride complex **41** with similar hydrogenation activity.^[62] The proposed mechanism involves reversible olefin insertion into the Ni-H bond with consecutive hydrogenolysis. The authors demonstrated the beneficial effect of the boryl ligand in **50** in comparison with isoelectronic and isostructural phenyl and amino functions (Table 2-16).

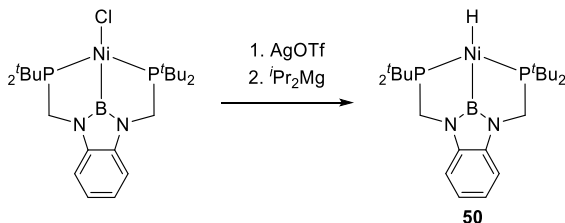
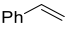
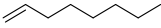
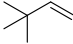


Figure 2-36. Synthesis of *P,B,P* nickel(I) hydride **50**

Table 2-16. Selected examples of the hydrogenation of terminal alkenes with the nickel complexes **46** and **50**

Entry	Substrate	TOF / h ⁻¹ (% Yield)	
		46	50
1		0.4 (100)	25 (100)
2		0.4 (70)	25 (64)
3		0.2 (97)	5 (100)

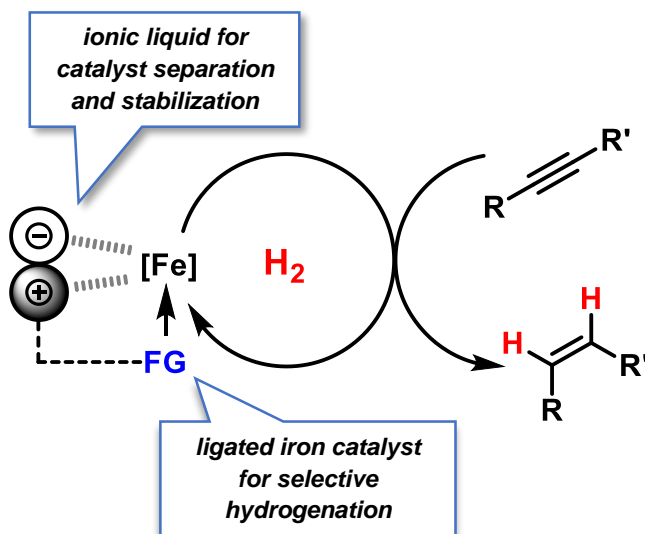
2.5 References

- [1] a) W. Keim, A. Behr, G. Schmitt, *Grundlagen der industriellen Chemie. Technische Produkte und Prozesse*, Salle, Frankfurt am Main, Berlin, **1986**. b) J. W. Veldsink, M. J. Bouma, N. H. Schöön, A. A. C. M. Beenackers, *Catal. Rev.* **1997**, 39, 253.
- [2] a) W. S. Knowles, *J. Chem. Educ.* **1986**, 63, 222; b) T. Ohta, H. Takaya, M. Kitamura, K. Nagai, R. Noyori, *J. Org. Chem.* **1987**, 52, 3174; c) G. Heydrich, G. Gralla, K. Ebel, W. Krause, N. Kashani-Shirazi, WO2009033870 A1, **2009**.
- [3] D. Wang, D. Astruc, *Chem. Rev.* **2015**, 115, 6621.
- [4] a) J. G. de Vries, C. J. Elsevier (Ed.) *The handbook of homogeneous hydrogenation*, WILEY-VCH, Weinheim, **2006**; b) N. B. Johnson, I. C. Lennon, P. H. Moran, J. A. Ramsden, *Acc. Chem. Res.* **2007**, 40, 1291.
- [5] M. C. White, *Adv. Synth. Catal.* **2016**, 358, 2364.
- [6] a) S. Shima, D. Chen, T. Xu, M. D. Wodrich, T. Fujishiro, K. M. Schultz, J. Kahnt, K. Ataka, X. Hu, *Nat. Chem.* **2015**, 7, 995; b) H.-J. Arpe, *Industrial organic chemistry*, WILEY-VCH, Weinheim, **2010**.
- [7] determined by title search on www.webofknowledge.com for “iron”, “cobalt”, “nickel” “AND” “hydrogenation”.
- [8] a) A. F. Thompson, S. B. Wyatt, *J. Am. Chem. Soc.* **1940**, 62, 2555; b) S.-I. Taira, *Bull. Chem. Soc. Jpn.* **1962**, 35, 840.
- [9] a) M. F. Sloan, A. S. Matlack, D. S. Breslow, *J. Am. Chem. Soc.* **1963**, 85, 4014; b) D. S. Breslow, A. S. Matlack, US3113986 A, **1963**.
- [10] W. M. Alley, I. K. Hamdemir, K. A. Johnson, R. G. Finke, *J. Mol. Catal. A: Chem.* **2010**, 315, 1.
- [11] a) N. Guo, M.-Y. Hu, Y. Feng, S.-F. Zhu, *Org. Chem. Front.* **2015**, 2, 692; b) T. N. Gieshoff, M. Villa, A. Welther, M. Plois, U. Chakraborty, R. Wolf, A. Jacobi von Wangelin, *Green Chem* **2015**, 17, 1408; c) T. N. Gieshoff, A. Welther, M. T. Kessler, M. H. G. Precht, A. Jacobi von Wangelin, *Chem. Commun.* **2014**, 50, 2261; d) D. J. Frank, L. Guet, A. Kaslin, E. Murphy, S. P. Thomas, *RSC Adv* **2013**, 3, 25698; e) A. Welther, M. Bauer, M. Mayer, A. Jacobi von Wangelin, *ChemCatChem* **2012**, 4, 1088; f) C. Rangheard, C. de Julián Fernández, P.-H. Phua, J. Hoorn, L. Lefort, J. G. de Vries, *Dalton Trans* **2010**, 39, 8464; g) P.-H. Phua, L. Lefort, J. A. F. Boogers, M. Tristany, J. G. de Vries, *Chem. Commun.* **2009**, 3747.
- [12] D. Astruc, F. Lu, J. R. Aranzas, *Angew. Chem. Int. Ed.* **2005**, 44, 7852; *Angew. Chem.* **2005**, 117, 8062.
- [13] a) V. Kelsen, B. Wendt, S. Werkmeister, K. Junge, M. Beller, B. Chaudret, *Chem. Commun.* **2013**, 49, 3416; b) L.-M. Lacroix, S. Lachaize, A. Falqui, T. Blon, J. Carrey, M. Respaud, F. Dumestre, C. Amiens, O. Margeat, B. Chaudret, *J. Appl. Phys.* **2008**, 103, 07D521.
- [14] R. Hudson, G. Hamasaka, T. Osako, Yamada, Yoichi M. A., C.-J. Li, Y. Uozumi, A. Moores, *Green Chem* **2013**, 15, 2141.
- [15] M. Stein, J. Wieland, P. Steurer, F. Tölle, R. Mülhaupt, B. Breit, *Adv. Synth. Catal.* **2011**, 353, 523.
- [16] E. N. Frankel, E. A. Emken, H. M. Peters, V. L. Davison, R. O. Butterfield, *J. Org. Chem.* **1964**, 29, 3292.
- [17] M. A. Schroeder, M. S. Wrighton, *J. Am. Chem. Soc.* **1976**, 98, 551.
- [18] E. J. Daida, J. C. Peters, *Inorg. Chem.* **2004**, 43, 7474.
- [19] Q. Knijnenburg, A. D. Horton, D. Van, A. W. Gal, P. Budzelaar, WO2003042131 A1, **2003**.
- [20] S. C. Bart, E. Lobkovsky, P. J. Chirik, *J. Am. Chem. Soc.* **2004**, 126, 13794.

- [21] S. C. Bart, K. Chlopek, E. Bill, M. W. Bouwkamp, E. Lobkovsky, F. Neese, K. Wieghardt, P. J. Chirik, *J. Am. Chem. Soc.* **2006**, *128*, 13901.
- [22] R. J. Trovitch, E. Lobkovsky, E. Bill, P. J. Chirik, *Organometallics* **2008**, *27*, 1470.
- [23] a) S. K. Russell, J. M. Darmon, E. Lobkovsky, P. J. Chirik, *Inorg. Chem.* **2010**, *49*, 2782; b) R. P. Yu, J. M. Darmon, J. M. Hoyt, G. W. Margulieux, Z. R. Turner, P. J. Chirik, *ACS Catal.* **2012**, *2*, 1760.
- [24] A. A. Danopoulos, J. A. Wright, W. B. Motherwell, *Chem. Commun.* **2005**, 784.
- [25] J. M. Darmon, R. P. Yu, S. P. Semproni, Z. R. Turner, S. C. E. Stieber, S. DeBeer, P. J. Chirik, *Organometallics* **2014**, *33*, 5423.
- [26] P. J. Chirik, *Acc. Chem. Res.* **2015**, *48*, 1687.
- [27] D. Srimani, Y. Diskin-Posner, Y. Ben-David, D. Milstein, *Angew. Chem. Int. Ed.* **2013**, *52*, 14131; *Angew. Chem.* **2013**, *125*, 14381.
- [28] E. Alberico, P. Sponholz, C. Cordes, M. Nielsen, H.-J. Drexler, W. Baumann, H. Junge, M. Beller, *Angew. Chem. Int. Ed.* **2013**, *52*, 14162; *Angew. Chem.* **2013**, *125*, 14412.
- [29] a) S. Chakraborty, W. W. Brennessel, W. D. Jones, *J. Am. Chem. Soc.* **2014**, *136*, 8564; b) R. Xu, S. Chakraborty, S. M. Bellows, H. Yuan, T. R. Cundari, W. D. Jones, *ACS Catal.* **2016**, *6*, 2127.
- [30] D. Gärtner, A. Welther, B. R. Rad, R. Wolf, A. Jacobi von Wangelin, *Angew. Chem. Int. Ed.* **2014**, *53*, 3722; *Angew. Chem.* **2014**, *126*, 3796.
- [31] W. W. Brennessel, R. E. Jilek, J. E. Ellis, *Angew. Chem. Int. Ed.* **2007**, *46*, 6132; *Angew. Chem.* **2007**, *119*, 6244.
- [32] P. Büschelberger, D. Gärtner, E. Reyes-Rodriguez, F. Kreyenschmidt, K. Koszinowski, A. Jacobi von Wangelin, R. Wolf, *manuscript in preparation*.
- [33] a) A. J. Frings, *dissertation*, University of Bochum, Germany, **1988**; b) K. Jonas, *Pure Appl. Chem.* **1990**, *62*, 1169 c) E.-M. Schnöckelborg, M. M. Khusniyarov, B. de Bruin, F. Hartl, T. Langer, M. Eul, S. Schulz, R. Pöttgen, R. Wolf, *Inorg. Chem.* **2012**, *51*, 6719.
- [34] a) B. V. Aller, *J. Appl. Chem.* **1958**, *8*, 492; b) M. G. Banwell, M. T. Jones, T. A. Reekie, B. D. Schwartz, S. H. Tan, L. V. White, *Org. Biomol. Chem.* **2014**, *12*, 7433.
- [35] W. M. Alley, I. K. Hamdemir, Q. Wang, A. I. Frenkel, L. Li, J. C. Yang, L. D. Menard, R. G. Nuzzo, S. Ozkar, K.-H. Yih, *Langmuir* **2011**, *27*, 6279.
- [36] F. Chen, A.-E. Surkus, L. He, M.-M. Pohl, J. Radnik, C. Topf, K. Junge, M. Beller, *J. Am. Chem. Soc.* **2015**, *137*, 11718.
- [37] S. U. Son, K. H. Park, Y. K. Chung, *Org. Lett.* **2002**, *4*, 3983.
- [38] a) I. Wender, R. Levine, M. Orchin, *J. Am. Chem. Soc.* **1950**, *72*, 4375; b) S. Friedman, S. Metlin, A. Svedi, I. Wender, *J. Org. Chem.* **1959**, *24*, 1287.
- [39] a) M. Hidai, T. Kuse, T. Hikita, Y. Uchida, A. Misono, *Tetrahedron Lett.* **1970**, *11*, 1715; b) G. F. Pregaglia, A. Andreetta, G. F. Ferrari, R. Ugo, *J. Organomet. Chem.* **1971**, *30*, 387; c) G. F. Ferrari, A. Andreetta, G. F. Pregaglia, R. Ugo, *J. Organomet. Chem.* **1972**, *43*, 209; d) H. M. Feder, J. Halpern, *J. Am. Chem. Soc.* **1975**, *97*, 7186.
- [40] Y. Ohgo, S. Takeuchi, Y. Natori, J. Yoshimura, *Bull. Chem. Soc. Jpn.* **1981**, *54*, 2124.
- [41] T. M. Kooistra, Q. Knijnenburg, J. M. M. Smits, A. D. Horton, P. H. M. Budzelaar, A. W. Gal, *Angew. Chem. Int. Ed.* **2001**, *40*, 4719; *Angew. Chem.* **2001**, *113*, 4855.
- [42] Q. Knijnenburg, A. D. Horton, H. van der Heijden, T. M. Kooistra, D. G. Hetterscheid, J. M. Smits, B. d. Bruin, P. H. Budzelaar, A. W. Gal, *J. Mol. Catal. A: Chem.* **2005**, *232*, 151.
- [43] Q. Knijnenburg, D. Hetterscheid, T. M. Kooistra, P. H. M. Budzelaar, *Eur. J. Inorg. Chem.* **2004**, 1204.

- [44] a) S. Monfette, Z. R. Turner, S. P. Semproni, P. J. Chirik, *J. Am. Chem. Soc.* **2012**, *134*, 4561; b) C. Bianchini, G. Mantovani, A. Meli, F. Migliacci, F. Zanobini, F. Laschi, A. Sommazzi, *Eur. J. Inorg. Chem.* **2003**, 1620.
- [45] a) K. H. Hopmann, *Organometallics* **2013**, *32*, 6388; b) M. R. Friedfeld, M. Shevlin, G. W. Margulieux, L.-C. Campeau, P. J. Chirik, *J. Am. Chem. Soc.* **2016**, *138*, 3314.
- [46] J. Chen, C. Chen, C. Ji, Z. Lu, *Org. Lett.* **2016**, *18*, 1594.
- [47] R. P. Yu, J. M. Darmon, C. Milsman, G. W. Margulieux, S. C. E. Stieber, S. DeBeer, P. J. Chirik, *J. Am. Chem. Soc.* **2013**, *135*, 13168.
- [48] G. Zhang, B. L. Scott, S. K. Hanson, *Angew. Chem. Int. Ed.* **2012**, *51*, 12102; *Angew. Chem.* **2012**, *124*, 12268.
- [49] T.-P. Lin, J. C. Peters, *J. Am. Chem. Soc.* **2013**, *135*, 15310.
- [50] W. W. Brennessel, Young, Jr., Victor G., J. E. Ellis, *Angew. Chem. Int. Ed.* **2002**, *41*, 1211; *Angew. Chem.* **2002**, *114*, 1259.
- [51] J. Camacho-Bunquin, M. J. Ferguson, J. M. Stryker, *J. Am. Chem. Soc.* **2013**, *135*, 5537.
- [52] M. R. Friedfeld, M. Shevlin, J. M. Hoyt, S. W. Krska, M. T. Tudge, P. J. Chirik, *Science* **2013**, *342*, 1076.
- [53] M. R. Friedfeld, G. W. Margulieux, B. A. Schaefer, P. J. Chirik, *J. Am. Chem. Soc.* **2014**, *136*, 13178.
- [54] M. Raney, US1628190 A, **1927**.
- [55] Y. Urushibara, S. Nishimura, H. Uehara, *Bull. Chem. Soc. Jpn.* **1955**, *28*, 446.
- [56] W. Keim, *Angew. Chem. Int. Ed. Engl.* **1990**, *29*, 235; *Angew. Chem.* **1990**, *102*, 251.
- [57] H. Itatani, J. C. Bailar, *J. Am. Chem. Soc.* **1967**, *89*, 1600.
- [58] I. M. Angulo, A. M. Kluwer, E. Bouwman, *Chem. Commun.* **1998**, 2689.
- [59] C. González-Arellano, E. Gutiérrez-Puebla, M. Iglesias, F. Sánchez, *Eur. J. Inorg. Chem.* **2004**, 1955.
- [60] K. V. Vasudevan, B. L. Scott, S. K. Hanson, *Eur. J. Inorg. Chem.* **2012**, 4898.
- [61] W. H. Harman, J. C. Peters, *J. Am. Chem. Soc.* **2012**, *134*, 5080.
- [62] T.-P. Lin, J. C. Peters, *J. Am. Chem. Soc.* **2014**, *136*, 13672.

3 Stereoselective iron-catalyzed alkyne hydrogenation in ionic liquids^{i,ii}



Iron(0) nanoparticles in ionic liquids (ILs) have been shown to catalyse the semi-hydrogenation of alkynes. In the presence of a nitrile-functionalised IL or acetonitrile, stereoselective formation of (*Z*)-alkenes was observed. The biphasic solvent system allowed facile separation and re-use of the catalyst.

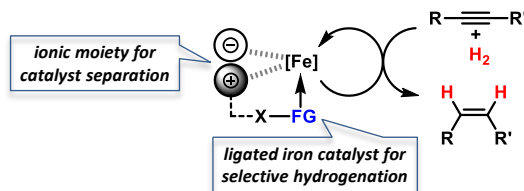
ⁱ Reproduced from T. N. Gieshoff, A. Welther, M. T. Kessler, M. H. G. Precht, A. Jacobi von Wangelin, *Chem. Commun.* **2014**, 50, 2261–2264 with permission from the Royal Society of Chemistry. Schemes, tables and text may differ from published version.

ⁱⁱ Authors contribution: Initial experiments were performed by A. Welther (Table 3-1, Table 3-2, Table 3-3, entries 2,3,7,11), see A. Welther, *Dissertation*, University Regensburg, **2013**. Table 3-3 entries 1,2,9-11, Table 3-4 entries 6,19,10,13-17, Scheme 3-2, Figure 3-2 were performed by T. N. Gieshoff, see T. N. Gieshoff, *Master Thesis*, University of Regensburg, **2013**. Ionic liquid synthesis and TEM measurement were performed by M. T. Kessler, University of Cologne.

3.1 Introduction

Iron-catalyzed hydrogenations are among the largest technical processes (Haber-Bosch, gas-to-liquid)^[1] but are underutilized on the smaller scales of fine chemical, agrochemical, and pharmaceutical manufacture and within academic synthesis programs. However, the current economic and environmental constraints have prompted reconsiderations of iron-catalyzed procedures.^[2] Hydrogenations of alkenes and alkynes with well-defined ligand-stabilized iron catalysts or heterogeneous species have been recently reported.^[3] Hydrogenations of alkynes in general bear the dual challenge of product- and stereo-selectivity. Lindlar-type catalysts exhibit especially high versatility and are the benchmark for semi-hydrogenations to (*Z*)-alkenes.^[4] This combination of an expensive noble metal catalyst (Pd/CaCO₃) and toxic additives (Pb(OAc)₂, quinoline) is clearly derogatory to the development of sustainable chemical processes, so an inexpensive nontoxic iron-catalyzed alternative is highly desirable.^[5] However, the search for new catalysts for technical applications is incomplete without the implementation of efficient catalyst separation and recycling technologies.^[6] Despite the higher selectivity of homogeneous catalysts, most technical processes use heterogeneous catalysts because of their ease of separation from the products. Within the scope of our iron catalysis program, we thus aimed at merging the benefits of a separable heterogeneous catalyst with that of a highly dispersive ligand-modified catalyst. We envisioned to capitalize on the hybrid concept of nanoparticulate iron catalysts^[7] in the presence of ligands which control the catalyst selectivity through coordination and an ionic liquid to allow catalyst separation. The potential of such modular systems was evaluated in stereoselective semi-hydrogenations of alkynes (Scheme 3-1).

Ionic liquids (ILs) based on azolium salts seemed perfectly suited for this task due to their ability to dissolve, stabilize, and modulate metal nanoparticles.^[8] Their physicochemical properties are widely adjustable by variation of substituents, the heterocycle, and counterion. Most importantly, azolium-ILs are immiscible with non-polar solvents and have a negligible vapor pressure. IL-stabilized precious metal nanoparticle catalysts were successfully applied to hydrogenations, whereas the generation and utilization of IL-embedded iron catalysts is as yet underutilized.^[9]

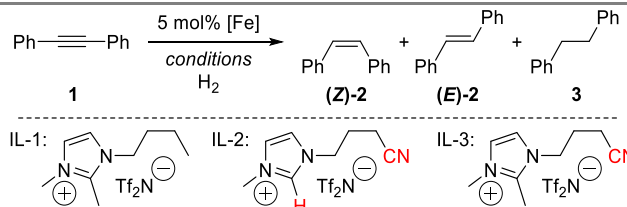


Scheme 3-1. Modular ion pair/ligand/iron catalysts for hydrogenations.

3.2 Reaction conditions and substrate scope

We set out to study the catalytic activity of heterogeneous iron species in low oxidation states generated by reduction of FeCl₃ with ethylmagnesium chloride (Table 3-1).^[3c,3e] Hydrogenation of diphenylacetylene (**1**) in the absence of a suitable ligand showed low selectivity toward stilbene (**2**). The use of imidazolium ILs generally required elevated pressure and temperature. Geared by literature precedents with Pd, Ru, and Au nanoparticles, we employed nitrile-functionalized ILs as catalyst modifiers.^[9,10] Notably, the presence of a nitrile function, the suppression of *N*-heterocyclic carbene formation,^[11] and the absence of THF were crucial to a selective *cis*-hydrogenation in IL-3.^[5] The replacement of THF with heptane also resulted in a high phase-partitioning at room temperature and allowed facile separation of the catalyst. The higher reaction temperature is believed to enhance dispersion of the viscous IL with the non-polar phase.

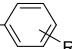
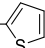
Table 3-1. Optimization of reaction conditions. ^a

				
Entry	Conditions ^b	Solvent(s)	1 / 2 / 3 in % ^c	Z/E (2) ^c
1	4 bar H ₂ , 45 °C, 8 h	THF	<1 / 2 / 93	n.d.
2	1 bar H ₂ , 18 °C, 8 h	THF	1 / 73 / 21	3 / 1
3	50 bar H ₂ , 50 °C, 16 h	THF/IL-1	2 / 3 / 93	n.d.
4	4 bar H ₂ , 18 °C, 16 h	THF/IL-2	94 / 2 / 2	n.d.
5	50 bar H ₂ , 50 °C, 16 h	THF/IL-2	82 / 15 / 2	6 / 1
6	50 bar H ₂ , 50 °C, 60 h	THF/IL-3	23 / 75 / 1	7 / 1
7	60 bar H₂, 80 °C, 44 h	hept/IL-3 ^d	1 / 94 / 3	19 / 1
8	30 bar H ₂ , 80 °C, 20 h	hept/IL-1 ^d	<1 / 1 / 98	n.d.

^a [Fe]: 5 mol% FeCl₃, 20 mol% EtMgCl, THF, r.t., 30 min; ^b For experimental details, see chapter 3.5.2; ^c determined by quantitative ¹H-NMR and GC-FID vs. hexamethyldisiloxane (¹H-NMR) or *n*-pentadecane (GC-FID) as internal standard; ^d removal of THF prior to reaction.

Application of the optimized conditions in a biphasic heptane/IL-3 mixture to other phenylacetylenes resulted in moderate to good yields of the corresponding alkenes and generally high stereoselectivities toward the (*Z*)-isomers (Table 3-2).

Table 3-2. Biphasic semi-hydrogenation of alkynes in heptane/IL-3.

$\text{R}-\text{C}\equiv\text{C}-\text{R}' \xrightarrow[\text{60 bar H}_2, 80^\circ\text{C}, 2\text{ d}]{5\text{ mol\% [Fe]}} \text{R}-\text{C}=\text{C}-\text{R}' + \text{R}-\text{CH}_2-\text{CH}_2-\text{R}'$ heptane/IL-3 (3/1)				
Entry	Alkyne	R	Yield alkene in % ^b	Z/E ^b
1		H	94	95 / 5
2		4- <i>t</i> Bu	86	95 / 5
3	Ph—C≡C— 	4-OMe	92	93 / 7
4		4-F	75	>99 / <1
5		3-OMe	52	96 / 4
6	Ph—C≡C— 	-	68	89 / 11
7	Ph—C≡C—Et	-	80	88 / 12

^a For experimental details, see chapter 3.5.2; ^b determined by quantitative ¹H-NMR and GC-FID vs. hexamethyldisiloxane (¹H-NMR) or *n*-pentadecane (GC-FID) as internal standard.

Our observation that ILs can effectively stabilise nanoparticles is in full accord with literature reports.^[9,10] Droplets of Fe-NPs in IL-1 and IL-3 were measured by transmission electron microscopy (TEM), respectively (Figure 3-1). Both species are approximately 4-5 nm in diameter and slowly grow during the catalytic reactions (to ~8-20 nm after 24 h under hydrogenation reaction conditions).

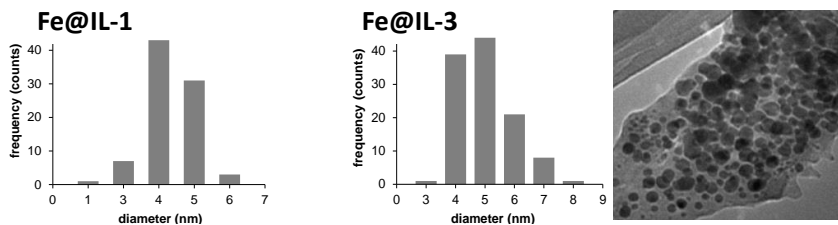
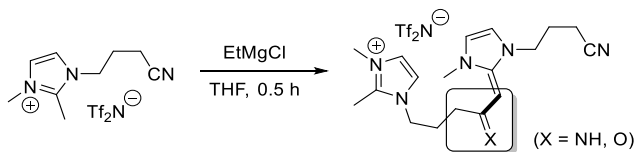
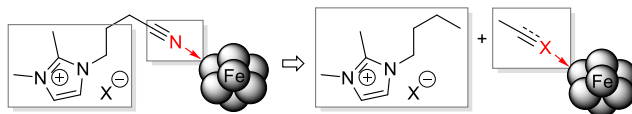


Figure 3-1. Particle sizes and TEM image (Fe@IL-3) of Fe@IL catalysts.

From a mechanistic point of view, the presence of two electrophilic functions (imidazolium cation, nitrile group) and a strong base/nucleophile (EtMgCl) poses the question of the actual nature of the ligand moiety that is present under the reaction conditions. We treated IL-1 with 1 equiv. EtMgCl at room temperature for 30 min followed by quenching with deuterium oxide (D_2O) which afforded a mixture of ring-deuterated (35%) and 2-deuteromethyl products (10%).^[12] IL-3 did not undergo deuteration under identical conditions (2H -NMR, MS). Instead, a dimer was formed which was detected by GC-MS and ESI-MS and tentatively assigned as shown in Scheme 3-2.^[13] If a nucleophile-assisted manipulation of the nitrile is relevant to the control of selectivity, simple alkylnitriles should exert a similar effect. We therefore examined whether the intramolecular bifunctional motif of IL-3 could also be expressed by a much simpler intermolecular combination of ionic liquid and nitrile functions. Furthermore, the potential occurrence of acetyl or imine moieties as degradation products of the nitrile prompted us to also investigate the activity of ternary catalyst systems comprising a pre-formed reduced iron species (5 mol%), the non-functionalized ionic liquid IL-1, and various carbonyl derivatives under the optimised conditions (Table 3-3, Scheme 3-3). Without additives, the hydrogenation of **1** in heptane/IL-1 afforded bibenzyl (**3**, >95% yield, Table 3-3, entry 1).



Scheme 3-2. Formation of a dimer of IL-3 by treatment with EtMgCl.



Scheme 3-3. Intramolecular vs. intermolecular mode of bifunctionality.

To our delight, identical productivity and stereoselectivity as with the bifunctional IL-3 was observed when adding acetonitrile (Table 3-3, entry 2), even at 20 bar H₂ (entry 3). The loading of acetonitrile could be varied from 50-200 mol% without any change of selectivity. Further addition of 100 mol% methyl benzoate, chlorobenzene^[14] or 1,1-diphenylethylene, respectively, resulted in no change of activity (entries 4-6). Iodobenzene slowed down conversion while nitrobenzene acted as inhibitor. Benzophenone and ethyl acetate showed only slightly lower activity and selectivity as MeCN (entries 10, 11). Nanoparticles prepared from EtMgCl and EtMgBr afforded identical catalytic results.

Table 3-3. Hydrogenation of **1** with ternary Fe/IL-1/additive catalysts.

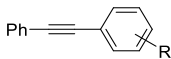
$ \begin{array}{c} \text{Ph} \text{---} \text{C} \equiv \text{C} \text{---} \text{Ph} \\ \mathbf{1} \end{array} \xrightarrow[\substack{60 \text{ bar H}_2, 80 \text{ }^\circ\text{C}, 16 \text{ h} \\ \text{heptane/IL-1}}]{\substack{5 \text{ mol\% [Fe]} \\ 50 \text{ mol\% additive}}} \begin{array}{c} \text{Ph} \text{---} \text{CH} = \text{CH} \text{---} \text{Ph} \\ \mathbf{2} \end{array} + \begin{array}{c} \text{Ph} \text{---} \text{CH}_2 \text{---} \text{CH}_2 \text{---} \text{Ph} \\ \mathbf{3} \end{array} $				
Entry	Additive	Conversion in %	2 in % ^d	<i>Z/E</i> (2) ^d
1	-	>99	3	n. d.
2	MeCN	96	93	96 / 4
3	MeCN ^{b,c}	99	85	96 / 4
4	MeCN + PhCO ₂ Me	99	95	97 / 3
5	MeCN + PhCl	>99	95	94 / 6
6	MeCN + Ph ₂ C=CH ₂	>99	95	96 / 4
7	MeCN + PhI	43	38	95 / 5
8	MeCN + PhNO ₂	5	<1	n. d.
9	MeC(O)Me ^b	25	22	91 / 9
10	PhC(O)Ph ^b	>99	84	94 / 6
11	MeCO ₂ Et	92	86	95 / 5

^aFor experimental details, see chapter 3.5.2. ^b100 mol% additive. ^c20 bar H₂
^ddetermined by quantitative GC-FID vs. *n*-pentadecane as internal standard.

The employment of a ternary Fe/IL-1/additive catalyst constitutes a significant simplification of the procedure and allows shorter reaction times than with the bifunctional IL-3 (16 h vs. 2 d). Table 3-4 shows selected examples of hydrogenations of

various alkynes in the presence of 5 mol% iron catalyst and 100 mol% acetonitrile in the biphasic solvent mixture IL-1/*n*-heptane. Generally, higher yields and stereoselectivities were obtained compared with the reactions in IL-3 (Table 3-2). Free NH₂ groups, esters, and alkenes were tolerated. Bulky groups (-SiMe₃) and carboxylates led to lower conversions. 1-Alkynes gave mixtures of alkenes and alkane. Hydrogenations proceeded also in mono-phasic THF/MeCN or toluene/MeCN (40 h) mixtures with similar selectivity, but the catalyst phase could not be separated. The catalyst species was found to rapidly age in the absence of IL-1 and lose activity after 48 h. On the other hand, effective catalyst separations and multiple re-uses without loss of catalytic activity were realized with the ternary catalyst Fe/IL-1/MeCN in hydrogenations of **1** under standard conditions (Figure 3-2). ICP-OES analysis of the product phase showed <0.03% leaching of iron (= 0.0015 mol%). Replacement of IL-1 with tetraalkyl-ammonium bromides (*n*-butyl, *n*-decyl) cleanly gave the alkanes, and product extraction with heptane failed. The heterogeneity of the catalyst species was further documented by the absence of inhibition by addition of dibenzo[*a,e*]cyclooctatetraene (dct).^[15]

Table 3-4. Biphasic semi-hydrogenations in MeCN/heptane/IL-1.

$\text{R}-\text{C}\equiv\text{C}-\text{R}' \xrightarrow[\text{heptane/IL-1 (3/1)}]{\substack{5 \text{ mol\% [Fe]} \\ 100 \text{ mol\% MeCN} \\ 60 \text{ bar H}_2, 80^\circ\text{C}, 18 \text{ h}}} \text{R}-\text{C}=\text{C}-\text{R}' + \text{R}-\text{CH}_2-\text{CH}_2-\text{R}'$				
Entry	Alkyne	R	Yield alkene in % ^c	Z/E ^c
1		H	97	96 / 4
2		4-'Bu	94	97 / 3
3		4-OMe	98	>99 / <1
4		4-NH ₂	76	>99 / <1
5		4-Br	84	>99 / <1
6		4-Cl	89	>99 / <1
7		4-F	83	99 / 1
8		4-CO ₂ Me	53 (74)	>99 / <1
9		2-Cl	79	>99 / <1
10		2-F	82	>99 / <1

11		-	76	99 / 1
12		-	90	>99 / <1
13		Et	79	95 / 5
14	$\text{Ph}-\text{C}\equiv\text{C}-\text{R}$	CO_2Me	13 (19)	96 / 4
15		SiMe_3	19 (40)	92 / 8
16		-	90	>99 / <1
17		-	38 (70)	>99 / <1

^a For experimental details, see chapter 3.5.2. ^b Conversion in parenthesis if not >90%;

^c determined by quantitative ^1H -NMR and GC-FID vs. hexamethyldisiloxane (^1H -NMR) or *n*-pentadecane (GC-FID) as internal standard.

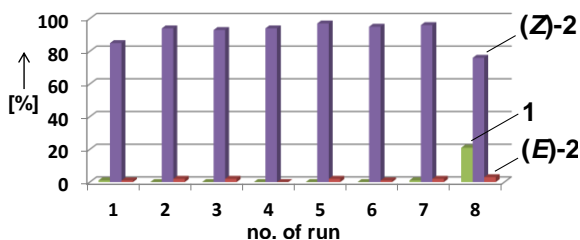


Figure 3-2. Consecutive hydrogenations of **1** with identical catalyst phase after liquid/liquid decantation.

3.3 Z-selective hydrogenation in absence of ionic liquids

The use of ionic liquids in the iron-catalyzed Z-selective semihydrogenation of alkynes clearly is beneficial for catalyst recycling and stability. On the other side, a polar and viscous catalyst in ionic liquid in combination with an unpolar substrate phase generates a two-phase system, presumably responsible for the need of high reaction temperatures and pressures. In order to develop an iron-based catalyst system which operates under mild conditions and is applicable with the use of standard laboratory inventory, catalytic hydrogenations were conducted in absence of ionic liquids (Table 3-5).

Table 3-5. Selected experiments in absence of ionic liquids.

$\text{Ph} \text{---} \text{C} \equiv \text{C} \text{---} \text{Ph} \xrightarrow[\text{H}_2]{\text{5 mol\% [Fe] conditions}} \text{Ph} \text{---} \text{CH} = \text{CH} \text{---} \text{Ph} + \text{Ph} \text{---} \text{CH} = \text{CH} \text{---} \text{Ph} + \text{Ph} \text{---} \text{CH}_2 \text{---} \text{CH}_2 \text{---} \text{Ph}$ <p style="text-align: center;">1 (Z)-2 (E)-2 3</p>				
Entry	Conditions ^a	Additive ^b	1 / 2 / 3 in % ^b	Z/E (2) ^c
1	4 bar H ₂ , 45 °C, 8 h	-	<1 / 2 / 93	n.d.
2	1 bar H ₂ , r.t., 8 h	-	1 / 73 / 21	3 / 1
3	10 bar H ₂ , r.t., 19 h	MeCN	88 / 8 / <1	n.d.
4	45 bar H ₂ , 80 °C, 15 h	MeCN	31 / 65 / <1	10 / 1
5	60 bar H ₂ , 80 °C, 20 h	MeCN	11 / 78 / <1	97 / 3

^a For experimental details, see chapter 3.5.2; ^b 100 mol% ^c determined by quantitative GC-FID vs. *n*-pentadecane as internal standard.

Under mild conditions, full hydrogenation to bibenzyl is achieved in absence of acetonitrile and ionic liquid (Table 3-5, entry 1). Addition of acetonitrile drastically decreases reactivity with low conversions even at elevated pressures. When employing harsh hydrogenation conditions (60 bar H₂, 80 °C) (Table 3-5, entry 5), high conversion with an excellent Z to E ratio is observed, identifying acetonitrile as the single responsible additive for high stereoselectivity. Harsh conditions are needed in order to activate the catalyst with acetonitrile as a very potent catalyst poison and are not a result of kinetic mass transport limitations implemented by viscous ionic liquids.

In order to remain high conversion with high stereoselectivity under less forcing conditions, a more active iron-based catalyst system was screened. The catalyst was derived from the reaction of Fe[N(SiMe₃)₂]₂ with LiAlH₄ or DiBAIH (see chapter 5) and shows excellent conversion of diphenylacetylene (Table 3-6, entry 1). Interestingly, the addition of acetonitrile resulted in selective semihydrogenations but with no stereoselectivity (Table 3-6, entries 2, 3). In the search for an alternative catalyst poison which enables stereoselective alkyne hydrogenation, CO₂ as a green and non-toxic alternative to acetonitrile showed promising results (entry 4-7). By the use of a mixture of H₂ and CO₂, catalysts FeCl₃-EtMgCl and Fe[N(SiMe₃)₂]₂-LiAlH₄ generated high Z to E stereoselectivity at elevated reaction pressures and temperatures. Milder reaction conditions resulted in little preference for Z-stilbene formation (entry 9). Further fine tuning of the H₂/CO₂ ratio might enhance stereocontrol under mild reaction conditions.

Table 3-6. Variation of catalyst and poison.

$ \begin{array}{c} \text{Ph} \text{---} \text{C} \equiv \text{C} \text{---} \text{Ph} \\ \mathbf{1} \end{array} \xrightarrow[\text{H}_2]{\begin{array}{c} [\text{cat}] \\ \text{conditions} \end{array}} \begin{array}{c} \text{Ph} \text{---} \text{CH} = \text{CH} \text{---} \text{Ph} \\ \mathbf{(Z)\text{-}2} \end{array} + \begin{array}{c} \text{Ph} \text{---} \text{CH} = \text{CH} \text{---} \text{Ph} \\ \mathbf{(E)\text{-}2} \end{array} + \begin{array}{c} \text{Ph} \text{---} \text{CH}_2 \text{---} \text{CH}_2 \text{---} \text{Ph} \\ \mathbf{3} \end{array} $				
A: [cat] = 5 mol% FeCl ₃ , 20 mol% EtMgCl B: [cat] = 5 mol% Fe[N(SiMe ₃) ₂] ₂ , 5 mol% LiAlH ₄ C: [cat] = 5 mol% Fe[N(SiMe ₃) ₂] ₂ , 5 mol% DiBAIH				
Entry	Conditions ^a	Additive ^b	1 / 2 / 3 in % ^b	Z/E (2) ^c
1	B , 1 bar H ₂ , r.t., 3 h	-	<1 / <1 / 93	n. d.
2	B , 45 bar H ₂ , 80 °C, 15 h	MeCN	<1 / 71 / 4	56 / 44
3	B , 45 bar H ₂ , 80 °C, 15 h	MeCN, IL-1	<1 / 59 / 3	54 / 46
4	B , 45 bar H ₂ , 80 °C, 15 h	5 bar CO ₂	13 / 75 / <1	89 / 11
5	B , 45 bar H ₂ , 80 °C, 15 h	5 bar CO ₂ , IL-1	2 / 71 / <1	87 / 13
6	A , 45 bar H ₂ , 80 °C, 15 h	5 bar CO ₂	65 / 33 / <1	88/12
7	A , 45 bar H ₂ , 80 °C, 15 h	5 bar CO ₂ , IL-1	3 / 67 / <1	96/4
8	B , 2 bar H ₂ , rt, 3 h	1 bar CO ₂	93 / 5 / <1	n. d.
9	C , 1 bar H ₂ , rt, 18 h	10 mol% CO ₂	<1 / 78 / 11	3 / 1
10	C , 1 bar H ₂ , rt, 2 h	100 mol% NaO ₂ CH	34 / 60 / 5	3 / 1

^aFor experimental details, see chapter 3.5.2; ^b100 mol% ^cdetermined by quantitative GC-FID vs. *n*-pentadecane as internal standard.

3.4 Summary

In summary, we have developed a simple ternary iron catalyst system that enables the (Z)-selective semi-hydrogenation of alkynes in a biphasic solvent mixture and the separation/reuse of the catalyst. The nanoparticle catalysts (~5 nm) form by reduction of FeCl₃ with EtMgCl. Acetonitrile effects stereocontrol; 1-butyl-2,3-dimethyl-1,3-imidazolium triflimide allows catalyst separation from the products and prevents particle aggregation.

3.5 Experimental

3.5.1 General

Analytical Thin-Layer Chromatography: TLC was performed using aluminium plates with silica gel and fluorescent indicator (*Merck*, 60, F254). Thin layer chromatography plates were visualized by exposure to ultraviolet light (366 or 254 nm) or by immersion in a staining solution of molybdatophosphoric acid in ethanol or potassium permanganate in water.

Column Chromatography: Flash column chromatography with silica gel 60 from *KMF* (0.040-0.063 mm). Mixtures of solvents used are noted in brackets.

Chemicals and Solvents: Commercially available chemicals were used without further purification, unless otherwise noted. Solvents (THF, Et₂O, *n*-heptane, toluene) were distilled over sodium and benzophenone and stored over molecular sieves (4 Å). EtMgCl in THF (2 M, *SigmaAldrich*) and iron(III)chloride (98%, anhydrous, *SigmaAldrich*) were stored and handled in a glovebox under argon (99.996%). Solvents used for column chromatography were distilled under reduced pressure prior use (ethyl acetate).

High Pressure Reactor: Hydrogenation reactions were carried out in 160 and 300 mL high pressure reactors (*Parr*TM) in 4 mL glass vials. The reactors were loaded under argon, purged with H₂ (1 min), sealed and the internal pressure was adjusted. Hydrogen (99.9992%) and CO₂ (≥99.5%) were purchased from *Linde*.

¹H- und ¹³C-NMR-Spectroscopy: Nuclear magnetic resonance spectra were recorded on a *Bruker Avance 300* (300 MHz) and *Bruker Avance 400* (400 MHz). ¹H-NMR: The following abbreviations are used to indicate multiplicities: s = singlet; d = doublet; t = triplet, q = quartet; m = multiplet, dd = doublet of doublet, dt = doublet of triplet, dq = doublet of quartet, ddt = doublet of doublet of quartet. Chemical shift δ is given in ppm to tetramethylsilane.

Fourier-Transformations-Infrared-Spectroscopy (FT-IR): Spectra were recorded on a *Varian Scimitar 1000 FT-IR* with ATR-device. All spectra were recorded at room temperature. Wave number is given in cm⁻¹. Bands are marked as s = strong, m = medium, w = weak and b = broad.

Gas chromatography with FID (GC-FID): HP6890 GC-System with injector 7683B and *Agilent 7820A* System. Column: HP-5, 19091J-413 (30 m × 0.32 mm × 0.25 μ m), carrier gas: N₂. GC-FID was used for reaction control and catalyst screening (Calibration with internal standard *n*-pentadecane and analytically pure samples).

Gas chromatography with mass-selective detector (GC-MS): *Agilent 6890N* Network GC-System, mass detector 5975 MS. Column: HP-5MS (30m × 0.25 mm × 0.25 μ m, 5%

phenylmethylsiloxane, carrier gas: H₂. Standard heating procedure: 50 °C (2 min), 25 °C/min -> 300 °C (5 min)

High resolution mass spectrometry (HRMS): The spectra were recorded by the Central Analytics Lab at the Department of Chemistry, University of Regensburg, on a MAT SSQ 710 A from Finnigan

Inductively coupled plasma optical emission spectrometry (ICP-OES): ICP-OES measurements were taken on a Spectro Analytical Instruments ICP Modula EOP.

3.5.2 General hydrogenation procedures

Preparation of precatalyst FeCl₃-EtMgCl

A Schlenk flask was charged with a solution of FeCl₃ (0.20 mmol, 33.1 mg) in dry THF (3.6 mL) in a glovebox. Under vigorous stirring EtMgCl in THF (2 M, 0.80 mmol, 0.40 mL) was added dropwise (1 min). The resulting black mixture was stirred at room temperature for 30 min before use.

Hydrogenation of alkynes with [Fe]/IL-3 (Table 3-2)

A 4 mL vial with screw cap and PTFE septum was charged with [BMMIM-CN][NTf₂] (IL-3) (150 µL) and 0.50 mL of the freshly prepared black precatalyst solution in a glove box and the mixture was stirred for 2 min, before THF was evaporated under reduced pressure (oil pump). The vial was transferred back into the glove box, charged with alkyne (0.50 mmol) and dry *n*-heptane (0.50 mL), put into a high pressure reactor, punctured with a short needle and the reactor was sealed. The reactor was purged three times with H₂ and pressurized with 52-55 bar of H₂, heated to 80 °C by a heating jacket (giving a pressure of 60 ± 2 bar) and stirred with an external magnetic stirrer for 2 d. The reactor was then cooled and depressurized, the vial removed, the heptane phase separated by decantation and the catalyst phase washed two more times with 1 mL *n*-heptane. The product mixture was analyzed by GC and ¹H-NMR.

Hydrogenation of alkynes with [Fe]/IL-1/Additive (Table 3-3, Table 3-4)

A 4 mL vial with screw cap and PTFE septum was charged with [BMMIM][NTf₂] (IL-1) (150 µL) and 0.50 mL of the freshly prepared black precatalyst solution in a glove box and the mixture was stirred for 2 min before THF was evaporated under reduced pressure (oil pump). The vial was transferred back into the glove box, charged with alkyne (0.50 mmol), dry acetonitrile (0.50 mmol) and dry *n*-heptane (0.50 mL), put into a high pressure reactor, punctured with a short needle and the reactor was sealed. The reactor was purged three times with H₂ and pressurized with 52-55 bar of H₂, heated to 80 °C by a heating jacket (giving a pressure of 60 ± 2 bar) and stirred with an external magnetic stirrer for 20 h. The reactor was then cooled and depressurized, the vial removed, the

heptane phase separated by decantation and the catalyst phase washed two more times with *n*-heptane (1 mL). The product mixture was analyzed by GC and $^1\text{H-NMR}$.

Quantifications via $^1\text{H-NMR}$ were performed vs. hexamethyldisiloxane as internal reference. For identification of the *E/Z* stereochemistry of the alkenes, their characteristic vinyl signals were analyzed and compared to literature.

Hydrogenation of alkynes with $\text{Fe}[\text{N}(\text{SiMe}_3)_2]_2\text{-LiAlH}_4$ in absence of IL (Table 3-6)

A 4 mL vial with screw cap and PTFE septum was charged with a solution of $\text{Fe}[\text{N}(\text{SiMe}_3)_2]_2$ in DME (0.5 mL, 0.025 mmol, 50 mM) in a glove box. A freshly prepared suspension of LiAlH_4 in DME (0.5 mL, 0.025 mmol, 50 mM) was added dropwise and the resulting black reaction mixture was stirred for 30 minutes. The vial was charged with alkyne (0.50 mmol), placed in a high pressure reactor and punctured with a short needle, and the reactor was sealed. The reactor was purged three times with dihydrogen and pressurized with 45 bar of H_2 and 5 bar of CO_2 , heated to 80 °C by a heating jacket (giving a pressure of 53 ± 2 bar) and stirred with an external magnetic stirrer for 18 h. The reactor was then cooled and depressurized, the vial removed and quenched with an aqueous solution of NaHCO_3 (1 mL). After extraction with ethyl acetate (1 mL), the product mixture was analyzed by quantitative GC-FID.

The $\text{Fe}[\text{N}(\text{SiMe}_3)_2]_2\text{-DiBAIH}$ catalyst was synthesized by using a solution of DiBAIH in toluene (0.5 mL, 0.05 mmol, 100 mM) instead.

Hydrogenation with 10 mol% CO_2 were conducted in a *COware* two-chamber system with reaction mixture (chamber A) and 15 mol% NaHCO_3 with 10 mol% *p*-toluenesulfonic acid (chamber B). The mixtures were frozen in liquid dinitrogen, then DMF (0.5 mL) was added (chamber B). The reactor was pumped down and thawed under H_2 atmosphere.

3.5.3 Mechanistic experimental details

Recycling experiments

For the recycling experiments, the general protocol of the hydrogenation of alkynes with $[\text{Fe}]/\text{IL-1}/\text{MeCN}$ was applied using diphenylacetylene. Reaction mixture was stirred for 24 h at 60 bar H_2 and 80 °C instead of 20 h. Then, the catalyst phase was extracted with *n*-heptane (3×0.5 mL) in a glove box. The combined organic layers were analyzed by GC-FID und GC-MS. The catalyst phase was charged again with acetonitrile (0.50 mmol, 26 μL), diphenylacetylene (0.5 mmol, 89.1 mg) and 0.5 mL *n*-heptane and transferred to the high pressure reactor for the next hydrogenation run.

Reaction of IL-1 and IL-3 with EtMgCl

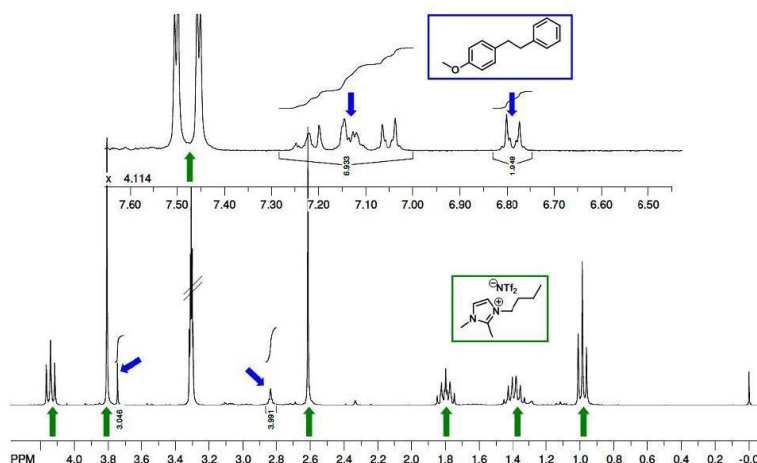
The ionic liquids IL-1 and IL-3 were tested in the reaction with EtMgCl for determination of side products. A 4 mL flask was charged with IL-1 or IL-3 (0.5 mmol, 150 μL) and

EtMgCl in THF (2 M in THF, 0.5 mmol, 0.25 mL) under argon atmosphere. The reaction mixture was stirred for 30 min, quenched with D₂O and dried (oil pump). The reaction mixture was analyzed by ESI-MS, ¹H-NMR and ²H-NMR.

Analysis of IL-1 after hydrogenation

To check if missing product after decantation and extraction of the catalyst phase (IL) is due to trapped residues of product in the IL, a ¹H-NMR of the IL after hydrogenation of 1-methoxy-4-(phenylethynyl) benzene with [Fe]/IL-1 was measured.

To that end, a small amount of the catalyst phase was diluted in MeOH-d₄ and filtered through a layer of celite (in a pipette) directly into the NMR tube.



Scheme 3-4. ¹H-NMR of IL-1 after hydrogenation of 1-methoxy-4-(phenylethynyl) benzene.

TEM-Analysis

A sample of the corresponding catalyst embedded in IL was dispersed in abs. THF. The highly diluted suspension was placed in an ultrasound bath for approx. 5 minutes. In a glove box, a small amount of the dispersion was placed on a carbon-coated copper grid and the solvent evaporated at ambient temperature. The particle size distribution was determined using *Lince24e*, by measuring 200-300 particles on the enlarged digital images. TEM measurements have been carried out three weeks after preparation of the samples. During this time, the samples fixed on the copper grid were stored in a glove box under an argon atmosphere.

Selective scavenging with dct

The heterogeneity of the catalyst species was further indicated by experiments in the presence of dibenzo[*a,e*]cyclooctatetraene (dct). Dct selectively binds homogeneous metal species due to its rigid tub-like structure and π -acceptor ability, and is resistant to hydrogenation. No inhibition of catalytic activity was observed in the hydrogenation of diphenylacetylene when dct was added at ~50% conversion. Standard procedure with 5 mol% Fe catalyst solution in 150 μ L IL-1, 0.5 mmol diphenylacetylene, 100 mol% MeCN, 0.5 mL heptane, 0.5 mmol *n*-pentadecane (GC reference). Reaction in a 4 mL vial at 80 °C, 20 bar H₂. After 5 h, the autoclave reactor was cooled and depressurized, transferred into a glovebox (argon) and a sample was taken for quantitative GC-FID analysis (entry 2). Then, 10 mol% (2 equiv. per Fe) dibenzo[*a,e*]cyclooctatetraene (dct) were added, and the reactor again pressurized and heated (20 bar, 80 °C). After another 3h, the sampling procedure was repeated (entry 4). A parallel reaction was run in a separate vial under identical conditions inside the same autoclave reactor but without addition of dct (entries 1 and 3). No hydrogenation of dct was observed after 8 h.

Table 3-7: Selective scavenging with dct.

$ \begin{array}{ccc} \text{Ph} \text{---} \text{C} \equiv \text{C} \text{---} \text{Ph} & \xrightarrow[\substack{20 \text{ bar H}_2, 80 \text{ }^\circ\text{C}, 16 \text{ h} \\ \text{heptane/IL-1} \\ 100 \text{ mol\% MeCN}}]{5 \text{ mol\% [Fe]}} & \text{Ph} \text{---} \text{CH} = \text{CH} \text{---} \text{Ph} + \text{Ph} \text{---} \text{CH}_2 \text{---} \text{CH}_2 \text{---} \text{Ph} \\ \mathbf{1} & & \mathbf{2} \qquad \qquad \mathbf{3} \end{array} $				
Entry	Conditions	Conversion in % ^a	2 in % ^a	Z / E (2) ^c
1	after 5 h	72	49	96 / 4
2	after 5 h	71	50	96 / 4
3	after 8 h	81	60	97 / 3
4	with dct, after 8 h	79	59	97 / 3

^a quantitative GC-FID vs. *n*-pentadecane as internal reference.

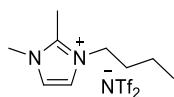
3.5.4 Synthesis of starting material

General procedure of ionic liquid synthesis

A 25 mL flask was charged with freshly distilled 1,2-dimethylimidazole (20.0 mmol, 1.92 g) and heated to 90 °C. 1-Chlorobutane (20.0 mmol, 2.09 mL) was added slowly and the reaction mixture was stirred at 90 °C for 5 days. For completion of the reaction 1-chlorobutane (1.00 mmol, 105 μ L) was added and the mixture was stirred for another 3 days. Then, LiNTf₂ (14.5 mmol, 4.16 g) and dist. H₂O (7.25 mL) were added and the mixture was stirred at room temperature for 12 h. The aqueous phase was removed and the organic phase washed with dist. H₂O (2 \times 4 mL) and dried at 130 °C for 3 days (oil pump).

[BMMIm][NTf₂] IL-1

Synthesis following the general procedure of ionic liquid synthesis.



C₁₁H₁₇F₆N₃O₄S₂

433.39 g/mol

Appearance

colorless liquid

Yield

6.24 g, 14.4 mmol (72%)

¹H-NMR

(400 MHz, MeOD) δ 7.49 (d, J = 2.0 Hz, 1H), 7.44 (d, J = 2 Hz, 1H), 4.13 (t, J = 7.4 Hz, 2H), 3.80 (s, 3H), 2.61 (s, 3H), 1.87–1.70 (m, 2H), 1.39 (m, 2H), 0.99 (t, J = 7.4 Hz, 3H).

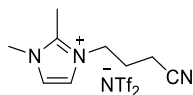
¹³C-NMR

(101 MHz, MeOD) δ 145.8, 126.0, 123.6, 122.9, 122.2, 119.7, 116.5, 35.5, 32.8, 20.5, 13.9, 9.6.

Analytical data were in full agreement with F. F. Bazito, Y. Kawano, R. M. Torresi, *Electrochim. Acta* **2007**, 52, 6427–6437.

[BMMIm-CN][NTf₂] IL-3

Synthesis following the general procedure of ionic liquid synthesis.



C₁₁H₁₄F₆N₄O₄S₂

444.37 g/mol

Appearance

yellow liquid

Yield

864 mg, 1.94 mmol (78%)

¹H-NMR	(400 MHz, MeOD) δ 7.56–7.42 (m, 2H), 4.26 (t, J = 7.2 Hz, 2H), 3.81 (s, 3H), 2.64 (s, 3H), 2.57 (t, J = 7.2 Hz, 2H), 2.18 (dt, J = 7.2 Hz, 2H).
¹³C-NMR	(101 MHz, MeOD) δ 146.4, 124.1, 122.9, 122.2, 120.0, 119.7, 48.0, 35.6, 26.6, 14.6, 9.7.

Analytical data were in full agreement with Z. Fei, D. Zhao, D. Pieraccini, W. H. Ang, T. J. Geldbach, R. Scopelliti, C. Chiappe, P. J. Dyson, *Organometallics* **2007**, *26*, 1588–1598.

General procedures for alkyne synthesis:

Method A

A 10 mL glass tube equipped with a stirring bar was charged with CuI (0.2 mmol, 38 mg), PPh₃ (0.4 mmol, 104 mg), Bu₄NBr (2.00 mmol, 644 mg), K₂CO₃ (4.00 mmol, 525 mg), aryl iodide (2.00 mmol) and deionized water (3 mL). The suspension was stirred at r.t. for 1 min. Then, phenylacetylene (3.00 mmol, 330 μ L) was added via syringe. The reaction vessel was purged with argon, sealed and placed into the microwave. The temperature was ramped to 120 °C within 1 min and then held at this temperature for 20 to 60 min. The reaction mixture was extracted with ethyl acetate (3 \times 10 mL), the combined organic layers were dried (MgSO₄) and the solvent removed by vacuum evaporation. The residue was then purified by silica gel column chromatography (*n*-pentane/dichloromethane).

Method B

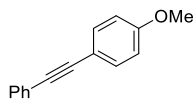
A 50 mL *Schlenk* tube with a screw cap was equipped with a stirring bar, charged with CuI (1.00 mmol, 190 mg), PPh₃ (2 mmol, 0.525 g) and KOH (20 mmol, 1.122 g), evacuated three times and purged with nitrogen. Then, deionized water (20 mL) was added. The suspension was stirred at r.t. for 10 min. Then, aryl iodide (10 mmol) and phenylacetylene (13 mmol, 1.328 g) were added via syringe. The reaction vessel was purged with nitrogen, sealed and stirred at 120 °C for 24 h. The reaction mixture was extracted with Et₂O (4 \times 20 mL), the combined organic layers were dried (MgSO₄) and the solvent removed by vacuum evaporation. The residue was then purified by silica gel column chromatography (*n*-pentane or *n*-pentane/dichloromethane).

Method C

A 50 mL *Schlenk* tube with a screw cap was equipped with a stirring bar, charged with CuI (0.14 mmol, 27.0 mg), Pd(Cl)₂(PPh₃)₂ (0.04 mmol, 25.2 mg) and the substituted iodobenzene (3.59 mmol), evacuated three times and purged with nitrogen. Then THF (4 mL) and Et₃N (4 mL) were added. Phenylacetylene (3.59 mmol, 395 μ L) was added slowly via syringe and the reaction mixture was stirred at room temperature for 15 h. Then, CH₂Cl₂ (25 mL) and aqueous HCl (25 mL, 1 M) were added and the reaction

mixture was extracted with CH_2Cl_2 (2×25 mL). The combined organic layers were dried (Na_2SO_4) and the solvent removed by vacuum evaporation. The residue was then purified by silica gel column chromatography (hexanes/ethyl acetate).

1-Methoxy-4-(phenylethynyl)benzene (Method A)



$\text{C}_{15}\text{H}_{12}\text{O}$

208.26 g/mol

Appearance

colorless solid

Yield

1.61 g, 7.71 mmol (77%)

TLC

$R_f = 0.29$ (SiO_2 , *n*-pentane/ CH_2Cl_2 9/1)

$^1\text{H-NMR}$

(300 MHz, CDCl_3) δ 7.49 (m, 4H), 7.33 (d, $J = 6.1$ Hz, 3H), 6.88 (d, $J = 8.6$ Hz, 2H), 3.83 (s, 3H).

$^{13}\text{C-NMR}$

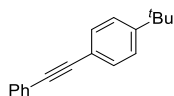
(75 MHz, CDCl_3) δ 159.60, 133.05, 131.44, 128.30, 127.92, 123.59, 115.37, 113.99, 89.36, 88.06, 55.31.

GC-MS

$t_R = 9.80$ min, (EI, 70 eV): $m/z = 208$ [M^+].

Analytical data were in full agreement with D. Yang, B. Li, H. Yang, H. Fu, L. Hu, *Synlett* **2011**, 5, 702-706.

1-*tert*-Butyl-4-(phenylethynyl)benzene (Method B)



$\text{C}_{18}\text{H}_{18}$

234.34 g/mol

Appearance

colorless solid

Yield

2.24 g, 9.54 mmol (95%)

TLC

$R_f = 0.44$ (SiO_2 , *n*-pentane)

$^1\text{H-NMR}$

(300 MHz, CDCl_3) δ 7.56-7.44 (m, 4H), 7.40-7.30 (m, 5H), 1.33 (s, 9H).

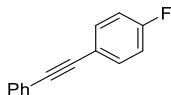
$^{13}\text{C-NMR}$

(75 MHz, CDCl_3) δ 151.55, 131.59, 131.34, 128.32, 128.08, 125.37, 123.52, 120.24, 89.53, 88.73, 34.81, 31.20.

GC-MS

$t_R = 10.27$ min, (EI, 70 eV): $m/z = 234$ [M^+].

Analytical data were in full agreement with J. Moon, M. Jeong, H. Nam, J. Ju, J. H. Moon, H. M. Jung, S. Lee, *Org. Lett.* **2008**, *10*, 945-948.

1-Fluoro-4-(phenylethynyl)benzene (Method B) $C_{14}H_9F$

196.22 g/mol

Appearance

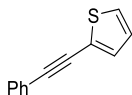
colorless solid

Yield

1.75 g, 8.93 mmol (89%)

TLC $R_f = 0.55$ (SiO_2 , *n*-pentane) **1H -NMR**(300 MHz, $CDCl_3$) δ 7.49-7.38 (m, 4H), 7.31-7.22 (m, 3H), 7.03-6.91 (m, 2H). **^{13}C -NMR**(75 MHz, $CDCl_3$) δ 164.16, 160.86, 133.55, 133.44, 131.57, 128.39, 128.35, 123.09, 119.40, 119.35, 115.80, 115.51, 89.05, 88.29.**GC-MS** $t_R = 8.63$ min, (EI, 70 eV): $m/z = 196$ [M^+].

Analytical data were in full agreement with H. Huang, H. Jiang, K. Chen, H. Liu, *J. Org. Chem.* **2008**, *73*, 9061-9064.

2-(Phenylethynyl)thiophene (Method B) $C_{12}H_8S$

184.26 g/mol

Appearance

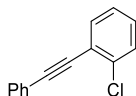
colorless solid

Yield

1.76 g, 9.57 mmol (96%)

TLC $R_f = 0.44$ (SiO_2 , *n*-pentane) **1H -NMR**(300 MHz, $CDCl_3$) δ 7.56-7.47 (m, 2H), 7.38- 7.31 (m, 3H), 7.31- 7.26 (m, 2H), 7.01 (dd, $J = 5.0, 3.8$ Hz, 1H). **^{13}C -NMR**(75 MHz, $CDCl_3$) δ 131.91, 131.43, 128.44, 128.39, 127.27, 127.12, 123.34, 122.94, 93.03, 82.61.**GC-MS** $t_R = 8.84$ min, (EI, 70 eV): $m/z = 184$ [M^+].

Analytical data were in full agreement with H. Huang, H. Jiang, K. Chen, H. Liu, *J. Org. Chem.* **2008**, *73*, 9061-9064.

1-Chloro-2-(phenylethynyl)benzene (Method B)C₁₄H₉Cl

212.67 g/mol

Appearance

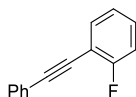
colorless liquid

Yield

1.82 g, 8.53 mmol (85%)

TLC $R_f = 0.50$ (SiO₂, *n*-pentane)**¹H-NMR**(400 MHz, CDCl₃) δ 7.58 (m, 3H), 7.44 (m, 1H), 7.37 (m, 3H), 7.30 – 7.22 (m, 2H).**¹³C-NMR**(101 MHz, CDCl₃) δ . 135.96, 133.24, 131.77, 129.33, 129.27, 128.67, 128.40, 126.48, 123.25, 122.94, 94.56, 86.20.**GC-MS** $t_R = 9.55$ min, (EI, 70 eV): $m/z = 212$ [M⁺].

Analytical data were in full agreement with T. Suzuka, Y. Okada, K. Ooshiro, Y. Uozumi, *Tetrahedron* **2010**, 66, 1064-1069.

1-Fluoro-2-(phenylethynyl)benzene (Method B)C₁₄H₉F

196.22 g/mol

Appearance

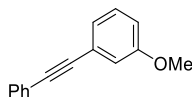
colorless solid

Yield

1.48 g, 7.55 mmol (76%)

TLC $R_f = 0.50$ (SiO₂, *n*-pentane)**¹H-NMR**(300 MHz, CDCl₃) δ 7.62 – 7.48 (m, 3H), 7.40 – 7.26 (m, 4H), 7.17 – 7.06 (m, 2H).**¹³C-NMR**(75 MHz, CDCl₃) δ . 133.45, 131.72, 130.02, 129.92, 128.60, 128.37, 123.99, 123.94, 122.91, 115.69, 115.41, 77.23.**GC-MS** $t_R = 8.70$ min, (EI, 70 eV): $m/z = 196$ [M⁺].

Analytical data were in full agreement with S. Enthaler, M. Haberberger, E. Irran, *Chem. Asian J.* **2011**, 6, 1613-1623.

1-Methoxy-3-(phenylethynyl)benzene (Method B)C₁₅H₁₂O

208.26 g/mol

Appearance

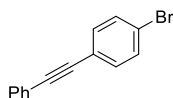
colorless solid

Yield

1.23 g, 5.92 mmol (59%)

TLC R_f = (SiO₂, *n*-pentane/CH₂Cl₂ 9/1)**¹H-NMR**(300 MHz, CDCl₃) δ 7.58 – 7.51 (m, 2H), 7.40 – 7.32 (m, 3H), 7.26 (m, 1H), 7.14 (m, 2H), 7.07 (m, 1H), 3.83 (s, 3H).**¹³C-NMR**(75 MHz, CDCl₃) δ 159.35, 131.65, 129.43, 128.37, 128.33, 124.20, 123.19, 116.32, 114.98, 89.30, 89.20, 55.32.**GC-MS** t_R = 9.90 min, (EI, 70 eV): m/z = 208 [M⁺].

Analytical data were in full agreement with K. G. Thakur, G. Sekar, *Synthesis* **2009**, 16, 2785-2789.

1-Bromo-4-(phenylethynyl)benzene (Method C)C₁₄H₉Br

257.13 g/mol

Appearance

colorless solid

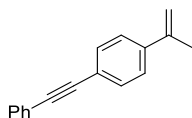
Yield

1.19 g, 4.64 mmol (83%)

TLC R_f = 0.59 (SiO₂, hexanes)**¹H-NMR**(300 MHz, CDCl₃) δ 7.57 – 7.45 (m, 4H), 7.43 – 7.31 (m, 5H).**¹³C-NMR**(75 MHz, CDCl₃) δ 133.04, 131.64, 131.61, 128.54, 128.42, 122.91, 122.49, 122.25, 90.53, 88.33.**GC-MS** t_R = 10.00 min, (EI, 70 eV): m/z = 257 [M⁺], 176, 151, 110, 98, 88, 75, 63, 51.

Analytical data were in full agreement with Che-Hung Lin, Yu-Jen Wang, Chin-Fa Lee, *Eur. J. Org. Chem.*, **2010**, 23, 4368–4371.

1-(Phenylethynyl)-4-(prop-1-en-2-yl)benzene (Method C)



$C_{17}H_{14}$

218.29 g/mol

Appearance

yellow solid

Yield

735 mg, 3.37 mmol (94%)

TLC

$R_f = 0.51$ (SiO₂, hexanes)

¹H-NMR

(300 MHz, CDCl₃) δ 7.59 – 7.42 (m, 6H), 7.40 – 7.31 (m, 3H), 5.43 (m, 1H), 5.14 (m, 1H), 2.16 (dd, $J = 1.4, 0.7$ Hz, 3H).

¹³C-NMR

(75 MHz, CDCl₃) δ 142.54, 140.94, 131.61, 131.50, 128.37, 128.26, 125.44, 123.32, 122.18, 113.25, 89.89, 89.42, 21.66.

GC-MS

$t_R = 10.20$ min, (EI, 70 eV): $m/z = 218$ [M^+], 202, 189, 178, 165, 152, 126, 115, 91, 77, 63, 51.

HRMS

(CI, m/z): found 218.1099 [M^+] (calculated 218.1096).

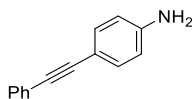
FT-IR

(ATR-film) in [cm⁻¹] 3077 (w), 2943 (w), 2363 (w), 2338 (w), 1961 (w), 1792 (w), 1620 (m), 1593 (m), 1503 (m), 1485(m), 1441 (m), 1403 (m), 1373 (m), 1119 (m), 1070 (m), 892 (s), 839 (s), 753 (s), 689 (s), 631 (m), 492 (s).

Melting point

77 °C

1-Amino-4-(phenylethynyl)benzene (Method C)



$C_{14}H_{11}N$

193.24 g/mol

Appearance

brown solid

Yield

2.35 g, 12.2 mmol (87%)

TLC

$R_f = 0.21$ (SiO₂, hexanes/ethyl acetate 4/1 + 1% Et₃N)

¹H-NMR

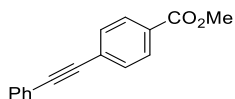
(300 MHz, CDCl₃) δ 7.54 – 7.46 (m, 2H), 7.39 – 7.28 (m, 5H), 6.65 (m, 2H), 3.86 (s, 2H).

^{13}C -NMR (75 MHz, CDCl_3) δ 146.56, 132.99, 131.37, 128.29, 127.69, 123.89, 114.81, 112.71, 90.09, 87.35.

GC-MS $t_R = 10.54$ min, (EI, 70 eV): $m/z = 193$ [M^+], 177, 165, 152, 139, 126, 115, 89, 74, 63, 52.

Analytical data were in full agreement with T. Schabel, C. Belge, B. Plietker, *Org. Lett.*, **2013**, *15*, 2858–2861.

Methyl 4-(phenylethynyl)benzoate (Method C)



$\text{C}_{16}\text{H}_{12}\text{O}_2$

236.27 g/mol

Appearance pale yellow solid

Yield 1.35 g, 5.71 mmol (82%)

TLC $R_f = 0.38$ (SiO_2 , hexanes/ethyl acetate = 9/1)

^1H -NMR (300 MHz, CDCl_3) δ 8.02 (m, 2H), 7.60 (m, 1H), 7.59 – 7.51 (m, 3H), 7.41 – 7.32 (m, 3H), 3.92 (s, 3H).

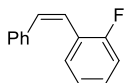
^{13}C -NMR (75 MHz, CDCl_3) δ 166.57, 131.76, 131.53, 129.55, 129.47, 128.80, 128.47, 128.02, 122.71, 92.40, 88.67, 52.26.

GC-MS $t_R = 10.59$ min, (EI, 70 eV): $m/z = 236$ [M^+], 205, 176, 151, 126, 102, 91, 76, 63, 51.

Analytical data were in full agreement with T. Schabel, C. Belger, B. Plietker, *Org. Lett.* **2013**, *15*, 2858–2861.

3.5.5 Hydrogenation products

(Z)-2-Fluoro stilbene



$\text{C}_{14}\text{H}_{11}\text{F}$

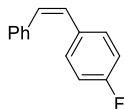
198.24 g/mol

^1H -NMR (400 MHz, CDCl_3) δ 7.33–7.21 (m, 7H), 7.13–7.05 (m, 1H), 6.99 (m, 1H), 6.79 (d, $J = 12.3$ Hz, 1H), 6.69 (d, $J = 12.3$ Hz, 1H).

GC-MS $t_R = 7.96$ min, (EI, 70 eV): m/z 198 [M^+], 183, 177, 170, 152, 144, 133, 120, 107, 98, 89, 75, 63.

Analytical data were in full agreement with J. Li, R. Hua, T. Liu, *J. Org. Chem.* **2010**, 75, 2966–2970.

(Z)-4-Fluoro stilbene



$C_{14}H_{11}F$

198.24 g/mol

1H -NMR

(300 MHz, $CDCl_3$) δ 7.23–7.17 (m, 7H), 6.92–6.85 (m, 2H), 6.58 (d, $J = 12.25$ Hz, 1H), 6.52 (d, $J = 12.25$ Hz, 1H).

^{13}C -NMR

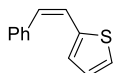
(75 MHz, $CDCl_3$) δ 161.74, 136.98, 133.13, 130.48, 130.21, 129.02, 128.78, 128.27, 127.15, 115.10.

GC-MS

$t_R = 7.98$ min, (EI, 70 eV): m/z 198 [M^+].

Analytical data were in full agreement with F. Luo, C. Pan, W. Wang, Z. Yea, J. Cheng, *Tetrahedron* **2010**, 66, 1399–1403.

(Z)-2-Styryl thiophene



$C_{12}H_{10}S$

186.27 g/mol

1H -NMR

(300 MHz, $CDCl_3$) δ 7.35–7.28 (m, 5H), 7.07 (d, $J = 5$ Hz, 1H), 6.96 (d, $J = 3.3$ Hz, 1H), 6.87 (dd, $J = 5$ Hz, 3.7 Hz, 1H), 6.69 (d, $J = 12$ Hz, 1H), 6.56 (d, $J = 12$ Hz, 1H).

^{13}C -NMR

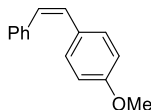
(75 MHz, $CDCl_3$) δ 139.72, 137.30, 128.82, 128.77, 128.49, 128.13, 127.48, 26.38, 125.48, 123.32.

GC-MS

$t_R = 8.21$ min, (EI, 70 eV): m/z 186 [M^+].

Analytical data were in full agreement with M. K. Deliomeroglu, C. Dengiz, R. Çalişkan, M. Balci, *Tetrahedron* **2012**, 68, 5838–5844.

(Z)-4-Methoxy stilbene



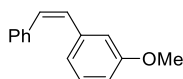
$C_{15}H_{14}O$

210.27 g/mol

$^1\text{H-NMR}$	(300 MHz, CDCl_3) δ 7.28 (m, 7H), 6.82 – 6.74 (m, 2H), 6.55 (m, 2H), 3.80 (s, 3H).
$^{13}\text{C-NMR}$	(75 MHz, CDCl_3) δ 158.70, 137.65, 130.20, 129.81, 128.86, 128.79, 128.37, 128.28, 126.95, 113.62, 55.22.
GC-MS	t_R = 9.27 min, (EI, 70 eV): m/z = 210 [M^+], 195, 179, 165, 152, 139, 128, 115, 102, 89, 77, 63, 51.

Analytical data were in full agreement with T. Schabel, C. Belge, B. Plietker, *Org. Lett.*, **2013**, 15, 2858–2861.

(Z)-3-Methoxy stilbene



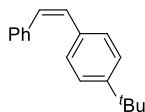
$\text{C}_{15}\text{H}_{14}\text{O}$

210.27 g/mol

$^1\text{H-NMR}$	^1H NMR (300 MHz, CDCl_3) δ 7.64 – 7.51 (m, 2H), 7.32 – 7.25 (m, 4H), 7.11 (dd, J = 2.7, 1.4 Hz, 1H), 6.90 – 6.82 (m, 2H), 6.71 – 6.56 (m, 2H), 3.67 (s, 3H).
$^{13}\text{C-NMR}$	(75 MHz, CDCl_3) δ 159.40, 138.58, 137.30, 130.53, 130.19, 129.28, 128.96, 128.27, 127.20, 121.56, 113.76, 113.35, 55.04.
GC-MS	t_R = 9.07 min, (EI, 70 eV): m/z = 210 [M^+], 194, 179, 165, 152, 139, 128, 115, 102, 89, 77, 63, 51.

Analytical data were in full agreement with J. C. Roberts, J. A. Pincock, *J. Org. Chem.*, **2004**, 69, 4279–4282.

(Z)-4-*tert*-Butyl stilbene



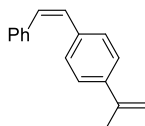
$\text{C}_{18}\text{H}_{20}$

236.35 g/mol

$^1\text{H-NMR}$	(300 MHz, CDCl_3) δ 7.29 (ddd, J = 6.3, 5.4, 4.5 Hz, 4H), 7.25 – 7.19 (m, 5H), 6.58 (s, 2H), 1.32 (s, 9H).
$^{13}\text{C-NMR}$	(75 MHz, CDCl_3) δ 150.19, 137.63, 134.21, 130.12, 129.61, 128.85, 128.62, 128.25, 127.00, 125.12, 34.59, 31.32.
GC-MS	t_R = 9.43 min, (EI, 70 eV): m/z = 236 [M^+], 221, 202, 193, 178, 165, 152, 143, 128, 115, 91, 77, 63, 51.

HRMS	(CI, m/z): found 234.1408 [M^+] (calculated 234.1409).
FT-IR	(ATR-film) in [cm^{-1}] 3014 (w), 2961 (m), 2868 (w), 1599 (w), 1509 (m), 1447 (m), 1363 (m), 1269 (m), 1200 (w), 1106 (w), 1073 (w), 1027 (w), 908 (s), 874 (m), 830 (m), 781 (s), 732 (s), 699 (s), 575 (s), 530 (m).

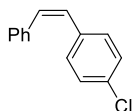
(Z)-1-(prop-1-en-2-yl)-4-styrylbenzene



$\text{C}_{17}\text{H}_{16}$
220.31 g/mol

$^1\text{H-NMR}$	(300 MHz, CDCl_3) δ 7.43 – 7.20 (m, 9H), 6.66 (d, $J = 12.3$ Hz, 1H), 6.61 (d, $J = 12.4$ Hz, 1H), 5.43 (s, 1H), 5.15 – 5.06 (m, 1H), 2.17 (s, 3H).
$^{13}\text{C-NMR}$	(75 MHz, CDCl_3) δ 142.76, 139.75, 137.42, 136.39, 130.30, 129.92, 128.92, 128.86, 128.33, 127.18, 125.30, 112.35, 21.74.
GC-MS	$t_R = 9.52$ min, (EI, 70 eV): $m/z = 220$ [M^+], 205, 191, 179, 165, 152, 127, 115, 91, 77, 95, 50.
HRMS	(CI, m/z): found 220.1254 [M^+] (calculated 220.1252).
FT-IR	(ATR-film) in [cm^{-1}] 3083 (w), 3011 (w), 2924 (w), 1626 (m), 1508 (m), 1446 (m), 1374 (m), 1310 (w), 1120 (w), 1073 (w), 890 (s), 874 (s), 836 (s), 797 (m), 733 (s), 694 (s), 647 (w), 567 (w).

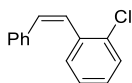
(Z)-4-Chloro stilbene



$\text{C}_{14}\text{H}_{11}\text{Cl}$
214.69 g/mol

$^1\text{H-NMR}$	(300 MHz, CDCl_3) δ 7.29–7.12 (m, 9H), 6.65 (d, $J = 12.2$ Hz, 1H), 6.54 (d, $J = 12.2$ Hz, 1H).
GC-MS	$t_R = 8.95$ min, (EI, 70 eV): m/z 214 [M^+], 179, 152, 139, 126, 113, 102, 89, 76, 63, 51.

Analytical data were in full agreement with V. K. Aggarwal, J. R. Fulton, C. G. Sheldon, J. de Vicente, *J. Am. Chem. Soc.* **2003**, *125*, 6034–6035.

(Z)-2-Chloro stilbene $C_{14}H_{11}Cl$

214.69 g/mol

 1H -NMR

(400 MHz, $CDCl_3$) δ 7.41 (d, $J = 8.0$ Hz, 1H), 7.23–7.12 (m, 7H), 7.04 (td, $J = 7.6, 1.0$ Hz, 1H), 6.73 (d, $J = 12.2$ Hz, 1H), 6.68 (d, $J = 12.2$ Hz, 1H).

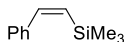
GC-MS

$t_R = 8.78$ min, (EI, 70 eV): m/z 214 [M^+], 179, 152, 139, 126, 113, 101, 89, 76, 63, 51.

Analytical data were in full agreement with D.-J. Dong, H.-H. Li, S.-K. Tian, *J. Am. Chem. Soc.* **2010**, 132, 5018–5020.

(Z)-Trimethyl(styryl)silane

Because of signal overlay in the 1H -NMR spectrum only characteristic vinyl signals are noted.

 $C_{11}H_{16}Si$

176.33 g/mol

 1H -NMR

(400 MHz, $CDCl_3$) δ 7.44 (dd, $J = 15.1, 1.4$ Hz, 1H), 5.91 (dd, $J = 15.1, 1.8$ Hz, 1H).

GC-MS

$t_R = 5.92$ min, (EI, 70 eV): m/z 176 [M^+], 161, 145, 135, 115, 77, 59, 51.

Analytical data were in full agreement with Y. Nishihara, D. Saito, K. Tanemura, S. Noyori, K. Takagi, *Org. Lett.* **2009**, 11, 3546–3549.

(Z)-But-1-ene-1-yl-benzene $C_{10}H_{12}$

132.20 g/mol

 1H -NMR

(400 MHz, $CDCl_3$) δ 7.40–7.31 (m, 4H), 7.26 (t, $J = 7.0$ Hz, 1H), 6.46 (d, $J = 11.6$ Hz, 1H), 5.71 (dt, $J = 11.6, 7.4$ Hz, 1H), 2.48–2.36 (m, 2H), 1.13 (t, $J = 7.4$ Hz, 3H).

GC-MS $t_R = 5.28$ min, (EI, 70 eV): m/z 132 [M^+], 115, 104, 91, 77, 65, 51.

Analytical data were in full agreement with E. H. P. Tan, G. C. Lloyd-Jones, J. N. Harvey, A. J. J. Lennox, B. M. Mills, *Angew. Chem. Int. Ed.* **2011**, 50, 9602–9606.

(Z)-Methyl cinnamate

Because of signal overlay in the 1H -NMR spectrum only characteristic vinyl signals are noted.



1H -NMR (300 MHz, $CDCl_3$) δ 6.95 (d, $J = 12.6$ Hz, 1H), 5.94 (d, $J = 12.6$ Hz, 1H).

GC-MS $t_R = 6.76$ min, (EI, 70 eV): m/z 162 [M^+], 131, 109, 91, 77, 63, 51.

Analytical data were in full agreement with C. Belger, N. M. Neisius, B. Plietker, *Chem. Eur. J.* **2010**, 16, 12214–12220.

(Z)-6-Dodecene



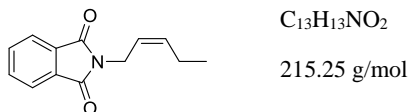
1H -NMR (400 MHz, $CDCl_3$) δ 5.36–5.20 (m, 2H), 1.94 (m, 4H), 1.27 (m, 12H), 0.82 (m, 6H).

GC-MS $t_R = 5.90$ min, (EI, 70 eV): m/z 168 [M^+], 140, 125, 111, 97, 83, 69, 55.

Analytical data were in full agreement with T. Hamatani, S. Matsubara, H. Matsuda, M. Schlosser, *Tetrahedron* **1988**, 44, 2875–2881.

(Z)-N-(Pent-2-ene-1-yl)phthalimide

Because of signal overlay in the 1H -NMR spectrum only characteristic vinyl signals are noted.

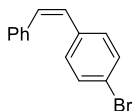


$^1\text{H-NMR}$ (300 MHz, CDCl_3) δ 5.58 (dt, $J = 10.7, 7.3$ Hz, 1H), 5.42 (dt, $J = 10.7, 7.0$ Hz, 1H).

GC-MS $t_R = 9.21$ min, (EI, 70 eV): m/z 215 [M^+], 186, 160, 148, 130, 104, 76, 67, 50.

Analytical data were in full agreement with C. Germon, A. Alexakis, J. F. Normant, *Synthesis* **1984**, 40, 40–43.

(Z)-4-Bromo stilbene



$\text{C}_{14}\text{H}_{11}\text{Br}$

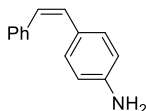
259.14 g/mol

$^1\text{H-NMR}$ (300 MHz, CDCl_3) δ 7.33 (d, $J = 8.4$ Hz, 2H), 7.25 – 7.20 (m, 5H), 7.10 (d, $J = 8.5$ Hz, 2H), 6.63 (d, $J = 12.2$ Hz, 1H), 6.49 (d, $J = 12.2$ Hz, 1H).

GC-MS $t_R = 9.44$ min, (EI, 70 eV): $m/z = 258$ [M^+], 179, 152, 126, 102, 89, 76, 63, 51.

Analytical data were in full agreement with T. Schabel, C. Belge, B. Plietker, *Org. Lett.* **2013**, 15, 2858–2861.

(Z)-4-Amino stilbene



$\text{C}_{14}\text{H}_{13}\text{N}$

195.26 g/mol

$^1\text{H-NMR}$ (300 MHz, CDCl_3) δ 7.32 (dd, $J = 8.1, 1.3$ Hz, 2H), 7.29 – 7.16 (m, 3H), 7.12 – 7.04 (m, 2H), 6.56 – 6.50 (m, 2H), 6.50 (d, $J = 12.2$ Hz, 1H), 6.44 (d, $J = 12.2$ Hz, 1H), 3.61 (s, 2H).

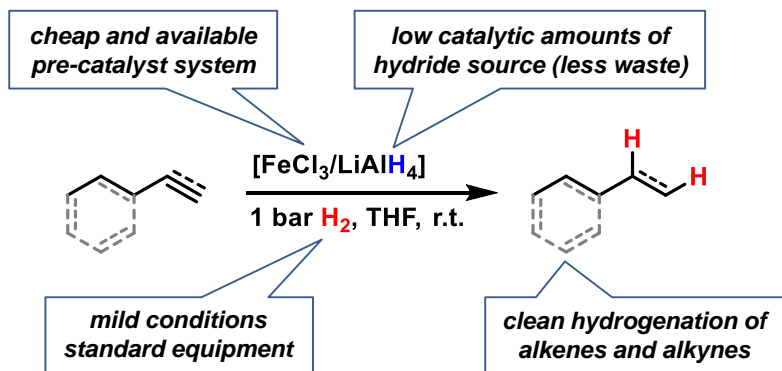
GC-MS $t_R = 9.76$ min, (EI, 70 eV): $m/z = 195$ [M^+], 180, 165, 152, 139, 117, 106, 89, 77, 65, 51.

Analytical data were in full agreement with T. Schabel, C. Belge, B. Plietker, *Org. Lett.* **2013**, 15, 2858–2861.

3.6 References

- [1] a) G. Ertl, *Catal. Rev. Sci. Eng.*, **1980**, *21*, 201-223; b) G. P. van der Laan and A. A. C. M. Beenackers, *Catal. Rev. Sci. Eng.*, **1999**, *41*, 255-318.
- [2] a) C. Bolm, J. Legros, J. Le Paih and L. Zani, *Chem. Rev.*, **2004**, *104*, 6217-6254; b) W. M. Czaplik, M. Mayer, J. Cvengros and A. Jacobi von Wangelin, *ChemSusChem*, **2009**, *2*, 396-407.
- [3] a) S. C. Bart, E. Lobkovsky and P. J. Chirik, *J. Am. Chem. Soc.*, **2004**, *126*, 13794-13807; b) R. J. Trovitch, E. Lobkovsky, E. Bill and P. J. Chirik, *Organometallics*, **2008**, *27*, 1470-1478; c) P. H. Phua, L. Lefort, J. A. F. Boogers, M. Tristany and J. G. de Vries, *Chem. Commun.*, **2009**, 3747-3749; d) M. Stein, J. Wieland, P. Steurer, F. Tölle, R. Mülhaupt and B. Breit, *Adv. Synth. Catal.*, **2011**, *353*, 523-527; e) A. Welther, M. Bauer, M. Mayer and A. Jacobi von Wangelin, *ChemCatChem*, **2012**, *4*, 1088-1093; f) V. Kelsen, B. Wendt, S. Werkmeister, K. Junge, M. Beller and B. Chaudret, *Chem. Commun.*, **2013**, 3416-3418.
- [4] H. Lindlar, *Helv. Chim. Acta*, **1952**, *35*, 446-450.
- [5] a) S. Enthaler, M. Haberberger and E. Irran, *Chem. Asian J.*, **2011**, *6*, 1613-1623; b) L. Ilies, T. Yoshida and E. Nakamura, *J. Am. Chem. Soc.*, **2012**, *134*, 16951-16954; c) C. Belger and B. Plietker, *Chem. Commun.*, **2012**, 5419-5421.
- [6] *Catalyst Separation, Recovery and Recycling*, eds. D. J. Cole-Hamilton, R. P. Tooze, Springer, Dordrecht, **2006**.
- [7] a) D. L. Huber, *Small*, **2005**, *1*, 485-501; b) A. Welther and A. Jacobi von Wangelin, *Curr. Org. Chem.*, **2013**, *17*, 326-335; c) R. Hudson, G. Hamasaka, T. Osako, Y. M. A. Yamada, C.-J. Li, Y. Uozumi and A. Moores, *Green Chem.*, **2013**, *15*, 2141-2148.
- [8] a) T. Welton, *Chem. Rev.*, **1999**, *99*, 2071-2084; b) N V. Plechkova and K. R. Seddon, *Chem. Soc. Rev.*, **2008**, *37*, 123-150; c) C. Vollmer and C. Janiak, *Coord. Chem. Rev.*, **2011**, *255*, 2039-2057; d) P. S. Campbell, M. H. G. Precht, C. C. Santini, P. H. Haumesser, *Curr. Org. Chem.*, **2013**, *17*, 414-429; e) M. H. G. Precht, J. D. Scholten and J. Dupont, *Molecules*, **2010**, *15*, 3441-3461.
- [9] a) C. Janiak, *Z. Naturforsch. B*, **2013**, *68*, 1056-1089; b) J. D. Scholten, B. C. Leal and J. Dupont, *ACS Catal.*, **2012**, *2*, 184-200; c) K. L. Luska and A. Moores, *ChemCatChem*, **2012**, *4*, 1534-1546; d) M. H. G. Precht, M. Scariot, J. D. Scholten, G. Machado, S. R. Teixeira and J. Dupont, *Inorg. Chem.*, **2008**, *47*, 8995-9001; e) R. Venkatesan, M. H. G. Precht, J. D. Scholten, R. P. Pezzi, G. Machado and J. Dupont, *J. Mater. Chem.*, **2011**, *21*, 3030-3036.
- [10] a) W. Zhu and Z. Hou, *Curr. Inorg. Chem.*, **2013**, *2*, 213-227; b) V. I. Parvulescu and C. Hardacre, *Chem. Rev.*, **2007**, *107*, 2615-2665; c) M. H. G. Precht, J. D. Scholten and J. Dupont, *J. Mol. Catal. A*, **2009**, *313*, 74-78; d) H. Wender, P. Migowski, A. F. Feil, L. F. de Oliveira, M. H. G. Precht, R. Leal, G. Machado, S. R. Teixeira and J. Dupont, *PhysChemChemPhys*, **2011**, *13*, 13552-13557.
- [11] D. Bézier, J.-B. Sortais and C. Darcel, *Adv. Synth. Catal.*, **2013**, *355*, 19-33.
- [12] R. Giernoth and D. Bankmann, *Eur. J. Org. Chem.*, **2008**, *17*, 2881-2886.
- [13] C. E. I. Knappke, J. M. Neudörfel and A. Jacobi von Wangelin, *Org. Biomol. Chem.*, **2010**, *8*, 1695-1705.
- [14] Fe-catalysed dehalogenation: W. M. Czaplik, S. Grupe, M. Mayer and A. Jacobi von Wangelin, *Chem. Commun.*, **2010**, 46, 6350-6352.
- [15] D. R. Anton and R. H. Crabtree, *Organometallics*, **1983**, *2*, 855-859.

4 Iron-catalyzed olefin hydrogenation at 1 bar H₂ with a FeCl₃-LiAlH₄ catalyst^{i,ii}



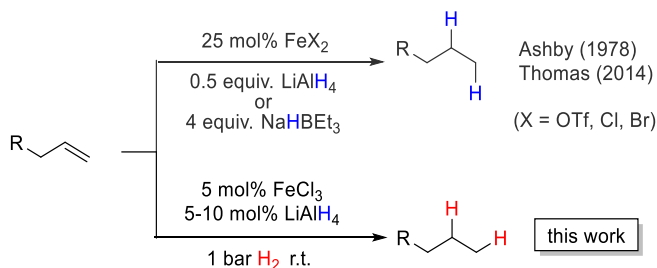
The scope and mechanism of a practical protocol for the iron-catalyzed hydrogenation of alkenes and alkynes at 1 bar H₂ pressure were studied. The catalyst is formed from cheap chemicals (5 mol% FeCl₃-LiAlH₄, THF). A homogeneous mechanism operates at early stages of the reaction while active nanoparticles form upon ageing of the catalyst solution.

ⁱⁱ Reproduced from T. N. Gieshoff, M. Villa, A. Welther, M. Plois, U. Chakraborty, R. Wolf, A. Jacobi von Wangelin, *Green Chem* **2015**, *17*, 1408–1413 with permission from the Royal Society of Chemistry. Schemes, tables and text may differ from published version.

ⁱ Authors contribution: Initial experiments were performed by A. Welther (Table 4-1, Table 4-2, Table 4-3 entries 1, 2, 3, 6, 10, 11), see A. Welther, *Dissertation*, University Regensburg, **2013**. Complex **4** (Scheme 4-3) was initially synthesized and analyzed by M. Plois and resynthesized by U. Chakraborty, see M. Plois, *Dissertation*, University Regensburg, **2012**. M. Villa contributed equally in Table 4-3 and Table 4-4).

4.1 Introduction

Catalytic hydrogenations of olefins constitute one of the strongholds of transition metal catalysis within organic synthesis and technical processes.^[1] The majority of methods involve noble metal catalysts based on Pd, Pt, Rh, Ir or toxic metals such as Ni or Co. Iron-catalyzed hydrogenations of olefins have only recently attracted great interest due to their expedient economic and environmental qualities.^[2] Homogeneous iron catalysts were mostly reported with phosphine and pyridyl-2,6-diimine ligands, sometimes requiring high pressures of H₂.^[3,4] Nanoparticle Fe catalysts could be prepared by reduction of iron salts with Grignard reagents in the absence of a suitable ligand or by decomposition of iron carbonyls.^[5] Fe-catalyzed reductions of olefins were recently reported with cheap ferrous salt pre-catalysts FeX₂ in the presence of an excess of lithium *N,N*-dimethylaminoborohydride (10 equiv.) or sodium triethylborohydride (4 equiv.) and required a high catalyst loading or the addition of tetra-dentate ligands.^[6] Reductions of alkenes and alkynes with LiAlH₄ in the presence of various transition metal halides (NiCl₂, TiCl₂, CoCl₂, FeCl₃) were already reported in the 1960s and postulated to involve metal hydride species that engage in formal hydrometalations of the olefin.^[7] Here, we wish to present a synthetic and mechanistic study on a hydrogenation protocol using catalytic amounts of a cheap Fe salt and catalytic amounts of lithium aluminiumhydride (LiAlH₄) as catalyst activator under an atmosphere of 1 bar H₂ as stoichiometric hydrogen source (Scheme 4-1).^[7e]



Scheme 4-1. Iron-catalyzed reductions of olefins: Hydride vs. hydrogen methods.

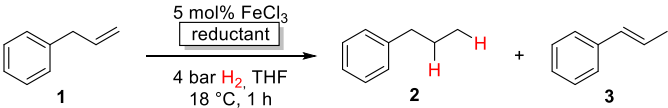
This method allows the use of standard (ambient pressure) equipment. H₂ is an abundant raw material; LiAlH₄ is an easy-to-handle reductant with numerous applications.^[8]

4.2 Reaction conditions and substrate scope

Initial experiments with the model substrate allylbenzene (**1**) aimed at the identification of a suitable catalytic reductant which assists the formation of a low-valent iron catalyst (with dark brown color) from the commercial pre-catalyst FeCl₃ (Table 4-1).^[9] LiAlH₄ displayed excellent selectivity which exceeded that of earlier protocols with Grignard reagents.^[5] Isomerization of the terminal double bond into conjugation – which occurred

in the related EtMgCl-mediated protocols (entries 2, 4) – was effectively suppressed.^[10] NaBH₄ was far less active even at elevated temperature and pressure (entries 6, 7). Interestingly, low ratios of LiAlH₄/FeCl₃ (1/1 to 2/1) fared optimal in the hydrogenation of **1** at 1 bar H₂. When employing a larger excess of LiAlH₄ (>2/1), the catalytic activity collapsed.^[7e] This stoichiometry differs from literature reports where large excess amounts of hydride reagents effected clean hydrogenations of olefins.^[6,7a-c] At 60 °C, the FeCl₃/LiAlH₄ catalyst decomposed upon decolorization.

Table 4-1. Selected optimization experiments.

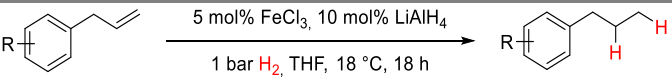
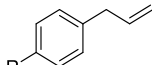
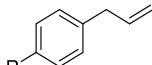
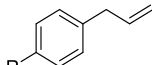
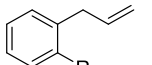
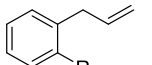
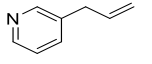
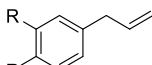
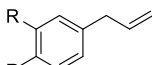
				
Entry	Reductant (mol%)	Deviation from conditions ^a	2 in % ^c	3 in % ^c
1	-	-	<1	2
2	EtMgCl (30)	-	42	56
3	EtMgCl (30)	- ^b	16	<1
4	EtMgCl (30)	1 bar H ₂ , 20 h	60	36
5	Et ₂ Zn (20)	30 bar H ₂ , 80 °C, 12 h	4	1
6	NaBH ₄ (100)	50 bar H ₂ , 24 h	8	<1
7	NaBH ₄ (100)	MeOH/THF (1:1), 50 bar H ₂ , 50 °C, 20 h	45	38
8	LiAlH ₄ (10)	-	97	3
9	LiAlH₄ (10)	1 bar H₂, 20 h	98	1
10	LiAlH ₄ (30)	as entry 9, open to air ^d	95	3
11	LiAlH ₄ (10)	FeCl ₂	96	1
12	LiAlH ₄ (10)	Fe(acac) ₃	20	15

^a Conditions: 5 mol% FeCl₃ in THF (0.5 mL) under argon, addition of reductant at r.t., after 10 min addition of **1**, after 1 min exchange of Ar with 4 bar H₂; ^b prior storage of [FeCl₃/red.] catalyst mixture in THF under argon for 3 d at r.t.; ^c quantitative GC-FID vs. *n*-pentadecane as internal reference; ^d during catalyst preparation.

The catalyst system comprises of cheap and easy-to-handle reagents (FeCl₃ or FeCl₂, LiAlH₄, THF); the reaction operates under ambient conditions (1 bar H₂, 20°C), which make the general protocol practical for every-day use in standard synthesis laboratories. The optimized conditions were applied to functionalized allylbenzenes and styrenes (Table 4-2 and Table 4-3).^[9]

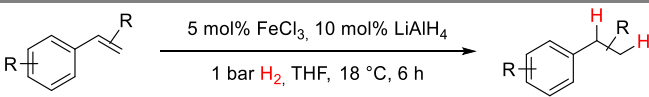
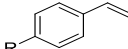
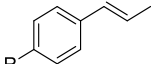
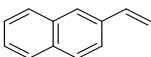
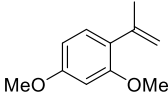
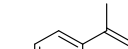
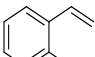
Allylbenzenes underwent only minimal olefin isomerization.^[10] Styrenes exhibited low propensity to undergo polymerization (entry 13, Table 4-3). The general protocol is compatible with several functional groups including F, Cl, Br, allyl and benzyl ethers, esters, carboxamides, pyridines and anilines. Clean hydrogenation was achieved with bulky, *ortho*-substituted, and electron-rich styrenes. For comparison, the FeCl₃/EtMgCl-derived catalyst effected undesired dehalogenation (Cl, Br)^[11] and allylether cleavage^[12], and showed no activity in the presence of carboxylates or cinnamates. Catalyst decomposition was effected by nitro groups, iodides, nitriles, ketones, and acidic protons (e.g. alkanols, pK_a~17), presumably by oxidation to catalytically inactive Fe(II) species (decolorization). Tri-substituted styrenes gave low conversions. In general, bulky and functionalized substrates were more reactive at elevated pressures (10 bar H₂).^[13]

Table 4-2. Hydrogenation of allylbenzenes at 1 bar H₂.

			
Entry	Allylbenzene	R	Yield in % ^a
1		H	93
2		Me	79 (92) ^b
3		OMe	84 (89) ^c
4		Me	95
5		OAc	93 (95) ^{c,d}
6		-	99
7		OMe	100
8		F	86

^a quantitative GC-FID vs. *n*-pentadecane as internal reference, conversion in % in parentheses if <95 %; ^b 7% 1-propen-1-ylbenzene (*E/Z* 9/1); ^c 24 h; ^d quantitative NMR (vs. CH₂Br₂)

Table 4-3. Hydrogenation of styrene derivatives.

			
Entry	Styrene	R	Yield in % ^a
1		H	100
2		Me	98
3		OMe	98
4		Cl	93 ^b
5		Br	94 ^b
6		F	77 ^c
7		OBn	100 ^d
8		NH ₂	97 ^c
9		CO ₂ Me	97
10		H	100 ^e
11		OMe	84
12		-	100
13		-	86 ^d
14		H	100 ^d
15		Cl	85 (89) ^f
16		Br	44 (56) ^f
17		Br	92 ^{c,f}
18		OMe	100 ^d
19		Cl	74 (86) ^b
20		OBn	100 ^d

Iron-catalyzed olefin hydrogenation at 1 bar H₂ with a FeCl₃-LiAlH₄ catalyst

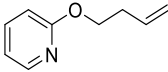
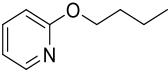
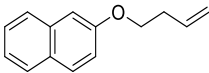
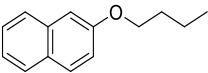
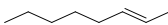
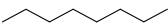
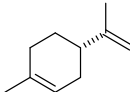
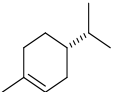
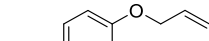
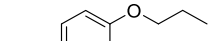


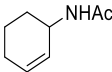
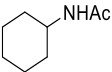
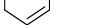
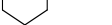
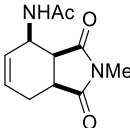
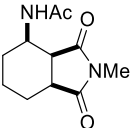
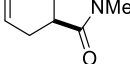
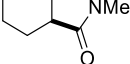
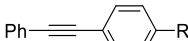
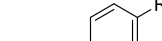
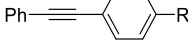
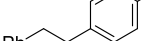
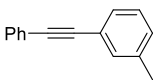
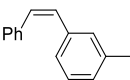
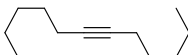

21		Ph	100 ^d
22		Bn	100 ^d
23		CO ₂ Et	100 ^d
24		-	48 (54)
25		-	88 ^c
26		-	33 (58) ^e
27		-	75 ^{d,g}
28		-	18 (18) ^c

^a quantitative GC-FID vs. *n*-pentadecane as internal reference, conversion in % in parentheses if <95 %; ^b <12 % ethylbenzene; ^c 20 h, 10 bar H₂; ^d 5 mol% LiAlH₄, 3 h; ^e 20 h; ^f <5 % cumene; ^g mixture of partial and full hydrogenation products (~6/1)

Hydrogenations of aliphatic alkenes were also catalyzed by FeCl₃-LiAlH₄ under similar conditions (Table 4-4).^[9] Terminal olefins were only slowly isomerized (~10%).^[10] Surprisingly, substrates containing moderately acidic protons (pK_a ~25)^[14] underwent hydrogenation with high selectivity (entries 10-13).^[15] Alkynes underwent *Z*-selective semi-hydrogenation,^[16] whereas complete hydrogenation to the alkanes was observed at longer reaction times or elevated pressures.

Table 4-4. Hydrogenation of other alkenes and alkynes.

$ \text{R}-\text{CH}=\text{CH}_2 \xrightarrow[1 \text{ bar H}_2, \text{ THF}, 18^\circ\text{C}, 3 \text{ h}]{5 \text{ mol\% FeCl}_3, 5 \text{ mol\% LiAlH}_4} \text{R}-\text{CH}_2-\text{CH}_2-\text{H} $			
Entry	Substrate	Product	Yield in % ^a
1			82 ^b
2			69 ^b
3			82 ^c

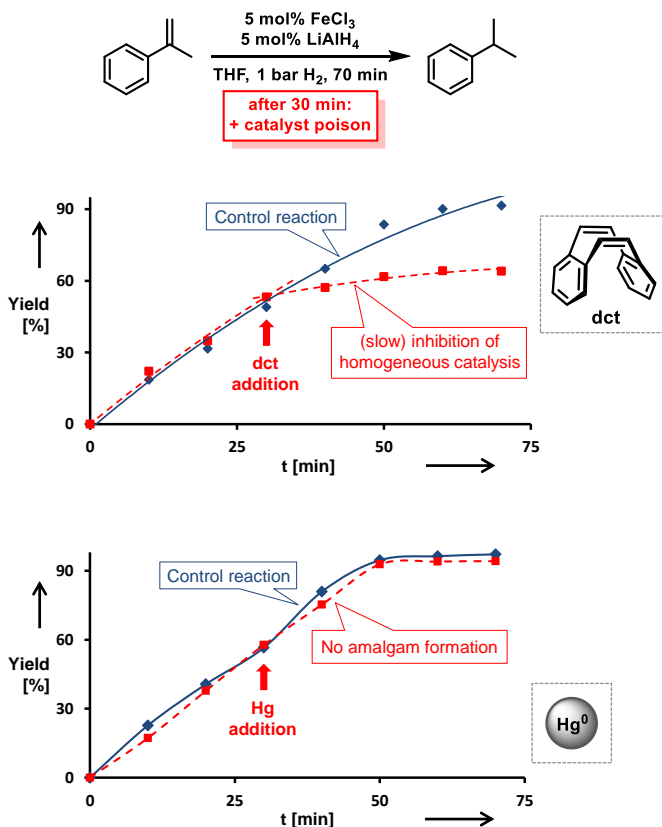
4			89 (89) ^c
5			65 (65) ^c
6			21 (41) ^b
7			100 ^d
8			2 (10)
9			64 (65) ^d
10			12 (16)
11			96 ^{d,e}
12			38 (38) ^{d,e}
13			69 (69) ^{d,e}
14			100 ^c (R=H)
15			92 ^c (R = CO ₂ Me)
16			75 (80) ^g
17			90 ^g

^a quantitative GC-FID vs. *n*-pentadecane as internal reference, conversion in % in parentheses if <95 %; ^b alkene isomers; ^c 20 h; ^d 10 bar, 20 h; ^e 10 mol% LiAlH₄; ^f 60 °C; ^g quantitative NMR vs. CH₂Br₂.

4.3 Mechanistic studies

The distinction between homogeneous and heterogeneous catalysts is a challenging task.^[17] However, kinetic experiments with selective poisons can provide valuable information on the topicity of the catalyst species. We have performed two sets of poisoning experiments which appear to support a homogeneous mechanism. Dibenzo[*a,e*]cycloocta-tetraene (dct) is a selective ligand for homogeneous metal species

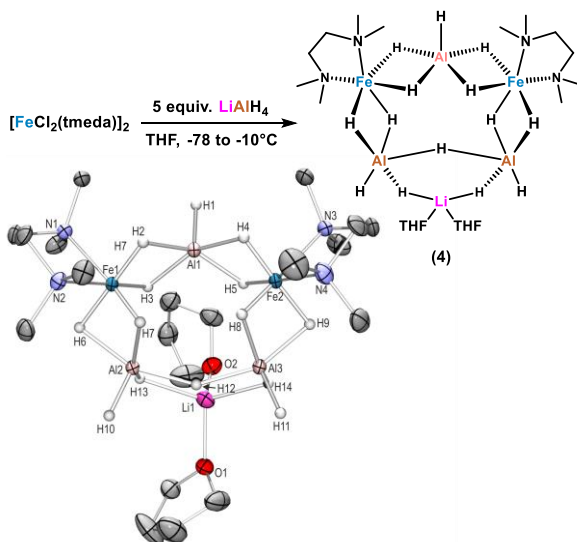
due to its rigid tub-like structure and π -acceptor properties.^[18] Upon addition of 30 mol% dct (6 equiv. per [Fe]) to the hydrogenation of α -methylstyrene at 1 bar H₂ after 30 min, the catalyst activity was significantly inhibited (Scheme 4-2, top).^[9,19] A similar conclusion can be derived from a poisoning experiment with 3 equiv. Hg (60 equiv. Hg per [Fe]). A potential amalgam formation^[20] was not observed and no significant change of the catalyst activity was observed in comparison with the control reaction (Scheme 4-2, bottom).^[9] These results suggest the operation of a homogeneous catalyst species during the early stage of the catalytic hydrogenation.



Scheme 4-2. Top: Poisoning experiment with 30 mol% dibenzo[*a,e*]cyclooctatetraene (dct, dashed curve) vs. control reaction (solid line). Bottom: Poisoning with 3 equiv. Hg (dashed) vs. control reaction (solid line).

Previous studies showed that the reaction of FeCl₃ with an excess of LiAlH₄ ultimately leads to the formation of iron metal and AlH₃ via the intermediate formation of a thermally

unstable iron(II) compound with the composition $\text{Fe}(\text{AlH}_4)_2$.^[21,22] In an attempt to gain deeper insight into the catalyst species operating in homogeneous solution, we treated $[\text{FeCl}_2(\text{tmeda})]_2$ ($\text{tmeda} = N,N,N',N'$ -tetramethylethylenediamine) with LiAlH_4 at -70°C and obtained dark red crystals of the oligohydride compound $[\text{Li}(\text{thf})_2\{\text{Fe}(\text{tmeda})\}_2(\text{AlH}_5)(\text{Al}_2\text{H}_9)]$ (**4**, Scheme 4-3).^[9] The hexa-metallic macrocyclic cage contains 14 bridging hydrido ligands and two Fe atoms with distorted octahedral coordination geometries. Unfortunately, the thermal instability prevented further spectroscopic characterization.



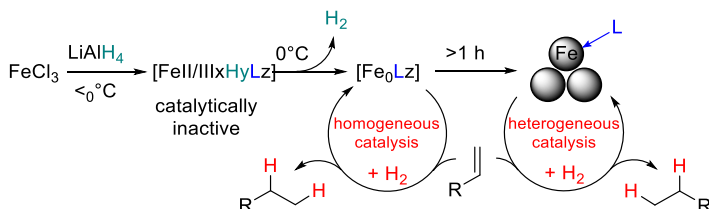
Scheme 4-3. Synthesis of the soluble LiAlFe-oligohydride complex **4**.

However, complex **4** showed no activity in hydrogenations of styrenes (1-10 bar H_2 , -10°C) and maintained its red color throughout the reaction. Above -10°C , the complex rapidly decomposed upon H_2 evolution to give a brown paramagnetic species which afforded good yields in hydrogenations at 20°C and 4 bar H_2 . The crystallographic characterization of **4** documents that this or similar oligonuclear Fe(II) alumino hydride complexes may be intermediates *en route* to the formation of catalytically active low-valent iron species.^[23]

The initially homogeneous dark-brown catalyst species (possibly in the oxidation states 0 and/or +1)^[23] experience rapid ageing and particle formation after approximately 1 h under reductive conditions. Several methods of synthesis and characterization techniques of naked Fe(0) nanoparticles (prepared by reduction of ferric and ferrous halides) have been reported.^[5,7,23,24] DLS measurements

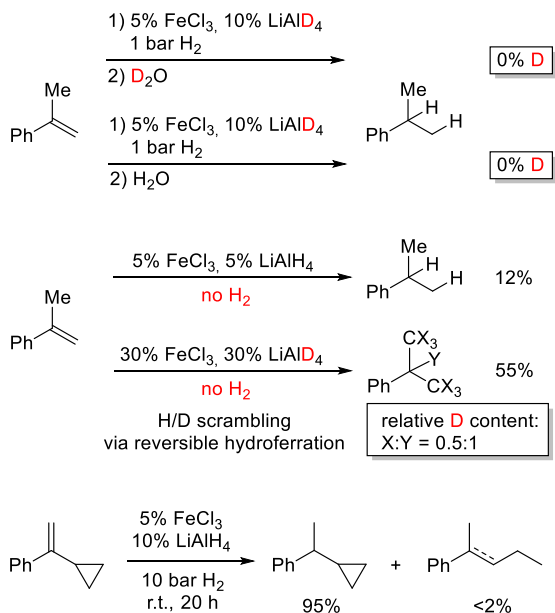
(dynamic light scattering) of freshly prepared catalyst solutions (5 mol% FeCl₃/LiAlH₄, THF, r.t., 10 min, then 100 nm nanofiltration) documented the presence of poly-disperse particles of 250-1500 nm size after 30 min of ageing under anaerobic conditions in the absence of substrates. The aged species are much less catalytically active than their homogeneous counterparts. Catalyst solutions (FeCl₃/LiAlH₄ (1/1) in THF) stored at 0°C under argon for 6 h, 24 h, and 48 h afforded 42%, 12%, and 5% conversion of α -methylstyrene under standard conditions (see entry 16 in Table 4-3), respectively.

We postulate a homogeneous mechanism of soluble, low-valent iron catalyst in the initial stage of the hydrogenation reactions (Scheme 4). Such species are formed by reduction of FeCl₃ (or L_nFeCl₂) with LiAlH₄ at above 0°C and are typically characterized by the dark brown color. The absence of suitable ligands leads to the formation of Fe(0) nanoclusters^[5,22,24] which require higher H₂ pressures than the homogeneous species to maintain catalytic activity.



Scheme 4-4. Proposed formation and catalysis of low-valent iron species.

Deuterium incorporation was observed at higher catalyst concentrations (30 mol% FeCl₃/LiAlD₄) in the absence of H₂ which gave ~55% hydrogenation product (Scheme 4-5, center).^[9] Such H₂-free conditions can effect H/D scrambling in the starting material and product (via reversible hydroferration) and the formation of radical intermediates (with participation of THF as H donor).^[9] However, the radical mechanism is very unlikely to operate under hydrogenation conditions in the presence of H₂ gas (Scheme 4-5):^[9] Reaction work-up with deuterium oxide (D₂O) and employment of lithium aluminium deuteride (LiAlD₄) showed no deuterium incorporation into the products, respectively (Scheme 4-5, top right). Further, the intermediacy of free C-radicals is unlikely: Employment of the radical probe 1-cyclopropyl-1-phenylethylene^[25] resulted in less than 2% ring opening (Scheme 5, bottom).^[9] The hydrogenation of various styrenes (1 bar H₂) was unaffected by the presence of 1 equiv. 1,1-diphenylethene. On the other hand, the addition of TEMPO (2,2,6,6-tetramethylpiperidinyloxy, 1 equiv.) inhibited conversion of α -methylstyrene (no TEMPO adduct detected), possibly by irreversible catalyst oxidation as indicated by the decolorization of the solution.



Scheme 4-5. Mechanistic studies with deuterated reagents (top), in the absence of H₂ (center), and with radical probe (bottom).

4.4 Conclusions

In summary, we have studied the iron-catalyzed hydrogenation of various styrenes, alkenes, and alkynes under an atmosphere of 1 bar H₂. This method uses cheap and easy-to-handle reagents (FeCl₃, LiAlH₄, THF, H₂) which allow facile implementation in standard synthesis labs. Alkynes underwent Z-selective semi-hydrogenation. Sterically hindered and functionalized olefins showed higher conversions at elevated H₂ pressures. Mechanistic studies support the notion of a homogeneous catalyst species at the outset of the hydrogenation reactions (<1 h) while catalyst ageing results in the formation of particles which exhibited somewhat lower catalytic activity. The crystallographically characterized homogeneous Fe(II) oligohydride complex **4** can serve as starting point for further model catalyst preparations.

4.5 Experimental

4.5.1 General

Analytical Thin-Layer Chromatography: TLC was performed using aluminium plates with silica gel and fluorescent indicator (*Merck*, 60, F254). Thin layer chromatography plates were visualized by exposure to ultraviolet light (366 or 254 nm) or by immersion in a staining solution of molybdatophosphoric acid in ethanol or potassium permanganate in water.

Column Chromatography: Flash column chromatography with silica gel 60 from *KMF* (0.040-0.063 mm). Mixtures of solvents used are noted in brackets.

Chemicals and Solvents: Commercially available olefins were distilled under reduced pressure prior use. Solvents (THF, Et₂O, *n*-hexane) were distilled over sodium and benzophenone and stored over molecular sieves (4 Å). Lithium aluminium hydride and iron(III)chloride (98%, anhydrous) were stored and handled in a glovebox under argon (99.996%). Commercial lithium aluminium hydride was purified by extraction with diethyl ether and subsequent removal of the solvent under high vacuum. Solvents used for column chromatography were distilled under reduced pressure prior use (ethyl acetate).

High Pressure Reactor: Hydrogenation reactions were carried out in 160 and 300 mL high pressure reactors (*Parr*TM) in 4 mL glass vials. The reactors were loaded under argon, purged with H₂ (1 min), sealed and the internal pressure was adjusted. Hydrogen (99.9992%) was purchased from *Linde*.

¹H- und ¹³C-NMR-Spectroscopy: Nuclear magnetic resonance spectra were recorded on a *Bruker* Avance 300 (300 MHz) and *Bruker* Avance 400 (400 MHz). ¹H-NMR: The following abbreviations are used to indicate multiplicities: s = singlet; d = doublet; t = triplet, q = quartet; m = multiplet, dd = doublet of doublet, dt = doublet of triplet, dq = doublet of quartet, ddt = doublet of doublet of quartet. Chemical shift δ is given in ppm to tetramethylsilane.

Fourier-Transformations-Infrared-Spectroscopy (FT-IR): Spectra were recorded on a *Varian* Scimitar 1000 FT-IR with ATR-device. All spectra were recorded at room temperature. Wave number is given in cm⁻¹. Bands are marked as s = strong, m = medium, w = weak and b = broad.

Gas chromatography with FID (GC-FID): HP6890 GC-System with injector 7683B and *Agilent* 7820A System. Column: HP-5, 19091J-413 (30 m × 0.32 mm × 0.25 μm), carrier gas: N₂. GC-FID was used for reaction control and catalyst screening (Calibration with internal standard *n*-pentadecane and analytically pure samples).

Gas chromatography with mass-selective detector (GC-MS): *Agilent* 6890N Network GC-System, mass detector 5975 MS. Column: HP-5MS (30m × 0.25 mm × 0.25 μm, 5%

phenylmethylsiloxane, carrier gas: H₂. Standard heating procedure: 50 °C (2 min), 25 °C/min -> 300 °C (5 min)

High resolution mass spectrometry (HRMS): The spectra were recorded by the Central Analytics Lab at the Department of Chemistry, University of Regensburg, on a MAT SSQ 710 A from Finnigan

Dynamic Light Scattering: Dynamic light scattering experiments were performed with the help of a goniometer CGS-II from ALV (Germany). The goniometer is equipped with an ALV-7004/Fast Multiple Tau digital correlator and a vertical-polarized 22 mW HeNe-laser (wavelength = 623.8 nm). All measurements were done at a scattering angle of 90° after thermostating to 25 °C. The measurement time was 300 s. The obtained correlation functions were fitted with the software TableCurve 2d v5.01 by a monomodal equation.

4.5.1 General hydrogenation procedures

General method for the hydrogenation with FeCl₃ (5mol%) and LiAlH₄ (10 mol%)

A 4 mL vial was charged with a freshly prepared solution of FeCl₃ in dry THF (0.50 mL, 0.05 M) and an aliquot of a vigorously stirred suspension of LiAlH₄ in dry THF (0.50 mL, 0.1 M) under argon atmosphere. After stirring for 30 min; the olefin (0.50 mmol) was added and the vial transferred to a high pressure reactor. The reactor was purged with H₂ (1 min), sealed, and the internal pressure adjusted to 1 bar H₂. After the designated reaction time, the vial was retrieved. The reaction was quenched with saturated aqueous NaHCO₃ (1 mL) and extracted with ethyl acetate (2 × 2 mL). The organic phases were dried (Na₂SO₄) and subjected to flash chromatography (SiO₂, pentane/ethyl acetate) or analyzed by quantitative GC-FID analysis vs. *n*-pentadecane as internal reference.

General method for the hydrogenation with FeCl₃ (5mol%) and LiAlH₄ (5 mol%)

A 25 mL flask was charged with a freshly prepared solution of FeCl₃ in dry THF (2 mL, 0.05 M) and an aliquot of a suspension of LiAlH₄ in dry THF (2 mL, 0.05 M) was added over 20 minutes at -78 °C under argon atmosphere via syringe pump. After stirring for additional 10 minutes, 1 mL of the catalyst suspension was added to a 4 mL vial with the olefin (0.50 mmol) and the vial was transferred to a high pressure reactor. The reactor was purged with H₂ (1 min), sealed, and the internal pressure adjusted to 1 bar H₂. After the designated reaction time, the vial was retrieved. The reaction was quenched with saturated aqueous NaHCO₃ (1 mL) and extracted with ethyl acetate (2 × 2 mL). The organic phases were dried (Na₂SO₄) and subjected to flash chromatography (SiO₂, pentane/ethyl acetate) or analyzed by quantitative GC-FID analysis vs. *n*-pentadecane as internal reference.

4.5.2 Mechanistic experimental details

Kinetic Experiments

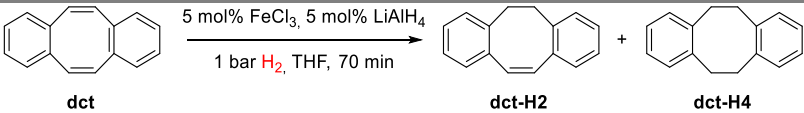
Kinetic studies were performed in a rubber septum sealed *Schlenk* tube under a dihydrogen atmosphere. Catalyst preparation according to the general method for the hydrogenation with FeCl₃ (5 mol%) and LiAlH₄ (5 mol%). Samples were taken via syringe (50 μ L) and quenched with an aqueous solution of sodium hydrogen carbonate. After extraction with ethyl acetate and filtration over a pad of silica, the samples were analyzed by GC-FID. Selected catalyst poisons (dct, Hg) were added after 30 minutes via syringe (dct as a solution in 100 μ L THF).

Table 4-5. Hydrogenation of α -methylstyrene with selective catalyst poisons.

$ \text{Ph}-\text{CH}=\text{CH}_2 \xrightarrow[1 \text{ bar H}_2, \text{ THF, 70 min}]{5 \text{ mol\% FeCl}_3, 5 \text{ mol\% LiAlH}_4} \text{Ph}-\text{CH}_2\text{CH}_3 $				
Entry	Time / min	Yield in % no additive	Yield in % + dct (30 mol%)	Yield in % + Hg (300 mol%)
1	0	0	0	0
2	10	23	22	17
3	20	41	35	38
4	30	57	53	58
5	40	81	57	75
6	50	95	62	93
7	60	96	64	94
8	70	97	64	94

^a quantitative GC-FID vs. *n*-pentadecane as internal reference

Table 4-6. Dct consumption in the hydrogenation of α -methylstyrene with 30 mol% dct.

				
Entry	Time / min	dct	dct-H2	dct-H4
1	30	100	0	0
2	40	58	40	2
3	50	36	59	5
4	60	28	65	7
5	70	27	66	7

^a determined by relative peak areas of GC-FID

Deuteration experiments

For deuterium exchange experiments the reaction mixture after hydrogenation of α -methylstyrene at 1 bar H_2 in 3 h was quenched with D_2O , extracted with Et_2O (2×1 mL), filtered over a pad of silica and analyzed by GC-FID, 1H and 2H -NMR to check for D-incorporation.

In a second experiment, $LiAlD_4$ was used instead of $LiAlH_4$. The reaction mixture after hydrogenation of α -methylstyrene at 1 bar H_2 in 3 h was quenched with H_2O , extracted with Et_2O (2×1 mL), filtered over a pad of silica and analyzed by GC-FID, 1H -NMR to check for D-incorporation.

In both experiments no incorporation of D has been detected.

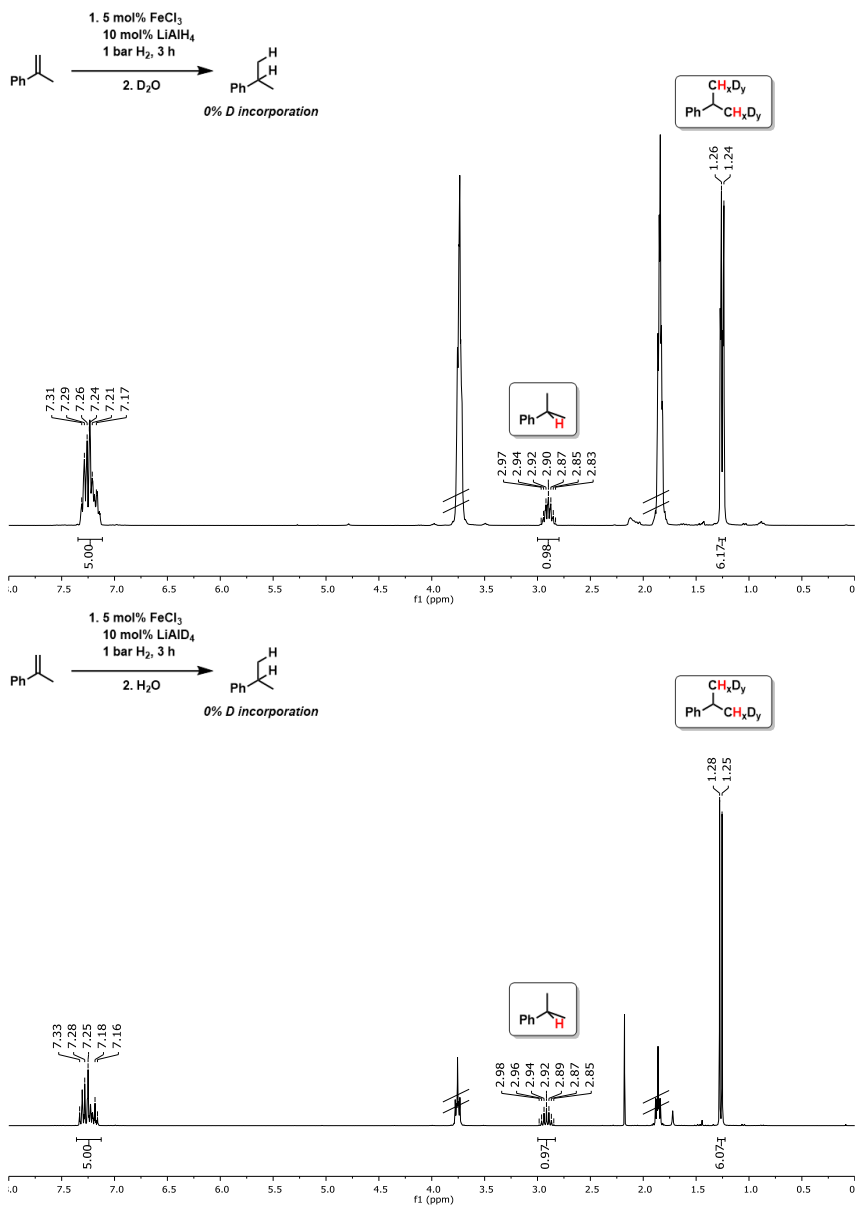


Figure 4-1. ¹H-NMR spectrum after hydrogenation of α -methylstyrene with 5 mol% FeCl₃ and 10 mol% LiAlH₄ and quench with D₂O (top) and after hydrogenation of α -methylstyrene with 5 mol% FeCl₃ and 10 mol% LiAlD₄ and quench with H₂O (bottom).

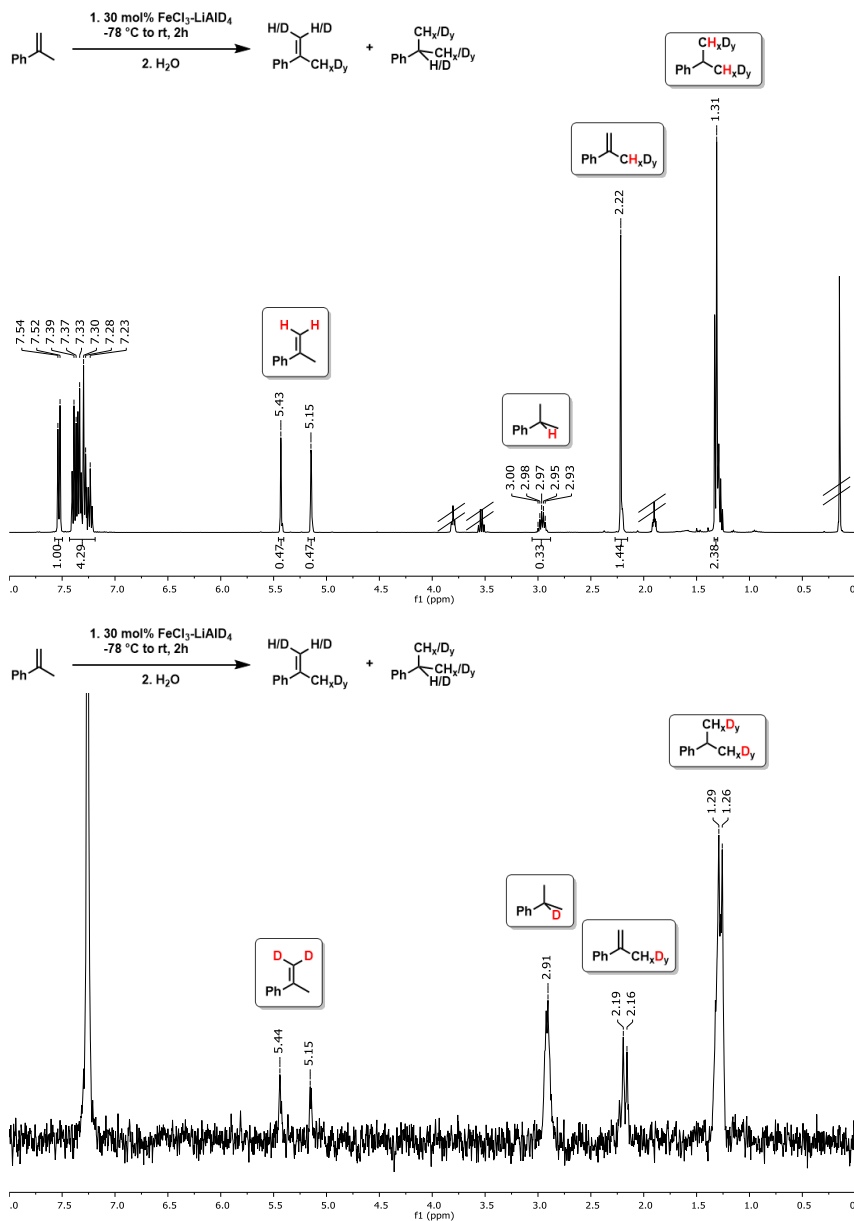


Figure 4-2. ¹H-NMR (top) and ²H-NMR (bottom) of crude reaction mixture after extraction. Substrate addition 20 min after catalyst preparation. ~55% product yield.

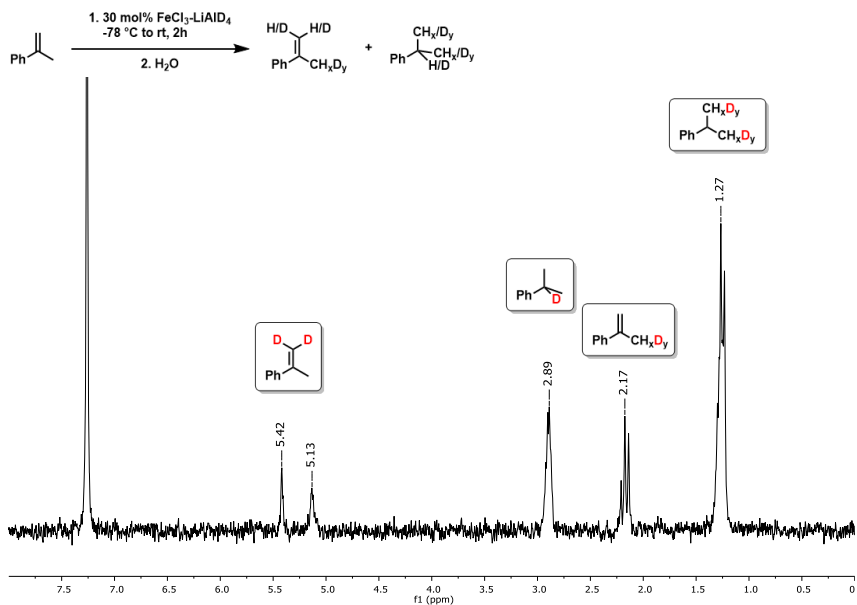
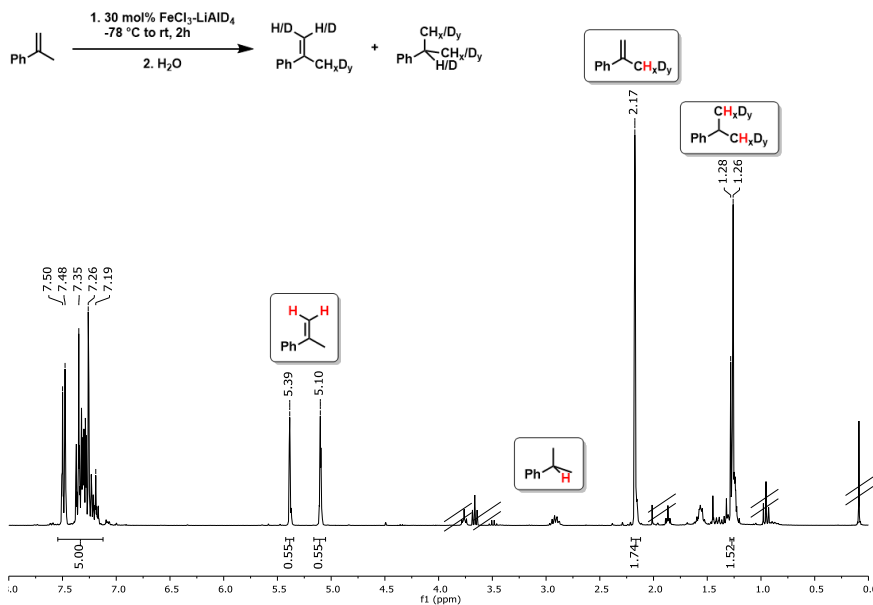


Figure 4-3. ¹H-NMR (top) and ²H-NMR (bottom) of crude reaction mixture after extraction. Substrate addition prior catalyst preparation. ~54% product yield.

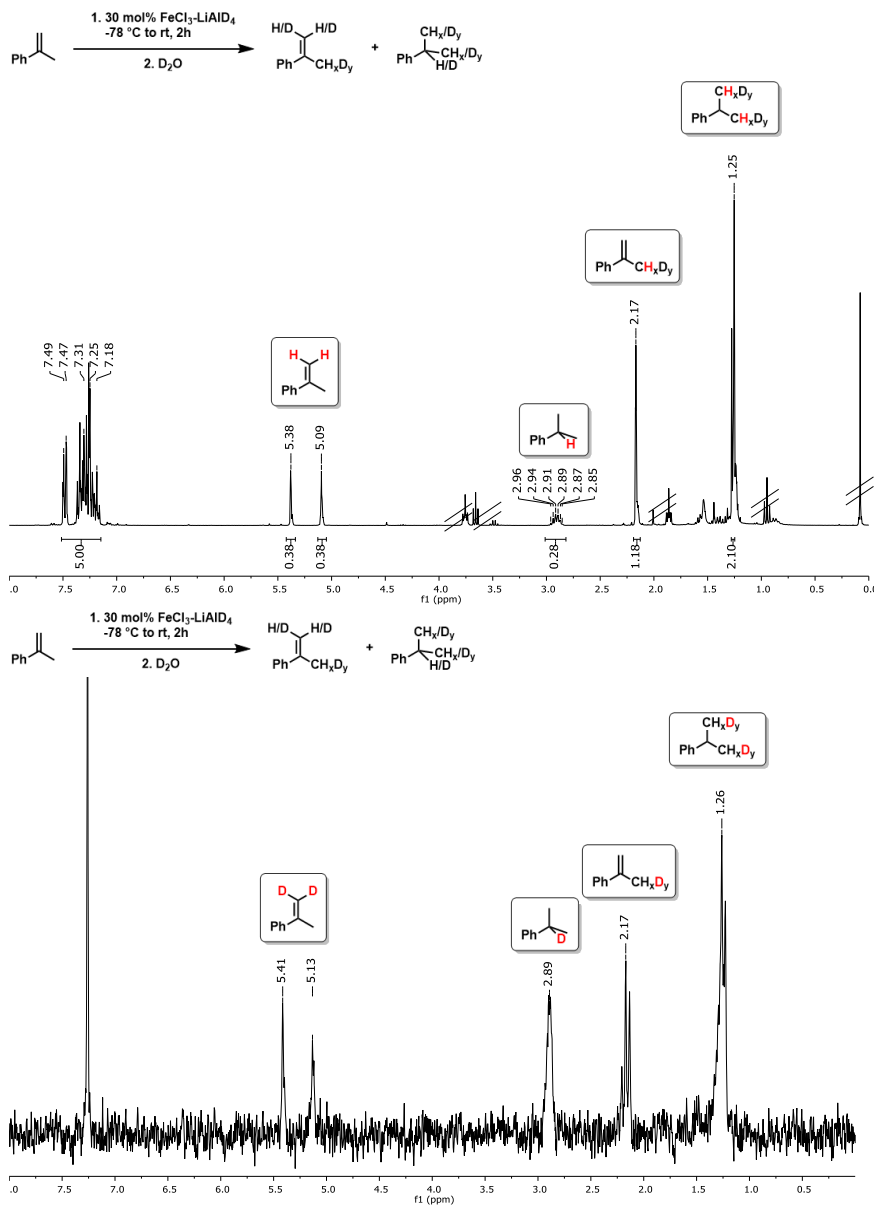


Figure 4-4. ^1H -NMR (top) and ^2H -NMR (bottom) of crude reaction mixture after extraction and D_2O quench. Substrate addition prior catalyst preparation. ~61% product yield.

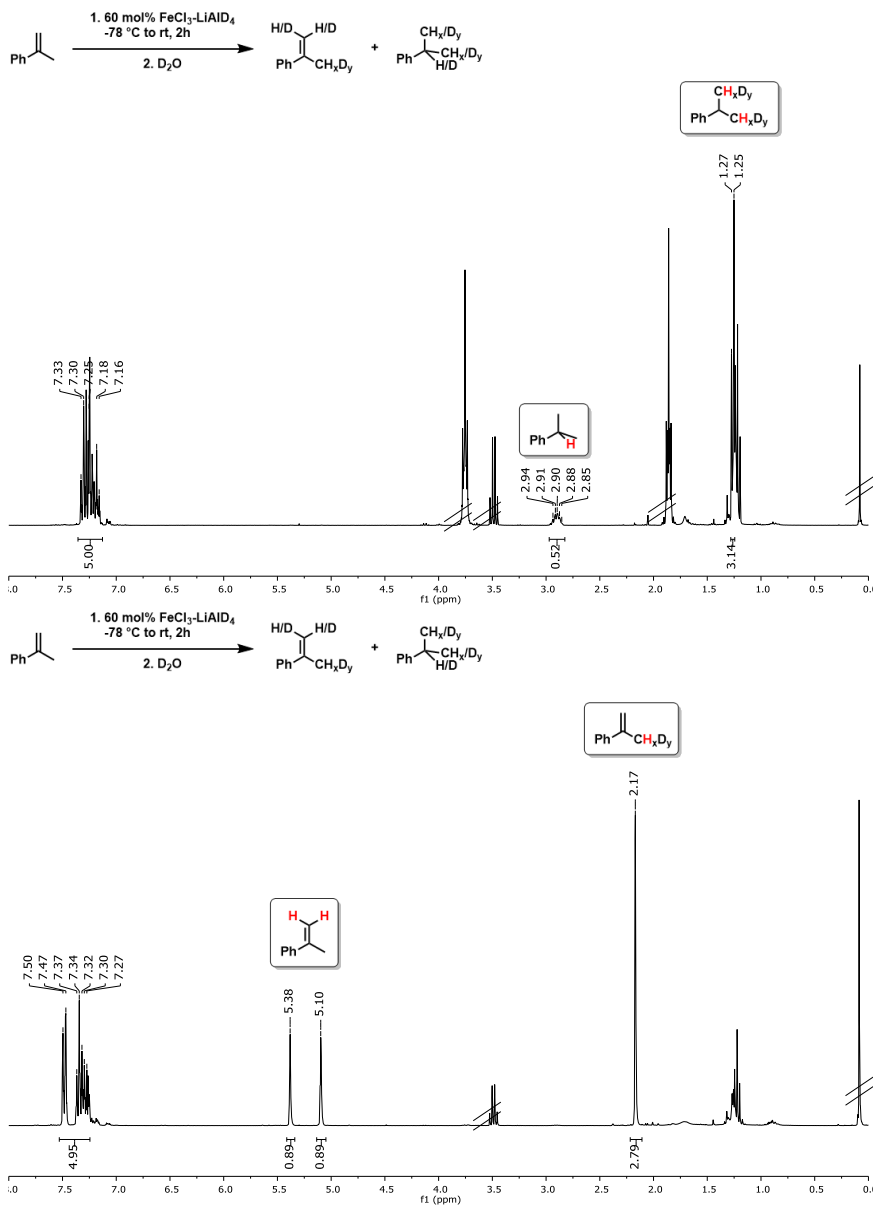
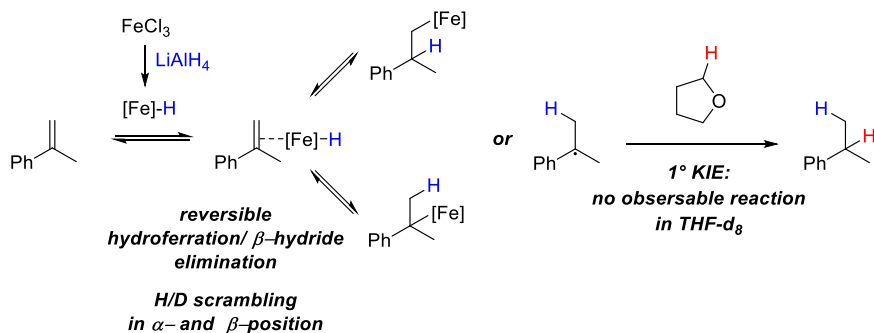
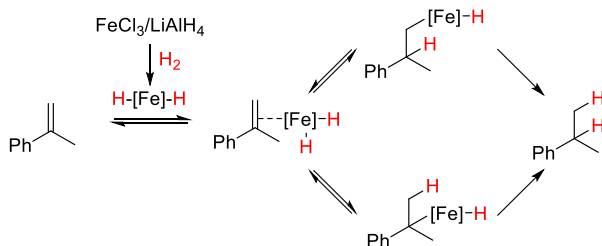


Figure 4-5. ¹H-NMR of crude reaction mixture in THF (top) and THF-d₈ (bottom) after extraction and D₂O quench. Substrate addition prior catalyst preparation. >95% product yield in THF (top), <5% product yield in THF-d₈ (bottom).

A) H₂-free reaction:
 -slower
 -radical intermediates?

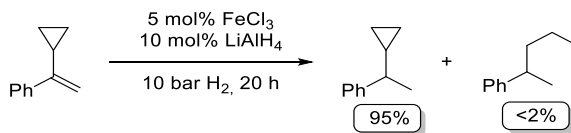


B) Hydrogenation reaction:
 -faster
 -no radical intermediates



Scheme 4-6. Mechanistic proposal of H₂ free reaction (A) and under dihydrogen atmosphere (B).

The observation of H/D scrambling in the olefin and product with D incorporation into the α- and β-positions suggests reversible hydroferration/β-hydride elimination at the Fe center. The very slow reaction in THF-d₈ under H₂-free conditions support the notion of a radical H/D-abstraction which is governed by a primary kinetic isotope effect (1° KIE). The operation of a radical mechanism is slower than the hydrogenation mechanism, especially at high H₂ pressures. See radical clock experiment at 10 bar H₂ below.



Scheme 4-7. Radical clock experiment.

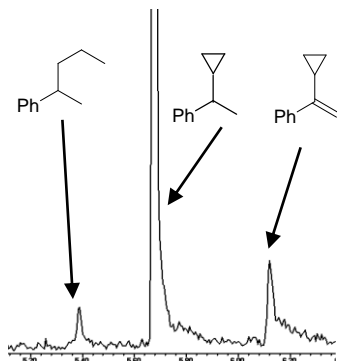


Figure 4-6. GC-MS spectrum of the reaction mixture of the hydrogenation of α -cyclopropylstyrene after work-up.

DLS measurement

The precatalyst was synthesized as described in the general procedure of hydrogenation reactions with FeCl₃/LiAlH₄ = 1/1 but in the absence of any unsaturated substrate. After stirring for additional 10 minutes, the mixture was diluted with anhydrous THF to achieve a final concentration $c[\text{Fe}] = 1.25 \text{ mM}$. The mixture was filtered through a 100 nm PTFE filter (sample B). The samples were measured after ageing at room temperature for 30 minutes.

Mean particle sizes:

Sample A:

$d = 297 \text{ nm } (\pm 30)$

Sample B (after filtration through 100 nm filter, three independent experiments):

$d = 334 \text{ nm } (\pm 30)$

$d = 1490 \text{ nm } (\pm 400)$

$d = 244 \text{ nm } (\pm 80)$ at higher dilution with $c[\text{Fe}] = 0.25 \text{ mM}$

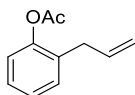
4.5.3 Synthesis of starting material

Preparation of allylbenzenes: Except for 2-allylphenyl acetate, allylbenzenes were prepared according to: M. Mayer, W. M. Czaplik and A. Jacobi von Wangelin, *Adv. Synth. Catal.* **2010**, 352, 2147. Analytical data were in full agreement with the literature reports.

Preparation of various styrenes, alkenes and alkynes: Non-commercial starting material was synthesized following the cited protocols.

2-Allylphenyl acetate

A 50 mL flask was charged with a solution of 2-allylphenol (1.4 mL, 10.6 mmol) in 15 mL CH_2Cl_2 . Then, triethylamine (4.6 mL, 33 mmol) was added at 0 °C followed by the slow addition of the acetyl chloride (11.6 mmol). The reaction mixture was stirred at room temperature for 15 h, diluted with 20 mL of ethyl acetate and washed with saturated aqueous NH_4Cl (10 mL). The organic phases were dried (MgSO_4), concentrated, and subjected to silica gel flash chromatography (cyclohexane/ethyl acetate).



$\text{C}_{11}\text{H}_{12}\text{O}_2$

176.22 g/mol

Appearance

colorless oil

$^1\text{H-NMR}$

(300 MHz, CDCl_3) δ 7.33-7.11 (m, 4H), 7.03 (d, 8.0 Hz, 1H), 5.90 (dt, J = 16.5, 6.4 Hz, 1H), 5.21-4.93 (m, 1H), 3.30 (d, J = 6.5 Hz, 1H), 2.30 (s, 3H).

GC-MS

t_R = 5.82 min, (EI, 70 eV): m/z = 176 [M^+].

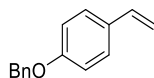
Analytical data were in full agreement with M. J. Gresser, S. M. Wales, P. A. Keller, *Tetrahedron* **2010**, 66, 6965-6976.

General procedure for styrene synthesis in a Wittig reaction

A 50 mL flask was charged with a suspension of methyltriphenylphosphonium bromide (6.94 mmol, 2.48 g) in THF (10 mL). Then, NaH-suspension in paraffine (60%, 6.94 mmol, 278 mg) was added in small portions. The reaction mixture was stirred at room temperature for 20 h followed by a dropwise addition of a solution of a ketone derivative (6.94 mmol) in THF (10 mL). The reaction mixture was stirred for 2 d at room temperature, quenched with H_2O (15 mL) and extracted with Et_2O (3×15 mL). The combined organic layers were dried (Na_2SO_4), concentrated and subjected to silica gel flash chromatography (*n*-pentane).

1-(Benzyloxy)-4-vinylbenzene

Synthesis following the general procedure for styrene synthesis in a Wittig reaction.



C₁₅H₁₄O

210.27 g/mol

Appearance

colorless solid

Yield

1.25 g, 5.97 mmol (74%)

TLC

R_f = 0.28 (SiO₂, *n*-pentane)

¹H-NMR

(300 MHz, CDCl₃) δ 7.49 – 7.29 (m, 7H), 6.99 – 6.90 (m, 2H), 6.67 (dd, *J* = 17.6, 10.9 Hz, 1H), 5.63 (dd, *J* = 17.6, 0.9 Hz, 1H), 5.14 (dd, *J* = 10.9, 0.9 Hz, 1H), 5.08 (s, 2H).

¹³C-NMR

(75 MHz, CDCl₃) δ 158.57, 136.94, 136.21, 130.69, 128.63, 128.02, 127.50, 127.43, 114.88, 111.75, 70.03.

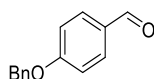
GC-MS

*t*_R = 9.40 min, (EI, 70 eV): *m/z* = 197 [M⁺], 183, 171, 156, 115, 102, 91, 75, 63, 51.

Analytical data were in full agreement with N. Kakusawa, K. Yamaguchi, J. Kouchichiro, *J. Organomet. Chem.* **2005**, *12*, 2956-2966.

4-(Benzyloxy)benzaldehyde

Synthesis following the procedure by S. K. Das, G. Panda, *Tetrahedron* **2008**, *19*, 4162-4173.



C₁₄H₁₂O₂

212.24 g/mol

Appearance

colorless solid

Yield

1.72 g, 8.12 mmol (81%)

TLC

R_f = 0.20 (SiO₂, hexanes/ethyl acetate = 9/1)

¹H-NMR

(300 MHz, CDCl₃) δ 9.89 (s, 1H), 7.84 (d, *J* = 8.7 Hz, 2H), 7.48 – 7.33 (m, 5H), 7.08 (d, *J* = 8.7 Hz, 2H), 5.16 (s, 2H).

¹³C-NMR

(75 MHz, CDCl₃) δ 190.82, 163.72, 135.93, 132.02, 130.11, 128.75, 128.36, 127.51, 115.15, 70.28.

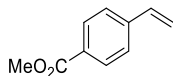
GC-MS

$t_R = 9.96$ min, (EI, 70 eV): $m/z = 212$ [M^+], 152, 121, 91, 77, 65, 51.

Analytical data were in full agreement with T. Shintou, T. Mukaiyama, *J. Am. Chem. Soc.*, **2004**, 23, 7359-7367.

Methyl-4-vinylbenzoate

Synthesis following the general procedure for styrene synthesis in a Wittig reaction.



$C_{10}H_{10}O_2$

162.19 g/mol

Appearance

colorless solid

Yield

234 mg, 1.44 mmol, 21%

TLC

$R_f = 0.11$ (SiO_2 , n -pentane)

 1H -NMR

(400 MHz, $CDCl_3$) δ 8.00 (d, $J = 8.4$ Hz, 2H), 7.46 (d, $J = 8.4$ Hz, 2H), 6.75 (dd, $J = 17.6, 10.9$ Hz, 1H), 5.86 (d, $J = 17.6$ Hz, 1H), 5.38 (d, $J = 10.9$ Hz, 1H), 3.91 (s, 3H).

 ^{13}C -NMR

(101 MHz, $CDCl_3$) δ 166.9, 141.9, 136.0, 129.9, 129.3, 126.1, 116.5, 52.1.

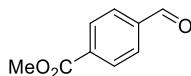
GC-MS

$t_R = 6.51$ min, (EI, 70 eV): $m/z = 197$ [M^+], 183, 171, 156, 115, 102, 91, 75, 63, 51.

Analytical data were in full agreement with A. Yokoyama, T. Maruyama, K. Tagami, H. Masu, K. Katagiri, I. Azumaya, T. Yokozawa, *Org. Lett.* **2008**, 10, 3207–3210.

Methyl-4-formylbenzoate

A 250 mL flask was charged with a solution of 4-formylbenzoic acid (15.0 mmol, 2.32 g) in dry methanol (75 mL). Trimethylsilylchloride (33.0 mmol, 4.20 mL) was added and the reaction mixture was stirred over night at room temperature. The product was isolated upon removal of the solvent under reduced pressure and silica gel flash chromatography (hexanes/ethyl acetate = 8/2).



$C_9H_8O_3$

164.16 g/mol

Appearance

colorless solid

Yield

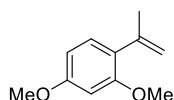
2.19 g, 13.3 mmol, 89%

TLC	$R_f = 0.24$ (SiO ₂ , hexanes/ethyl acetate = 8/2)
¹H-NMR	(400 MHz, CDCl ₃) δ 10.09 (s, 1H), 8.19 (d, $J = 8.1$ Hz, 2H), 7.94 (d, $J = 8.3$ Hz, 2H), 3.95 (s, 3H).
¹³C-NMR	(101 MHz, CDCl ₃) δ 191.7, 166.1, 139.2, 135.1, 130.2, 129.5, 52.6.
GC-MS	$t_R = 7.13$ min, (EI, 70 eV): $m/z = 164$ [M ⁺], 150, 133, 119, 105, 91, 77, 62, 51.

Analytical data were in full agreement with V. P. Baillargeon, J. K. Stille, *J. Am. Chem. Soc.* **1986**, *108*, 452–461.

2,4-Dimethoxy- α -methylstyrene

Synthesis following the general procedure for styrene synthesis in a Wittig reaction.



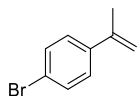
C₁₁H₁₄O₂

178.23 g/mol

Appearance	pale yellow solid
Yield	570 mg, 3.20 mmol (64%)
¹H-NMR	(300 MHz, CDCl ₃) δ 7.12 (d, $J = 8.6$ Hz, 1H), 6.30 – 6.15 (m, 2H), 5.10 (s, 1H), 5.05 (s, 1H), 3.81 (s, 6H), 2.10 (s, 3H).
¹³C-NMR	(75 MHz, CDCl ₃) δ 160.07, 157.69, 143.73, 129.72, 114.55, 103.95, 98.72, 55.41, 23.42.
GC-MS	$t_R = 7.23$ min, (EI, 70 eV): $m/z = 178$ [M ⁺], 163, 148, 135, 120, 115, 105, 91, 77, 69, 63, 51.
HRMS	(EI, m/z): found 178.0996 [M ⁺⁺] (calculated 178.0994).
IR	(ATR-film) in [cm ⁻¹] 2969 (w), 2955 (w), 2835 (w), 1737 (m), 1607 (s), 1578 (m), 1502 (s), 1463 (m), 1413 (w), 1371 (w), 1298 (m), 1257 (m), 1243 (m), 1206 (s), 1158 (s), 1102 (m), 1035 (s), 936 (w), 912 (w), 832 (m), 800 (m), 733 (m), 681 (w), 635 (m), 607 (w), 505 (m).

4-Bromo- α -methylstyrene

Synthesis following the general procedure for styrene synthesis in a Wittig reaction.



C_9H_9Br

197.08 g/mol

Appearance

colorless oil

Yield

1.06 g, 5.39 mmol, 77%

TLC

R_f = 0.59 (SiO₂, *n*-pentane)

¹H-NMR

(400 MHz, CDCl₃) δ 7.50-7.35 (m, 2H), 7.42-7.29 (m, 2H), 5.36 (s, 1H), 5.10 (s, 1H), 2.12 (s, 3H).

¹³C-NMR

(101 MHz, CDCl₃) δ 142.2, 140.1, 131.3, 127.2, 121.4, 113.1, 21.7.

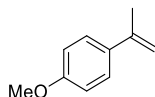
GC-MS

t_R = 6.51 min, (EI, 70 eV): m/z = 197 [M⁺], 183, 171, 156, 115, 102, 91, 75, 63, 51.

Analytical data were in full agreement with T. Taniguchi, A. Yajima, H. Ishibashi, *Adv. Synth. Catal.* **2011**, 353, 2643–2647.

4-Methoxy- α -methylstyrene

Synthesis following the general procedure for styrene synthesis in a Wittig reaction.



$C_{10}H_{12}O$

148.20 g/mol

Appearance

colorless liquid

Yield

1.04 g, 7.02 mmol (35%)

TLC

R_f = 0.25 (SiO₂, *n*-pentane)

¹H-NMR

(300 MHz, CDCl₃) δ 7.42 (d, J = 8.9 Hz, 2H), 6.87 (d, J = 8.9 Hz, 2H), 5.29 (s, 1H), 4.99 (s, 1H), 3.82 (s, 3H), 2.13 (s, 3H).

¹³C-NMR

(75 MHz, CDCl₃) δ 159.05, 142.56, 133.74, 126.60, 113.54, 110.68, 55.30, 21.94.

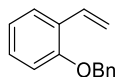
GC-MS

t_R = 6.39 min, (EI, 70 eV): m/z = 148 [M⁺], 127, 133, 115, 105, 89, 77, 63, 51.

Analytical data were in full agreement with A. Fryszkowska, K. Fisher, J. M. Gardiner, G. M. Stephens, *J. Org. Chem.* **2008**, 73, 4295-4298.

1-(Benzyloxy)-2-vinylbenzene

Synthesis following the general procedure for styrene synthesis in a Wittig reaction.



C₁₅H₁₄O

210.27 g/mol

Appearance

colorless oil

Yield

800 mg, 3.81 mmol (87%)

TLC

R_f = 0.21 (SiO₂, *n*-pentane)

¹H-NMR

(300 MHz, CDCl₃) δ 7.54 (dd, *J* = 7.6, 1.7 Hz, 1H), 7.50 – 7.34 (m, 5H), 7.25 – 7.10 (m, 2H), 6.97 (ddd, *J* = 8.2, 5.9, 2.1 Hz, 2H), 5.79 (dd, *J* = 17.8, 1.5 Hz, 1H), 5.28 (dd, *J* = 11.2, 1.5 Hz, 1H), 5.12 (s, 2H).

¹³C-NMR

(75 MHz, CDCl₃) δ 155.88, 137.16, 131.65, 128.85, 128.59, 127.91, 127.33, 127.11, 126.53, 120.99, 114.49, 112.43, 70.27.

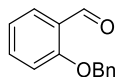
GC-MS

*t*_R = 9.13 min, (EI, 70 eV): *m/z* 210 [M⁺], 193, 119, 91, 77, 65, 51.

Analytical data were in full agreement with M. Barbasiewicz, M. Bieniek, A. Michrowska, A. Szadkowska, A. Makal, K. Wozniak, K. Grela, *Adv. Synth. Catal.* **2007**, 349, 193-203.

2-(Benzyloxy)benzaldehyde

Synthesis following the procedure by S. K. Das, G. Panda, *Tetrahedron* **2008**, 19, 4162-4173.



C₁₄H₁₂O₂

212.24 g/mol

Appearance

yellowish liquid

Yield

943 mg, 4.40 mmol (44%)

TLC

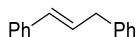
R_f = 0.31 (SiO₂, hexanes/ethyl acetate = 9/1)

$^1\text{H-NMR}$	(300 MHz, CDCl_3) δ 10.57 (d, $J = 0.7$ Hz, 1H), 7.87 (dd, $J = 8.0, 1.8$ Hz, 1H), 7.58 – 7.50 (m, 1H), 7.48 – 7.31 (m, 5H), 7.09 – 7.01 (m, 2H), 5.20 (s, 2H).
$^{13}\text{C-NMR}$	(75 MHz, CDCl_3) δ 189.77, 161.05, 136.08, 135.94, 128.75, 128.46, 128.30, 127.31, 125.16, 121.02, 113.02, 70.45.
GC-MS	$t_R = 9.74$ min, (EI, 70 eV): $m/z = 212$ [M^+], 183, 121, 91, 77, 65, 51.

Analytical data were in full agreement with S. K. Das, G. Panda, *Tetrahedron*, **2008**, *19*, 4162-4173.

(*E*)-1,3-Diphenylpropene

A round-bottom flask was charged with 1,3-diphenylpropan-1-ol (7.50 mmol, 1.59 g) and a tip of a spatula of *p*-toluenesulfonic acid in toluene (50 mL). The solution was stirred under reflux for 20 h. After cooling to room temperature the reaction mixture was extracted with Et_2O (3×25 mL). The combined organic layers were washed with brine (25 mL), dried over Na_2SO_4 and subjected to silica gel flash chromatography (*n*-pentane).



$\text{C}_{15}\text{H}_{14}$

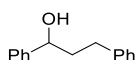
194.28 g/mol

Appearance	colorless oil
Yield	1.25 g, 6.44 mmol (86%)
TLC	$R_f = 0.33$ (SiO_2 , <i>n</i> -pentane)
$^1\text{H-NMR}$	(300 MHz, CDCl_3) δ 7.47 – 7.27 (m, 10H), 6.53 (d, $J = 15.9$ Hz, 1H), 6.43 (dt, $J = 15.7, 6.4$ Hz, 1H), 3.62 (d, $J = 6.3$ Hz, 2H).
$^{13}\text{C-NMR}$	(75 MHz, CDCl_3) δ 140.25, 137.55, 131.15, 129.32, 128.78, 128.60, 127.21, 126.29, 126.22, 39.45.
GC-MS	$t_R = 9.01$ min, (EI, 70 eV): $m/z = 194$ [M^+], 179, 165, 152, 115, 103, 91, 78, 65, 51.

Analytical data were in full agreement with E. Alacid, C. Nájera, *Org. Lett.* **2008**, *10*, 5011–5014.

1,3-diphenylpropan-1-ol

A round-bottom flask was charged with benzaldehyde (35.0 mmol, 3.61 g) in THF (40 mL) under inert atmosphere and cooled to 0 °C. A freshly prepared solution of benzyl magnesium bromide in THF (40 mmol; 0.5 M) was added dropwise. The solution was allowed to warm to room temperature and was stirred overnight. After 18 h an aqueous solution of hydrochloric acid (1 M, 100 mL) was added slowly. The crude product was extracted with diethyl ether Et₂O (3 × 50 mL) and the combined organic layers were dried over Na₂SO₄ and subjected to silica gel flash chromatography (hexanes/ethyl acetate 9/1).



C₁₅H₁₆O

212.29 g/mol

Appearance

yellowish oil

Yield

4.43 g, 20.9 mmol (60%)

TLC

R_f = 0.14 (SiO₂, hexanes/ethyl acetate = 9/1)

¹H-NMR

(300 MHz, CDCl₃) δ 7.48 – 7.33 (m, 7H), 7.27 (dd, *J* = 7.7, 1.4 Hz, 3H), 4.70 (dd, *J* = 7.7, 5.6 Hz, 1H), 2.88 (s, 1H), 2.76 (m, 2H), 2.31 – 1.95 (m, 2H).

¹³C-NMR

(75 MHz, CDCl₃) δ 144.70, 141.97, 128.61, 128.53, 127.71, 126.14, 125.99, 73.88, 40.56, 32.16.

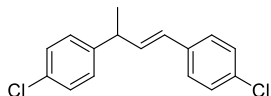
GC-MS

t_R = 9.57 min, (EI, 70 eV): *m/z* = 212 [M⁺], 194, 179, 165, 152, 133, 116, 107, 91, 79, 65, 51.

Analytical data were in full agreement with R. Martínez, D. J. Ramón, M. Yus, *Tetrahedron* **2006**, 62, 8988–9001.

1,3-Bis-(4-chloro-phenyl)-1-butene

Synthesis following the procedure described by J. R. Cabrero-Antonino, A. Leyva-Pérez, A. Corma, *Adv. Synth. Catal.* **2010**, 352, 1571–1576.



C₁₆H₁₄Cl₂

277.19 g/mol

Appearance

yellowish liquid

Yield

470 mg, 1.70 mmol, 34%

TLC

R_f = 0.46 (SiO₂, *n*-pentane)

¹H-NMR	(400 MHz, CDCl ₃) δ 7.33–7.11 (m, 8H), 6.41–6.21 (m, 2H), 3.61 (m, 1H), 1.44 (d, <i>J</i> = 7.0 Hz, 3H).
¹³C-NMR	(101 MHz, CDCl ₃) δ 145.5, 140.6, 131.7, 131.5, 129.7, 128.6, 128.4, 128.4, 39.7, 38.9, 33.2, 22.5.
GC-MS	<i>t</i> _R = 10.97 min, (EI, 70 eV): <i>m/z</i> = 276 [M ⁺], 241, 212, 191, 149, 125, 103, 91, 77, 65, 51.

Analytical data were in full agreement with J. R. Cabrero-Antonino, A. Leyva-Pérez, A. Corma, *Adv. Synth. Catal.* **2010**, 352, 1571–1576.

N-(1-Phenylvinyl)acetamide

Synthesis following the procedure described by J. T. Reeves, Z. Tan, Z. S. Han, G. Li, Y. Zhang, Y. Xu, D. C. Reeves, N. C. Gonnella, S. Ma, H. Lee, B. Z. Lu, C. H. Senanayake, *Angew. Chem. Int. Ed.* **2012**, 51, 1400–1404.



C₁₀H₁₁NO

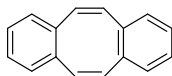
161.20 g/mol

Appearance	colorless solid
Yield	235 mg, 1.48 mmol (15%)
¹H-NMR	(300 MHz, DMSO- <i>d</i> ₆) δ 9.34 (s, 1H), 7.49 – 7.31 (m, 5H), 5.62 (s, 1H), 4.98 (s, 1H), 2.01 (s, 3H).
¹³C-NMR	(75 MHz, DMSO- <i>d</i> ₆) δ 169.04, 141.36, 140.94, 137.93, 128.18, 126.13, 101.78, 23.64.
GC-MS	<i>t</i> _R = 7.87 min, (EI, 70 eV): <i>m/z</i> = 161 [M ⁺], 146, 132, 119, 104, 77, 63, 51.

Analytical data were in full agreement with J. T. Reeves, Z. Tan, Z. S. Han, G. Li, Y. Zhang, Y. Xu, D. C. Reeves, N. C. Gonnella, S. Ma, H. Lee et al., *Angew. Chem. Int. Ed.* **2012**, 51, 1400–1404.

Dibenzo[*a,e*]cyclooctatetraene (dct)

Synthesis following the procedure described by G. Franck, M. Brill, G. Helmchen, *J. Org. Chem.* **2012**, 89, 55–65.



C₁₆H₁₂

204.27 g/mol

Appearance	colorless solid
Yield	912 mg, 4.46 mmol (47%)
¹H-NMR	(300 MHz, CDCl ₃): δ = 7.19–7.13 (m, 4H), 7.10–7.02 (m, 4H), 6.76 (s, 4H).
¹³C-NMR	(75 MHz, CDCl ₃): δ = 137.1, 133.3, 129.1, 126.8.
GC-MS	<i>t</i> _R = 9.35 min, (EI, 70 eV): <i>m/z</i> = 204 [M ⁺].

Analytical data were in full agreement with G. Franck, M. Brill, G. Helmchen, *J. Org. Chem.* **2012**, 89, 55-65.

1-Phenylcyclohexene

A solution of phenylmagnesiumbromide in THF (1 M, 50.0 mmol, 50.0 mL) was added dropwise to a solution of cyclohexanone (30.0 mmol, 3.20 mL) in THF (30 mL) at 0 °C. The reaction mixture was allowed to gain room temperature while stirring for 2 h. Then, the reaction mixture was cooled to 0 °C and quenched with aqueous HCl (5%, 25 mL) and extracted with Et₂O (3 × 15 mL). The combined organic layers were dried (MgSO₄), concentrated and dissolved in toluene (50 mL). After addition of a tip of a spatula *p*-toluenesulfonic acid the reaction mixture was heated under reflux for 12 h. The reaction mixture was concentrated and subjected to silica gel flash chromatography (*n*-pentane).



C₁₂H₁₄

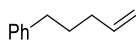
158.24 g/mol

Appearance	colorless liquid
Yield	1.14 g, 7.22 mmol (24%)
TLC	<i>R</i> _f = 0.36 (SiO ₂ , <i>n</i> -pentane)
¹H-NMR	(300 MHz, CDCl ₃) δ 7.49–7.38 (m, 2H), 7.34 (m, 2H), 7.27–7.19 (m, 1H), 6.15 (m, 1H), 2.44 (m, 2H), 2.30–2.14 (m, 2H), 1.90–1.75 (m, 2H), 1.75–1.61 (m, 2H).
¹³C-NMR	(101 MHz, CDCl ₃) δ 142.8, 136.7, 128.3, 126.6, 125.0, 124.8, 27.5, 26.0, 23.2, 22.3.
GC-MS	<i>t</i> _R = 7.35 min, (EI, 70 eV): <i>m/z</i> = 158 [M ⁺], 143, 129, 113, 91, 77, 51.

Analytical data were in full agreement with M. A. Reichle, B. Breit, *Angew. Chem. Int. Ed.* **2012**, 51, 5730–5734.

Pent-4-en-1-ylbenzene

A flask was equipped with 2-phenylethylbromide (3.40 mmol, 629 mg) and dissolved in THF (4 mL) under inert atmosphere. A freshly prepared solution of allylmagnesiumchloride in THF (4 mL, 2 M) was added dropwise and the resulting reaction mixture was stirred for 1 h under reflux. After cooling to room temperature, the reaction mixture was quenched with a saturated aqueous solution of NH_4Cl (10 mL) and extracted with CH_2Cl_2 (3×10 mL). The combined organic layers were dried over Na_2SO_4 , concentrated and subjected to silica gel flash chromatography (hexanes/ethyl acetate = 98/2).

 $\text{C}_{11}\text{H}_{14}$

146.23 g/mol

Appearance

colorless oil

Yield

348 mg, 2.38 mmol (70%)

 ^1H -NMR

(300 MHz, CDCl_3) δ 7.30 – 7.13 (m, 5H), 5.82 (ddt, J = 16.9, 10.2, 6.6 Hz, 1H), 5.06 – 4.93 (m, 2H), 2.65 – 2.57 (m, 2H), 2.08 (dd, J = 14.6, 6.9 Hz, 2H), 1.77 – 1.65 (m, 2H).

 ^{13}C -NMR

(75 MHz, CDCl_3) δ 141.42, 137.57, 127.42, 127.23, 124.64, 113.67, 34.28, 32.26, 29.59.

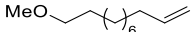
GC-MS

t_R = 5.77min, (EI, 70 eV): m/z = 146 [M^+], 131, 117, 105, 92, 77, 65, 55, 51.

Analytical data were in full agreement with J. C. Anderson, R. H. Munday, *J. Org. Chem.* **2004**, 69, 8971–8974.

11-Methoxyundec-1-ene

A 100 mL flask was charged with NaH-suspension in paraffine (60%, 22.5 mmol, 0.90 g) in THF (30 mL) and cooled to 0 °C. After dropwise addition of 11-undec-1-enol (15 mmol, 2.55 g) the reaction mixture was allowed to gain room temperature while stirring for 2 h. Methyl iodide (15 mmol, 2.55 g) was added and the reaction mixture was heated under reflux for 3 h. Then, the reaction mixture was quenched with an aqueous saturated solution of NH_4Cl (5 mL) and H_2O (5 mL) and extracted with Et_2O (3×10 mL). The combined organic layers were dried (Na_2SO_4), concentrated and subjected to silica gel flash chromatography (hexanes/ethyl acetate = 98/2).

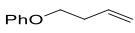
	C ₁₂ H ₂₄ O
	184.32 g/mol
Appearance	colorless liquid
Yield	2.48 g, 13.5 mmol, 90%
TLC	<i>R</i> _f = 0.36 (SiO ₂ , hexanes/ethyl acetate = 98/2)
¹H-NMR	(400 MHz, CDCl ₃) δ 5.81 (ddt, <i>J</i> = 16.9, 10.2, 6.7 Hz, 1H), 4.99 (ddd, <i>J</i> = 17.1, 3.7, 1.6 Hz, 1H), 4.93 (ddt, <i>J</i> = 10.2, 2.3, 1.2 Hz, 1H), 3.36 (t, <i>J</i> = 6.7 Hz, 2H), 3.33 (s, 3H), 2.08 – 1.99 (m, 2H), 1.61 – 1.51 (m, 2H), 1.36 – 1.24 (m, 11H).
¹³C-NMR	(101 MHz, CDCl ₃) δ 139.25, 114.10, 72.99, 58.53, 33.81, 29.65, 29.54, 29.49, 29.43, 29.13, 28.94, 26.14.
GC-MS	<i>t</i> _R = 6.73 min, (EI, 70 eV): <i>m/z</i> = 184 [M ⁺], 169, 152, 137, 124, 109, 95, 82, 67, 55.
HRMS	(CI, <i>m/z</i>): found 184.1829 [M ⁺] (calculated 184.1827).
FT-IR	(ATR-film) in [cm ⁻¹] 3077 (w), 2978 (w), 2924 (s), 2854 (s), 1641 (m), 1461 (m), 1387 (w), 1196 (w), 1119 (s), 992 (m), 908 (s), 722 (m), 635 (w).

General procedure for phenylalkenylether synthesis

A flask was charged with a phenol derivative (15.0 mmol) and triphenylphosphine (15.0 mmol, 3.93 g) under an inert atmosphere. After solvation in dry THF (25 mL) 3-buten-1-ol (15.0 mmol, 1.08 g) was added and the stirred solution was cooled by an external ice/water bath. Diisopropyl azodicarboxylate (16.5 mmol, 3.33 g) was added dropwise and the solution was allowed to come to room temperature and stirred for additional 18 h. After evaporation of the solvent under reduced pressure, the residue was purified by silica gel flash chromatography (hexanes).

(But-3-en-1-yloxy)benzene

Synthesis following the general procedure for phenylalkenylether synthesis.

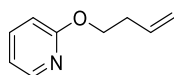
	C ₁₀ H ₁₂ O
	148.20 g/mol
Appearance	colorless liquid
Yield	1.14 g, 7.69 mmol (51%)

TLC	$R_f = 0.26$ (SiO ₂ , hexanes)
¹H-NMR	(300 MHz, CDCl ₃) δ 7.37 – 7.28 (m, 2H), 7.03 – 6.90 (m, 3H), 5.96 (ddt, $J = 17.0, 10.2, 6.7$ Hz, 1H), 5.27 – 5.11 (m, 2H), 4.05 (t, $J = 6.7$ Hz, 2H), 2.59 (qt, $J = 6.7, 1.2$ Hz, 2H).
¹³C-NMR	(75 MHz, CDCl ₃) δ 158.94, 134.56, 129.49, 120.73, 117.05, 114.61, 67.12, 33.74.
GC-MS	$t_R = 5.93$ min, (EI, 70 eV): $m/z = 148$ [M ⁺], 120, 107, 94, 77, 65, 55.

Analytical data were in full agreement with J. Niu, H. Zhou, Z. Li, J. Xu, S. Hu, *J. Org. Chem.* **2008**, 73, 7814–7817.

2-(but-3-en-1-yloxy)pyridine

Synthesis following the general procedure for phenylalkenylether synthesis.



C₉H₁₁NO

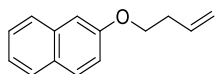
198.26 g/mol

Appearance	yellowish liquid
Yield	949 mg, 6.36 mmol (42%)
TLC	$R_f = 0.26$ (SiO ₂ , hexanes/Et ₂ O = 30/1)
¹H-NMR	(300 MHz, CDCl ₃) δ 8.15 (ddd, $J = 5.1, 2.0, 0.7$ Hz, 1H), 7.56 (ddd, $J = 8.4, 7.1, 2.0$ Hz, 1H), 6.85 (ddd, $J = 7.1, 5.1, 0.9$ Hz, 1H), 6.73 (dt, $J = 8.4, 0.8$ Hz, 1H), 5.91 (ddt, $J = 17.0, 10.2, 6.7$ Hz, 1H), 5.16 (ddd, $J = 17.2, 3.4, 1.6$ Hz, 1H), 5.09 (ddd, $J = 10.2, 3.1, 1.2$ Hz, 1H), 4.35 (t, $J = 6.8$ Hz, 2H), 2.54 (qt, $J = 6.8, 1.4$ Hz, 2H).
¹³C-NMR	(75 MHz, CDCl ₃) δ 163.77, 146.76, 138.64, 134.72, 116.84, 116.64, 111.19, 65.09, 33.47.
GC-MS	$t_R = 5.70$ min, (EI, 70 eV): $m/z = 149$ [M ⁺], 132, 120, 108, 95, 78, 67, 51.
HRMS	(APCI, m/z): found 150.0917 [M+H ⁺] (calculated 150.0913).

FT-IR (ATR-film) in [cm⁻¹] 3079 (w), 3018 (w), 2945 (w), 1595 (m), 1571 (m), 1468 (m), 1433 (m), 1312 (w), 1288 (m), 1272 (w), 1252 (w), 1143 (w), 1043 (w), 1020 (w), 989 (w), 912 (w), 779 (m), 548 (m), 533 (m), 495 (m).

2-(But-3-en-1-yloxy)naphthalene

Synthesis following the general procedure for phenylalkenylether synthesis.



C₁₄H₁₄O

198.26 g/mol

Appearance yellowish liquid

Yield 2.50 g, 12.61 mmol (84%)

TLC *R*_f = 0.32 (SiO₂, hexanes)

¹H-NMR (300 MHz, CDCl₃) δ 7.81 – 7.69 (m, 3H), 7.44 (ddd, *J* = 8.2, 6.9, 1.3 Hz, 1H), 7.34 (ddd, *J* = 8.1, 6.9, 1.3 Hz, 1H), 7.20 – 7.12 (m, 2H), 5.97 (ddt, *J* = 17.0, 10.2, 6.7 Hz, 1H), 5.22 (dq, *J* = 17.2, 1.6 Hz, 1H), 5.15 (ddd, *J* = 10.2, 3.0, 1.2 Hz, 1H), 4.15 (t, *J* = 6.7 Hz, 2H), 2.63 (qt, *J* = 6.7, 1.3 Hz, 2H).

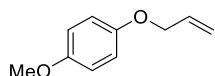
¹³C-NMR (75 MHz, CDCl₃) δ 156.88, 134.57, 134.50, 129.39, 128.97, 127.66, 126.74, 126.35, 123.58, 119.01, 117.12, 106.67, 67.21, 33.65.

GC-MS *t*_R = 8.99 min, (EI, 70 eV): *m/z* = 198 [M⁺], 183, 170, 157, 143, 126, 114, 101, 89, 77, 63, 53.

Analytical data were in full agreement with B. Branchi, C. Galli, P. Gentili, *Eur. J. Org. Chem.* **2002**, 2002, 2844–2854.

1-(Allyloxy)-4-methoxybenzene

Synthesis following the procedure described by H. B. Mereyala, S. R. Gurralla, S. K. Mohan, *Tetrahedron*, **1999**, 55, 11331-11342.



C₁₀H₁₂O₂

164.20 g/mol

Appearance colorless liquid

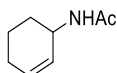
Yield 1.41 g, 8.59 mmol (86%)

TLC	$R_f = 0.27$ (SiO ₂ , PE/EE = 95/5)
¹H-NMR	(300 MHz, CDCl ₃) δ 6.91 – 6.79 (m, 4H), 6.06 (ddt, $J = 17.3, 10.6, 5.3$ Hz, 1H), 5.41 (dq, $J = 17.3, 1.6$ Hz, 1H), 5.28 (dq, $J = 10.6, 1.4$ Hz, 1H), 4.49 (dt, $J = 5.3, 1.5$ Hz, 2H), 3.77 (s, 3H).
¹³C-NMR	(75 MHz, CDCl ₃) δ 153.89, 152.74, 133.62, 117.55, 115.71, 114.60, 69.51, 55.72.
GC-MS	$t_R = 6.88$ min, (EI, 70 eV): $m/z = 164$ [M ⁺], 123, 109, 95, 80, 63, 51.

Analytical data were in full agreement with A. B. Naidu, E. A. Jaseer and G. Sekar *J. Org. Chem.* **2009**, 74, 3675–3679.

N-(cyclohex-2-en-1-yl)acetamide

A mixture of 3-bromocyclohexene (9.3 mmol, 1.50 g) in CCl₄ (15 mL) and sodiumazide (30.9 mmol, 2.00 g) in H₂O (15 mL) was stirred at room temperature for 2 days. The aqueous phase was extracted with CH₂Cl₂ (2 × 25 mL) and ethyl acetate (1 × 25 mL). The combined organic layers were dried (Na₂SO₄), concentrated and diluted in THF (6 mL). After the addition of triphenylphosphine (16.8 mmol, 4.40 g) the reaction mixture was stirred for 2 h. Then, aqueous NaOH (1 M, 40 mL) was added, the reaction mixture was stirred for 18 h, extracted with ethyl acetate (1 × 50 mL) and the organic layer was extracted with aqueous HCl (1 M, 3 × 15 mL). The combined aqueous layers were concentrated and suspended in CH₂Cl₂. After the addition of Et₃N (27.9 mmol, 3.87 mL), 4-(dimethylamino)-pyridine (0.9 mmol, 113.6 mg) and acetyl chloride (10.2 mmol, 0.73 mL) the reaction mixture was stirred at room temperature for 3 h. The reaction mixture was washed with aqueous saturated NaCl, dried (Na₂SO₄), concentrated and subjected to silica gel flash chromatography (hexanes/ethyl acetate = 1/4).



C₈H₁₃NO

139.19 g/mol

Appearance	colorless solid
Yield	643 mg, 4.60 mmol, 50%
TLC	$R_f = 0.2$ (SiO ₂ , hexanes/ethyl acetate = 1/4)
¹H-NMR	(400 MHz, CDCl ₃) δ 5.95–5.77 (m, 1H), 5.74–5.32 (m, 2H), 4.46 (m, 1H), 1.99 (m, 2H), 1.96 (s, 3H), 1.93–1.81 (m, 1H), 1.71–1.58 (m, 2H), 1.58–1.42 (m, 1H)

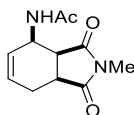
¹³C-NMR (101 MHz, CDCl₃) δ 169.2, 130.9, 127.7, 44.7, 29.5, 24.8, 23.5, 19.7.

GC-MS *t*_R = 6.68 min, (EI, 70 eV): *m/z* = 139 [M⁺], 111, 97, 79, 69, 60, 54.

Analytical data were in full agreement with Y. Leblanc, R. Zamboni, M. A. Bernstein, *J. Org. Chem.* **1991**, 56, 1971–1972.

***N*-Methyl-3-acetamido-1,2,3,6-tetrahydrophthalimide**

Synthesis following the procedure described by R. Fichtler, J.-M. Neudörfl, A. Jacobi von Wangelin, *Org. Biomol. Chem.* **2011**, 9, 7224–7236.



C₁₁H₁₄N₂O₃

222.24 g/mol

Appearance colorless solid

Yield 488 mg, 2.2 mmol (15%)

TLC *R*_f = 0.13 (SiO₂, hexanes/ethyl acetate = 1/4)

¹H-NMR (300 MHz, CDCl₃) δ 7.27 (s, 1H), 5.86 (m, 1H), 5.72 (m, 1H), 4.81–4.61 (m, 1H), 3.19 (m, 2H), 2.94 (s, 3H), 2.71 (m, 1H), 2.21 (m, 1H), 2.08 (s, 3H).

¹³C-NMR (75 MHz, CDCl₃) δ 179.3, 179.2, 169.9, 132.9, 127.4, 45.2, 42.5, 38.8, 25.0, 24.1, 23.5.

GC-MS *t*_R = 9.76 min, (EI, 70 eV): *m/z* = 222 [M⁺], 204, 179, 165, 151, 136, 120, 105, 94, 79, 69, 58.

Analytical data were in full agreement with D. Strübing, H. Neumann, A. Jacobi von Wangelin, S. Klaus, S. Hübner, M. Beller, *Tetrahedron* **2006**, 62, 10962–10967.

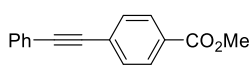
General procedure for alkyne synthesis by Sonogashira coupling

A 50 mL *Schlenk* tube with a screw cap was equipped with a stirring bar, charged with CuI (0.14 mmol, 27.0 mg), (0.04 mmol, 25.2 mg) Pd(Cl)₂(PPh₃)₂ and 3.59 mmol of the substituted iodo-benzene, evacuated three times and purged with nitrogen. Then 4 mL THF and 4 mL Et₃N were added. Phenylacetylene (3.59 mmol, 395 μL) was added slowly via syringe and the reaction mixture was stirred at room temperature for 15 h. Then, CH₂Cl₂ (25 mL) and aqueous HCl (25 mL, 1 M) were added and the reaction mixture was extracted with CH₂Cl₂ (2 × 25 mL). The combined organic layers were dried (Na₂SO₄)

and the solvent removed by vacuum evaporation. The residue was then purified by silica gel flash chromatography (hexanes)

Methyl 4-(phenylethynyl)benzoate

Synthesis following the general procedure for alkyne synthesis by Sonogashira coupling.



$C_{16}H_{12}O_2$

236.27 g/mol

Appearance

pale yellow solid

Yield

1.35 g, 5.71 mmol (82%)

TLC

R_f = 0.38 (SiO₂, hexanes/ethyl acetate = 9/1)

¹H-NMR

(300 MHz, CDCl₃) δ 8.02 (m, 2H), 7.60 (m, 1H), 7.59 – 7.51 (m, 3H), 7.41 – 7.32 (m, 3H), 3.92 (s, 3H).

¹³C-NMR

(75 MHz, CDCl₃) δ 166.57, 131.76, 131.53, 129.55, 129.47, 128.80, 128.47, 128.02, 122.71, 92.40, 88.67, 52.26.

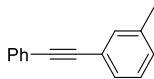
GC-MS

t_R = 10.59 min, (EI, 70 eV): m/z = 236 [M⁺], 205, 176, 151, 126, 102, 91, 76, 63, 51.

Analytical data were in full agreement with T. Schabel, C. Belger, B. Plietker, *Org. Lett.* **2013**, *15*, 2858–2861.

1-Methyl-3-(phenylethynyl)benzene

Synthesis following the general procedure for alkyne synthesis by Sonogashira coupling.



$C_{15}H_{12}$

192.26 g/mol

Appearance

colorless solid

Yield

1.76 g, 9.14 mmol (91%)

TLC

R_f = 0.55 (SiO₂, *n*-pentane)

¹H-NMR

(300 MHz, CDCl₃) δ 7.57 – 7.48 (m, 2H), 7.40 – 7.31 (m, 5H), 7.24 (t, J = 7.5 Hz, 1H), 7.15 (d, J = 7.6 Hz, 1H), 2.36 (s, 3H).

¹³C-NMR (75 MHz, CDCl₃) δ 138.04, 132.20, 131.61, 129.19, 128.70, 128.35, 128.26, 128.19, 77.45, 77.03, 76.61, 21.27.

GC-MS *t*_R = 9.23 min, (EI, 70 eV): *m/z* = 192 [M⁺], 176, 165, 152, 139, 126, 115, 95, 74, 63, 51.

Analytical data were in full agreement with H. Kim, P. H. Lee, *Adv. Synth. Catal.* **2009**, 351, 2827–2832.

(1-cyclopropylvinyl)benzene

Synthesis following the general procedure for styrene synthesis in a Wittig reaction.



C₁₁H₁₂

144.22 g/mol

Appearance colorless liquid

Yield 1.27 g, 8.8 mmol (80%)

TLC *R*_f = 0.53 (SiO₂, hexanes)

¹H-NMR (300 MHz, CDCl₃) δ = 7.67 – 7.57 (m, 2H), 7.42 – 7.26 (m, 3H), 5.30 (d, *J*=1.0, 1H), 4.95 (t, *J*=1.2, 1H), 1.67 (tt, *J*=8.3, 5.4, 1.2, 1H), 0.92 – 0.79 (m, 2H), 0.61 (ddd, *J*=6.4, 5.4, 4.1, 2H).

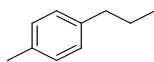
¹³C-NMR (75 MHz, CDCl₃) δ 149.47, 141.75, 128.28, 127.58, 126.25, 109.15, 77.58, 77.16, 77.16, 76.74, 15.78, 6.83.

GC-MS *t*_R = 6.31 min, (EI, 70 eV): *m/z* = 144 [M⁺], 129, 115, 103, 91, 77, 63, 51.

Analytical data were in full agreement with C. Chatalova-Sazepin, Q. Wang, G. M. Sammis, J. Zhu, *Angew. Chem. Int. Ed.* **2015**, 54, 5443–5446.

4.5.4 Hydrogenation products

1-Methyl-4-propylbenzene

 $C_{10}H_{14}$

134.22 g/mol

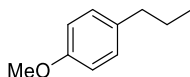
 1H -NMR(300 MHz, $CDCl_3$) δ 7.07 (s, 4H), 2.54 (t, 2H), 2.31 (s, 3H), 1.61 (m, 2H), 0.93 (t, 3H). ^{13}C -NMR(75 MHz, $CDCl_3$) δ 139.55, 134.92, 128.83, 128.28, 37.51, 37.58, 24.65, 20.94, 13.80.

GC-MS

 t_R = 5.09 min, (EI, 70 eV): m/z = 134 [M^+].

Analytical data were in full agreement with N. Sakai, K. Nagasawa, R. Ikeda, Y. Nakaïke, T. Konakahara, *Tetrahedron Lett.* **2011**, 52, 3133-3136.

1-Methoxy-4-propylbenzene

 $C_{10}H_{14}O$

150.22 g/mol

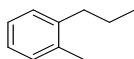
 1H -NMR(300 MHz, $CDCl_3$) δ 7.08 (d, J = 8.1 Hz, 2H), 6.81 (d, J = 8.2 Hz, 2H), 3.76 (s, 3H), 2.51 (t, J = 7.6 Hz, 2H), 1.71-1.46 (m, 2H), 0.92 (t, J = 7.3 Hz, 3H) ^{13}C -NMR(75 MHz, $CDCl_3$) δ 157.58, 134.71, 129.24, 113.55, 55.12, 37.42, 37.09, 24.75, 13.71.

GC-MS

 t_R = 5.07 min, (EI, 70 eV): m/z = 150 [M^+].

Analytical data were in full agreement with A. Dhakshinamoorthy, A. Sharmila, K. Pitchumani, *Chem. Eur. J.* **2010**, 16, 1128-1132.

1-Methyl-2-propylbenzene

 $C_{10}H_{14}$

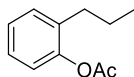
134.22 g/mol

 1H -NMR(300 MHz, $CDCl_3$) δ 7.14-7.09 (m, 4H), 2.6-2.54 (m, 2H), 2.3 (s, 3H), 1.67-1.54 (m, 2H), 0.98 (t, 3H). ^{13}C -NMR(75 MHz, $CDCl_3$) δ 140.86, 135.87, 130.03, 128.83, 125.76, 125.71, 35.39, 23.35, 19.28, 14.17.

GC-MS $t_R = 5.18$ min, (EI, 70 eV): $m/z = 134$ [M⁺].

Analytical data were in full agreement with X. Qian, L. N. Dawe, C. M. Kozak, *Dalton Trans.* **2011**, 40, 933-943.

2-Propylphenyl acetate



C₁₁H₁₄O₂

178.23 g/mol

¹H-NMR (300 MHz, CDCl₃) δ 7.18 (dd, $J = 13.8, 6.0$ Hz, 3H), 7.00 (d, $J = 7.5$ Hz, 1H), 2.53–2.40 (t, 2H), 2.29 (s, 3H), 1.59 (m, $J = 15.0, 7.5$ Hz, 2H), 0.93 (t, $J = 7.3$ Hz, 3H).

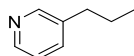
¹³C-NMR (75 MHz, CDCl₃) δ 169.64, 148.97, 134.27, 130.26, 126.89, 126.04, 122.22, 32.21, 23.10, 20.89, 14.00.

GC-MS $t_R = 5.84$ min, (EI, 70 eV): $m/z = 178$ [M⁺].

HRMS (EI, 70 eV): $m/z = 178.009 \pm 5$ ppm

FT-IR (ATR-film) in [cm⁻¹]: 3466 (w), (w), 3026 (w), 2958 (m), 2926 (m), 2866 (m), 1759 (s), 1636 (w), 1580 (w), 1487 (s), 1453 (s), 1367 (s), 1201 (s), 1179 (s), 1115 (s), 1036 (m), 1009 (m), 940 (m), 856 (w), 830 (m), 786 (m), 751 (s), 660 (m).

3-Propylpyridine



C₈H₁₁N

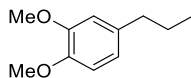
121.18 g/mol

¹H-NMR (300 MHz, CDCl₃) δ 8.43 (d, $J = 4.8$ Hz, 2H), 7.49 (d, $J = 7.5$ Hz, 1H), 7.26–7.12 (m, 1H), 2.59 (t, $J = 7.6$ Hz, 2H), 1.78–1.32 (m, 2H), 0.95 (t, $J = 7.3$ Hz, 3H).

¹³C-NMR (75 MHz, CDCl₃) δ 149.87, 147.07, 137.69, 135.85, 123.34, 123.20, 34.99, 24.21, 23.98, 13.60.

GC-MS $t_R = 4.20$ min, (EI, 70 eV): $m/z = 121$ [M⁺].

Analytical data were in full agreement with A. Fischer, M. J. King, F. P. Robinson, *Can. J. Chem.* **1978**, 56, 3072-3077.

1,2-Dimethoxy-4-propylbenzene $C_{11}H_{16}O_2$

180.24 g/mol

 1H -NMR

(300 MHz, $CDCl_3$) δ 6.83-6.64 (m, 3H), 3.87 (s, 3H), 3.85 (s, 3H), 2.53 (t, $J = 7.8$ Hz, 2H), 1.72-1.50 (m, 2H), 0.94 (t, $J = 7.3$ Hz, 3H).

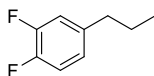
 ^{13}C -NMR

(75 MHz, $CDCl_3$) δ 148.72, 147.03, 135.36, 120.19, 111.79, 111.13, 55.81, 37.66, 24.77, 13.80.

GC-MS

$t_R = 6.59$ min, (EI, 70 eV): $m/z = 180$ [M^+].

Analytical data were in full agreement with A. R. Katritzky, S. C. Jurczyk, M. Szajda, I. V. Shcherbakova, J. N. Lam, *Synthesis* **1994**, 1994, 499-504.

1,2-Difluoro-4-propylbenzene $C_9H_{10}F_2$

156.17 g/mol

 1H -NMR

(300 MHz, $CDCl_3$) δ 7.10-6.90 (m, 3H), 2.58 (t, 2H), 1.69-1.57 (m, 2H), 0.94 (t, 3H).

 ^{13}C -NMR

(75 MHz, $CDCl_3$) δ 150.97, 147.71, 139.55, 124.13, 117.01, 116.75, 37.14, 24.35, 13.57.

GC-MS

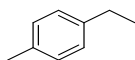
$t_R = 6.38$ min, (EI, 70 eV): $m/z = 156$ [M^+].

HRMS

(EI, 70 eV): $m/z = 156.038 \pm 5$ ppm

FT-IR

(ATR-film) in $[cm^{-1}]$: 3066 (w), 2920 (s), 2851 (m), 2358 (w), 2326 (w), 1731 (w), 1604 (w), 1518 (s), 1487 (m), 1454 (m), 1376 (w), 1260 (s), 1220 (w), 1190 (w), 1116 (m), 1093 (m), 1020, 950 (w), 916 (w), 870 (m), 812 (s), 770 (m), 756(w).

1-Ethyl-4-methylbenzene C_9H_{12}

120.19 g/mol

 1H -NMR

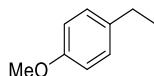
(300 MHz, $CDCl_3$) δ 7.09 (s, 4H), 2.60 (q, $J = 7.6$ Hz, 2H), 2.31 (s, 3H), 1.21 (t, $J = 7.6$ Hz, 3H).

GC-MS

$t_R = 4.36$ min, (EI, 70 eV): $m/z = 120$ [M⁺].

Analytical data were in full agreement with M. L. Kantam, R. Kishore, J. Yadav, M. Sudhakar, A. Venugopal, *Adv. Synth. Catal.* **2012**, 354, 663-669.

1-Ethyl-4-methoxybenzene



C₉H₁₂O

136.19 g/mol

¹H-NMR

(300 MHz, CDCl₃) δ 7.1 (d, 2H), 6.82 (d, 2H), 3.77 (s, 3H), 2.58 (t, 2H), 1.20 (t, 3H).

¹³C-NMR

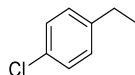
(75 MHz, CDCl₃) 157.5, 136.4, 128.7, 115.38, 55.3, 28, 15.9.

GC-MS

$t_R = 5.75$ min, (EI, 70 eV): $m/z = 136$ [M⁺].

Analytical data were in full agreement with B. Wang, H.-X. Sun, Z.-H. Sun, *Eur. J. Org. Chem.* **2009**, 22, 3688-3692.

1-Ethyl-4-chlorobenzene



C₈H₉Cl

140.61 g/mol

¹H-NMR

(300 MHz, CDCl₃) δ 7.23 (d, $J = 8.0$ Hz, 2H), 7.10 (d, $J = 8.0$ Hz, 2H), 2.60 (q, $J = 7.6$ Hz, 2H), 1.23 (t, 3H).

¹³C-NMR

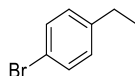
(75 MHz, CDCl₃) δ 142.63, 131.26, 129.22, 128.37, 28.28, 15.55.

GC-MS

$t_R = 4.92$ min, (EI, 70 eV): $m/z = 140$ [M⁺], 125, 105, 89, 77, 63, 51.

Analytical data were in full agreement with M. E. Sloan, A. Staubitz, K. Lee, I. Manners, *Eur. J. Org. Chem.* **2011**, 4, 672-675.

1-Ethyl-4-bromobenzene



C₈H₉Br

185.06 g/mol

¹H-NMR

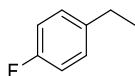
(400 MHz, CDCl₃) δ 7.45–7.35 (m, 2H), 7.09–6.96 (m, 2H), 2.59 (q, $J = 7.6$ Hz, 2H), 1.20 (t, $J = 7.6$ Hz, 3H).

^{13}C -NMR (101 MHz, CDCl_3) δ 143.2, 131.4, 129.7, 119.3, 28.4, 15.5.

GC-MS $t_R = 5.76$ min, (EI, 70 eV): $m/z = 184$ [M^+], 169, 105, 89, 77, 63, 51.

Analytical data were in full agreement with T. Maegawa, T. Takahashi, M. Yoshimura, H. Suzuka, Y. Monguchi, H. Sajiki, *Adv. Synth. Catal.* **2009**, 351, 2091–2095.

1-Ethyl-4-fluorobenzene



$\text{C}_8\text{H}_9\text{F}$

124.16 g/mol

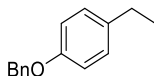
^1H -NMR (300 MHz, CDCl_3) δ 7.12–7.01 (m, 2H), 6.94–6.83 (m, 2H), 2.55 (q, $J = 7.6$ Hz, 2H), 1.15 (t, $J = 6.6$ Hz, 3H).

^{13}C -NMR (75 MHz, CDCl_3) δ 162.75, 139.78, 129.18, 129.08, 115.15, 114.84, 28.11, 15.80.

GC-MS $t_R = 3.54$ min, (EI, 70 eV): $m/z = 124$ [M^+].

Analytical data were in full agreement with E. C. Taylor, E. C. Bigham, D. K. Johnson, *J. Org. Chem.* **1977**, 42, 362–363.

1-Benzyloxy-4-ethylbenzene



$\text{C}_{15}\text{H}_{16}\text{O}$

212.29 g/mol

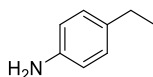
^1H -NMR (300 MHz, CDCl_3) δ 7.51 – 7.30 (m, 5H), 7.18 – 7.11 (m, 2H), 6.97 – 6.89 (m, 2H), 5.07 (s, 2H), 2.62 (q, $J = 7.6$ Hz, 2H), 1.24 (t, $J = 7.6$ Hz, 3H).

^{13}C -NMR (75 MHz, CDCl_3) δ 156.89, 137.30, 136.72, 128.78, 128.60, 127.92, 127.52, 114.72, 70.08, 28.03, 15.93.

GC-MS $t_R = 9.17$ min, (EI, 70 eV): $m/z = 212$ [M^+], 122, 107, 91, 77, 65, 51.

Analytical data were in full agreement with C. Zhu, N. Yukimura, M. Yamane, *Organometallics* **2010**, 29, 2098–2103.

4-Ethylaniline



C₈H₁₁N

121.18 g/mol

¹H-NMR

(400 MHz, CDCl₃) δ 6.98 (d, 2H), 6.61 (d, 2H), 3.34 (bs, 2H), 2.53 (q, 2H), 1.19 (t, 3H).

¹³C-NMR

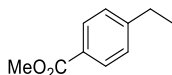
(101 MHz, CDCl₃) δ 144.1, 134.5, 128.6, 115.4, 28, 16.

GC-MS

*t*_R = 5.75 min, (EI, 70 eV): *m/z* = 121 [M⁺].

Analytical data were in full agreement with B. Wang, H.-X. Sun, G.-Q. Lin, Z.-H. Sun, *Adv. Synth. Catal.* **2009**, 351, 415-422.

Methyl 4-ethylbenzoate



C₁₀H₁₂O₂

164.20 g/mol

¹H-NMR

(400 MHz, CDCl₃) δ 7.96 (m, 2H), 7.27 (m, 2H), 3.90 (s, 3H), 2.71 (q, *J* = 7.6 Hz, 2H), 1.26 (t, *J* = 7.6 Hz, 3H).

¹³C-NMR

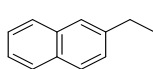
(101 MHz, CDCl₃) δ 167.2, 149.8, 129.7, 127.9, 127.7, 52.0, 29.0, 15.2.

GC-MS

*t*_R = 6.81 min, (EI, 70 eV): *m/z* = 164 [M⁺], 149, 133, 121, 105, 89, 77, 63, 51.

Analytical data were in full agreement with R. J. Rahaim, R. E. Maleczka, *Org. Lett.* **2011**, 13, 584–587.

2-Ethynaphthalene



C₁₂H₁₂

156.22 g/mol

¹H-NMR

(400 MHz, CDCl₃) δ 7.84–7.73 (m, 3H), 7.62 (s, 1H), 7.48–7.31 (m, 3H), 2.81 (q, *J* = 7.6 Hz, 2H), 1.33 (t, *J* = 7.6 Hz, 3H).

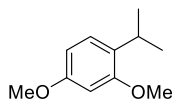
¹³C-NMR

(101 MHz, CDCl₃) δ 141.8, 133.7, 132.0, 127.8, 127.6, 127.4, 127.1, 125.8, 125.6, 125.0, 77.4, 77.0, 76.7, 29.1, 15.5.

GC-MS $t_R = 7.33$ min, (EI, 70 eV): $m/z = 156$ [M^+], 141, 128, 115, 102, 89, 77, 63, 51.

Analytical data were in full agreement with M. E. Sloan, A. Staubitz, K. Lee, I. Manners, *Eur. J. Org. Chem.* **2011**, 4, 672–675.

1-Isopropyl-2,4-dimethoxybenzene



$C_{11}H_{16}O_2$

180.25 g/mol

1H -NMR (300 MHz, $CDCl_3$) δ 7.15 – 7.05 (m, 1H), 6.50 – 6.40 (m, 2H), 3.81 (s, 3H), 3.80 (s, 3H), 3.23 (hept, $J = 6.9$ Hz, 1H), 1.19 (d, $J = 6.9$ Hz, 6H).

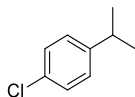
^{13}C -NMR (75 MHz, $CDCl_3$) δ 158.67, 157.67, 129.52, 126.23, 103.81, 98.50, 55.33, 26.24, 22.89.

GC-MS $t_R = 7.11$ min, (EI, 70 eV): $m/z = 180$ [M^+], 166, 150, 135, 121, 105, 91, 77, 65, 51.

HRMS (EI, m/z): found 180.1153 [M^{++}] (calculated 180.1150).

FT-IR (ATR-film) in $[cm^{-1}]$: 2961 (m), 2870 (w), 2835 (w), 1612 (m), 1587 (m), 1504 (s), 1462 (m), 1446 (w), 1298 (m), 1257 (m), 1205 (s), 1151 (s), 1115 (w), 1096 (m), 1036 (s), 937 (w), 924 (w), 833 (m), 831 (m), 795 (m), 692 (w), 635 (w), 557 (w).

1-Chloro-4-isopropylbenzene



$C_9H_{11}Cl$

154.64 g/mol

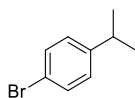
1H -NMR (300 MHz, $CDCl_3$) δ 7.25 (m, 2H), 7.21–7.09 (m, 2H), 2.89 (m, 1H), 1.23 (d, $J = 6.9$ Hz, 6H).

^{13}C -NMR (75 MHz, $CDCl_3$) δ 142.3, 131.3, 128.4, 127.8, 33.6, 23.9.

GC-MS $t_R = 5.37$ min, (EI, 70 eV): $m/z = 154$ [M^+], 139, 125, 119, 105, 89, 77, 63, 51.

Analytical data were in full agreement with S. S. Kim, C. S. Kim, *J. Org. Chem.* **1999**, 64, 9261–9264.

1-Bromo-4-isopropylbenzene



C₉H₁₁Br

199.09 g/mol

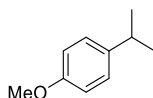
¹H-NMR (400 MHz, CDCl₃) δ 7.47–7.32 (m, 2H), 7.08 (m, 2H), 2.85 (sept, *J* = 6.9 Hz, 1H), 1.21 (d, *J* = 6.9 Hz, 6H).

¹³C-NMR (101 MHz, CDCl₃) δ 147.8, 131.3, 128.2, 119.3, 33.7, 30.9, 23.8.

GC-MS *t*_R = 6.16 min, (EI, 70 eV): *m/z* = 198 [M⁺], 185, 169, 158, 143, 119, 104, 91, 77, 63, 51.

Analytical data were in full agreement with M. A. Hall, J. Xi, C. Lor, S. Dai, R. Pearce, W. P. Dailey, R. G. Eckenhoff, *J. Med. Chem.* **2010**, 53, 5667–5675.

1-Isopropyl-4-methoxybenzene



C₁₀H₁₄O

180.24 g/mol

¹H-NMR (300 MHz, CDCl₃) δ 7.15 (d, *J* = 8.8 Hz, 2H), 6.84 (d, *J* = 8.7 Hz, 2H), 3.79 (s, 3H), 2.95 – 2.78 (m, 1H), 1.24 (s, 3H), 1.21 (s, 3H).

¹³C-NMR (75 MHz, CDCl₃) δ 156.86, 141.06, 127.26, 113.77, 55.27, 33.28, 24.24.

GC-MS *t*_R = 5.93 min, (EI, 70 eV): *m/z* = 150 [M⁺], 120, 105, 91, 77, 65, 51.

Analytical data were in full agreement with Cahiez, G.; Foulgoc, L.; Moyeux, A. *Angew. Chem. Int. Ed.* **2009**, 48, 2969–2972.

1-Chloro-2-ethylbenzene



C₈H₉Cl

140.61 g/mol

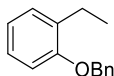
¹H-NMR (300 MHz, CDCl₃) δ 7.33 (d, *J* = 7.7 Hz, 2H), 7.25–7.07 (m, 2H), 2.76 (q, *J* = 7.5 Hz, 2H), 1.23 (t, *J* = 7.5 Hz, 3H).

^{13}C -NMR (75 MHz, CDCl_3) δ 141.59, 133.77, 129.50, 129.33, 127.05, 126.79, 26.73, 14.03.

GC-MS $t_R = 4.77$ min, (EI, 70 eV): $m/z = 140$ [M^+]

Analytical data were in full agreement with J. L. O'Connell, J. S. Simpson, P. G. Dumanski, G. W. Simpson, C. J. Easton, *Org. Biomol. Chem.* **2006**, 4, 2716-2723.

1-Benzylloxy-2-ethylbenzene



$\text{C}_{15}\text{H}_{16}\text{O}$

212.29 g/mol

^1H -NMR (300 MHz, CDCl_3) δ 7.51 – 7.30 (m, 5H), 7.19 (m, 2H), 6.98 – 6.88 (m, 2H), 5.11 (s, 2H), 2.74 (q, $J = 7.5$ Hz, 2H), 1.26 (t, $J = 7.5$ Hz, 3H).

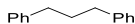
^{13}C -NMR (75 MHz, CDCl_3) δ 156.49, 137.59, 133.03, 129.09, 128.55, 127.74, 127.09, 126.79, 120.77, 111.50, 69.77, 23.44, 14.26.

GC-MS $t_R = 8.86$ min, (EI, 70 eV): $m/z = 212$ [M^+], 122, 107, 91, 77, 65, 51.

HRMS (CI, m/z): found 212.1203 [M^{++}] (calculated 212.1201).

FT-IR (ATR-film) in $[\text{cm}^{-1}]$ 3063 (w), 3035 (w), 2965 (m), 2928 (m), 2873 (w), 1601 (m), 1587 (m), 1491 (s), 1450 (s), 1379 (m), 1290 (w), 1236 (s), 1186 (w), 1125 (m), 1042 (m), 1020 (m), 851 (w), 747 (s), 733 (s), 694 (s), 624 (m), 462 (m).

1,3-Diphenylpropane



$\text{C}_{15}\text{H}_{16}$

196.29 g/mol

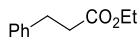
^1H -NMR (300 MHz, CDCl_3) δ 7.37 – 7.27 (m, 4H), 7.25 – 7.17 (m, 6H), 2.77 – 2.59 (m, 4H), 2.05 – 1.90 (m, 2H).

^{13}C -NMR (75 MHz, CDCl_3) δ 142.33, 128.49, 128.35, 125.78, 35.48, 33.02.

GC-MS $t_R = 8.65$ min, (EI, 70 eV): $m/z = 196$ [M^+], 179, 165, 152, 115, 105, 92, 79, 65, 51.

Analytical data were in full agreement with C.-T. Yang, Z.-Q. Zhang, Y.-C. Liu, L. Liu, *Angew. Chem. Int. Ed. Engl.* **2011**, *50*, 3904–3907.

Ethyl 3-phenylpropanoate



C₁₁H₁₄O₂

178.23 g/mol

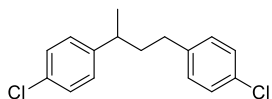
¹H-NMR (400 MHz, CDCl₃) δ 7.33–7.26 (m, 2H), 7.24–7.16 (m, 3H), 4.13 (q, *J* = 7.1 Hz, 2H), 3.01–2.90 (m, 2H), 2.66–2.58 (m, 2H), 1.24 (t, *J* = 7.1 Hz, 3H).

¹³C-NMR (101 MHz, CDCl₃) δ 172.9, 140.6, 128.5, 128.3, 126.2, 60.4, 36.0, 31.0, 14.2.

GC-MS *t*_R = 6.99 min, (EI, 70 eV): *m/z* = 178 [M⁺], 133, 104, 91, 77, 65, 51.

Analytical data were in full agreement with M. Amatore, C. Gosmini, J. Périchon, *J. Org. Chem.* **2006**, *71*, 6130–6134.

1,3-Bis-(4-chlorophenyl)-butane



C₁₆H₁₆Cl₂

279.20 g/mol

¹H-NMR (400 MHz, CDCl₃) δ 7.34–6.97 (m, 8H), 2.79–2.61 (m, 1H), 2.55–2.39 (m, 2H), 1.95–1.82 (m, 2H), 1.25 (d, *J* = 6.9 Hz, 3H).

¹³C-NMR (101 MHz, CDCl₃) δ 145.5, 140.6, 131.7, 131.5, 129.7, 128.6, 128.4, 128.4, 39.7, 38.9, 33.2, 22.5.

GC-MS *t*_R = 10.61 min, (EI, 70 eV): *m/z* = 279 [M⁺], 191, 166, 139, 121, 103, 77, 51.

HRMS (CI, *m/z*): found 278.0632 [M⁺] (calculated 278.0629).

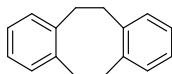
FT-IR (ATR-film) in [cm⁻¹] 3025 (w), 2960 (m), 2926 (m), 2859(w), 1894 (w), 1597 (w), 1491 (s), 1455 (m), 1408 (m), 1091 (s), 1013 (s), 825 (s), 531 (s), 489 (m).

***N*-(1-Phenylethyl)acetamide** $C_{10}H_{13}NO$

163.22 g/mol

 1H -NMR(300 MHz, $CDCl_3$) δ 7.38 – 7.23 (m, 5H), 5.80 (s, 1H), 5.19 – 5.07 (m, 1H), 2.00 (s, 3H), 1.50 (d, $J = 6.9$ Hz, 3H). **^{13}C -NMR**(75 MHz, $CDCl_3$) δ 143.03, 128.73, 127.47, 126.23, 48.90, 23.47, 21.69.**GC-MS** $t_R = 7.58$ min, (EI, 70 eV): $m/z = 163$ [M^+], 148, 120, 106, 91, 77, 65, 51

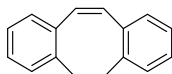
Analytical data were in full agreement with B. V. Subba Reddy, N. Sivasankar Reddy, C. Madan, J. S. Yadav *Tetrahedron Lett.* **2010**, 51, 4827–4829.

Dibenzo-1,5-cyclooctadiene $C_{16}H_{16}$

208.30 g/mol

 1H -NMR(300 MHz, $CDCl_3$) δ 7.00 (m, 8H), 3.07 (s, 8H). **^{13}C -NMR**(75 MHz, $CDCl_3$) δ 140.62, 129.69, 126.12, 35.16.**GC-MS** $t_R = 9.27$ min, (EI, 70 eV): $m/z = 208$ [M^+], 193, 178, 165, 152, 128, 115, 104, 91, 78, 63, 51.

Analytical data were in full agreement with D. Guijarro, B. Mancheno, M. Yus, *Tetrahedron.* **1992**, 48, 4593–4600.

Dibenzo-1,3,5-cyclooctatriene $C_{16}H_{14}$

206.29 g/mol

 1H -NMR(300 MHz, $CDCl_3$) δ 7.22 – 7.16 (m, 2H), 7.16 – 7.09 (m, 6H), 6.79 (s, 2H), 3.24 (s, 4H). **^{13}C -NMR**(101 MHz, $CDCl_3$) δ 139.85, 136.82, 131.51, 130.22, 129.97, 127.05, 125.55, 35.84.

GC-MS $t_R = 9.50$ min, (EI, 70 eV): $m/z = 206$ [M⁺], 191, 178, 165, 151, 139, 115, 106, 89, 77, 67, 51.

Analytical data were in full agreement with A. C. Cope, R. D. Smith, *J. Am. Chem. Soc.* **1955**, 77, 4596–4599.

Phenylcyclohexane



C₁₂H₁₆

160.26 g/mol

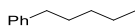
¹H-NMR (300 MHz, CDCl₃) δ 7.41–7.10 (m, 5H), 2.49 (m, 1H), 2.02–1.68 (m, 5H), 1.56–1.15 (m, 5H).

¹³C-NMR (75 MHz, CDCl₃) δ 148.1, 128.3, 126.9, 125.8, 44.7, 34.52, 27.0, 26.2.

GC-MS $t_R = 6.88$ min, (EI, 70 eV): $m/z = 160$ [M⁺], 131, 117, 104, 91, 78, 65, 51.

Analytical data were in full agreement with W. M. Czaplik, M. Mayer, A. Jacobi von Wangelin, *Angew. Chem. Int. Ed.* **2009**, 48, 607–610.

n-Pentylbenzene



C₁₁H₁₆

148.25 g/mol

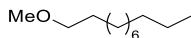
¹H-NMR (300 MHz, CDCl₃) δ 7.31 – 7.13 (m, 5H), 2.64 – 2.56 (m, 2H), 1.62 (dt, $J = 15.2$, 7.4 Hz, 2H), 1.38 – 1.26 (m, 4H), 0.89 (t, $J = 6.9$ Hz, 3H).

¹³C-NMR (75 MHz, CDCl₃) δ 141.93, 127.37, 127.18, 124.51, 34.93, 30.50, 30.20, 21.53, 13.01.

GC-MS $t_R = 5.81$ min, (EI, 70 eV): $m/z = 148$ [M⁺], 133, 105, 91, 78, 65.

Analytical data were in full agreement with L. Ackermann, A. R. Kapdi, C. Schulzke, *Org. Lett.* **2010**, 12, 2298–2301.

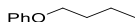
1-Methoxyundecane



C₁₂H₂₆O

186.33 g/mol

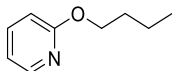
$^1\text{H-NMR}$	(400 MHz, CDCl_3) δ 3.36 (t, $J = 6.7$ Hz, 2H), 3.32 (s, 3H), 1.61–1.50 (m, 2H), 1.39–1.18 (m, 16H), 0.87 (t, $J = 6.9$ Hz, 3H).
$^{13}\text{C-NMR}$	(101 MHz, CDCl_3) δ 73.0, 58.5, 31.9, 29.7, 29.6, 29.5, 29.4, 26.2, 22.7, 14.1.
GC-MS	$t_{\text{R}} = 6.76$ min, (EI, 70 eV): $m/z = 186$ [M^+], 154, 126, 111, 97, 83, 69, 56.
HRMS	(CI, m/z): found 186.1987 [M^{++}] (calculated 186.1984).
FT-IR	(ATR-film) in $[\text{cm}^{-1}]$ 2923 (s), 2853 (s), 1745 (w), 1459 (m), 1379 (w), 1238 (w), 1195 (w), 1118 (s), 965 (w), 722 (w).

***n*-Butoxybenzene** $\text{C}_{10}\text{H}_{14}\text{O}$

150.22 g/mol

$^1\text{H-NMR}$	(300 MHz, CDCl_3) δ 7.34 – 7.26 (m, 2H), 6.99 – 6.87 (m, 3H), 3.97 (t, $J = 6.5$ Hz, 2H), 1.85 – 1.70 (m, 2H), 1.62 – 1.41 (m, 2H), 0.98 (t, $J = 7.4$ Hz, 3H).
$^{13}\text{C-NMR}$	(75 MHz, CDCl_3) δ 159.13, 129.43, 120.46, 114.49, 67.56, 31.38, 19.29, 13.90.
GC-MS	$t_{\text{R}} = 6.00$ min, (EI, 70 eV): $m/z = 150$ [M^+], 94, 77. 65. 51.

Analytical data were in full agreement with J. Niu, H. Zhou, Z. Li, J. Xu, S. Hu, *J. Org. Chem.* **2008**, 73, 7814–7817.

2-(*n*-Butoxy)pyridine $\text{C}_9\text{H}_{13}\text{NO}$

151.21 g/mol

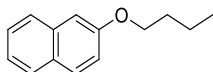
$^1\text{H-NMR}$	(300 MHz, CDCl_3) δ 8.14 (ddd, $J = 5.1, 2.0, 0.7$ Hz, 1H), 7.55 (ddd, $J = 8.4, 7.1, 2.0$ Hz, 1H), 6.83 (ddd, $J = 7.1, 5.1, 0.9$ Hz, 1H), 6.76 – 6.66 (m, 1H), 4.27 (t, $J = 6.7$ Hz, 2H), 1.81 – 1.69 (m, 2H), 1.48 (m, 2H), 0.97 (t, $J = 7.4$ Hz, 3H).
------------------------------------	--

¹³C-NMR (75 MHz, CDCl₃) δ 164.08, 146.89, 138.48, 116.45, 111.08, 65.70, 31.17, 19.29, 13.91.

GC-MS *t_R* = 5.82 min, (EI, 70 eV): *m/z* = 151 [M⁺], 121, 108, 95, 78, 67, 51.

Analytical data were in full agreement with D. Chambers, Richard, M. Parsons, G. Sandford, J. Skinner, Christopher, J. Atherton, Malcolm, S. Moilliet, John, *J. Chem. Soc., Perkin Trans. 1* **1999**, 803–810.

2-(*n*-Butoxy)naphthalene



C₁₄H₁₆O

200.28 g/mol

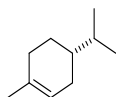
¹H-NMR (300 MHz, CDCl₃) δ 7.80 – 7.70 (m, 3H), 7.44 (ddd, *J* = 8.2, 7.0, 1.3 Hz, 1H), 7.33 (ddd, *J* = 8.1, 6.9, 1.2 Hz, 1H), 7.19 – 7.10 (m, 2H), 4.09 (t, *J* = 6.5 Hz, 2H), 1.93 – 1.77 (m, 2H), 1.63 – 1.47 (m, 2H), 1.02 (t, *J* = 7.4 Hz, 3H).

¹³C-NMR (75 MHz, CDCl₃) δ 157.13, 134.63, 129.32, 128.88, 127.65, 126.71, 126.30, 123.47, 119.06, 106.52, 67.71, 31.34, 19.36, 13.93.

GC-MS *t_R* = 9.01 min, (EI, 70 eV): *m/z* = 200 [M⁺], 144, 127, 115, 89, 57.

Analytical data were in full agreement with C. Cazorla, E. Pfordt, M.-C. Duclos, E. Metay, M. Lemaire, *Green Chem* **2011**, 13, 2482–2488.

(*R*)-4-Isopropyl-1-methyl-cyclohex-1-ene



C₁₀H₁₈

138.25 g/mol

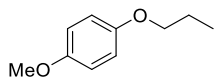
¹H-NMR (300 MHz, CDCl₃) δ 5.42 – 5.33 (m, 1H), 2.05 – 1.91 (m, 3H), 1.79 – 1.67 (m, *J* = 14.3, 4.6 Hz, 2H), 1.64 (s, 3H), 1.52 – 1.39 (m, *J* = 6.7 Hz, 1H), 1.25 – 1.15 (m, *J* = 13.8, 7.9 Hz, 2H), 0.89 (d, *J* = 4.3 Hz, 3H), 0.87 (d, *J* = 4.3 Hz, 3H).

¹³C-NMR (75 MHz, CDCl₃) δ 133.97, 121.03, 40.01, 32.30, 30.83, 28.97, 26.49, 23.50, 20.02, 19.70.

GC-MS $t_R = 4.81$ min, (EI, 70 eV): $m/z = 138$ [M^+], 123, 95, 79, 67, 55.

Analytical data were in full agreement with D. F. Schneider, M. S. Viljoen, *Tetrahedron* **2002**, 58, 5307-5315.

1-Methoxy-4-*n*-propoxybenzene



$C_{10}H_{14}O_2$

166.22 g/mol

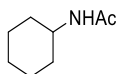
1H -NMR (300 MHz, $CDCl_3$) δ 6.84 (s, 4H), 3.87 (t, $J = 6.6$ Hz, 2H), 3.77 (s, 3H), 1.87 – 1.70 (m, 2H), 1.03 (t, $J = 7.4$ Hz, 3H).

^{13}C -NMR (75 MHz, $CDCl_3$) δ 153.65, 153.29, 115.43, 114.61, 70.17, 55.75, 22.70, 10.56.

GC-MS $t_R = 6.87$ min, (EI, 70 eV): $m/z = 166$ [M^+], 124, 109, 95, 81, 64, 53.

Analytical data were in full agreement with A. B. Naidu, E. A. Jaseer, G. Sekar, *J. Org. Chem.* **2009**, 74, 3675–3679.

N-Cyclohexylacetamide



$C_8H_{15}NO$

141.21 g/mol

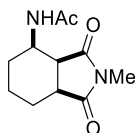
1H -NMR (400 MHz, $CDCl_3$) δ 5.32 (s, 1H), 3.87–3.65 (m, 1H), 1.95 (s, 3H), 1.94–1.87 (m, 2H), 1.75–1.66 (m, 2H), 1.66–1.55 (m, 1H), 1.43–1.29 (m, 2H), 1.23–1.04 (m, 3H).

^{13}C -NMR (101 MHz, $CDCl_3$) δ 169.0, 48.2, 33.3, 25.6, 24.9, 23.6.

GC-MS $t_R = 6.71$ min, (EI, 70 eV): $m/z = 141$ [M^+], 112, 82, 60.

Analytical data were in full agreement with R. Pelagalli, I. Chiarotto, M. Feroci, S. Vecchio, *Green Chem.* **2012**, 14, 2251-2255.

N-Methyl-3-(acetamido)-hexahydrophthalimide

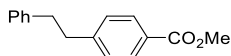


$C_{11}H_{16}N_2O_3$

224.26 g/mol

¹H-NMR	(400 MHz, CDCl ₃) δ 7.16 (s, 1H), 4.31 (ddt, <i>J</i> = 12.7, 9.0, 5.3 Hz, 1H), 3.10–2.99 (m, 2H), 2.98 (s, 3H), 2.09–2.02 (m, 1H), 2.01 (s, 3H), 2.00–1.93 (m, 1H), 1.68–1.50 (m, 2H), 1.40 (m, 1H), 1.15 (m, 1H).
¹³C-NMR	(101 MHz, CDCl ₃) δ 179.2, 179.2, 169.5, 44.9, 42.3, 41.3, 27.6, 24.7, 24.6, 23.5, 20.5.
GC-MS	<i>t</i> _R = 9.81 min, (EI, 70 eV): <i>m/z</i> = 224 [M ⁺], 207, 181, 165, 153, 138, 126, 112, 96, 80, 70, 60, 51.
HRMS	(CI, <i>m/z</i>): found 225.1234 [M+H ⁺] (calculated 225.1234).
FT-IR	(ATR-film) in [cm ⁻¹] 3324 (m), 2957 (w), 2924 (w), 2861 (w), 1769 (m), 1703 (s), 1647 (s), 1539 (s), 1460 (w), 1431 (s), 1378 (s), 1306 (m), 1271 (s), 1197 (w), 1162 (w), 1113 (m), 1050 (m), 982 (m), 952 (m), 910 (m), 762 (m), 682 (s), 596 (s), 543 (s), 454 (m).
Melting Point	128 °C

Methyl 4-phenylethylbenzoate



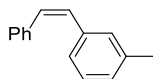
C₁₆H₁₆O₂

240.30 g/mol

¹H-NMR	(300 MHz, CDCl ₃) δ 7.99 (d, <i>J</i> = 8.1 Hz, 2H), 7.32 – 7.27 (m, 2H), 7.27 – 7.21 (m, 3H), 7.21 – 7.15 (m, 2H), 3.92 (s, 3H), 3.07 – 2.90 (m, 4H).
¹³C-NMR	(75 MHz, CDCl ₃) δ 167.17, 147.22, 141.19, 129.74, 128.60, 128.50, 128.45, 127.97, 126.14, 52.03, 37.94, 37.50.
GC-MS	<i>t</i> _R = 10.13 min, (EI, 70 eV): <i>m/z</i> = 240 [M ⁺], 209, 178, 165, 149, 118, 105, 91, 78, 65, 50.

Analytical data were in full agreement with P. J. Rushworth, D. G. Hulcoop, D. J. Fox, *J. Org. Chem.* **2013**, 78, 9517–9521.

(Z)-1-Methyl-3-styrylbenzene



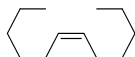
C₁₅H₁₄

194.28 g/mol

$^1\text{H-NMR}$	(400 MHz, CDCl_3) δ 7.29 – 6.98 (m, 9H), 6.58 (s, 2H), 2.27 (s, 3H).
$^{13}\text{C-NMR}$	(101 MHz, CDCl_3) δ 137.91, 137.47, 137.33, 129.31, 129.01, 128.84, 128.47, 128.39, 127.98, 127.18, 126.00, 123.54, 21.47.
GC-MS	t_{R} = 8.37 min, (EI, 70 eV): m/z = 194 [M^+], 179, 165, 152, 128, 115, 105, 91, 83, 65, 50.

Analytical data were in full agreement with F. Alonso, P. Riente, M. Yus, *Eur. J. Org. Chem.* **2009**, 2009, 6034–6042.

(Z)-6-dodecene



$\text{C}_{12}\text{H}_{24}$

168.32 g/mol

$^1\text{H-NMR}$	(300 MHz, CDCl_3) δ 5.43 – 5.28 (m, 2H), 2.08 – 1.93 (m, 4H), 1.39 – 1.24 (m, 12H), 0.89 (t, J = 6.8 Hz, 6H).
$^{13}\text{C-NMR}$	(75 MHz, CDCl_3) δ 129.92, 31.55, 29.47, 27.18, 22.60, 14.10.
GC-MS	t_{R} = 5.91 min, (EI, 70 eV): m/z = 168 [M^+], 140, 125, 111, 97, 83, 69, 55.

Analytical data were in full agreement with T. Hamatani, S. Matsubara, H. Matsuda, M. Schlosser, *Tetrahedron* **1988**, 44, 2875–2881.

1-Cyclopropyl-1-phenylethane



$\text{C}_{11}\text{H}_{14}$

146.23 g/mol

$^1\text{H-NMR}$	(300 MHz, CDCl_3) δ 7.41 – 7.26 (m, 4H), 7.25 – 7.17 (m, 1H), 1.99 (dq, J = 9.2, 7.0 Hz, 1H), 1.35 (d, J = 7.0 Hz, 3H), 0.96 (qt, J = 9.1, 8.0, 5.0 Hz, 1H), 0.65 – 0.36 (m, 2H), 0.27 – 0.09 (m, 2H).
$^{13}\text{C-NMR}$	(75 MHz, CDCl_3) δ 147.38, 128.23, 127.00, 125.89, 44.67, 21.62, 18.56, 4.64, 4.34.
GC-MS	t_{R} = 6.88 min, (EI, 70 eV): m/z = 146 [M^+], 131, 117, 105, 91, 77, 65, 51.

Analytical data were in full agreement with R. T. Hrubiec, M. B. Smith, *J. Org. Chem.* **1984**, *49*, 385-388.

4.5.5 [Li(thf)₂{Fe(tmeda)}₂(μ-AlH₅)(μ-Al₂H₉)] (**4**)

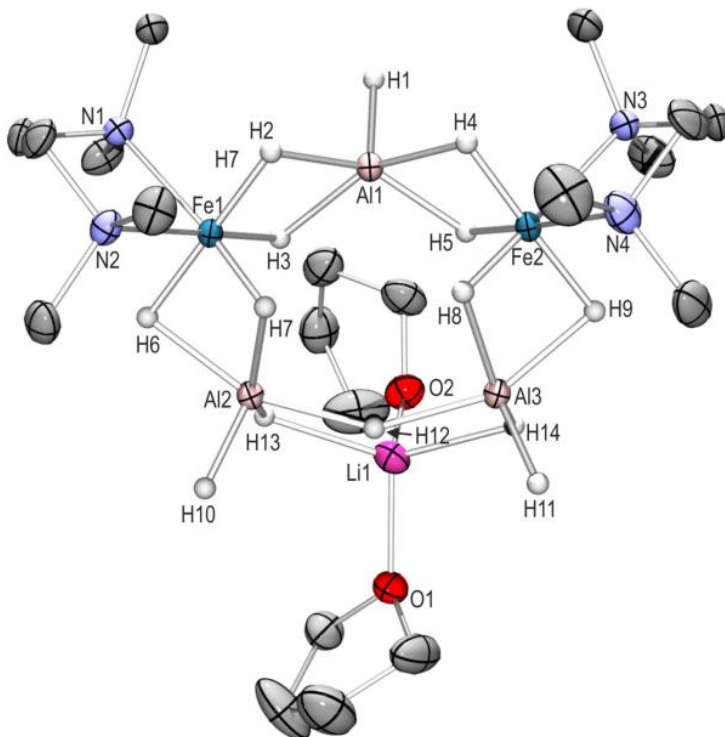
All manipulations were carried out under an inert atmosphere of purified argon, using standard *Schlenk* or glovebox techniques. Solvents (THF, *n*-hexane) were dried by refluxing over sodium and distilled under argon prior to use. Commercial lithium aluminium hydride was purified by extraction with diethyl ether and subsequent removal of the solvent under high vacuum. [FeCl₂(tmeda)]₂ was prepared according to: S. C. Davies, D. L. Hughes, G. J. Leigh, J. R. Sanders, J. S. de Souza, *J. Chem. Soc., Dalton Trans.* **1997**, 1981.

Synthesis of **4**: [FeCl₂(tmeda)]₂ (2.490 g, 5.12 mmol, 1.0 equiv.) was dissolved in THF (120 mL). The cooled (−78 °C) solution was added to a suspension of LiAlH₄ (0.912 g, 23.38 mmol) in 120 mL THF, which was also cooled at −78 °C with a dry ice acetone bath. A deep red suspension formed that was stirred for 30 min at −78 °C. Subsequently, the cold solution was filtered through a P4 frit. The filtrate was layered with pre-cooled (−20 °C) *n*-hexane. Storage at −78 °C gave a deep red crystalline solid. The mother liquor was removed with a cannula. Dark red crystals of **4** were obtained by dissolving the remaining solid in cold toluene (50 mL) at −78 °C and layering this solution with pre-cooled *n*-hexane. A suitable crystal was selected, transferred to paratone oil that was cooled under a stream of cooled N₂ gas, and mounted on a glass fibre in the cooled nitrogen stream of the diffractometer for the X-ray structure determination. The further spectroscopic characterization of the compound was prevented by its high thermal instability. Decomposition to a dark brown residue was observed at temperatures above −10 °C in the solid state as well as in solution. The crystallographic data of **4** were collected on a Bruker APEXII diffractometer equipped with a rotating anode (Mo-*K*α radiation, λ = 0.71073 Å). A red plate with the dimensions 0.19 × 0.11 × 0.05 mm^{−3}. The structures were solved using direct methods and refined against *F*² using the program suite SHELXTL-97.23.

a) *SHELXTL-Plus*, REL. 4.1; Siemens Analytical X-RAY Instruments Inc.: Madison, WI, **1990**; b) Sheldrick, G. M. *SHELXL 97*, Program for the Refinement of Structures, University of Göttingen, **1997**; c) Sheldrick, G.M., *Acta Cryst.*, 2008, **A64**, 112.

The positions of the hydrogen atoms bound to aluminium and iron were located on the Fourier difference map and refined freely. All other hydrogen atoms were placed on calculated positions and refined using a riding model. Crystal Data for C₂₀H₆₂Al₃Fe₂LiN₄O₂ (M = 590.32 g mol^{−1}): orthorhombic, space group *Pca*2₁, *a* = 15.4965(7) Å, *b* = 16.8579(7) Å, *c* = 12.6159(6) Å, *V* = 3295.8(3) Å³, *Z* = 4, *T* = 153(1) K, μ(Mo *K*α) = 0.981 mm^{−1}, *D*_{calc} = 1.190 g mm^{−3}, 30041 reflections measured (6.86 ≤ θ ≤ 27.10), 5799 unique (*R*_{int} = 0.0617, *R*_{sigma} = 0.0489) which were used in all calculations. The final *R*₁ was 0.0329 (*I* ≥ 2σ(*I*)) and *wR*₂ was 0.1674 (all data). The

crystallographic information file (CIF) has been deposited at the **CCDC**, 12 Union Road, Cambridge, CB21EZ, U.K., and can be obtained on request free of charge, by quoting the publication citation and deposition number **1034372**.



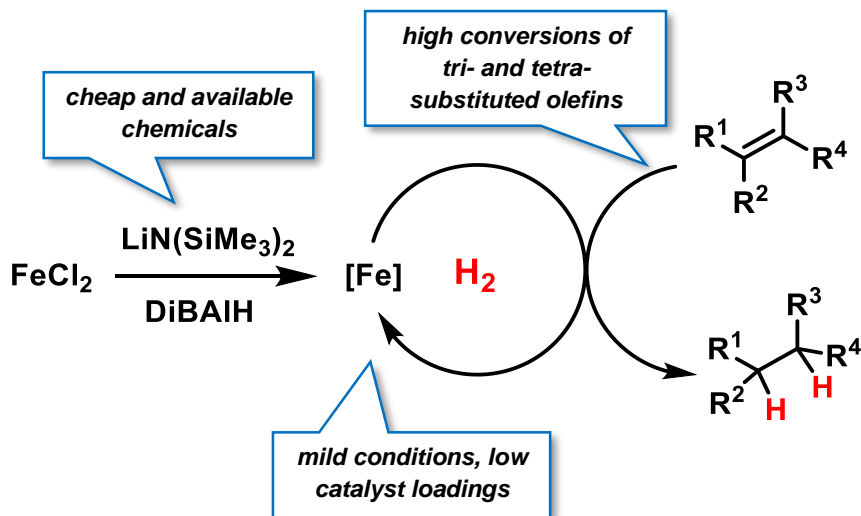
4.6 References

- [1] a) *Catalytic Hydrogenation*; L. Cerveny (ed.); Elsevier: Amsterdam, 1986. b) *The Handbook of Homogeneous Hydrogenation*; J. G. de Vries and C. J. Elsevier (eds.); Wiley-VCH: Weinheim, 2007. (c) S. Nishimura, *Handbook of Heterogeneous Catalytic Hydrogenation for Organic Synthesis*; Wiley: New York, **2001**.
- [2] a) K. Junge, K. Schröder and M. Beller, *Chem. Commun.*, **2011**, 47, 4849; b) B. A. F. Le Bailly and S. P. Thomas, *RSC Adv.*, **2011**, 1, 1435.
- [3] a) E. J. Daida and J. C. Peters, *Inorg. Chem.*, **2004**, 43, 7474; b) C. Bianchini, A. Meli, M. Peruzzini, P. Frediani, C. Bohanna, M. A. Esteruelas and L. A. Oro, *Organometallics*, **1992**, 11, 138.
- [4] a) R. P. Yu, J. M. Darmon, J. M. Hoyt, G. W. Margulieux, Z. R. Turner and P. J. Chirik, *ACS Catal.*, **2012**, 2, 1760; b) R. J. Trovitch, E. Lobkovsky, E. Bill and P. J. Chirik, *Organometallics*, **2008**, 27, 1470; c) S. C. Bart, E. Lobkovsky and P. J. Chirik, *J. Am. Chem. Soc.*, **2004**, 126, 13794; d) T. S. Carter, L. Guiet, D. J. Frank, J. West and S. P. Thomas, *Adv. Synth. Catal.*, **2013**, 355, 880.
- [5] a) P. H. Phua, L. Lefort, J. A. F. Boogers, M. Tristany and J. G. de Vries, *Chem. Commun.*, **2009**, 45, 3747; b) M. Stein, J. Wieland, P. Steurer, F. Tölle, R. Mülhaupt and B. Breit, *Adv. Synth. Catal.*, **2011**, 353, 523; c) A. Welther, M. Bauer, M. Mayer and A. Jacobi von Wangelin, *ChemCatChem*, **2012**, 4, 1088; d) R. Hudson, A. Rivière, C. M. Cirtiu, K. L. Luska and A. Moores, *Chem. Commun.*, **2012**, 48, 3360; e) A. Welther and A. Jacobi von Wangelin, *Curr. Org. Chem.*, **2013**, 17, 326; f) R. Hudson, G. Hamasaka, T. Osako Y. M. A. Yamada, C. J. Li, Y. Uozumi and A. Moores, *Green Chem.*, **2013**, 15, 2141.
- [6] a) B. A. F. Le Bailly, M. D. Greenhalgh and S. P. Thomas, *Chem. Commun.*, **2012**, 48, 1580; b) D. J. Frank, L. Guiet, A. Käslin, E. Murphy and S. P. Thomas, *RSC Adv.*, **2013**, 3, 25698.
- [7] LiAlH₄ as hydride source in metal-catalyzed reductions: a) G. Dozzi, S. Cucinella, A. Mazzei, *J. Organomet. Chem.*, **1979**, 164, 1; b) E. C. Ashby and J. J. Lin, *J. Org. Chem.*, **1978**, 43, 2567; c) E. C. Ashby and J. J. Lin, *Tetrahedron Lett.*, **1977**, 51, 4481. For early reports of H₂ evolution from iron hydride species and catalytic olefin hydrogenations, see: d) Y. Takegami, T. Ueno and T. Fujii, *Kogyo Kagaku Zasshi (J. Chem. Soc. Jpn., Ind. Chem. Sec.)*, **1964**, 67, 1009; e) Y. Takegami, T. Ueno and T. Fujii, *Bull. Chem. Soc. Jpn.*, **1965**, 38, 1279.
- [8] a) Technical production and use of H₂: H.-J. Arpe, *Industrial Organic Chemistry*; Wiley-VCH: Weinheim, **2010**; b) selected applications of LiAlH₄: S. Yaragorla, *Synlett*, **2008**, 19, 3073.
- [9] Please see chapter 4.5 for detailed experimental and analytical data.
- [10] Olefin isomerization with iron carbonyls: a) J. V. Crivello, S. Kong, *J. Org. Chem.*, **1998**, 63, 6745; b) M. R. Reddy, M. Periasamy, *J. Organomet. Chem.*, **1995**, 491, 263; c) P. A. Tooley, L. W. Arndt, M. Y. Darensbourg, *J. Am. Chem. Soc.*, **1985**, 107, 2422; d) R. Jennerjahn, R. Jackstell, I. Piras, R. Franke, H. Jiao, M. Bauer and M. Beller, *ChemSusChem*, **2012**, 5, 734; e) naked Fe(0) species: M. Mayer, A. Welther and A. Jacobi von Wangelin, *ChemCatChem*, **2011**, 3, 1567. Allylbenzenes were prepared according to: f) M. Mayer, W. M. Czaplik and A. Jacobi von Wangelin, *Adv. Synth. Catal.*, **2010**, 352, 2147.
- [11] a) F. Alonso, I. P. Beletskaya and M. Yus, *Chem. Rev.*, **2002**, 102, 4009; b) W. M. Czaplik, S. Grupe, M. Mayer and A. Jacobi von Wangelin, *Chem. Commun.*, **2010**, 46, 6350.
- [12] D. Gärtner, H. Konnerth and A. Jacobi von Wangelin, *Catal. Sci. Technol.*, **2013**, 3, 2541.

- [13] a) α -Methylstyrene was hydrogenated at 4 bar H₂ in the presence of various functionalized additives (1 equiv.). No decrease of hydrogenation selectivity was observed when adding PhCl, PhBr, PhCO₂Me, PhNH₂, PhCONH₂, and 1,1-diphenylethylene, respectively. With PhNO₂, PhCN, PhI, and MeCN, no conversion of α -methylstyrene was observed, respectively, neither was the additive significantly consumed (<5%). b) At 1-2 bar H₂, much lower tolerance of functional groups was observed. We assume that the presence of functionalized substrates or polar moieties enhances catalyst ageing and formation of a heterogeneous species which appeared to somewhat less active. It should also be noted that sporadic cases of somewhat lower reproducibilities of reactions at 1 bar H₂ pressure were observed with substrates bearing polar functional groups.
- [14] *N*-Methylacetamide (AcNHMe), pK_a 25.9. F. G. Bordwell, J. A. Harrelson and T.-Y. Lynch, *J. Org. Chem.*, **1990**, 55, 3337.
- [15] *N*-Acetylaminocyclohexenes were prepared according to: a) D. Strübing, H. Neumann, A. Jacobi von Wangelin, S. Klaus, S. Hübner and M. Beller, *Tetrahedron*, **2006**, 62, 10962; b) S. Hübner, H. Neumann, A. Jacobi von Wangelin, S. Klaus, D. Strübing, H. Klein, M. Beller, *Synthesis*, **2005**, 2084; c) S. Klaus, S. Hübner, H. Neumann, D. Strübing, A. Jacobi von Wangelin, D. Gördes and M. Beller, *Adv. Synth. Catal.*, **2004**, 346, 970; d) A. Jacobi von Wangelin, H. Neumann, D. Gördes, A. Spannenberg and M. Beller, *Org. Lett.*, **2001**, 3, 2895.
- [16] Fe-catalyzed Z-selective semihydrogenation of alkynes: a) S. Enthaler, M. Haberberger and E. Irran, *Chem. Asian J.*, 2011, **6**, 1613; b) L. Ilies, T. Yoshida and E. Nakamura, *J. Am. Chem. Soc.*, 2012, **134**, 16951; (c) C. Belger and B. Plietker, *Chem. Commun.*, **2012**, 48, 5419; d) T. N. Gieshoff, A. Welther, M. T. Kessler, M. H. G. Precht and A. Jacobi von Wangelin, *Chem. Commun.*, **2014**, 50, 2261.
- [17] a) J. A. Widegren and R. G. Finke, *J. Mol. Catal. A*, **2003**, 198, 317; b) D. Astruc, F. Lu and J. Ruiz Aranzaes, *Angew. Chem. Int. Ed.*, **2005**, 44, 7852; c) R. H. Crabtree, *Chem. Rev.*, **2012**, 112, 1536.
- [18] a) D. R. Anton and R. H. Crabtree, *Organometallics*, **1983**, 2, 855; b) G. Franck, M. Brill and G. Helmchen, *J. Org. Chem.*, **2012**, 89, 55; c) J. F. Sonnenberg and R. H. Morris, *Catal. Sci. Technol.*, **2014**, 4, 3426.
- [19] The observation of a partial inhibition by dct results from a superposition of an effective catalyst inhibition by the presence of dct and (a slower) hydrogenation of dct as substrate itself (see entry 27 in Table 4-3).
- [20] Iron forms only metastable alloys with mercury (amalgam). The maximum concentration of Fe(0) in Hg was reported to be 2-3 wt.%. a) S. Mørup, S. Linderroth, J. Jacobsen and M. Holmblad, *Hyperfine Interact.*, **1991**, 69, 489; b) S. Linderroth and S. Mørup *J. Phys. Condens. Matter*, **1992**, 4, 8627.
- [21] a) G. W. Schaeffer, J. S. Roscoe and A. C. Stewart, *J. Am. Chem. Soc.*, **1956**, 78, 729; b) H. Neumaier, D. Büchel and G. Ziegelmaier, *Z. Anorg. Allg. Chem.*, **1966**, 345, 46; c) M. E. Kost and A. L. Golovanova, *Izv. Akad. Nauk SSSR, Ser. Khim.*, **1957**, 5, 991.
- [22] The stable low-spin iron(II) aluminohydride complex [(Me³tacn)₂Fe₂(μ-AlH₆)]⁺ has recently been reported (tacn = 1,4,7-triazacyclononane): M. Oishi, T. Endo, M. Oshima and H. Suzuki, *Inorg. Chem.*, **2014**, 53, 5100.
- [23] a) A. Füstner, R. Martin, H. Krause, G. Seidel, R. Goddard and C. W. Lehmann, *J. Am. Chem. Soc.*, **2008**, 130, 8773; b) A. Hedström, E. Lindstedt and P.-O. Norrby, *J. Organomet. Chem.*, **2013**, 748, 51.
- [24] a) C. Rangheard, C. de Julian Fernandez, P.-H. Phua, J. Hoorn, L. Lefort and J. G. de Vries, *Dalton Trans.*, **2010**, 39, 8464; b) R. Schoch, W. Desens, T. Werner and M.

- Bauer, *Chem. Eur. J.*, **2013**, *19*, 15816; c) V. Kelsen, B. Wendt, S. Werkmeister, K. Junge, M. Beller and B. Chaudret, *Chem. Commun.*, **2013**, *49*, 3416.
[25] a) D. Griller and K. U. Ingold, *Acc. Chem. Res.*, **1980**, *13*, 317; b) M. Newcomb, *Tetrahedron*, **1993**, *49*, 1151.

5 Iron-catalyzed hydrogenation of sterically hindered alkenes^{i,ii}



The reaction of $\text{Fe}[\text{N}(\text{SiMe}_3)_2]_2$ with DiBAIH generates a Ziegler-type hydrogenation catalyst, highly active in the hydrogenation of sterically hindered olefins under mild conditions. Key mechanistic experiments reveal elemental steps of the reaction of $\text{Fe}[\text{N}(\text{SiMe}_3)_2]_2$ with DiBAIH and hint toward a catalytically active nanocluster or nanoparticle formation.

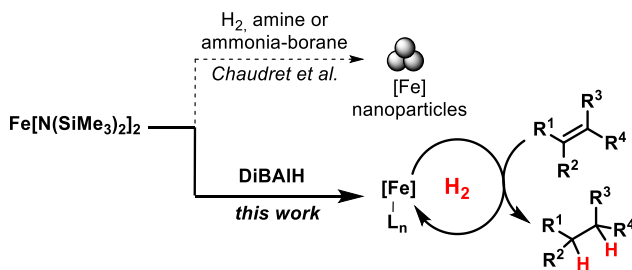
ⁱ Manuscript in preparation.

ⁱⁱ Synthesis and characterization of complexes $(\text{SiNpEt})\text{Fe}[\text{N}(\text{SiMe}_3)_2]_2$ and $(\text{BnNpMe})\text{Fe}[\text{N}(\text{SiMe}_3)_2]_2$ were performed by D. Herrmann, University Regensburg.

5.1 Introduction

In the development of transition metal complexes with low coordination numbers, two-coordinated transition metal complexes (Co, Mn, Ni, Zn, Hg, Cd) were synthetically available for the first time by the use of bulky silylamido ligands in the 1960's.^[1] The synthesis of the bis(bis(trimethylsilyl)amido)iron was first reported in 1988 by Anderson *et al.*^[2] The complex gained interest as a useful synthetic alternative for iron halides in iron complex synthesis and the synthesis of biologically relevant iron-sulfur clusters.^[3] More recently, Chaudret *et al.* synthesized zerovalent iron nanoparticles with a size of 1.5 ± 0.2 nm, by reduction of $\text{Fe}[\text{N}(\text{SiMe}_3)_2]_2$ with H_2 .^[4] Upon reduction, the release of $\text{HN}(\text{SiMe}_3)_2$ was detected, which is believed to prevent further agglomeration by coordination. The particles have been extensively characterized (WAXS, TEM, SQUID, Mössbauer) and studied in the hydrogenation of terminal and di-substituted alkenes as well as alkynes at 10 bar H_2 .^[5] Similarly, iron nanoparticles were synthesized by the reduction of $\text{Fe}[\text{N}(\text{SiMe}_3)_2]_2$ with long chain amines or ammonia borane.^[6]

The use of aluminium organyls as reductants to form low-valent transition metal catalysts has been known for decades and established the class of Ziegler-type hydrogenation catalysts (see chapter 2.2). Iron Ziegler-type hydrogenation catalysts derived by $\text{Fe}(\text{acac})_3$ or $\text{Fe}(\text{2-ethylhexanoate})_3$ with AlR_3 ($\text{R} = \text{Et}, ^i\text{Bu}$) or $^n\text{BuLi}$ usually make use of an excess of the organometallic activation reagent (6 to 32 equivalents referred to iron) or are restricted to simple terminal and di-substituted alkene hydrogenation.^[7]



Scheme 5-1. Synthesis of low-valent iron hydrogenation catalysts from $\text{Fe}[\text{N}(\text{SiMe}_3)_2]_2$.

Tri- and tetra-substituted alkenes are highly challenging substrates and most iron-catalyzed protocols fail to provide high conversions under mild conditions.^[8] Only recently, Chirik *et al.* reported about defined iron pincer complexes, which were able to hydrogenate challenging alkenes at 4 bar H_2 .^[9] Although the complexes showed excellent reaction rates and broad functional group tolerance, an easily accessible alternative using cheaper ligands is highly desirable.

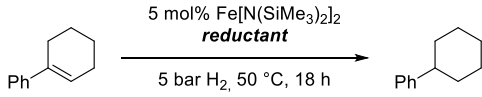
Inspired by Chaudret *et al.*, we envisioned to exploit our experience in the generation of low-valent iron hydrogenation catalysts by activation of simple iron precursors (FeCl_2 ,

FeCl₃) with cheap reductants (EtMgCl, LiAlH₄) to develop a protocol based on the use of Fe[N(SiMe₃)₂]₂ as iron source.

5.2 Results and discussion

Initial experiments with 1-phenylcyclohexene as a model substrate aimed to reveal a suitable reductant for Fe[N(SiMe₃)₂]₂ to generate a catalyst system able to hydrogenate the tri-substituted olefin under mild conditions (Table 5-1). Activation with molecular hydrogen at high temperatures (150 °C) is known to generate catalytically active nanoparticles but failed in the hydrogenation of 1-phenylcyclohexene.^[4,5] Various commonly used reductants were screened, where only aluminium hydrides and organyls enabled clean conversion to phenylcyclohexane (entries 12, 13, 15). NaBH₄ as activation agent failed to be active under mild conditions (1 bar H₂, rt) (entry 10).

Table 5-1. Screen of various reductants in the hydrogenation of 1-phenylcyclohexene with Fe[N(SiMe₃)₂]₂.

<div style="text-align: center;">  </div>		
Entry	Reductant (mol%)	Yield in % ^a
1	H ₂ ^b	<1 (<1)
2	NaOCHO (20 mol)	<1 (<1)
3	PhSiH ₃ (10 mol%)	<1 (<1)
4	[NaNaph] (10 mol%)	<1 (5)
5	EtMgCl (20 mol%)	5 (9)
6	Zn (10 mol%)	<1 (<1)
7	Al (10 mol%)	<1 (<1)
8	NaH (20 mol%)	<1 (8)
9	NaBH ₄ (5 mol%)	>99 (>99)
10		<1 (<1) ^c
11	LiAlH ₄ (5 mol%)	>99 (>99)
12		>99 (>99) ^c
13	Al(ⁱ Bu) ₃ (10 mol%)	93 (>99) ^d

Overall high conversion (>90%) of 1-phenylcyclohexene was achieved under Ziegler-type conditions with all aluminium organyls (AlMe₃, Al(*i*Bu)₃, DiAlH), whereas the resulting bimetallic catalysts presented severe differences in stability and turnover frequencies (see experimental, Table S-9). For AlMe₃, precipitation of a black solid was observed after 20 h (see experimental, Figure S-2) with complete loss of activity (TOF_{fresh} = 13 h⁻¹ vs. TOF_{20 h} = <1 h⁻¹). In contrast, DiAlH enabled storage of the catalyst solution for 5 days with only minimal loss of activity (TOF_{fresh} = 41 h⁻¹ vs TOF_{5 d} = 37 h⁻¹).

Reaction scheme for the synthesis of 1-(4-chlorophenyl)ethene (10) from 1-(4-chlorophenyl)ethane (9):

1-(4-chlorophenyl)ethane (9) reacts with 5 mol% $\text{Fe}[\text{N}(\text{SiMe}_3)_2]_2$ and 5 mol% LiAlH_4 under 1 bar H_2 at 23 °C for 3 h to form 1-(4-chlorophenyl)ethene (10) in 77% yield.

1-(4-chlorophenyl)ethane (9) reacts with 5 mol% $\text{Fe}[\text{N}(\text{SiMe}_3)_2]_2$ and 10 mol% DiBAIH under 1 bar H_2 at 23 °C for 3 h to form 1-(4-chlorophenyl)ethene (10) in >99% yield.

In blank experiments, the necessity of all components (bis(bis(trimethylsilyl)amido) iron, DiBAIH and H₂ as the quantitative reductant) was studied (Table 5-2). In absence of DiBAIH, or by exchange of Fe[N(SiMe₃)₂]₂ with FeCl₂(thf)_{1.5} no hydrogenation of 1-phenylcyclohexene was observed (entries 2 and 3). DiBAIH was not effective as a stoichiometric reductant (entries 5 and 6), even in addition of an oxidant for catalyst reoxidation. Interestingly, *in situ* generation of the precatalyst was possible by reacting lithium bis(trimethylsilyl)amide with FeCl₂(thf)_{1.5} for one hour, prior addition of DiBAIH (entry 7). A lower productivity (see experimental, Table 5-9) in comparison to preformed

$\text{Fe}[\text{N}(\text{SiMe}_3)_2]_2$ indicated incomplete conversion after 1 h ($\text{TOF}_{in\ situ} = 27\text{ h}^{-1}$ vs. $\text{TOF}_{preformed} = 41\text{ h}^{-1}$). Nevertheless, *in situ* formation simplifies the synthesis of the active species and enables a fast access by the use of standard organic laboratory chemicals.

Table 5-2. Blank experiments and *in situ* precatalyst formation.

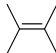
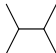
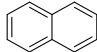
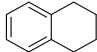
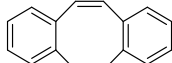
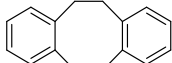
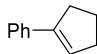
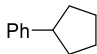
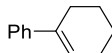
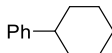
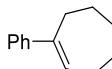
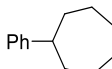
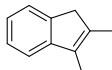
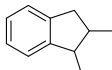
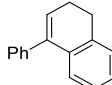
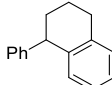
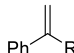
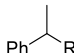
Entry	Catalyst	Reaction conditions	Yield in % ^a
1	5 mol% $\text{Fe}[\text{N}(\text{SiMe}_3)_2]_2$ 10 mol% DiBAIH	1.3 bar H_2 , rt, 0.5 h	>99 (>99)
2	5 mol% $\text{Fe}[\text{N}(\text{SiMe}_3)_2]_2$	5 bar H_2 , 150 °C, 18 h	<1 (<1)
3	5 mol% $\text{FeCl}_2(\text{thf})_{1.5}$ 10 mol% DiBAIH	1.3 bar H_2 , rt, 0.5 h	1 (1)
4	5 mol% $\text{HN}(\text{SiMe}_3)_2$ 5 mol% DiBAIH	5 bar H_2 , 50 °C, 15 h	1 (5)
5	5 mol% $\text{Fe}[\text{N}(\text{SiMe}_3)_2]_2$ 100 mol% DiBAIH	no H_2 , rt, 3 h	5 (6)
6	5 mol% $\text{Fe}[\text{N}(\text{SiMe}_3)_2]_2$ 100 mol% DiBAIH 185 mol% oxidant ^b	no H_2 , rt, 3 h	2 (3)
7	5 mol% $\text{FeCl}_2(\text{thf})_{1.5}$ 10 mol% DiBAIH 11 mol% $\text{HN}(\text{SiMe}_3)_2$ 10 mol% ⁿ BuLi	1.3 bar H_2 , rt, 0.5 h	98 (>99)

^a quantitative GC-FID vs. *n*-pentadecane as internal reference, conversion in % in parentheses; ^b *p*-bromochlorobenzene. See chapter 5.6 for experimental detail.

Using the optimized protocol (5 mol% $\text{Fe}[\text{N}(\text{SiMe}_3)_2]_2$, 10 mol% DiBAIH) a broad scope of largely unfunctionalized alkenes and alkynes was screened under hydrogenation conditions. Terminal and internal alkenes (Table 5-3, entries 1, 2, 15) were hydrogenated in excellent yield at 2 bar H_2 in 3 h. Farnesene, a sesquiterpene which is commercially produced by fermentation of ligno-cellulosic sugars, required harsher reaction conditions (80 °C, 10 bar H_2 , 20 h) for excellent conversion to farnesane, a component in jet fuel.^[10] Styrenic di- and tri-substituted substrates showed good to excellent conversion at 2 bar H_2 in 3 h in general, with 1-phenylcyclopentene as the only exception. Remarkably, highly

challenging tetra-substituted alkenes, were hydrogenated in moderate to good yield (entries 3, 9) at elevated temperature or pressure. Internal alkynes were hydrogenated in excellent yield, whereas terminal alkynes underwent fast polymerization and [2+2+2]-cycloisomerization (see chapter 6).

Table 5-3. Hydrogenation of largely unfunctionalized alkenes and alkynes.

$ \begin{array}{ccc} \begin{array}{c} \text{R}^1 \quad \text{R}^3 \\ \diagdown \quad \diagup \\ \text{C}=\text{C} \\ \diagup \quad \diagdown \\ \text{R}^2 \quad \text{R}^4 \end{array} & \xrightarrow[\text{2 bar H}_2, \text{ toluene, rt, 3 h}]{\begin{array}{c} \text{5 mol\% Fe[N(SiMe}_3)_2]_2 \\ \text{10 mol\% DiBAIH} \end{array}} & \begin{array}{c} \text{R}^1 \quad \text{R}^3 \\ \quad \\ \text{C}-\text{C} \\ \quad \\ \text{R}^2 \quad \text{R}^4 \end{array} \end{array} $				
Entry	Substrate	R	Product	Yield in % ^a
1	1-octene		<i>n</i> -octane	>99 (>99)
2	(<i>E</i>)-4-octene			>99 (>99) ^b
3				47 (91) ^c
4				>99 (>99) ^c
5				89 ^d
6				<5
7				>99 (>99) 95 (>99) ^g
8				87 ^d
9				93 (>99) ^e
10				82 ^d
11		Me		>99 (>99)
12		Ph		>99 (>99)
13		cyclopropyl		81 ^{b,d}

14			>99 (>99)
15			92 (>99) ^f
16	farnesene ^f	farnesane	91 ^{d,e}
17			90 (>99) >99 (>99) ^g
18			96 (>99)
19	6-dodecyne	<i>n</i> -dodecane	99 (>99)

^a quantitative GC-FID vs. *n*-pentadecane as internal reference, conversion in % in parentheses; ^b 0.5 mol% Fe[N(SiMe₃)₂]₂, 1 mol% DiBAIH ^c 80 °C, 15 h; ^d isolated yield; ^e 10 bar, 80 °C, 15 h; ^f mixture of isomers; ^g 5 mol% FeCl₂(thf)_{1.5} 10 mol% LiN(SiMe₃)₂, 10 mol% DiBAIH.

Table 5-4. Determination of turnover frequencies for selected alkenes.

$ \begin{array}{ccc} \begin{array}{c} \text{R}^1 \\ \diagup \\ \text{C} \\ \diagdown \\ \text{R}^2 \end{array} & \begin{array}{c} \text{R}^3 \\ \diagdown \\ \text{C} \\ \diagup \\ \text{R}^4 \end{array} & \xrightarrow[\text{2 bar H}_2, \text{ toluene, rt, 5 min}]{\begin{array}{c} 0.5 \text{ mol\% Fe[N(SiMe}_3)_2]_2 \\ 1 \text{ mol\% DiBAIH} \end{array}} \begin{array}{c} \text{R}^1 \\ \diagup \\ \text{C} \\ \diagdown \\ \text{R}^2 \end{array} \begin{array}{c} \text{R}^3 \\ \diagdown \\ \text{C} \\ \diagup \\ \text{R}^4 \end{array} \end{array} $			
Entry	Substrate	Yield after 5 min in % ^a	TOF / h ⁻¹
1	1-octene	19	466
2	α -methylstyrene	11	261
3	1-phenylcyclohexene	18 ^b	44

^a quantitative GC-FID vs. *n*-pentadecane as internal reference, conversion in % in parentheses; ^b 5 mol% Fe[N(SiMe₃)₂]₂, 10 mol% DiBAIH, no reaction with lower catalyst loadings.

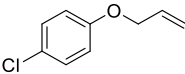
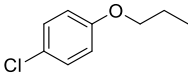
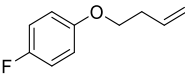
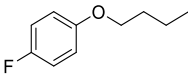
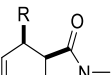
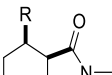
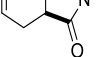
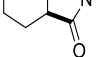
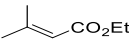
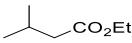
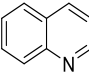
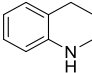
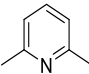
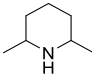
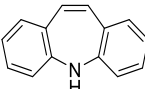
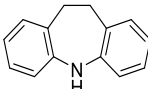
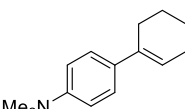
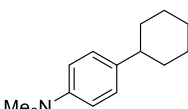
Turnover frequencies were determined for the hydrogenation of 1-octene, 1-phenylcyclohexene and α -methylstyrene yielding high productivity. Notably, catalyst loadings as low as 0.5 mol% Fe[N(SiMe₃)₂]₂, 1 mol% DiBAIH could be applied for 1-octene and α -methylstyrene. Lower catalyst loadings (0.1 mol% Fe[N(SiMe₃)₂]₂ with 0.2 mol% DiBAIH) were not productive. Additionally, lower catalyst loadings (<5 mol%)

in the hydrogenation of 1-phenylcyclohexene resulted in a complete inhibition of the hydrogenation reaction. Presumably, residual contaminations of 1-phenylcyclohexene acted as catalyst poisons.

Functional group tolerance was studied by employing various functionalized alkenes under hydrogenation conditions (Table 5-5). Excellent selectivity was maintained upon hydrogenation of 4-chloro- and 4-bromo- α -methylstyrenes (entries 1 and 2). Various functional groups including methyl- and benzylethers (entries 4, 8) as well as amines (entries 9, 16, 18, 19) were tolerated. Nitriles, nitro groups and iodo groups acted as inhibitors. Thioethers, vinyl ethers and conjugated esters (entries 5, 10, 15) slowed down the reaction rate and required harsher conditions for moderate conversion. Allylic ethers were not tolerated, allylether cleavage was observed in traces. Notably, the catalyst system was effective in the selective hydrogenation of quinoline to 1,2,3,4-tetrahydroquinoline (entry 16). No hydrogenation was observed for 2,6-lutidine (entry 17).

Table 5-5. Functional group tolerance in the hydrogenation with $\text{Fe}[\text{N}(\text{SiMe}_3)_2]_2$ -DiBAIH.

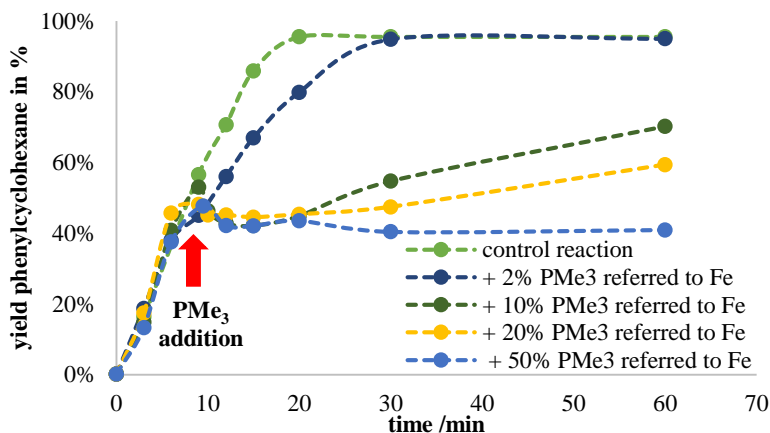
$ \begin{array}{ccc} \begin{array}{c} \text{R}^1 \quad \text{R}^3 \\ \diagdown \quad \diagup \\ \text{C}=\text{C} \\ \diagup \quad \diagdown \\ \text{R}^2 \quad \text{R}^4 \end{array} & \xrightarrow[\text{2 bar H}_2, \text{ toluene, rt, 3 h}]{\begin{array}{c} \text{5 mol\% Fe}[\text{N}(\text{SiMe}_3)_2]_2 \\ \text{10 mol\% DiBAIH} \end{array}} & \begin{array}{c} \text{R}^1 \quad \text{R}^3 \\ \quad \\ \text{C}-\text{C} \\ \quad \\ \text{R}^2 \quad \text{R}^4 \end{array} \end{array} $				
Entry	Substrate	R	Product	Yield in % ^a
1		Cl		>99 (>99)
2		Br		95 (>99) ^g
3		I		<5
4		OMe		>99 (>99)
5		SMe		54 (54)
6		CN		<5
7		NO ₂		<5
8		OBn		93 (>99) ^c
9		NH ₂		99 (>99) ^g
10				94 ^b
10				57 (80) ^d

11				<5
12				75 ^b
13		H		89 ^b
14		NHAc		<5
15				53 (73) ^d
16				90 ^{b,e}
17				<5
18				91 ^b
19				97 ^b

^a quantitative GC-FID vs. *n*-pentadecane as internal reference, conversion in % in parentheses; ^b isolated yield; ^c 0.5 mol% Fe[N(SiMe₃)₂]₂, 1 mol% DiBAIH ^d 80 °C; 15 h; ^e 10 bar, 80 °C, 15 h; ^f mixture of isomers; ^g 5 mol% FeCl₂(thf)_{1.5}, 10 mol% LiN(SiMe₃)₂, 10 mol% DiBAIH.

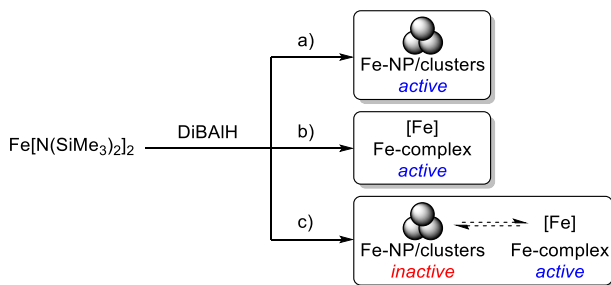
5.3 Mechanistic experiments

In key mechanistic experiments, the nature of the active species was studied. Kinetic experiments with the addition of selective catalyst poisons were conducted to address the challenging distinction between a homotopic and heterotopic catalyst.^[11] In a first set of experiments, the kinetics of the hydrogenation of 1-phenylcyclohexene was measured upon addition of PMe_3 as a catalyst poison (Scheme 5-3). PMe_3 has been shown to effectively poison iron nanoparticles as reported by Morris and coworkers.^[12] For homotopic catalysts with one active site per metal atom, at least 1 equivalent of poison is necessary for complete inhibition. Contrary, a minority of metal atoms are available for catalytic reactions in nanoparticles, since the inner core contains a major fraction of metal atoms. Therefore, less active sites are expected per metal atom and substoichiometric amounts of catalyst poison referred to metal atoms are able to inhibit the catalytic activity (ref^[12]: 10% PMe_3 referred to iron-nanoparticle catalyst resulted in complete stop of hydrogenation activity). Studying the hydrogenation of 1-phenylcyclohexene with $\text{Fe}[\text{N}(\text{SiMe}_3)_2]_2\text{-DiBAIH}$, 50% of catalyst poison referred to iron inhibited the activity completely. Less catalyst poison slowed down the reaction rate, whereas 2% of PMe_3 to iron resulted in only minimal inhibition.



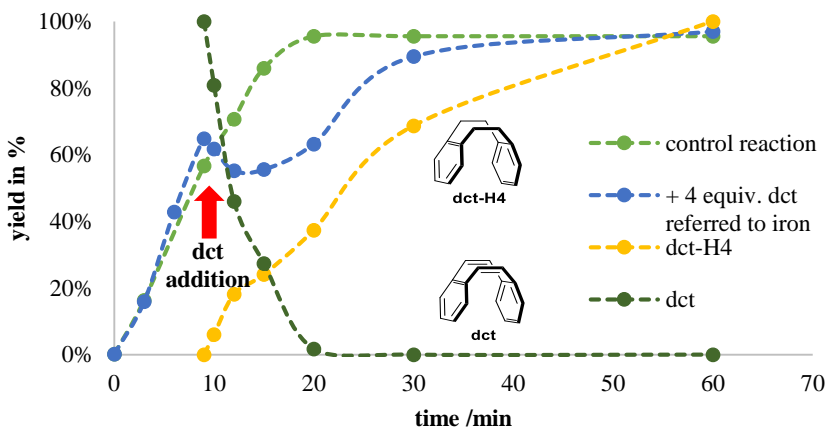
Scheme 5-3. Poisoning experiment of the iron-catalyzed hydrogenation of 1-phenylcyclohexene with PMe_3 .

These results support a heterotopic catalyst with less than one active site per metal atom, which would be consistent with a metal cluster or nanoparticle as the active species (Scheme 5-4, a). Alternatively, a homotopic catalyst with one active site is possible, as well under the implication, that the conversion of $\text{Fe}[\text{N}(\text{SiMe}_3)_2]_2$ to the active species is not quantitative or unselective, yielding only a fraction of active catalyst (Scheme 5-4, c).



Scheme 5-4. Possible topocities of the active species; a) active heterotopic iron clusters or nanoparticles, b) active homotopic iron complex, c) active homotopic iron complex with inactive or less active iron clusters or nanoparticles.

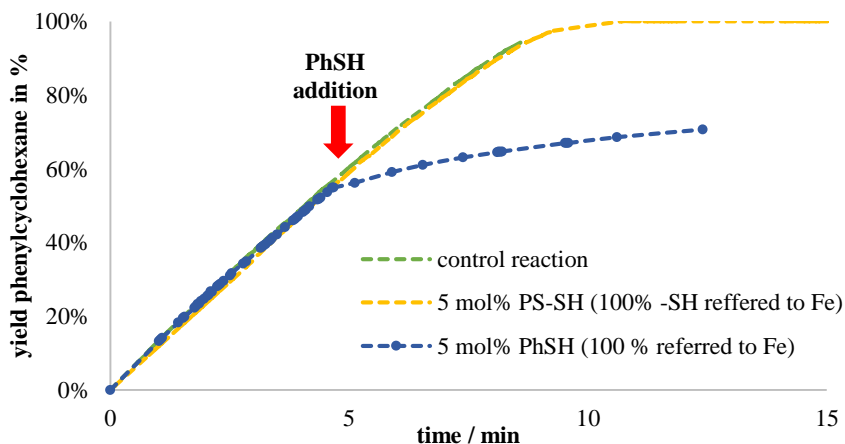
A second set of experiment was conducted with dibenzo[*a,e*]cyclooctatetraene (dct) as selective catalyst poison. Dct, a rigid tub-shaped molecule is reported to bind selectively to metal complexes and leads to fast inhibition of homotopic hydrogenation catalysts.^[11,13] Addition of dct to the hydrogenation of 1-phenylcyclohexene with $\text{Fe}[\text{N}(\text{SiMe}_3)_2]_2$ - DiBAIH resulted in immediate inhibition of product formation. Instead, dct was hydrogenated within minutes to form the fully hydrogenated dibenzo[*a,e*]cyclooctane (dct-H4). Upon consumption of dct, hydrogenation of 1-phenylcyclohexene resumed until full conversion.



Scheme 5-5. Poisoning experiment of the iron-catalyzed hydrogenation of 1-phenylcyclohexene with the selective poison dct.

Assuming that dct indeed is effectively inhibiting homotopic mononuclear catalysts as proposed and observed in earlier reports, the results support a heterotopic iron cluster or nanoparticle catalyst (Scheme 5-4, a). The heterotopic catalyst is less affected by dct and preferably consumes the stronger binding diene and remains overall hydrogenation productivity. Nevertheless, the side by side operation of a homotopic molecular and heterotopic active species cannot be ruled out with this test. In that scenario, the homotopic active species is blocked by dct, which is consumed by present heterotopic catalyst species.

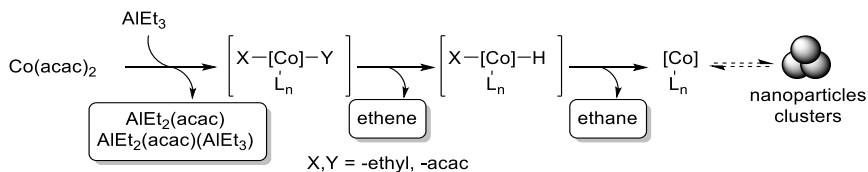
A third set of experiments was performed by addition of thiophenol-linked polystyrene (PS-SH). This test is a variation of the three-phase test, in which the substrate is bound to a polymer.^[11] In this example, the catalyst poison is bound to the polymer. By polymer bead swelling, the free thiol moieties are accessible for small, soluble homotopic catalysts. Nanoparticles or clusters are excluded to enter the cavities and only minimally affected by the inner thiol-groups.^[14] To ensure sufficient swelling, the poison-linked polymer bead was stirred within the catalyst solution for 24 h prior use of the catalyst solution in hydrogenation reactions. Interestingly, no change of reaction rate was observed in comparison to a freshly prepared catalyst solution. This result clearly supports the formation of a heterotopic catalyst as the sole active species. To verify the implied catalyst deactivation by thiol-groups, free thiophenol was added to a freshly prepared reaction mixture after 5 minutes, resulting in drastic inhibition of the hydrogenation rate.



Scheme 5-6. Poisoning experiment of the iron-catalyzed hydrogenation of 1-phenylcyclohexene with thiophenol-linked polystyrene (PS-SH) and thiophenol (PhSH).

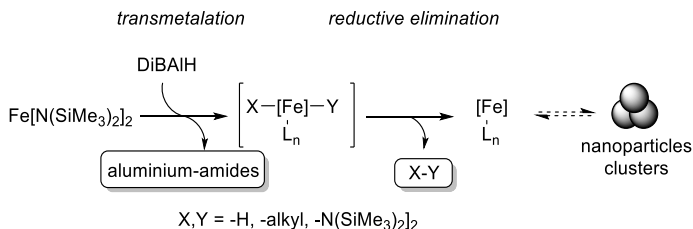
In summary, all three poisoning tests support the formation of a heterotopic catalyst species, although particle formation was not detected by dynamic light scattering. Supplementary, the isolation of a tetranuclear $[\text{Fe}_4]$ -cluster (see chapter 6) upon reaction of $\text{Fe}[\text{N}(\text{SiMe}_3)_2]_2$ with one equivalent DiBAIH indicates selective cluster formation as an intermediate species. In excess of DiBAIH (>1 equivalents), the cluster presumably undergoes further reduction with sequential nanoparticle formation.

The reaction of $\text{Fe}[\text{N}(\text{SiMe}_3)_2]_2$ with DiBAIH was studied in detail by key mechanistic experiments to gain further indications on the catalytically active species. Mechanistic proposals for the formation of Ziegler-type hydrogenation catalysts were made for various combinations of iron and cobalt precursors.^[15] Major effort including extensive spectroscopic analysis was conducted for the catalyst derived from the reaction $\text{Co}(\text{acac})_2$ with AlEt_3 . Here, the detection of ethane and ethene led to the assumption of a mechanism shown in Scheme 5-7.^[16] Additionally, Schmidt and coworkers observed the formation of $\text{AlEt}_2(\text{acac})$ as well as $\text{AlEt}_2(\text{acac})(\text{Al})\text{Et}_3$ by IR.^[17]



Scheme 5-7. Mechanistic proposal for Ziegler-type hydrogenation catalyst formation from $\text{Co}(\text{acac})_2$ - AlEt_3 .

In general, reductive synthesis of a low-valent iron species with DiBAIH should involve similar steps (Scheme 5-8). In analogy, analysis of the by-products was performed to rationalize the formation of a low-valent iron catalyst from $\text{Fe}[\text{N}(\text{SiMe}_3)_2]_2$ and DiBAIH.

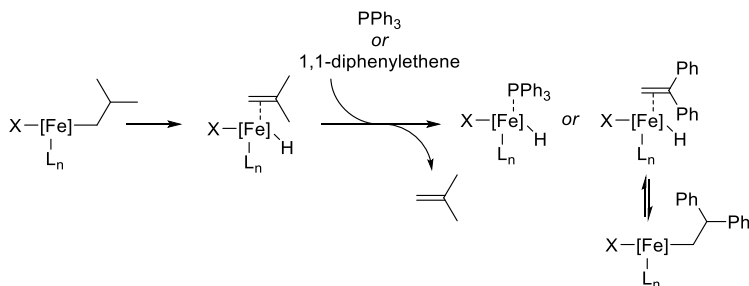


Scheme 5-8. General postulation of reductive synthesis of a low-valent iron species with $\text{Fe}[\text{N}(\text{SiMe}_3)_2]_2$ and DiBAIH.

The formation of aluminium amides was analyzed by ^1H -NMR of the crude reaction mixture of $\text{Fe}[\text{N}(\text{SiMe}_3)_2]_2$ -DiBAIH (see experimental, chapter 5.6.3). Comparison with spectra of analytically pure samples of $\text{HN}(\text{SiMe}_3)_2$, DiBAIH as well as with a reaction

mixture of $\text{HN}(\text{SiMe}_3)_2$ with one equivalent DiBAIH identified the formation of at least three different aluminium amides. By distillation under reduced pressure (10^{-3} mbar, 100°C) a mixture of $\text{Al}(\text{tBu})_2\text{N}(\text{SiMe}_3)_2$ and $\text{Al}(\text{tBu})[\text{N}(\text{SiMe}_3)_2]_2$ was isolated and analyzed by $^1\text{H-NMR}$. Further characterization with mass spectrometry was unsuccessful.

Free $\text{HN}(\text{SiMe}_3)_2$ as a product of reductive elimination forms only in traces as evidenced by $^1\text{H-NMR}$. Instead, *iso*-butane and *iso*-butene were detected by Headspace-GC-MS (see experimental, Table 5-10) as well as $^1\text{H-NMR}$ (see experimental, Figure 5-8). By addition of PPh_3 or 1,1-diphenylethene, enhanced release of *iso*-butane was measured (see experimental, Table 5-10), presumably as a result of saturation of coordination sites (Scheme 5-9).



Scheme 5-9. Release of *iso*-butene by addition of PPh_3 or 1,1-diphenylethene.

The evolution of H_2 by reductive elimination from a putative dihydrido iron species was not observed upon reaction of $\text{Fe}[\text{N}(\text{SiMe}_3)_2]_2$ with DiBAIH. In contrast, $\text{FeCl}_2(\text{thf})_{1.5}$ with DiBAIH evolved 0.73 equivalents of H_2 highlighting the ligand effect on the reaction pathway to form a low-valent iron species (see experimental, Table 5-11).

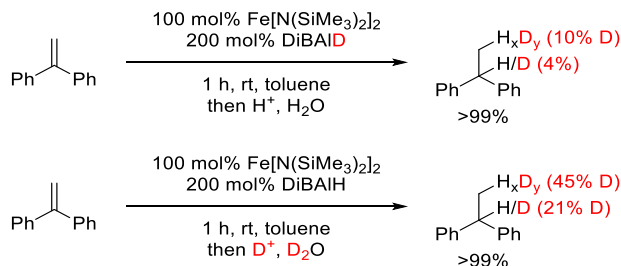
The iron-hydride intermediate formation was tracked by trapping with 1,1-diphenylethene in absence of H_2 (Table 5-6). Full conversion to 1,1-diphenylethane was obtained by reaction with 1 equivalent of $\text{Fe}[\text{N}(\text{SiMe}_3)_2]_2$ and 2 equivalents of DiBAIH after aqueous quench, indicating the quantitative formation of an iron-hydride intermediate (entry 1). No conversion was detected in absence of $\text{Fe}[\text{N}(\text{SiMe}_3)_2]_2$. Interestingly, if DiBAIH was exchanged by $\text{Al}(\text{tBu})_3$ ~50% conversion was observed, indicating a major iron hydride formation by alkyl transmetalation from aluminium to iron with sequential β -hydride elimination (Scheme 5-11). In line, no conversion was observed with $\text{Fe}[\text{N}(\text{SiMe}_3)_2]_2\text{-AlMe}_3$ (entry 6), which lacks aluminium hydrides and β -hydrogen atoms for generation of an iron-hydride intermediate.

Table 5-6. Stoichiometric hydrogenation of 1,1-diphenylethene in absence of H₂.

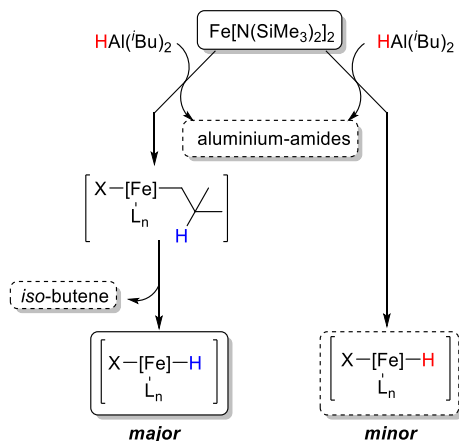
$ \begin{array}{c} \text{Ph} \quad \text{C}=\text{C} \quad \text{Ph} \\ \text{1} \end{array} \xrightarrow[\text{toluene, rt, 1 h then H}^+, \text{H}_2\text{O}]{[\text{Fe}], [\text{Al}]} \begin{array}{c} \text{Ph} \quad \text{CH}(\text{H})\text{CH}(\text{H}) \quad \text{Ph} \\ \text{2} \end{array} $				
Entry	[Fe]	[Al]	[Fe]/[Al]/1	2/1 ^a
1	Fe[N(SiMe ₃) ₂] ₂	DiBAIH	1/2/1	full conversion
2	Fe[N(SiMe ₃) ₂] ₂	DiBAIH	0.5/1/1	1/1
3	Fe[N(SiMe ₃) ₂] ₂	DiBAIH	1/1/1	1/1
4	Fe[N(SiMe ₃) ₂] ₂	DiBAIH	0.5/2/1	1/1
5	none	DiBAIH	0/1/1	no conversion
6	Fe[N(SiMe ₃) ₂] ₂	AlMe ₃	1/2/1	no conversion
7		Al(ⁱ Bu) ₃	1/2/1	1/1
8	FeCl ₂ (thf) _{1.5}	DiBAIH	1/2/1	1/1

^a relative ratio of peak areas of GC-MS.

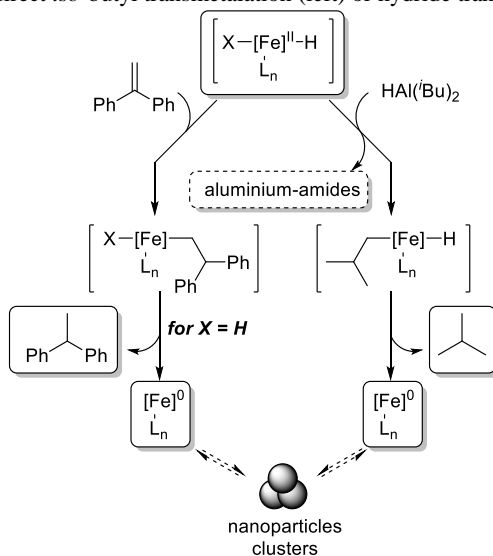
H/D scrambling experiments by stoichiometric hydrogenation of 1,1-diphenylethene support the minor iron-hydride formation by hydride transfer from Al to Fe (Scheme 5-11, right), as only ~14% of deuterium incorporation was observed upon use of DiBAID (Scheme 5-10). *Vice versa*, high deuterium incorporation (~66%) was detected in the reaction with DiBAIH and D₂O quench. Similar results were obtained by performing the same reactions with 10 mol% Fe[N(SiMe₃)₂]₂ and 20 mol% DiBAIH (Figure 5-3, Figure 5-4).

**Scheme 5-10.** Deuterium exchange in the absence of H₂.

A radical reaction pathway involving H-atom transfer from toluene to the substrate is not dominating in the H_2 -free stoichiometric hydrogenation of alkenes, as only minor deuterium incorporation was detected, when the reaction was performed in d_8 -toluene (see experimental, Figure 5-5).



Scheme 5-11. Postulated reaction pathways for the formation of an iron-hydride intermediate via direct *iso*-butyl transmetalation (left) or hydride transmetalation (right).



Scheme 5-12. Postulated reductive elimination to form a low-valent iron species in presence of an alkene (left) and in absence of a substrate (right).

In absence of an alkene, the iron-hydride intermediate undergoes fast reductive elimination of *iso*-butane (Scheme 5-12, right) as observed by GC-MS and NMR (see experimental Table 5-10, Figure 5-8).

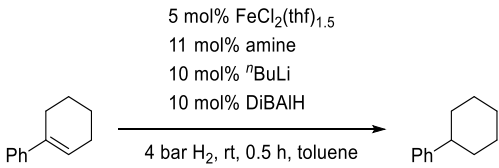
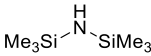
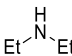
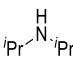
5.4 Hydrogenation with similar chiral catalysts

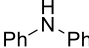
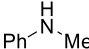
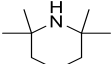
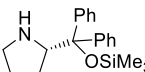
Stereoselective hydrogenations of alkenes are highly desirable as this transformation are often employed as key steps in the synthesis of bioactive compounds (see chapter 2.1). Typically, metals like Rh, Ru, Pd and more recently Co are used, a protocol for iron-catalyzed stereoselective alkene hydrogenation with molecular hydrogen is yet unknown.

As shown in chapter 5.2, *in situ* generation of $\text{Fe}[\text{N}(\text{SiMe}_3)_2]_2$ by deprotonation of bis(trimethylsilyl)amine with $n\text{BuLi}$ and reaction with $\text{FeCl}_2(\text{thf})_{1.5}$ resulted in a reactive catalyst upon activation with DiBAIH. This protocol allows easy exchange of the amine by other commercially available, chiral amines. In a first set of experiments, the amine substitution pattern was varied to gain insight into the limits and possibilities of the introduction of chiral substituents as possible inducer of enantioselective transformations.

A screen of various secondary amines (Table 5-7) revealed drastic differences in the hydrogenation performance in combination with $\text{FeCl}_2(\text{thf})_{1.5}$ and DiBAIH. In general, hydrogenation reactions with amines bearing bulky substituents (entries 2, 5, 7) afforded high conversions. In contrast, addition of amines with small substituents especially in presence of β -hydrogens, inhibited reactivity (entries 3, 4, 6), indicating a different operating mechanism. In line with these observations, the use of the chiral Hayashi-Jørgensen catalyst (entry 8) afforded no conversion in the hydrogenation of 1-phenylcyclohexene.

Table 5-7. Variation of amines in the hydrogenation of 1-phenylcyclohexene.

<div style="text-align: center;">  </div>		
Entry	Amine ^a	Yield (Conversion) in % ^b
1	none	<1 (<1)
2		>99 (>99)
3		<1 (<1)
4		24 (24)

5		76 (76)
6		10 (12)
7		>99 (>99)
8		<1 (7)

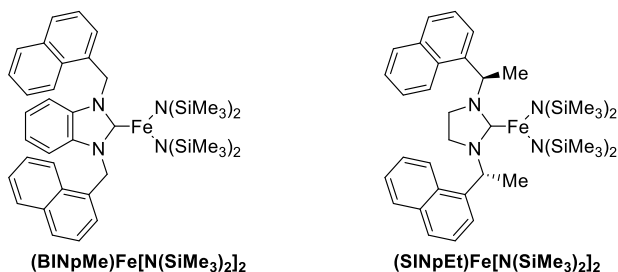
^a Catalyst preparation: Deprotonation of 11 mol% amine with 10 mol% ⁿBuLi (10 min) prior to addition of 5 mol% FeCl₂(thf)_{1.5} (30 min), then DiBAIH addition.; ^b quantitative GC-FID vs. *n*-pentadecane as internal reference, conversion in % in parenthesis.

Chiral secondary amines fulfilling the requirements (bulky substituents, absence of β -hydrogens) as shown in Scheme 5-13 are known, but their synthesis is tedious.^[18] Additionally, the strategy of chiral amine addition might not be successful in enantioselective hydrogenations, since the mechanistic experiments (see chapter 5.3) suggest the dissociation of the amide-ligand upon reaction with DiBAIH. The so formed aluminium-amides might participate in the hydrogenation, whereas a strategy involving a closely bound chiral ligand seems to be more expedient.



Scheme 5-13. Examples of sterically hindered chiral secondary amines.

In collaboration with the group of Prof. Wolf, *NHC* ligands were introduced to the Fe[N(SiMe₃)₂]₂ complex and tested for catalytic activity. As template, a chiral 1,3-bis(1-(1-naphthyl)ethyl)imidazolium ligand, initially synthesized by Hermann *et al.*, was used.^[19] The two isolated complexes (BINpMe)Fe[N(SiMe₃)₂]₂ and chiral (SiNpEt)Fe[N(SiMe₃)₂]₂ (Scheme 5-14) were screened in the hydrogenation of 1-phenylcyclohexene (Table 5-8).



Scheme 5-14. $(NHC)Fe[N(SiMe_3)_2]_2$ complexes synthesized by D. Herrmann, University Regensburg.

As observed earlier, activation with DiBAIH was obligatory to induce reactivity. Activation with 50 bar H_2 was not successful (entries 1-5). Interestingly, $(BINpMe)Fe[N(SiMe_3)_2]_2$ reacted slowly with DiBAIH as indicated by color change from pale brown to dark green over 24 h. Upon storage of the reaction mixture for 2 d at $-30\text{ }^\circ\text{C}$ in *n*-hexane, a crystalline compound was collected, which was identified as the starting material by X-ray crystallography. The incomplete reaction with DiBAIH results in the necessity of higher reaction pressures and longer reaction times (4 bar H_2 , 18 h) compared to $Fe[N(SiMe_3)_2]_2$ -DiBAIH. In contrast, $(SINpEt)Fe[N(SiMe_3)_2]_2$ with DiBAIH turned dark brown immediately indicating fast reduction of the iron precursor. The catalyst mixture showed excellent conversion at elevated pressures (entry 6) which identifies it as promising candidate for stereoselective alkene hydrogenations.

Table 5-8. Hydrogenation of 1-phenylcyclohexene with $(BINpMe)Fe[N(SiMe_3)_2]_2$ and $(SINpEt)Fe[N(SiMe_3)_2]_2$.

Entry	[Fe]	Conditions	Yield (Conversion) in % ^a
1	$(BINpMe)Fe[N(SiMe_3)_2]_2$	10 bar H_2 , rt, 18 h	>99 (>99)
2	$(BINpMe)Fe[N(SiMe_3)_2]_2$	4 bar H_2 , rt, 18 h	95 (95)
3	$(BINpMe)Fe[N(SiMe_3)_2]_2$	1.9 bar H_2 , rt, 0.5 h	<1 (<1)
4	$(BINpMe)Fe[N(SiMe_3)_2]_2$	1.9 bar H_2 , rt, 0.5 h ^b	<1 (<1)
5	$(BINpMe)Fe[N(SiMe_3)_2]_2$	no DiBAIH, 50 bar H_2 , rt, 18 h	<1 (<1)

6 (SINpEt)Fe[(N(SiMe₃)₂)₂] 10 bar H₂, rt, 18 h >99 (>99)

^a quantitative GC-FID vs. *n*-pentadecane as internal reference; ^b catalyst preparation 18 h prior reaction.

In a following set of experiments, (SINpEt)Fe[(N(SiMe₃)₂)₂] was used for the hydrogenation of prochiral alkenes (Figure 5-1). Full conversion was observed in all cases in less than 4 h at 1.9 bar H₂. Unfortunately, no enantiomeric enrichment was detected. Most probably, the chiral *NHC*-ligand is dissociated upon reaction with DiBAIH. When (SINpEt)Fe[(N(SiMe₃)₂)₂] was treated with LiBEtH in an independent reaction, a mixture of products of the addition of LiBEtH with the free *NHC*-ligand was detected by X-ray crystallography. A screen for a less reducing activation agent might prevent *NHC*-dissociation and allow enantioselective alkene hydrogenation, but is not part of this work.

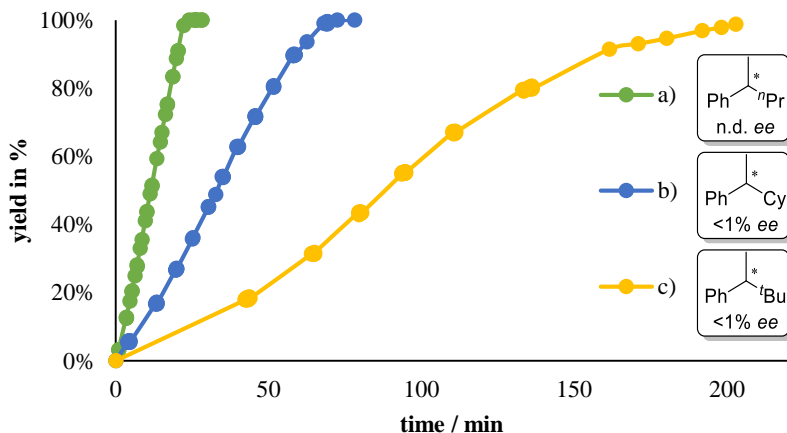


Figure 5-1. Hydrogenation of a) α -(*n*-propyl)styrene, b) α -(cyclohexyl)styrene c) α -(*tert*-butyl)styrene with 5 mol% (SINpEt)Fe[(N(SiMe₃)₂)₂] and 10 mol% DiBAIH at 1.9 bar H₂.

5.5 Conclusions

In summary, we have studied the iron-catalyzed hydrogenation of a broad scope of sterically hindered alkenes and alkynes. A new Ziegler-type catalyst was developed using Fe[(N(SiMe₃)₂)₂] and DiBAIH as activation agent providing a stable and highly active system. Examination of by-products in the generation of the active species support an alkyl transfer from aluminium to iron, β -hydride elimination of *iso*-butene under

formation of an iron-hydride intermediate. In absence of an alkene, the intermediate undergoes reductive elimination of *iso*-butane by second alkyl transfer and hydride transfer from DiBALH. Kinetic poisoning experiments hint toward a heterotopic hydrogenation catalyst, whereas the additional formation of a homotopic active species cannot be excluded. Stereoselective hydrogenations of prochiral alkenes by the use of a chiral *NHC*-Fe[N(SiMe₃)₂]₂ complex failed, presumably due to dissociation of the chiral ligand upon reaction with DiBALH.

5.6 Experimental

5.6.1 General

Analytical Thin-Layer Chromatography: TLC was performed using aluminium plates with silica gel and fluorescent indicator (*Merck*, 60, F254). Thin layer chromatography plates were visualized by exposure to ultraviolet light (366 or 254 nm) or by immersion in a staining solution of molybdatophosphoric acid in ethanol or potassium permanganate in water.

Column Chromatography: Flash column chromatography with silica gel 60 from *KMF* (0.040-0.063 mm). Mixtures of solvents used are noted in brackets.

Chemicals and Solvents: Commercially available olefins were distilled under reduced pressure prior use. Solvents (THF, Et₂O, *n*-hexane, toluene) were distilled over sodium and benzophenone and stored over molecular sieves (4 Å). LiN(SiMe₃)₂ (*SigmaAldrich*, 97%) was sublimated and stored under argon. HN(SiMe₃)₂, HNEt₂, HN(*i*Pr)₂, HNPhMe and 2,2,6,6-tetramethylpiperidine were distilled over CaH₂ and stored under argon prior use. HNPh₂ was recrystallized in *n*-pentane. Solvents used for column chromatography were distilled under reduced pressure prior use (ethyl acetate). DiBAIH (1 M in toluene), AlMe₃ (2 M in toluene), Al(*t*Bu)₃ were used as received from *SigmaAldrich* or diluted before use.

High Pressure Reactor: Hydrogenation reactions were carried out in 160 and 300 mL high pressure reactors (*Parr*TM) in 4 mL glass vials. The reactors were loaded under argon, purged with H₂ (1 min), sealed and the internal pressure was adjusted. Hydrogen (99.9992%) was purchased from *Linde*.

¹H- und ¹³C-NMR-Spectroscopy: Nuclear magnetic resonance spectra were recorded on a *Bruker Avance 300* (300 MHz) and *Bruker Avance 400* (400 MHz). ¹H-NMR: The following abbreviations are used to indicate multiplicities: s = singlet; d = doublet; t = triplet, q = quartet; m = multiplet, dd = doublet of doublet, dt = doublet of triplet, dq = doublet of quartet, ddt = doublet of doublet of quartet. Chemical shift δ is given in ppm to tetramethylsilane.

Fourier-Transformations-Infrared-Spectroscopy (FT-IR): Spectra were recorded on a *Varian Scimitar 1000 FT-IR* with ATR-device. All spectra were recorded at room temperature. Wave number is given in cm⁻¹. Bands are marked as s = strong, m = medium, w = weak and b = broad.

Gas chromatography with FID (GC-FID): HP6890 GC-System with injector 7683B and *Agilent 7820A* System. Column: HP-5, 19091J-413 (30 m × 0.32 mm × 0.25 μ m), carrier gas: N₂. GC-FID was used for reaction control and catalyst screening (Calibration with internal standard *n*-pentadecane and analytically pure samples).

Gas chromatography with mass-selective detector (GC-MS): Agilent 6890N Network GC-System, mass detector 5975 MS. Column: HP-5MS (30m × 0.25 mm × 0.25 µm, 5% phenylmethylsiloxane, carrier gas: H₂. Standard heating procedure: 50 °C (2 min), 25 °C/min → 300 °C (5 min)

Chiral gas chromatography with FID (chiral GC-FID): Fisons GC 8000. Column: CP-Chirasil-Dex CB (25 m × 0.25 mm ID, 0.25 µm film), carrier gas: Ar. Injection 0.1 µL. Inlet: 200 °C, Detector: 200 °C, Column 50-200 °C with 3 to 10 °C per minute.

Headspace gas chromatography with TCD (HS-GC-TCD): Inficon 3000 Micro GC. Column: 5 Å molecular sieves, carrier gas: argon. Standard heating procedure: 120 °C (3 min). Headspace GC-TCD was used for quantification of H₂, CH₄ and C₂H₆ in the reduction of FeX₂ salts (X = N(SiMe₃)₂, Cl) with aluminium organyls (DiAlH, Al(^{*i*}Bu)₃, AlMe₃). Calibrations of examined gases were conducted by hydrolization of LiAlH₄ (H₂), MeMgCl (CH₄) and EtMgCl (C₂H₆).

Headspace gas chromatography with mass-selective detector (HS-GC-MS): Agilent 7890 B GC-system, mass detector AccuTOF GCX from Jeol. Column: HP 5 (30 m × 0.25 mm × 0.25 µm) from Agilent, carrier gas: helium. Standard heating procedure: 22.2 °C (2 min), 1 °C/min (17.8 min) → 40 °C (3 min) with a flow of 0.6 mL/min. Split 50:1. Injection: 1 µL at 120 °C.

High resolution mass spectrometry (HRMS): The spectra were recorded by the Central Analytics Lab at the Department of Chemistry, University of Regensburg, on a MAT SSQ 710 A from Finnigan.

Gas-uptake reaction monitoring: Gas-uptake was monitored with a *Man On the Moon* X201 kinetic system to maintain a constant reaction pressure. The system was purged with hydrogen prior use. Reservoir pressure was set to about 9 bar H₂. Calibration of the reservoir pressure drop in relation to H₂ consumption was performed by quantitative hydrogenation of various amounts of α -methylstyrene with a Pd/C catalyst in 1 mL of THF.

Dynamic Light Scattering: Dynamic light scattering experiments were performed with the help of a goniometer CGS-II from ALV (Germany). The goniometer is equipped with an ALV-7004/Fast Multiple Tau digital correlator and a vertical-polarized 22 mW HeNe-laser (wavelength = 623.8 nm). All measurements were done at a scattering angle of 90° after thermostating to 25 °C. The measurement time was 300 s. The obtained correlation functions were fitted with the software TableCurve 2d v5.01 by a monomodal equation.

5.6.2 Hydrogenation procedures

General method for catalyst preparation

In an argon-filled glovebox a flame-dried flask was charged with a solution of $\text{Fe}[\text{N}(\text{SiMe}_3)_2]_2$ in toluene (50 mM, 1 mL, 50 μmol). A solution of DiBAI^{H} in toluene (100 mM, 1 mL, 100 μmol) was added via syringe. The solution turned black immediately and was stirred at room temperature for 5 minutes prior use.

General method for *in situ* catalyst preparation with $\text{LiN}(\text{SiMe}_3)_2$

In an argon-filled glovebox a flame-dried flask was charged with $\text{LiN}(\text{SiMe}_3)_2$ (16.7 mg; 100 μmol) and suspended in toluene (1 mL). $\text{FeCl}_2(\text{thf})_{1.5}$ (11.7 mg, 50 μmol) was added and the resulting suspension was stirred at room temperature. After 60 minutes a solution of DiBAI^{H} in toluene (100 mM, 1 mL, 100 μmol) was added via syringe. The solution turned black immediately and was stirred at room temperature for 5 minutes prior use.

General method for *in situ* catalyst preparation with various amines

In an argon-filled glovebox a flame-dried flask was charged with an amine (110 μmol) and toluene (0.8 mL). A solution of $n\text{BuLi}$ in toluene (50 mM, 0.2 mL, 100 μmol) was added at room temperature. After 30 minutes of stirring, $\text{FeCl}_2(\text{thf})_{1.5}$ (11.7 mg, 50 μmol) was added and the resulting suspension was stirred for 60 minutes. After that, a solution of DiBAI^{H} in toluene (100 mM, 1 mL, 100 μmol) was added via syringe. The solution turned black immediately and was stirred at room temperature for 5 minutes prior use.

General method for catalytic hydrogenation

In an argon-filled glovebox a flame-dried 4 mL reaction vial was charged with the substrate (0.2 mmol) and *n*-pentadecane as internal reference for GC-FID quantification (0.2 mmol). After addition of freshly prepared catalyst suspension (400 μL ; 5 mol% $[\text{Fe}]$), the reaction vial was transferred to a high pressure reactor which was sealed and removed from the glovebox. The reactor was purged with H_2 (3×3 bar) and the reaction pressure and temperature were set. After the indicated reaction time, the vial was retrieved and hydrolyzed with a saturated aqueous solution of sodium hydrogen carbonate (0.5 mL). The reaction mixture was extracted with ethyl acetate (1×0.5 mL) and analyzed by GC-FID and GC-MS.

For product isolation, 0.5 to 1 mmol of the starting material was used. After quenching, the product was extracted with ethyl acetate (3×3 mL), washed with brine (10 mL), dried over sodium sulfate and filtered over a pad of silica. Removal of the solvent at reduced pressure afforded the product in high purity.

General method for kinetic examination in catalytic hydrogenation

A flame-dried 10 mL 2-neck flask was connected to a *Man on the Moon X201* gas-uptake system and kept at 23 °C with the help of a water bath. After purging with H₂, the system was set to a reaction pressure of 1.9 bar. Freshly prepared catalyst mixture (1 mL) was added via syringe and stirred for 2 minutes. Monitoring of the hydrogen uptake started with the addition of the substrate (0.5 mmol).

5.6.3 Mechanistic experimental details**Stability of the catalyst**

The catalyst stability was determined by comparison of the hydrogenation rate of 1-phenylcyclohexene after several catalyst treatments. Turnover frequencies were calculated upon the yield after 7 minutes.

Table 5-9. Comparison of TOF after various catalyst pretreatments.

Entry	Reductant	Catalyst pretreatment	TOF ^a / h ⁻¹
1	DiBAIH	freshly prepared	41
2	DiBAIH	storage for 5 d in solution	37
3	DiBAIH	removal of solvent and resolution	30
4	DiBAIH	removal of solvent, storage for 5 d under argon and resolution	27
5	AlMe ₃	freshly prepared	13
6	AlMe ₃	storage for 20 h in solution	<1
7	DiBAIH	<i>in situ</i> synthesis of Fe[N(SiMe ₃) ₂] ₂	27

^a determined with yield after 7 minutes.

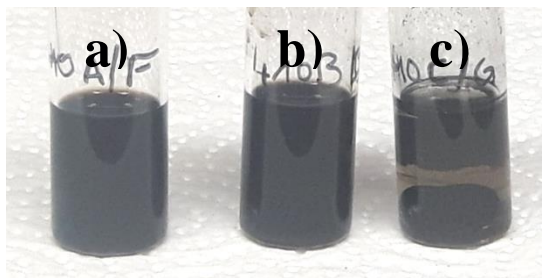


Figure 5-2. Catalyst in solution after 20 h storage under argon; a) $\text{Fe}[\text{N}(\text{SiMe}_3)_2]_2\text{-DiBAIH}$; b) $\text{FeCl}_2(\text{thf})_{1.5}\text{-LiN}(\text{SiMe}_3)_2\text{-DiBAIH}$; c) $\text{Fe}[\text{N}(\text{SiMe}_3)_2]_2\text{-AlMe}_3$.

Determination of degree of deuteration

For deuterium exchange experiments, a reaction mixture of 1,1-diphenylethene with 10 mol% $\text{Fe}[\text{N}(\text{SiMe}_3)_2]_2$ and 20 mol% DiBAIH was quenched after 1 h with D_2O . The reaction mixture was extracted with Et_2O ($2 \times 1 \text{ mL}$), filtered over a pad of silica and analyzed by GC-FID, ^1H and ^2H -NMR to check for D-incorporation.

In a second experiment, DiBAID was used instead of DiBAIH. The reaction mixture of 1,1-diphenylethene with 10 mol% $\text{Fe}[\text{N}(\text{SiMe}_3)_2]_2$ and 20 mol% DiBAID was quenched after 1 h with H_2O and extracted with Et_2O ($2 \times 1 \text{ mL}$). The organic phase was filtered over a pad of silica and analyzed by GC-FID, ^1H -NMR and ^2H -NMR to check for D-incorporation.

For examination of a radical pathway involving the transfer of hydrogen atoms from the solvent, a third reaction of 1,1-diphenylethene with 10 mol% $\text{Fe}[\text{N}(\text{SiMe}_3)_2]_2$ and 20 mol% DiBAIH was performed in toluene- d_8 . After 1 h, the reaction mixture was quenched with H_2O , extracted with Et_2O ($2 \times 1 \text{ mL}$), filtered over a pad of silica and analyzed by GC-FID, ^1H -NMR and ^2H -NMR to check for D-incorporation.

For complete conversion, the reactions were repeated with 100 mol% $\text{Fe}[\text{N}(\text{SiMe}_3)_2]_2$ and 200 mol% DiBAIH (D_2O -quench) or 200 mol% DiBAID (H_2O -quench).

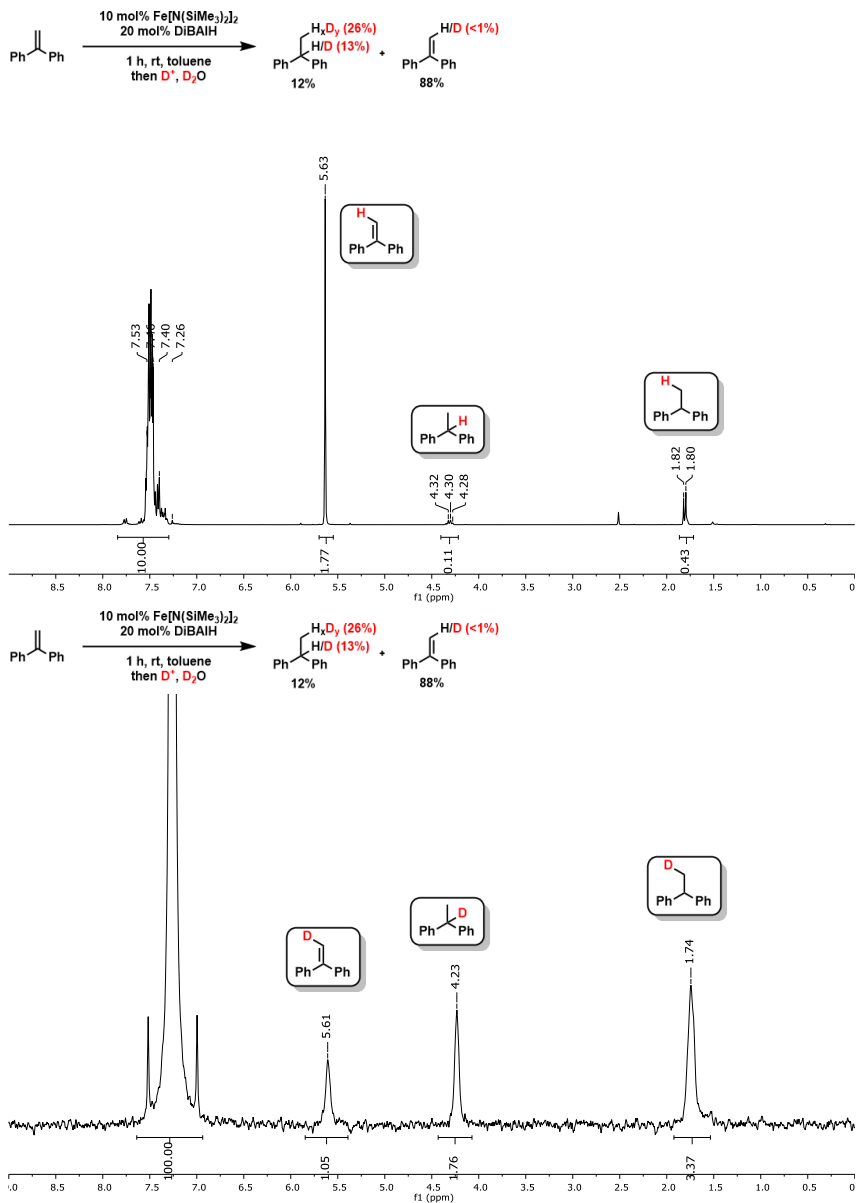


Figure 5-3. $^1\text{H-NMR}$ (top) and $^2\text{H-NMR}$ (bottom) of crude reaction mixture after extraction. Quantification ($^2\text{H-NMR}$) via addition of CDCl_3 (99.95 mg) as internal reference, m (product mixture) = 171 mg.

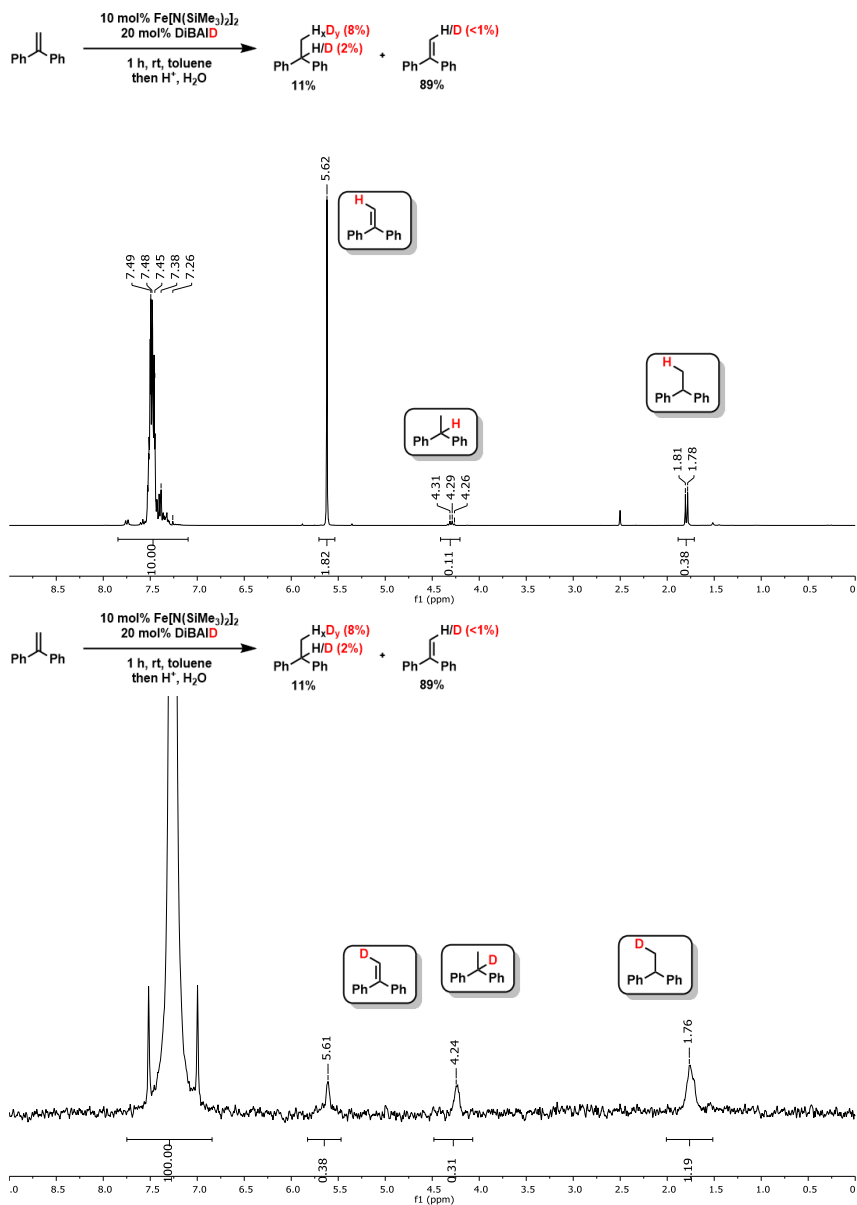


Figure 5-4. $^1\text{H-NMR}$ (top) and $^2\text{H-NMR}$ (bottom) of crude reaction mixture after extraction. Quantification ($^2\text{H-NMR}$) via addition of CDCl_3 (100.84 mg) as internal reference, m (product mixture) = 171 mg.

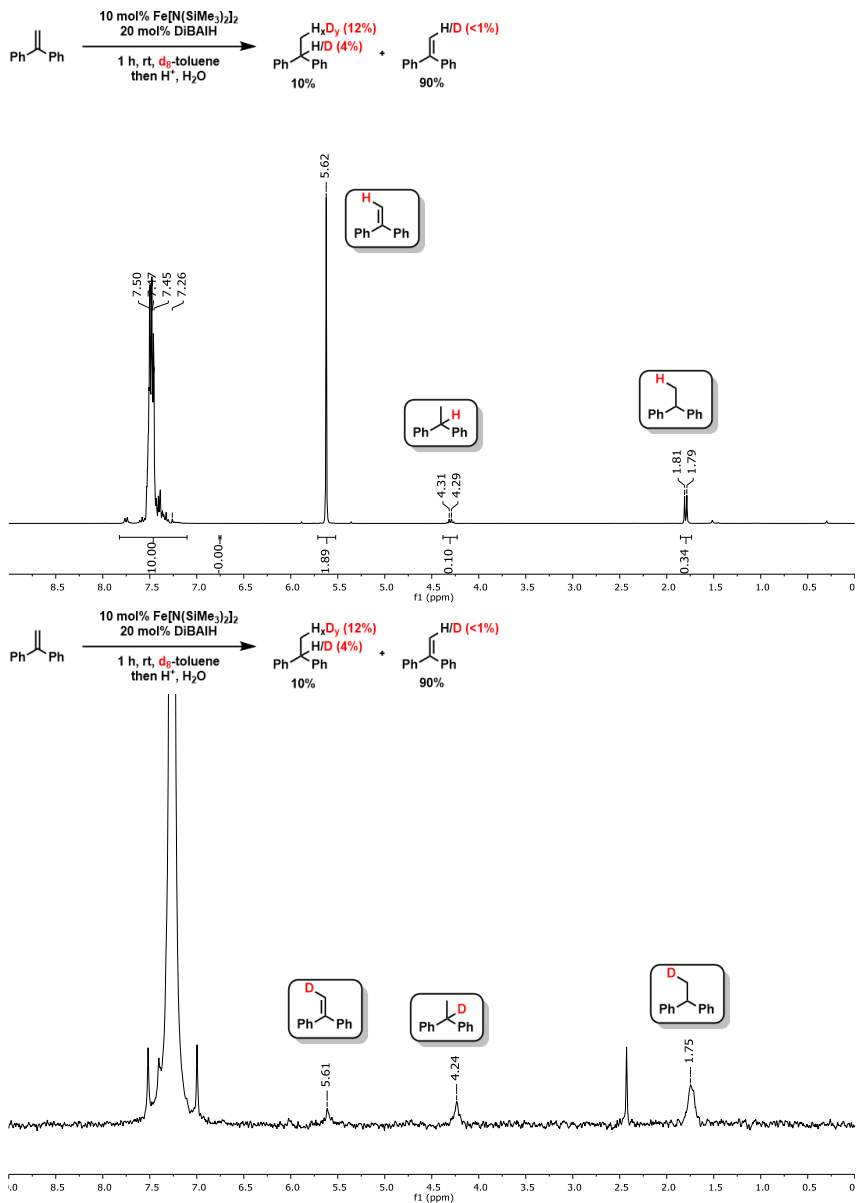


Figure 5-5. ^1H -NMR (top) and ^2H -NMR (bottom) of crude reaction mixture after extraction. Quantification (^2H -NMR) via addition of CDCl_3 (104.61 mg) as internal reference, m (product mixture) = 171 mg.

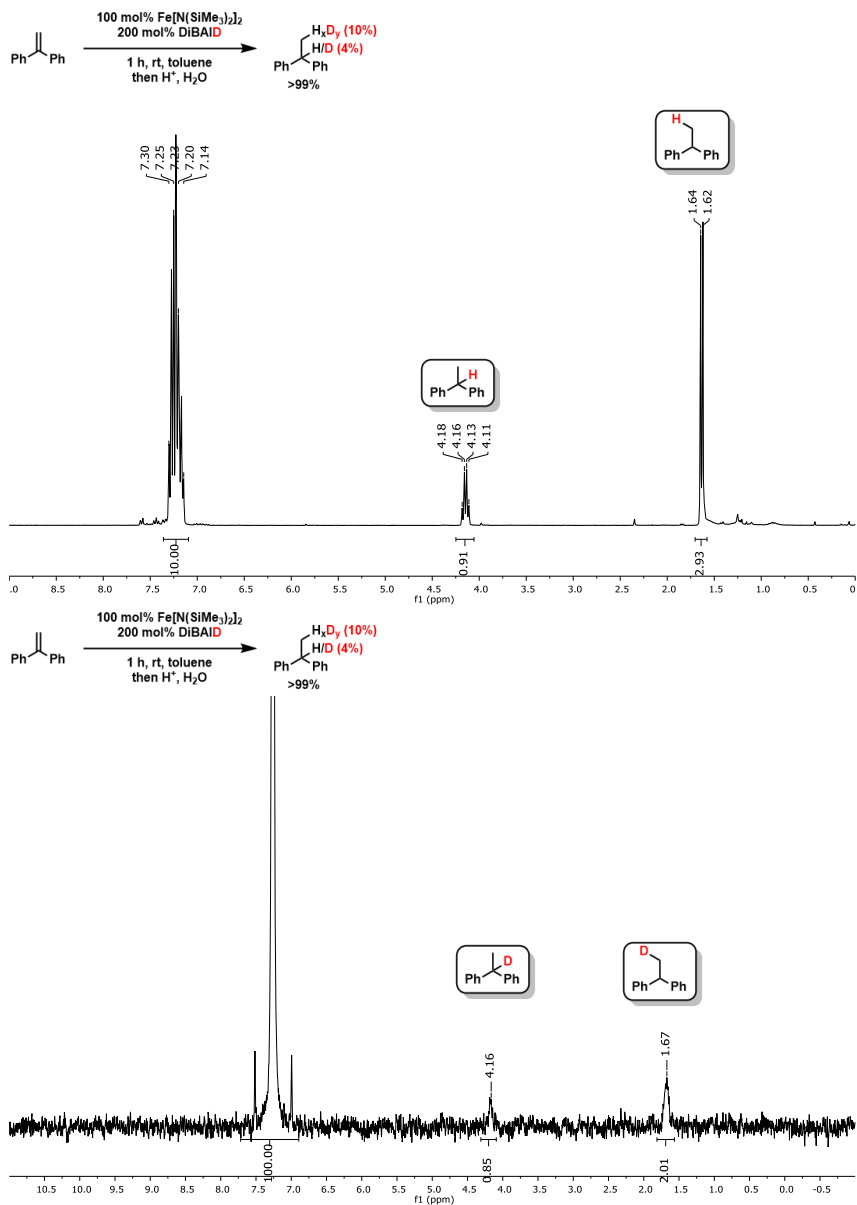


Figure 5-6. $^1\text{H-NMR}$ (top) and $^2\text{H-NMR}$ (bottom) of crude reaction mixture after extraction. Quantification ($^2\text{H-NMR}$) via addition of CDCl_3 (79 mg) as internal reference, m (product mixture) = 25 mg.

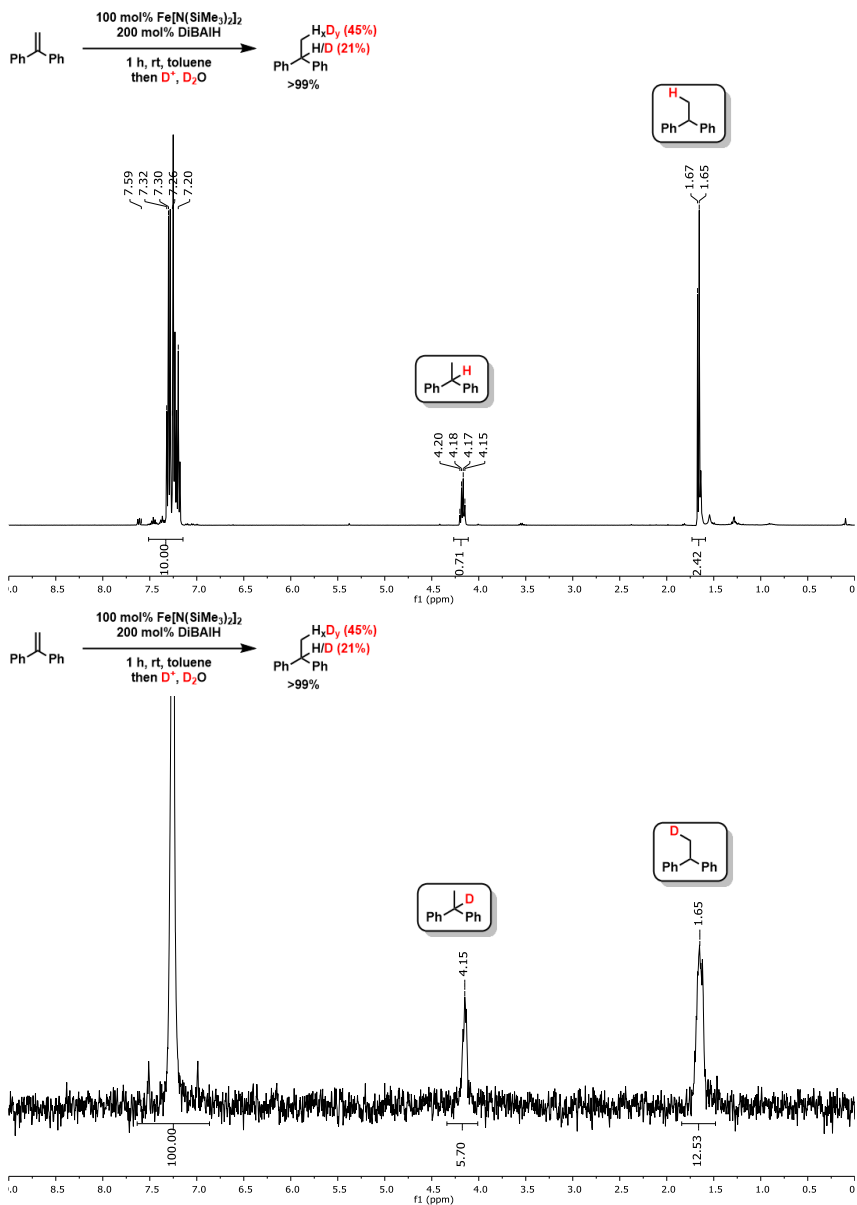


Figure 5-7. $^1\text{H-NMR}$ (top) and $^2\text{H-NMR}$ (bottom) of crude reaction mixture after extraction. Quantification ($^2\text{H-NMR}$) via addition of CDCl_3 (33 mg) as internal reference, m (product mixture) = 14 mg.

Determination of gaseous by-products in the reaction of Fe[N(SiMe₃)₂]₂ with DiBAIH

Headspace GC-MS measurements were performed for detection of gaseous alkanes (C₄-C₈) in the reaction of Fe[N(SiMe₃)₂]₂ with various aluminium organyls.

Therefore, a solution of Fe[N(SiMe₃)₂]₂ in toluene (0.1 mmol, 0.5 M, 0.2 mL) was filled into a 2 mL GC-vial. The vial was closed with a septum screw cap after which a solution of DiBAIH in toluene (0.2 mmol, 1 M, 0.2 mL) was added at room temperature via syringe (10 s). The vial was stirred for 5 minutes prior analysis by Headspace GC-MS. Additives were added after DiBAIH addition. Only *iso*-butene and *iso*-butane were detected.

Table 5-10. Determination of gaseous by-products in the reaction of Fe[N(SiMe₃)₂]₂ with various aluminium organyls by Headspace GC-MS.

$\text{Fe}[\text{N}(\text{SiMe}_3)_2]_2 \xrightarrow[\text{toluene}]{2 \text{ equiv. [Al]}} \text{iso-butene } \mathbf{3} + \text{iso-butane } \mathbf{4} + [\text{Fe}]/[\text{Al}]\text{-products}$			
Entry	[Al]	Additive	3/4 ^a
1	DiBAIH	-	1/300
2	DiBALD	-	0/1 ^b
3	Al(^{<i>i</i>} Bu) ₃	-	1/2
4	DiBAIH	PPh ₃	1/10
5	DiBAIH	Ph ₂ C=CH ₂	1/10

^a relative ratio of peak areas of Headspace GC-MS; ^b partial deuteration of **4** detected.

The evolution of *iso*-butene and *iso*-butane was additionally analyzed by ¹H-NMR.

Therefore, a solution of Fe[N(SiMe₃)₂]₂ in toluene (0.1 mmol, 0.5 M, 0.2 mL) was filled into a 4 mL vial and closed with a septum screw cap. A NMR tube with a septum screw cap and C₆D₆ (0.6 mL) was connected via cannula and cooled to -78 °C with the help of an acetone/dry ice bath. A solution of DiBAIH in toluene (0.2 mmol, 1 M, 0.2 mL) was added via syringe into the 4 mL vial, which was then heated to 60 °C. After 20 minutes, the NMR tube was disconnected and measured.

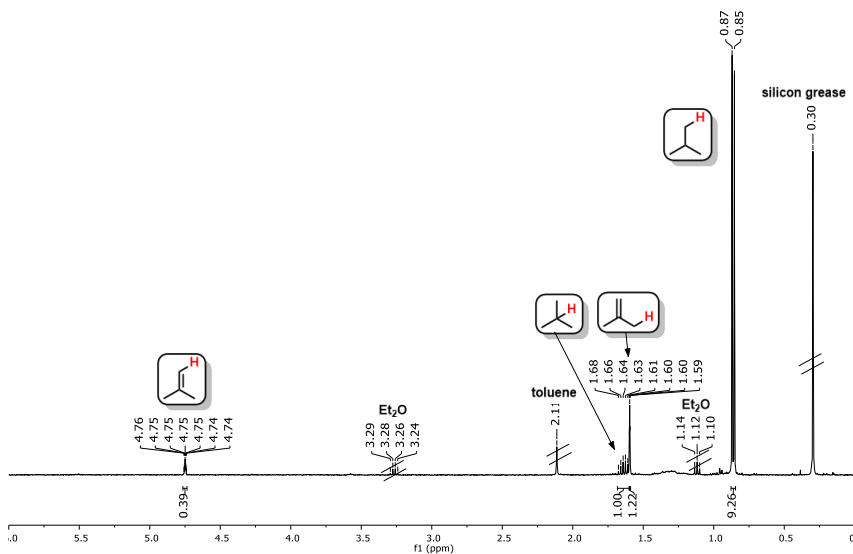


Figure 5-8. ^1H -NMR of volatile products of $\text{Fe}[\text{N}(\text{SiMe}_3)_2]_2$ with 2 equivalents DiBAIH.

The evolution of H_2 , CH_4 and C_2H_6 was analyzed by Headspace GC-TCD.

Therefore, 4 mL vials were filled with a solution of the iron salt in DME or toluene (0.1 mmol, 0.1 M, 1 mL) and closed with a septum screw cap and connected to the inlet of the Headspace GC-TCD. A solution of the aluminium organyl/hydride (0.1-0.2 mmol, 1 mL) was added, the injection started after 3 minutes.

Evolved H_2 in % is based on the peak area of H_2 in the hydrolysis of 0.025 mmol LiAlH_4 (0.1 mmol H_2).

Evolved CH_4 in % is based on the peak area of CH_4 in the hydrolysis of 0.1 mmol MeMgCl (0.1 mmol CH_4).

Evolved C_2H_6 in % is based on the peak area of C_2H_6 in the hydrolysis of 0.1 mmol EtMgCl (0.1 mmol C_2H_6).

Table 5-11. Evolution of H₂ measured by Headspace GC-TCD.

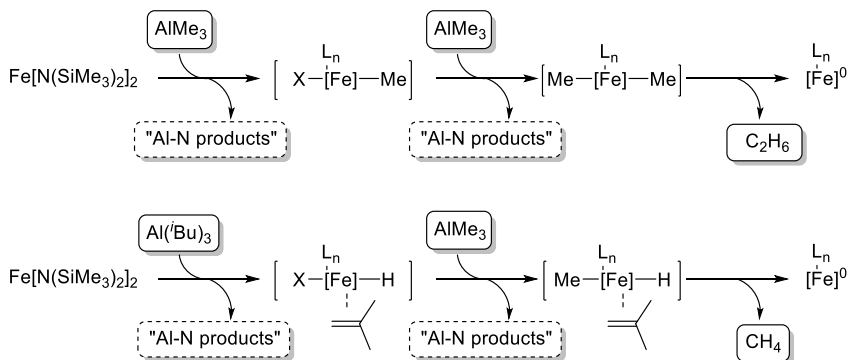
$\text{FeX}_2 \xrightarrow[\text{solvent}]{[\text{Al}]} \text{H}_2 + [\text{Fe}]/[\text{Al}]\text{-products}$				
Entry	[Fe] (mmol)	[Al] (mmol)	solvent	H ₂ in % ^a
1	Fe[N(SiMe ₃) ₂] ₂ (0.1)	DiBAIH (0.2)	toluene	<1
2			DME	9
3	Fe[N(SiMe ₃) ₂] ₂ (0.1)	LiAlH ₄ (0.1)	toluene	<1
4			DME	35
5	FeCl ₂ (thf) _{1.5} (0.1)	DiBAIH (0.2)	toluene	73
6			DME	34
7	FeCl ₂ (thf) _{1.5} (0.1)	LiAlH ₄ (0.1)	toluene	107
8			DME	39
9	Fe[N(SiMe ₃) ₂] ₂ (0.1)	AlMe ₃ (0.2)	toluene	<1
10		AlMe ₃ (0.1) + Al(ⁱ Bu) ₃	toluene	<1

^a ratio of peak area (H₂) and peak area (H₂) by hydrolysis of 0.025 mmol of LiAlH₄.

Table 5-12. Evolution of CH₄ and C₂H₆ measured by Headspace GC-TCD.

$\text{Fe}[\text{N}(\text{SiMe}_3)_2]_2 \xrightarrow[\text{toluene}]{[\text{Al}]} \text{CH}_4 + \text{C}_2\text{H}_6 + [\text{Fe}]/[\text{Al}]\text{-products}$				
Entry	[Fe] (mmol)	[Al] (mmol)	CH ₄ in % ^a	C ₂ H ₆ in % ^a
1	Fe[N(SiMe ₃) ₂] ₂ (0.1)	AlMe ₃ (0.2)	8	13
2		AlMe ₃ (0.1) + Al(ⁱ Bu) ₃ (0.1)	60	<1

^a ratio of peak area (CH₄) and peak area (CH₄) by hydrolysis of 0.1 mmol of MeMgCl;
^b ratio of peak area (C₂H₆) and peak area (C₂H₆) by hydrolysis of 0.1 mmol of EtMgCl.



Scheme 5-15. Postulated pathway of CH_4 and C_2H_6 formation by reaction of $\text{Fe}[\text{N}(\text{SiMe}_3)_2]_2$ with AlMe_3 and $\text{AlMe}_3/\text{Al}(\text{iBu})_3$.

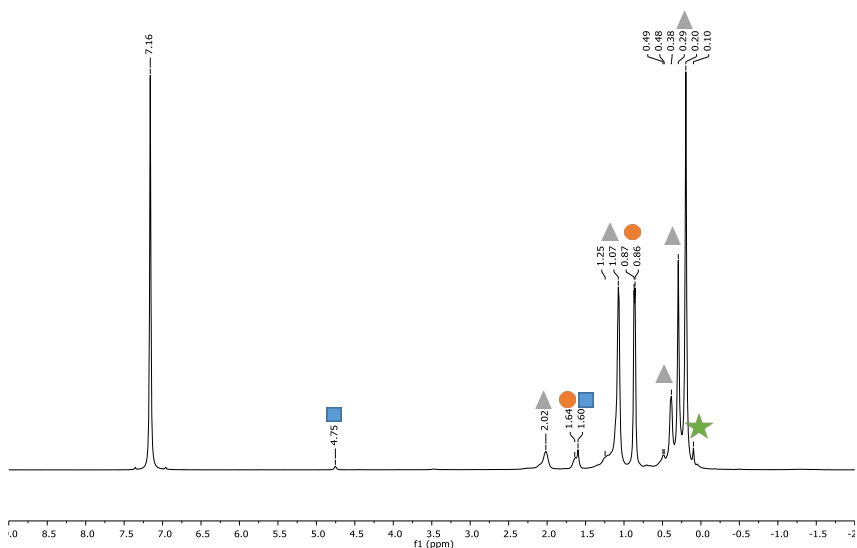


Figure 5-9. ^1H -NMR of $\text{Fe}[\text{N}(\text{SiMe}_3)_2]_2 + 2$ equiv. DiBAIH in C_6D_6 . Peak assignment: *iso*-butene (■), *iso*-butane (●), “Al-N products” (▲), $\text{HN}(\text{SiMe}_3)_2$ (★).

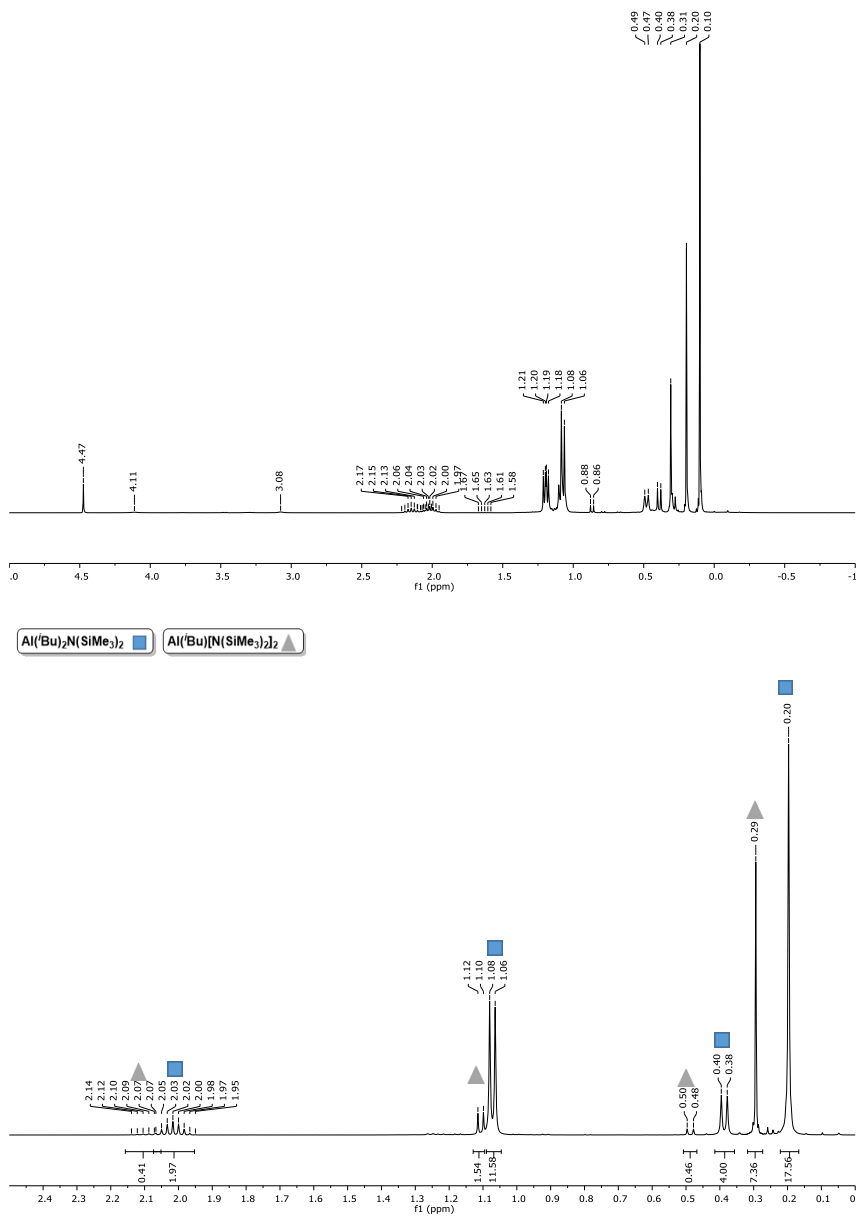


Figure 5-10. ^1H -NMR in C_6D_6 of $\text{HN}(\text{SiMe}_3)_2$ + 1 equiv. DiBAIh (top), distillate of $\text{Fe}[\text{N}(\text{SiMe}_3)_2]_2$ + 2 equiv. DiBAIh (bottom).

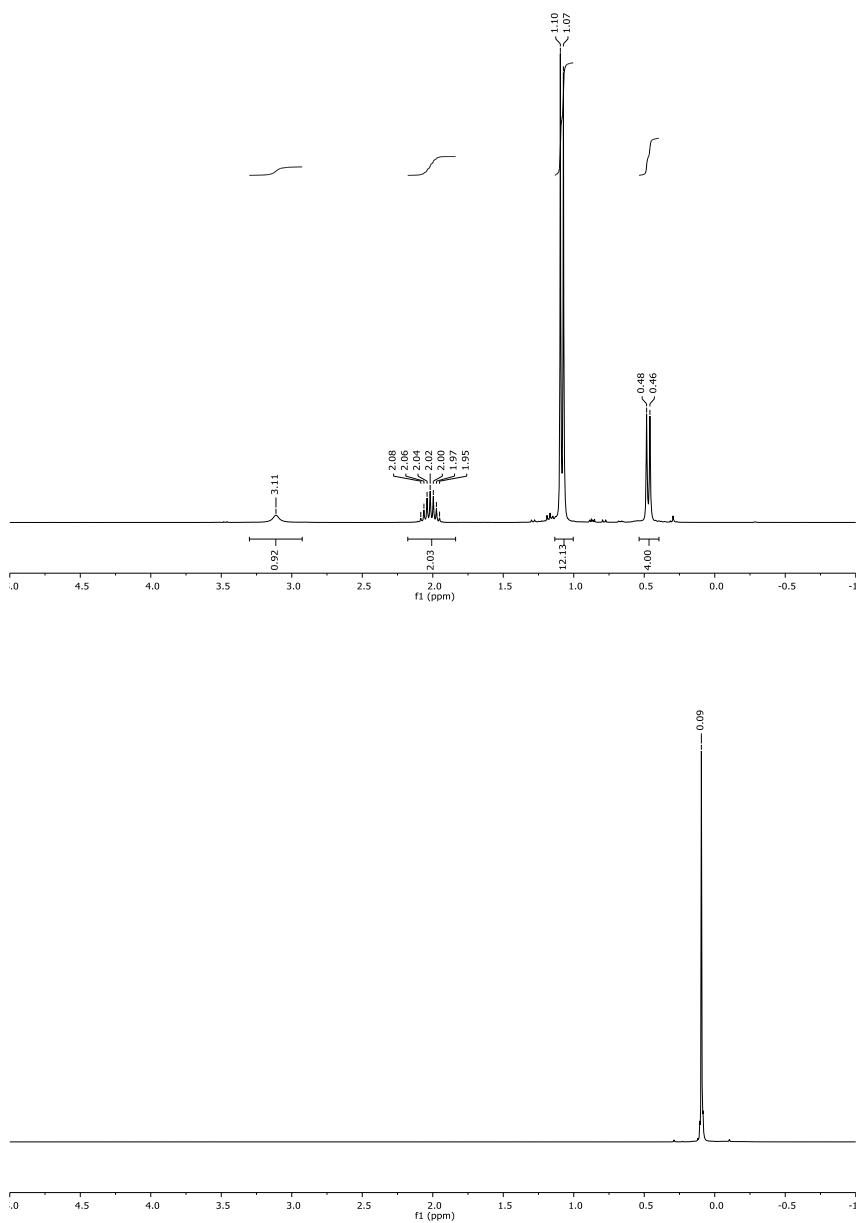


Figure 5-11. ^1H -NMR in C_6D_6 of DiBALH (top), $\text{HN}(\text{SiMe}_3)_2$ (bottom).

5.6.4 Synthesis of starting material

Synthesis of $\{\text{Fe}[\text{N}(\text{SiMe}_3)_2]_2\}$

Synthesis according to R. A. Andersen, K. Faegri, J. C. Green, A. Haaland, M. F. Lappert, W. P. Leung, K. Rypdal, *Inorg. Chem.* **1988**, 27, 1782–1786 with slight modifications.

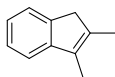
A flame-dried *Schlenk*-flask under argon was charged with $\text{LiN}(\text{SiMe}_3)_2$ (6.37 g, 2.2 equiv., 38.1 mmol) in diethyl ether (60 mL). At 0 °C FeCl_2 (2.24 g, 1.0 equiv., 17.1 mmol, 97%) was added in portions. The resulting reaction mixture was allowed to warm to room temperature and stirred for 24 h. The solid residue was suspended in *n*-hexane (25 mL) filtered over a glass frit and washed with *n*-hexane (5×3 mL). After removing the solvent under reduced pressure, the crude product was purified by distillation under reduced pressure (90 °C, 10^{-3} mbar) to obtain a dark green oil which crystallizes upon standing at room temperature.

	$\text{C}_{24}\text{H}_{72}\text{Fe}_2\text{N}_4\text{Si}_8$
$\{\text{Fe}[\text{N}(\text{SiMe}_3)_2]_2\}_2$	753.24 g/mol
Yield	4.71 g, 12.5 mmol (73%)
$^1\text{H-NMR}$	(400 MHz, C_6D_6) δ = 64.10 (bs).

Analytical data were in full agreement with R. A. Andersen, K. Faegri, J. C. Green, A. Haaland, M. F. Lappert, W. P. Leung, K. Rypdal, *Inorg. Chem.* **1988**, 27, 1782–1786.

2,3-Dimethyl-1*H*-indene

Synthesis following the procedure described by M. V. Troutman, D. H. Appella, S. L. Buchwald, *J. Am. Chem. Soc.* **1999**, 121, 4916–4917.



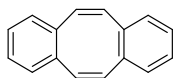
	$\text{C}_{11}\text{H}_{12}$
	144.22 g/mol
Appearance	colorless liquid
Yield	1.49 g, 10.3 mmol (69%)
TLC	R_f = 0.66 (SiO_2 , <i>n</i> -pentane)
$^1\text{H-NMR}$	(300 MHz, CDCl_3) δ 7.37 (dp, J = 7.3, 0.9 Hz, 1H), 7.31 – 7.21 (m, 2H), 7.12 (td, J = 7.2, 1.5 Hz, 1H), 3.31 – 3.21 (m, 2H), 2.07 (q, J = 1.0 Hz, 3H), 2.04 (tq, J = 2.1, 1.1 Hz, 3H).

^{13}C-NMR	(75 MHz, CDCl_3) δ 126.05, 123.55, 122.97, 117.91, 42.46, 13.95, 10.17.
GC-MS	t_R = 6.77 min, (EI, 70 eV): m/z = 144 [M^+], 129, 115, 89, 77, 63, 51.

Analytical data were in full agreement with M. G. Schrems, E. Neumann, A. Pfaltz, *Angew. Chem. Int. Ed.* **2007**, 46, 8274–8276.

Dibenzo[*a,e*]cyclooctatetraene (dct)

Synthesis following the procedure described by G. Franck, M. Brill, G. Helmchen, *J. Org. Chem.* **2012**, 89, 55-65.



$\text{C}_{16}\text{H}_{12}$

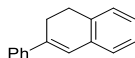
204.27 g/mol

Appearance	colorless solid
Yield	912 mg, 4.46 mmol (47%)
TLC	R_f = 0.46 (SiO_2 , hexanes)
^1H-NMR	(300 MHz, CDCl_3): δ 7.19–7.13 (m, 4H), 7.10–7.02 (m, 4H), 6.76 (s, 4H).
^{13}C-NMR	(75 MHz, CDCl_3): δ 137.1, 133.3, 129.1, 126.8.
GC-MS	t_R = 9.35 min, (EI, 70 eV): m/z = 204 [M^+].

Analytical data were in full agreement with G. Franck, M. Brill, G. Helmchen, *J. Org. Chem.* **2012**, 89, 55-65.

4-Phenyl-1,2-dihydronaphthalene

Synthesis was performed by Schachtner, Josef, *Dissertation* **2016**, Regensburg.



$\text{C}_{16}\text{H}_{14}$

206.29 g/mol

Appearance	colorless liquid
Yield	912 mg, 4.46 mmol (47%)
TLC	R_f = 0.41 (SiO_2 , hexanes)

¹H-NMR	(300 MHz, CDCl ₃) δ 7.43 – 7.27 (m, 5H), 7.24 – 7.05 (m, 3H), 7.01 (dd, <i>J</i> = 7.4, 1.6 Hz, 1H), 6.09 (t, <i>J</i> = 4.7 Hz, 1H), 2.86 (t, <i>J</i> = 7.9 Hz, 2H), 2.42 (ddd, <i>J</i> = 9.1, 7.2, 4.7 Hz, 2H).
¹³C-NMR	(75 MHz, CDCl ₃) δ 128.9, 128.3, 127.8, 127.7, 127.2, 126.3, 125.6, 28.4, 23.7.
GC-MS	<i>t</i> _R = 9.37 min, (EI, 70 eV): <i>m/z</i> = 206 [M] ⁺ , 178, 165, 152, 128, 102, 78, 51.

Analytical data were in full agreement with P. Peach, D. J. Cross, J. A. Kenny, I. Houson, L. Campbell, T. Walsgrove, M. Wills, *Tetrahedron*, **2006**, 62, 1864-1876.

1-Phenylcyclopentene

Synthesis was performed by Schachtner, Josef, *Dissertation* **2016**, Regensburg.



C₁₁H₁₂

144.22 g/mol

Appearance	colorless liquid
Yield	1.99 g, 13.8 mmol (69%)
TLC	<i>R</i> _f = 0.66 (SiO ₂ , hexanes)
¹H-NMR	(300 MHz, CDCl ₃) δ 7.48 – 7.42 (m, 2H), 7.36 – 7.27 (m, 2H), 7.25 – 7.18 (m, 1H), 6.19 (h, <i>J</i> = 2.1 Hz, 1H), 2.82 – 2.61 (m, 2H), 2.54 (tq, <i>J</i> = 7.6, 2.5 Hz, 2H), 2.15 – 1.93 (m, 2H).
¹³C-NMR	(75 MHz, CDCl ₃) δ 128.29, 128.27, 127.60, 126.82, 126.12, 125.91, 125.54, 66.45, 33.37, 33.18, 28.91, 28.08, 23.37, 19.35.
GC-MS	<i>t</i> _R = 6.94 min, (EI, 70 eV): <i>m/z</i> = 144 [M] ⁺ , 129, 115, 103, 91, 77, 63, 51.

Analytical data were in full agreement with W. Su, S. Urgaonkar, P. A. McLaughlin, J. G. Verkade, *J. Am. Chem. Soc.* **2004**, 126, 16433–16439.

1-Phenylcycloheptene

Synthesis was performed by Schachtner, Josef, *Dissertation* **2016**, Regensburg.



$C_{13}H_{16}$

172.27 g/mol

Appearance

colorless liquid

Yield

2.89 g, 16.8 mmol (84%)

TLC

$R_f = 0.69$ (SiO₂, hexanes)

¹H-NMR

(300 MHz, CDCl₃) δ 7.42 – 7.16 (m, 5H), 6.13 (td, $J = 6.8, 1.3$ Hz, 1H), 2.75 – 2.52 (m, 2H), 2.43 – 2.25 (m, 2H), 1.94 – 1.80 (m, 2H), 1.74 – 1.50 (m, 4H).

¹³C-NMR

(75 MHz, CDCl₃) δ 144.99, 130.45, 128.13, 126.26, 125.67, 32.86, 32.82, 28.92, 26.98, 26.85.

GC-MS

$t_R = 7.97$ min, (EI, 70 eV): $m/z = 172$ [M⁺], 157, 144, 129, 115, 104, 91, 77, 63, 51.

Analytical data were in full agreement with G. Baddeley, J. Chadwick, H. T. Taylor, *J. Chem. Soc.* **1956**, 451.

(1-cyclopropylvinyl)benzene

Synthesis following the general procedure for styrene synthesis in a Wittig reaction in chapter 4.5.3.



$C_{11}H_{12}$

144.22 g/mol

Appearance

colorless liquid

Yield

1.27 g, 8.8 mmol (80%)

TLC

$R_f = 0.53$ (SiO₂, hexanes)

¹H-NMR

(300 MHz, CDCl₃) δ 7.67 – 7.57 (m, 2H), 7.42 – 7.26 (m, 3H), 5.30 (d, $J=1.0$, 1H), 4.95 (t, $J=1.2$, 1H), 1.67 (ttd, $J=8.3, 5.4, 1.2$, 1H), 0.92 – 0.79 (m, 2H), 0.61 (ddd, $J=6.4, 5.4, 4.1$, 2H).

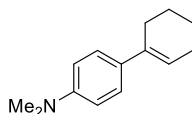
^{13}C -NMR (75 MHz, CDCl_3) δ 149.47, 141.75, 128.28, 127.58, 126.25, 109.15, 77.58, 77.16, 77.16, 76.74, 15.78, 6.83.

GC-MS t_R = 6.31 min, (EI, 70 eV): m/z = 144 $[\text{M}^+]$, 129, 115, 103, 91, 77, 63, 51.

Analytical data were in full agreement with C. Chatalova-Sazepin, Q. Wang, G. M. Sammis, J. Zhu, *Angew. Chem. Int. Ed.* **2015**, 54, 5443–5446.

4-(Cyclohex-1-enyl)-*N,N*-dimethylaniline

Synthesis was performed by Schachtner, Josef, *Dissertation* **2016**, Regensburg.



$\text{C}_{14}\text{H}_{19}\text{N}$

201.31 g/mol

Appearance colorless liquid

Yield 1.65 g, 8.20 mmol (82%)

TLC R_f = 0.82 (SiO_2 , hexanes)

^1H -NMR (300 MHz, CDCl_3) δ 7.41 – 7.19 (m, 2H), 6.76 (ddd, J = 13.1, 6.8, 2.8 Hz, 2H), 6.06 – 6.00 (m, 1H), 2.96 (d, J = 2.8 Hz, 6H), 2.35 – 2.49 (m, 2H), 2.27 – 2.14 (m, 2H), 1.87 – 1.73 (m, 2H), 1.61 – 1.72 (m, 2H).

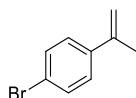
^{13}C -NMR (75 MHz, CDCl_3) δ 149.4, 136.0, 129.1, 125.6, 121.7, 116.7, 112.7, 112.6, 40.8, 40.7, 27.4, 25.9, 23.2, 22.4.

GC-MS t_R = 9.59 min, (EI, 70 eV): m/z = 202 $[\text{M}]^+$, 180, 157, 129, 101, 77, 51.

Analytical data were in full agreement with K. Ishiuka, H. Seike, T. Hatakeyama, M. Nakamura, *J. Am. Chem. Soc.* **2010**, 132, 13117–13119.

4-Bromo- α -methylstyrene

Synthesis following the general procedure for styrene synthesis in a Wittig reaction in chapter 4.5.3.



$\text{C}_9\text{H}_9\text{Br}$

197.08 g/mol

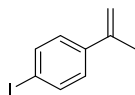
Appearance colorless oil

Yield	1.06 g, 5.39 mmol (77%)
TLC	$R_f = 0.59$ (SiO ₂ , <i>n</i> -pentane)
¹H-NMR	(400 MHz, CDCl ₃) δ 7.50-7.35 (m, 2H), 7.42-7.29 (m, 2H), 5.36 (s, 1H), 5.10 (s, 1H), 2.12 (s, 3H).
¹³C-NMR	(101 MHz, CDCl ₃) δ 142.2, 140.1, 131.3, 127.2, 121.4, 113.1, 21.7.
GC-MS	$t_R = 6.51$ min, (EI, 70 eV): $m/z = 197$ [M ⁺], 183, 171, 156, 115, 102, 91, 75, 63, 51.

Analytical data were in full agreement with T. Taniguchi, A. Yajima, H. Ishibashi, *Adv. Synth. Catal.* **2011**, 353, 2643–2647.

4-Iodo- α -methylstyrene

Synthesis following the general procedure for styrene synthesis in a Wittig reaction in chapter 4.5.3.



C₉H₉I

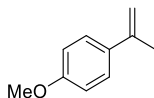
244.08 g/mol

Appearance	colorless solid
Yield	1.21 g, 4.96 mmol (71%)
TLC	$R_f = 0.84$ (SiO ₂ , <i>n</i> -pentane)
¹H-NMR	(300 MHz, CDCl ₃) δ 7.70 – 7.59 (m, 2H), 7.24 – 7.15 (m, 2H), 5.40 – 5.33 (m, 1H), 5.12 – 5.07 (m, 1H), 2.14 – 2.09 (m, 3H).
¹³C-NMR	(75 MHz, CDCl ₃) δ 142.28, 140.70, 137.27, 134.97, 127.41, 113.15, 92.88, 21.62.
GC-MS	$t_R = 7.14$ min, (EI, 70 eV): $m/z = 244$ [M ⁺], 127, 115, 102, 91, 75, 63, 50.

Analytical data were in full agreement with G. B. Bachman, C. L. Carlson, M. Robinson, *J. Am. Chem. Soc.* **1951**, 73, 1964–1965.

4-Methoxy- α -methylstyrene

Synthesis following the general procedure for styrene synthesis in a Wittig reaction in chapter 4.5.3.



$C_{10}H_{12}O$

148.20 g/mol

Appearance

colorless liquid

Yield

1.04 g, 7.02 mmol (35%)

TLC

$R_f = 0.25$ (SiO_2 , n -pentane)

 1H -NMR

(300 MHz, $CDCl_3$) δ 7.42 (d, $J = 8.9$ Hz, 2H), 6.87 (d, $J = 8.9$ Hz, 2H), 5.29 (s, 1H), 4.99 (s, 1H), 3.82 (s, 3H), 2.13 (s, 3H).

 ^{13}C -NMR

(75 MHz, $CDCl_3$) δ 159.05, 142.56, 133.74, 126.60, 113.54, 110.68, 55.30, 21.94.

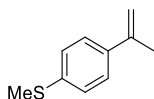
GC-MS

$t_R = 6.39$ min, (EI, 70 eV): $m/z = 148$ [M^+], 127, 133, 115, 105, 89, 77, 63, 51.

Analytical data were in full agreement with A. Fryszkowska, K. Fisher, J. M. Gardiner, G. M. Stephens, *J. Org. Chem.* **2008**, 73, 4295-4298.

Methyl(4-(prop-1-en-2-yl)phenyl)sulfane

Synthesis following the general procedure for styrene synthesis in a Wittig reaction in chapter 4.5.3.



$C_{10}H_{12}S$

164.27 g/mol

Appearance

colorless solid

Yield

1.09 g, 6.63 mmol (33%)

TLC

$R_f = 0.44$ (SiO_2 , n -pentane)

 1H -NMR

(300 MHz, $CDCl_3$) δ 7.45 – 7.35 (m, 2H), 7.25 – 7.18 (m, 2H), 5.36 (dq, $J=1.6, 0.8$, 1H), 5.06 (dq, $J=1.5, 1.5$, 1H), 2.49 (s, 3H), 2.14 (dd, $J=1.5, 0.8$, 3H).

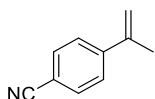
^{13}C -NMR (75 MHz, CDCl_3) δ 142.51, 138.01, 137.49, 126.37, 125.90, 111.96, 21.75, 15.91.

GC-MS t_{R} = 7.38 min, (EI, 70 eV): m/z = 164 [M^+], 149, 134, 115, 102, 91, 77, 69, 51.

Analytical data were in full agreement with G. Fraenkel, J. M. Geckle, *J. Am. Chem. Soc.* **1980**, 102, 2869–2880.

4-Cyano- α -methylstyrene

Synthesis following the general procedure for styrene synthesis in a Wittig reaction in chapter 4.5.3.



$\text{C}_{10}\text{H}_9\text{N}$

143.19 g/mol

Appearance colorless liquid

Yield 1.09 g, 7.61 mmol (38%)

TLC R_{f} = 0.10 (SiO_2 , n -pentane)

^1H -NMR (300 MHz, CDCl_3) δ 7.67 – 7.56 (m, 2H), 7.59 – 7.48 (m, 2H), 5.47 (dq, J =0.9, 1H), 5.24 (dq, J =1.4, 1H), 2.15 (dd, J =1.5, 0.8, 3H).

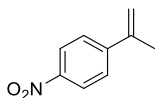
^{13}C -NMR (75 MHz, CDCl_3) δ 145.63, 141.78, 132.10, 126.12, 119.00, 115.67, 110.83, 21.46.

GC-MS t_{R} = 6.79 min, (EI, 70 eV): m/z = 143 [M^+], 128, 116, 101, 89, 75, 63, 51.

Analytical data were in full agreement with O. Pytela, B. Trlida, *Collect. Czech. Chem. Commun.* **2007**, 72, 1025–1036.

4-Nitro- α -methylstyrene

Synthesis following the general procedure for styrene synthesis in a Wittig reaction in chapter 4.5.3.



$\text{C}_9\text{H}_9\text{NO}_2$

163.18 g/mol

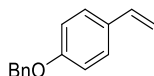
Appearance orange solid

Yield	312 mg, 1.91 mmol (10%)
TLC	$R_f = 0.18$ (SiO ₂ , <i>n</i> -pentane)
¹H-NMR	(300 MHz, CDCl ₃) δ 8.22 – 8.15 (m, 2H), 7.64 – 7.55 (m, 2H), 5.55 – 5.50 (m, 1H), 5.32 – 5.27 (m, 1H), 2.22 – 2.16 (m, 3H).
¹³C-NMR	(75 MHz, CDCl ₃) δ 147.63, 141.56, 126.23, 123.60, 116.41, 21.61.
GC-MS	$t_R = 7.43$ min, (EI, 70 eV): $m/z = 163$ [M ⁺], 133, 115, 105, 91, 75, 63, 51.

Analytical data were in full agreement with N. Kornblum, L. Cheng, T. M. Davies, G. W. Earl, N. L. Holy, R. C. Kerber, M. M. Kestner, J. W. Manthey, M. T. Musser, *J. Org. Chem.* **1987**, 52, 196–204.

1-(Benzyloxy)-4-vinylbenzene

Synthesis following the general procedure for styrene synthesis in a Wittig reaction in chapter 4.5.3.



C₁₅H₁₄O

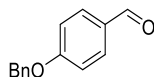
210.27 g/mol

Appearance	colorless solid
Yield	1.25 g, 5.97 mmol (74%)
TLC	$R_f = 0.28$ (SiO ₂ , <i>n</i> -pentane)
¹H-NMR	(300 MHz, CDCl ₃) δ 7.49 – 7.29 (m, 7H), 6.99 – 6.90 (m, 2H), 6.67 (dd, $J = 17.6, 10.9$ Hz, 1H), 5.63 (dd, $J = 17.6, 0.9$ Hz, 1H), 5.14 (dd, $J = 10.9, 0.9$ Hz, 1H), 5.08 (s, 2H).
¹³C-NMR	(75 MHz, CDCl ₃) δ 158.57, 136.94, 136.21, 130.69, 128.63, 128.02, 127.50, 127.43, 114.88, 111.75, 70.03.
GC-MS	$t_R = 9.40$ min, (EI, 70 eV): $m/z = 197$ [M ⁺], 183, 171, 156, 115, 102, 91, 75, 63, 51.

Analytical data were in full agreement with N. Kakusawa, K. Yamaguchi, J. Kouchichiro, *J. Organomet. Chem.* **2005**, 12, 2956–2966.

4-(Benzyloxy)benzaldehyde

Synthesis following the procedure by S. K. Das, G. Panda, *Tetrahedron* **2008**, *19*, 4162-4173.

C₁₄H₁₂O₂

212.24 g/mol

Appearance

colorless solid

Yield

1.72 g, 8.12 mmol (81%)

TLC R_f = 0.20 (SiO₂, hexanes/ethyl acetate = 9/1)**¹H-NMR**(300 MHz, CDCl₃) δ 9.89 (s, 1H), 7.84 (d, J = 8.7 Hz, 2H), 7.48 – 7.33 (m, 5H), 7.08 (d, J = 8.7 Hz, 2H), 5.16 (s, 2H).**¹³C-NMR**(75 MHz, CDCl₃) δ 190.82, 163.72, 135.93, 132.02, 130.11, 128.75, 128.36, 127.51, 115.15, 70.28.**GC-MS** t_R = 9.96 min, (EI, 70 eV): m/z = 212 [M⁺], 152, 121, 91, 77, 65, 51.

Analytical data were in full agreement with T. Shintou, T. Mukaiyama, *J. Am. Chem. Soc.*, **2004**, *23*, 7359-7367.

N-(1-Phenylvinyl)acetamide

Synthesis following the procedure described by J. T. Reeves, Z. Tan, Z. S. Han, G. Li, Y. Zhang, Y. Xu, D. C. Reeves, N. C. Gonnella, S. Ma, H. Lee, B. Z. Lu, C. H. Senanayake, *Angew. Chem. Int. Ed.* **2012**, *51*, 1400-1404.

C₁₀H₁₁NO

161.20 g/mol

Appearance

colorless solid

Yield

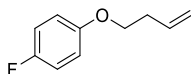
235 mg, 1.48 mmol (15%)

¹H-NMR(300 MHz, DMSO-*d*₆) δ 9.34 (s, 1H), 7.49 – 7.31 (m, 5H), 5.62 (s, 1H), 4.98 (s, 1H), 2.01 (s, 3H).**¹³C-NMR**(75 MHz, DMSO-*d*₆) δ 169.04, 141.36, 140.94, 137.93, 128.18, 126.13, 101.78, 23.64.**GC-MS** t_R = 7.87 min, (EI, 70 eV): m/z = 161 [M⁺], 146, 132, 119, 104, 77, 63, 51.

Analytical data were in full agreement with J. T. Reeves, Z. Tan, Z. S. Han, G. Li, Y. Zhang, Y. Xu, D. C. Reeves, N. C. Gonnella, S. Ma, H. Lee et al., *Angew. Chem. Int. Ed.* **2012**, 51, 1400–1404.

1-(but-3-en-1-yloxy)-4-fluorobenzene

Synthesis following the procedure by J. A. Murphy, F. Schoenebeck, N. J. Findlay, D. W. Thomson, S. Zhou, J. Garnier; *J. Am. Chem. Soc.* **2009**, 131, 6475–6479.



C₁₀H₁₁FO

166.20 g/mol

Appearance

colorless liquid

Yield

1.89 g, 11.38 mmol (76%)

TLC

R_f = 0.80 (SiO₂, hexanes/ethyl acetate = 99/1)

¹H-NMR

(300 MHz, CDCl₃) δ 7.03 – 6.91 (m, 2H), 6.88 – 6.78 (m, 2H), 5.90 (ddt, J = 17.0, 10.2, 6.7 Hz, 1H), 5.14 (qdd, J = 3.0, 2.6, 1.4 Hz, 2H), 3.97 (t, J = 6.7 Hz, 2H), 2.53 (qt, J = 6.7, 1.3 Hz, 2H).

¹³C-NMR

(75 MHz, CDCl₃) δ 158.81, 155.66, 155.00, 134.37, 117.11, 115.92, 115.62, 115.59, 115.49, 67.86, 33.67.

GC-MS

t_R = 5.96 min, (EI, 70 eV): m/z = 166 [M⁺], 138, 125, 112, 95, 83, 75, 55.

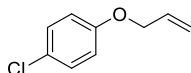
HRMS

(EI, m/z): found 166.0798 [M⁺] (calculated 166.0794).

FT-IR

(ATR-film) in [cm⁻¹] 2872 (w), 1642 (w), 1504 (s), 1472 (m), 1431 (w), 1388 (w), 1294 (w), 1247 (m), 1202 (s), 1096 (m), 1036 (m), 988 (m), 916 (s), 825 (s), 744 (s), 513 (s).

1-(allyloxy)-4-chlorobenzene



C₉H₉ClO

168.62 g/mol

Appearance

colorless liquid

Yield

1.53 g, 9.07 mmol (91%)

TLC

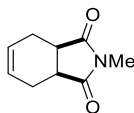
R_f = 0.20 (SiO₂, hexanes/ethyl acetate = 9/1)

¹H-NMR	(300 MHz, CDCl ₃) δ 7.29 – 7.19 (m, 2H), 6.89 – 6.79 (m, 2H), 6.04 (ddt, <i>J</i> = 17.3, 10.5, 5.3 Hz, 1H), 5.41 (dq, <i>J</i> = 17.3, 1.6 Hz, 1H), 5.30 (dq, <i>J</i> = 10.4, 1.4 Hz, 1H), 4.51 (dt, <i>J</i> = 5.3, 1.5 Hz, 2H).
¹³C-NMR	(75 MHz, CDCl ₃) δ 157.17, 132.91, 129.32, 125.69, 117.95, 116.02, 69.06.
GC-MS	<i>t</i> _R = 6.59 min, (EI, 70 eV): <i>m/z</i> = 168 [M ⁺], 153, 133, 127, 111, 105, 99, 73, 63, 50.

Analytical data were in full agreement with K. Huang, H. Wang, V. Stepanenko, M. de Jesús, C. Torruellas, W. Correa, M. Ortiz-Marciales, *J. Org. Chem.* **2011**, 76, 1883–1886.

***N*-Methyl-1,2,3,6-tetrahydrophthalimide**

Synthesis was performed by Schachtner, Josef, *Dissertation* **2016**, Regensburg.



C₉H₁₁NO₂

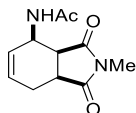
165.19 g/mol

Appearance	colorless solid
Yield	5.7 g, 34.5 mmol (70%)
TLC	<i>R</i> _f = 0.42 (SiO ₂ , hexanes/ethyl acetate 2/1)
¹H-NMR	(400 MHz, CDCl ₃): δ 5.92-5.85 (m, 2H), 3.12-3.05 (m, 2H), 2.96 (s, 3H), 2.64-2.58 (m, 2H), 2.27-2.19 (m, 2H).
GC-MS	<i>t</i> _R = 7.58 min (EI, 70 eV): <i>m/z</i> = 165 [M ⁺], 150, 136, 107, 80, 65, 57, 51.

Analytical data were in full agreement with E. Schefczik, *Chem. Ber.* **1965**, 98, 1270–1281.

N-Methyl-3-acetamido-1,2,3,6-tetrahydropthalimide

Synthesis following the procedure described by R. Fichtler, J.-M. Neudörfl, A. Jacobi von Wangelin, *Org. Biomol. Chem.* **2011**, 9, 7224–7236.


 $C_{11}H_{14}N_2O_3$

222.24 g/mol

Appearance

colorless solid

Yield

488 mg, 2.2 mmol (15%)

TLC $R_f = 0.13$ (SiO₂, hexanes/ethyl acetate = 1/4)**¹H-NMR**

(300 MHz, CDCl₃) δ 7.27 (s, 1H), 5.86 (m, 1H), 5.72 (m, 1H), 4.81–4.61 (m, 1H), 3.19 (m, 2H), 2.94 (s, 3H), 2.71 (m, 1H), 2.21 (m, 1H), 2.08 (s, 3H).

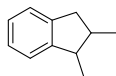
¹³C-NMR

(75 MHz, CDCl₃) δ 179.3, 179.2, 169.9, 132.9, 127.4, 45.2, 42.5, 38.8, 25.0, 24.1, 23.5.

GC-MS

$t_R = 9.76$ min, (EI, 70 eV): $m/z = 222$ [M⁺], 204, 179, 165, 151, 136, 120, 105, 94, 79, 69, 58.

Analytical data were in full agreement with D. Strübing, H. Neumann, A. Jacobi von Wangelin, S. Klaus, S. Hübner, M. Beller, *Tetrahedron* **2006**, 62, 10962–10967.

5.6.5 Hydrogenation products**1,2-dimethyl-2,3-dihydro-1H-indene**
 $C_{11}H_{14}$

146.23 g/mol

¹H-NMR

(400 MHz, CDCl₃) δ 7.23 – 7.10 (m, 4H), 3.17 (p, $J = 7.1$ Hz, 1H), 3.04 – 2.92 (m, 1H), 2.63 – 2.53 (m, 2H), 1.15 (d, $J = 7.2$ Hz, 3H), 0.99 (d, $J = 6.8$ Hz, 3H).

¹³C-NMR

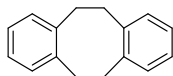
(75 MHz, CDCl₃) δ 148.81, 142.95, 126.10, 126.04, 124.48, 123.59, 42.39, 39.39, 37.84, 15.20, 14.67.

GC-MS

$t_R = 6.03$ min, (EI, 70 eV): $m/z = 146$ [M⁺], 131, 115, 103, 91, 77, 63, 51.

Analytical data were in full agreement with R. P. Yu, J. M. Darmon, J. M. Hoyt, G. W. Margulieux, Z. R. Turner, P. J. Chirik, *ACS Catal.* **2012**, 2, 1760–1764.

5,6,11,12-tetrahydridibenzo[*a,e*][8]annulene



C₁₆H₁₆

208.30 g/mol

Yield 87 mg, 0.42 mmol (89%)

¹H-NMR (300 MHz, CDCl₃) δ 7.06 – 6.93 (m, 8H), 3.07 (s, 8H).

¹³C-NMR (75 MHz, CDCl₃) δ 140.60, 129.67, 126.10, 35.16.

GC-MS *t*_R = 9.45 min, (EI, 70 eV): *m/z* = 208 [M⁺], 193, 178, 165, 115, 104, 91, 78, 63, 51.

Analytical data were in full agreement with D. Guijarro, B. Mancheño, M. Yus, *Tetrahedron* **1992**, 48, 4593–4600.

Phenylcyclohexane



C₁₂H₁₆

160.26 g/mol

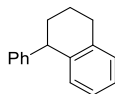
¹H-NMR (300 MHz, CDCl₃) δ 7.34 – 7.25 (m, 2H), 7.24 – 7.14 (m, 3H), 2.60 – 2.39 (m, 1H), 2.00 – 1.79 (m, 4H), 1.80 – 1.73 (m, 1H), 1.51 – 1.19 (m, 5H).

¹³C-NMR (75 MHz, CDCl₃) δ 148.1, 128.3, 126.5, 125.8, 44.7, 34.52, 27.0, 26.2.

GC-MS *t*_R = 7.30 min, (EI, 70 eV): *m/z* = 160 [M⁺], 143, 129, 115, 102, 91, 77, 63, 51.

Analytical data were in full agreement with W. M. Czaplik, M. Mayer, Jacobi von Wangelin, Axel, *Angew. Chem. Int. Ed.* **2009**, 48, 607–610.

1-Phenyl-1,2,3,4-tetrahydronaphthalene



C₁₆H₁₆

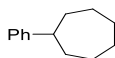
208.30 g/mol

Yield 166 mg, 0.80 mmol (82%)

$^1\text{H-NMR}$	(300 MHz, CDCl_3) δ 7.37 – 7.10 (m, 7H), 7.09 – 7.01 (m, 1H), 6.86 (d, J = 7.8 Hz, 1H), 4.14 (t, J = 6.6 Hz, 1H), 3.04 – 2.76 (m, 2H), 2.31 – 2.10 (m, 1H), 2.03 – 1.68 (m, 3H).
$^{13}\text{C-NMR}$	(75 MHz, CDCl_3) δ 147.55, 139.40, 137.61, 130.21, 128.99, 128.88, 128.25, 125.96, 125.92, 125.66, 45.65, 33.30, 29.82, 21.00.
GC-MS	t_R = 9.33 min, (EI, 70 eV): m/z = 208 [M^+], 179, 165, 152, 130, 115, 104, 91, 78, 63, 51.

Analytical data were in full agreement with S. T. Bright, J. M. Coxon, P. J. Steel, *J. Org. Chem.* **1990**, 55, 1338–1344.

Phenylcycloheptane



$\text{C}_{13}\text{H}_{18}$

174.29 g/mol

Yield	153 mg, 0.88 mmol (87%)
$^1\text{H-NMR}$	(300 MHz, CDCl_3) δ 7.35 – 7.11 (m, 5H), 2.76 – 2.56 (m, 1H), 2.00 – 1.75 (m, 4H), 1.74 – 1.49 (m, 8H).
$^{13}\text{C-NMR}$	(75 MHz, CDCl_3) δ 150.05, 128.31, 126.70, 125.52, 47.10, 36.86, 27.99, 27.27.
GC-MS	t_R = 7.80 min, (EI, 70 eV): m/z = 174 [M^+], 117, 104, 91, 78, 65, 55.

Analytical data were in full agreement with S. Kawamura, K. Ishizuka, H. Takaya, M. Nakamura, *Chem. Commun.* **2010**, 46, 6054–6056.

1,1-Diphenylethane



$\text{C}_{14}\text{H}_{14}$

182.27 g/mol

$^1\text{H-NMR}$	(300 MHz, CDCl_3) δ 7.35 – 7.11 (m, 10H), 4.15 (q, J = 7.1, 1H), 1.63 (d, J = 7.2, 3H).
GC-MS	t_R = 7.97 min, (EI, 70 eV): m/z = 182 [M^+], 167, 152, 139, 128, 115, 103, 89, 77, 63, 51.

Analytical data were in full agreement with F. Schoenebeck, J. A. Murphy, S.-z. Zhou, Y. Uenoyama, Y. Miclo, T. Tuttle, *J. Am. Chem. Soc.* **2007**, *129*, 13368–13369.

1-Cyclopropyl-1-phenylethane



$C_{11}H_{14}$

146.23 g/mol

Yield 63 mg, 0.43 mmol (81%)

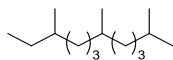
1H -NMR (300 MHz, $CDCl_3$) δ 7.41 – 7.26 (m, 4H), 7.25 – 7.17 (m, 1H), 1.99 (dq, J = 9.2, 7.0 Hz, 1H), 1.35 (d, J = 7.0 Hz, 3H), 0.96 (qt, J = 9.1, 8.0, 5.0 Hz, 1H), 0.65 – 0.36 (m, 2H), 0.27 – 0.09 (m, 2H).

^{13}C -NMR (75 MHz, $CDCl_3$) δ 147.38, 128.23, 127.00, 125.89, 44.67, 21.62, 18.56, 4.64, 4.34.

GC-MS t_R = 5.87 min, (EI, 70 eV): m/z = 146 [M^+], 131, 117, 105, 91, 77, 65, 51.

Analytical data were in full agreement with T. N. Gieshoff, M. Villa, A. Welther, M. Plois, U. Chakraborty, R. Wolf, A. Jacobi von Wangelin, *Green Chem* **2015**, *17*, 1408–1413.

2,6,10-Trimethyldodecane



$C_{15}H_{32}$

212.42 g/mol

Yield 191 mg, 0.90 mmol (91%)

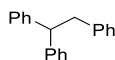
1H -NMR (300 MHz, $CDCl_3$) δ 1.77 – 1.44 (m, 4H), 1.42 – 0.98 (m, 14H), 0.93 – 0.75 (m, 14H).

^{13}C -NMR (75 MHz, $CDCl_3$) δ 42.41, 39.43, 39.39, 37.88, 37.48, 37.43, 37.41, 37.32, 37.01, 36.97, 35.76, 35.64, 34.47, 34.44, 34.42, 33.07, 32.83, 32.80, 30.56, 29.59, 29.49, 28.47, 28.00, 25.31, 24.84, 24.53, 22.78, 22.74, 22.64, 19.76, 19.70, 19.28, 19.22, 16.22, 11.46, 11.43.

GC-MS t_R = 7.18 min, (EI, 70 eV): m/z = 212 [M^+], 183, 127, 113, 85, 71, 57.

Analytical data were in full agreement with D. K. Dalling, R. J. Pugmire, D. M. Grant, W. E. Hull, *Magn. Reson. Chem.* **1986**, 24, 191–198.

1,1,2-Triphenylethane



$C_{20}H_{18}$

258.36 g/mol

1H -NMR (300 MHz, $CDCl_3$) δ 7.30 – 7.09 (m, 13H), 7.05 – 6.95 (m, 2H), 4.24 (t, $J = 7.8$ Hz, 1H), 3.37 (d, $J = 7.8$ Hz, 2H).

^{13}C -NMR (75 MHz, $CDCl_3$) δ 144.45, 140.26, 129.08, 128.34, 128.05, 126.19, 125.88, 53.11, 42.11.

GC-MS $t_R = 10.67$ min, (EI, 70 eV): $m/z = 258$ [M^+], 167, 152, 139, 128, 115, 102, 91, 77, 65, 51.

Analytical data were in full agreement with T. C. Fessard, H. Motoyoshi, E. M. Carreira, *Angew. Chem. Int. Ed.* **2007**, 46, 2078–2081.

Pinane

Mixture of diastereomers.



$C_{10}H_{18}$

138.25 g/mol

1H -NMR complex mixture of isomers

^{13}C -NMR (75 MHz, $CDCl_3$) δ 67.98, 65.88, 48.07, 47.62, 41.35, 40.88, 39.49, 38.82, 35.95, 33.96, 29.35, 28.30, 26.84, 26.54, 25.63, 24.61, 23.93, 23.83, 23.22, 23.04, 22.90, 21.61, 20.09, 15.29.

GC-MS $t_R = 4.67$ min, (EI, 70 eV): $m/z = 138$ [M^+], 123, 95, 81, 67, 55.

Analytical data were in full agreement with A. Stolle, B. Ondruschka, W. Bonrath, T. Netscher, M. Findeisen, M. M. Hoffmann, *Chemistry* **2008**, 14, 6805–6814.

1,2,3,4-Tetrahydroquinoline



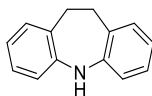
$C_9H_{11}N$

133.19 g/mol

Yield	124 mg, 0.93 mmol (90%)
¹H-NMR	(300 MHz, CDCl ₃) δ 7.03 – 6.92 (m, 2H), 6.62 (td, <i>J</i> = 7.4, 1.2 Hz, 1H), 6.50 (d, <i>J</i> = 7.8 Hz, 1H), 3.98 (s, 1H), 3.37 – 3.25 (m, 2H), 2.78 (t, <i>J</i> = 6.4 Hz, 2H), 2.03 – 1.88 (m, 2H).
¹³C-NMR	(75 MHz, CDCl ₃) δ 144.82, 129.56, 126.76, 121.48, 116.97, 114.23, 42.03, 27.02, 22.22.
GC-MS	<i>t</i> _R = 7.17 min, (EI, 70 eV): <i>m/z</i> = 133 [M ⁺], 118, 104, 91, 77, 63, 51.

Analytical data were in full agreement with M. Ortiz-Marciales, L. D. Rivera, M. de Jesus, S. Espinosa, J. A. Benjamin, O. E. Casanova, I. G. Figueroa, S. Rodriguez, W. Correa, *J. Org. Chem.* **2005**, 70, 10132–10134.

10,11-Dihydro-5H-dibenzo[b,f]azepine

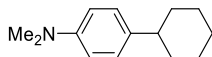


C₁₄H₁₃N
195.27 g/mol

Yield	179 mg, 0.92 mmol (91%)
¹H-NMR	(300 MHz, CDCl ₃) δ 7.18 – 7.04 (m, 4H), 6.89 – 6.66 (m, 4H), 6.02 (s, 1H), 3.12 (s, 4H).
¹³C-NMR	(75 MHz, CDCl ₃) δ 141.38, 129.62, 127.57, 125.76, 118.38, 116.86, 33.87.
GC-MS	<i>t</i> _R = 10.16 min, (EI, 70 eV): <i>m/z</i> = 195 [M ⁺], 180, 167, 152, 118, 97, 89, 77, 63, 51.

Analytical data were in full agreement with J. A. Profitt, H. H. Ong, *J. Org. Chem.* **1979**, 44, 3972–3974.

4-Cyclohexyl-*N,N*-dimethylaniline



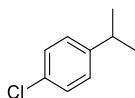
C₁₄H₂₁N
203.33 g/mol

Yield	197 mg, 0.97 mmol (97%)
--------------	-------------------------

$^1\text{H-NMR}$	(300 MHz, CDCl_3) δ 7.15 – 7.07 (m, 2H), 6.77 – 6.72 (m, 2H), 2.93 (s, 6H), 2.52 – 2.38 (m, 1H), 1.94 – 1.80 (m, 4H), 1.78 – 1.70 (m, 1H), 1.48 – 1.34 (m, 4H), 1.34 – 1.25 (m, 1H).
$^{13}\text{C-NMR}$	(75 MHz, CDCl_3) δ 127.34, 113.11, 43.53, 41.06, 34.75, 27.05, 26.26.
GC-MS	t_R = 9.30 min, (EI, 70 eV): m/z = 203, 160, 146, 134, 118, 103, 91, 77, 65, 55.

Analytical data were in full agreement with Z. Li, H.-M. Sun, Q. Shen, *Org. Biomol. Chem.* **2016**, *14*, 3314–3321.

1-Chloro-4-isopropylbenzene

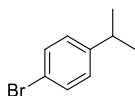


$\text{C}_9\text{H}_{11}\text{Cl}$
154.64 g/mol

$^1\text{H-NMR}$	(300 MHz, CDCl_3) δ 7.25 (m, 2H), 7.21–7.09 (m, 2H), 2.89 (m, 1H), 1.23 (d, J = 6.9 Hz, 6H).
$^{13}\text{C-NMR}$	(75 MHz, CDCl_3) δ 142.3, 131.3, 128.4, 127.8, 33.6, 23.9.
GC-MS	t_R = 5.37 min, (EI, 70 eV): m/z = 154 [M^+], 139, 125, 119, 105, 89, 77, 63, 51.

Analytical data were in full agreement with S. S. Kim, C. S. Kim, *J. Org. Chem.* **1999**, *64*, 9261–9264.

1-Bromo-4-isopropylbenzene

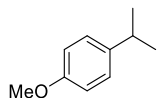


$\text{C}_9\text{H}_{11}\text{Br}$
199.09 g/mol

Yield	99 mg, 0.50 mmol (91%)
$^1\text{H-NMR}$	(300 MHz, CDCl_3) δ 7.47 – 7.36 (m, 2H), 7.15 – 7.04 (m, 2H), 2.87 (hept, J = 6.9 Hz, 1H), 1.23 (d, J = 6.9 Hz, 6H).
$^{13}\text{C-NMR}$	(101 MHz, CDCl_3) δ 147.8, 131.3, 128.2, 119.3, 33.7, 30.9, 23.8.
GC-MS	t_R = 6.16 min, (EI, 70 eV): m/z = 198 [M^+], 185, 169, 158, 143, 119, 104, 91, 77, 63, 51.

Analytical data were in full agreement with M. A. Hall, J. Xi, C. Lor, S. Dai, R. Pearce, W. P. Dailey, R. G. Eckenhoff, *J. Med. Chem.* **2010**, 53, 5667–5675.

1-Isopropyl-4-methoxybenzene



$C_{10}H_{14}O$

180.24 g/mol

1H -NMR

(300 MHz, $CDCl_3$) δ 7.15 (d, J = 8.8 Hz, 2H), 6.84 (d, J = 8.7 Hz, 2H), 3.79 (s, 3H), 2.95 – 2.78 (m, 1H), 1.24 (s, 3H), 1.21 (s, 3H).

^{13}C -NMR

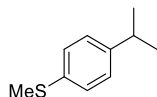
(75 MHz, $CDCl_3$) δ 156.86, 141.06, 127.26, 113.77, 55.27, 33.28, 24.24.

GC-MS

t_R = 5.93 min, (EI, 70 eV): m/z = 150 [M^+], 120, 105, 91, 77, 65, 51.

Analytical data were in full agreement with Cahiez, G.; Foulgoc, L.; Moyeux, A. *Angew. Chem. Int. Ed.* **2009**, 48, 2969–2972.

Methyl(4-(prop-2-yl)phenyl)sulfane



$C_{10}H_{14}S$

166.28 g/mol

1H -NMR

(300 MHz, $CDCl_3$) δ 7.26 – 7.19 (m, 2H), 7.19 – 7.13 (m, 2H), 2.88 (p, J = 6.9 Hz, 1H), 2.48 (s, 3H), 1.24 (d, J = 6.9 Hz, 6H).

^{13}C -NMR

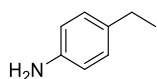
(75 MHz, $CDCl_3$) δ 146.11, 135.05, 127.20, 127.01, 77.47, 77.04, 76.62, 33.65, 24.00, 16.42.

GC-MS

t_R = 7.20 min, (EI, 70 eV): m/z = 166 [M^+], 151, 136, 104, 91, 77, 51.

Analytical data were in full agreement with X.-m. Wu, J.-m. Lou, G.-b. Yan, *Synlett* **2016**, 27, 2269–2273.

4-Ethylaniline



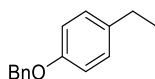
$C_8H_{11}N$

121.18 g/mol

Yield	116 mg, 0.96 mmol (94%)
¹H-NMR	(300 MHz, CDCl ₃) δ 7.01 (d, <i>J</i> = 8.5 Hz, 2H), 6.68 (d, <i>J</i> = 8.3 Hz, 2H), 3.78 (s, 2H), 2.56 (q, <i>J</i> = 7.6 Hz, 2H), 1.20 (t, <i>J</i> = 7.6 Hz, 3H).
¹³C-NMR	(101 MHz, CDCl ₃) δ 143.23, 134.98, 128.64, 115.64, 28.03, 15.98.
GC-MS	<i>t</i> _R = 6.11 min, (EI, 70 eV): <i>m/z</i> = 121 [M ⁺], 106, 93, 77, 65, 51.

Analytical data were in full agreement with B. Wang, H.-X. Sun, G.-Q. Lin, Z.-H. Sun, *Adv. Synth. Catal.* **2009**, 351, 415-422.

1-Benzyloxy-4-ethylbenzene



C₁₅H₁₆O
212.29 g/mol

¹H-NMR	(300 MHz, CDCl ₃) δ 7.51 – 7.30 (m, 5H), 7.18 – 7.11 (m, 2H), 6.97 – 6.89 (m, 2H), 5.07 (s, 2H), 2.62 (q, <i>J</i> = 7.6 Hz, 2H), 1.24 (t, <i>J</i> = 7.6 Hz, 3H).
¹³C-NMR	(75 MHz, CDCl ₃) δ 156.89, 137.30, 136.72, 128.78, 128.60, 127.92, 127.52, 114.72, 70.08, 28.03, 15.93.
GC-MS	<i>t</i> _R = 9.17 min, (EI, 70 eV): <i>m/z</i> = 212 [M ⁺], 122, 107, 91, 77, 65, 51.

Analytical data were in full agreement with C. Zhu, N. Yukimura, M. Yamane, *Organometallics* **2010**, 29, 2098–2103.

Trimethyl-(1-phenylethoxy)silane

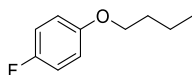


C₁₁H₁₈OSi
194.35 g/mol

¹H-NMR	(300 MHz, CDCl ₃) δ 7.36 – 7.18 (m, 5H), 4.86 (q, <i>J</i> = 6.4 Hz, 1H), 1.43 (d, <i>J</i> = 6.3 Hz, 3H), 0.07 (s, 9H).
¹³C-NMR	(75 MHz, CDCl ₃) δ 146.33, 128.02, 126.73, 125.24, 70.48, 26.78, 0.00.
GC-MS	<i>t</i> _R = 5.74 min, (EI, 70 eV): <i>m/z</i> = 179 [M-CH ₃], 105, 75, 51.

Analytical data were in full agreement with Y. Onishi, Y. Nishimoto, M. Yasuda, A. Baba, *Org. Lett.* **2011**, *13*, 2762–2765.

4-Fluorobenzyl-*n*-butylether



$C_{10}H_{13}FO$

168.21 g/mol

Yield 65 mg, 0.39 mmol (75%)

1H -NMR (300 MHz, $CDCl_3$) δ 7.02 – 6.91 (m, 2H), 6.87 – 6.78 (m, 2H), 3.92 (t, J = 6.5 Hz, 2H), 1.75 (m, 2H), 1.56 – 1.41 (m, 2H), 0.97 (t, J = 7.4 Hz, 3H).

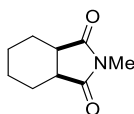
^{13}C -NMR (75 MHz, $CDCl_3$) δ 158.68, 155.53, 155.28, 115.87, 115.56, 115.44, 115.33, 77.46, 77.24, 77.04, 76.62, 68.31, 31.35, 19.24, 13.87.

GC-MS t_R = 6.04 min, (EI, 70 eV): m/z = 168 [M^+], 112, 95, 83, 75, 57, 50.

HRMS (EI, m/z): found 168.0954 [M^+] (calculated 168.0950).

FT-IR (ATR-film) in $[cm^{-1}]$ 2961 (m), 2937 (m), 2874 (w), 1504 (s), 1472 (m), 1390 (w), 1292 (w), 1247 (m), 1206 (s), 1096 (w), 1069 (w), 1028 (w), 974 (w), 825 (s), 755 (s), 723 (m), 512 (m).

2-Methylhexahydro-1*H*-isoindole-1,3(2*H*)-dione



$C_9H_{13}NO_2$

167.21 g/mol

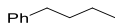
Yield 149 mg, 0.89 mmol (89%)

1H -NMR (300 MHz, $CDCl_3$) δ 2.97 (s, 3H), 2.85 (td, J = 4.5, 2.2 Hz, 2H), 1.98 – 1.80 (m, 2H), 1.80 – 1.68 (m, 2H), 1.53 – 1.35 (m, 4H).

^{13}C -NMR (75 MHz, $CDCl_3$) δ 179.95, 77.46, 77.04, 76.62, 39.77, 24.67, 23.71, 21.61.

GC-MS t_R = 7.77 min, (EI, 70 eV): m/z = 167 [M^+], 138, 113, 82, 67, 54.

Analytical data were in full agreement with B. Bailey, R. D. Haworth, J. McKenna, *J. Chem. Soc.* **1954**, 967.

***n*-Butylbenzene** $C_{10}H_{14}$

134.22 g/mol

 ^1H -NMR

(300 MHz, CDCl_3) δ 7.38 – 7.27 (m, 2H), 7.20 (m, 3H), 2.68 – 2.57 (m, 2H), 1.71 – 1.54 (m, 2H), 1.37 (dq, $J = 14.5, 7.3$ Hz, 2H), 0.94 (t, $J = 7.3$ Hz, 3H).

 ^{13}C -NMR

(75 MHz, CDCl_3) δ 142.95, 128.44, 128.24, 125.57, 35.71, 33.73, 22.42, 14.01.

GC-MS

$t_R = 5.09$ min, (EI, 70 eV): $m/z = 134$ [M^+], 128, 115, 105, 92, 77, 65, 51.

Analytical data were in full agreement with L. Ackermann, A. R. Kapdi, C. Schulzke, *Org. Lett.* **2010**, 12, 2298–2301.

5.6.6 Hydrogenation with chiral iron-complexes

Synthesis of **(SINpEt)Fe[N(SiMe₃)₂]₂** and **(BnNpMe)Fe[N(SiMe₃)₂]₂** was performed by D. Hermann, University Regensburg.

bis(bis(trimethylsilyl)amido)((*R,R*)-1,3-bis(1-(1-naphthyl)ethyl)imidazolidin-2-ylidene) iron(II), **(SINpEt)Fe[N(SiMe₃)₂]₂**

376.6 mg (1.00 mmol, 1.0 equivalent) of bis(bis(trimethylsilyl)amido)iron and 183.4 mg (1.00 mmol, 1.0 equivalent) of sodium bis(trimethylsilyl)amide were dissolved in 5 mL of toluene and stirred for 10 minutes. 466.3 mg (1.00 mmol, 1.0 equivalent) of 1,3-bis(1-(1-naphthyl)ethyl)imidazolinium tetrafluoroborate was added and the mixture was stirred for one hour at room temperature. All volatiles were removed *in vacuo*. The solid residue was washed with 1 mL of cold *n*-pentane and subsequently extracted with toluene. After filtration, the solvent was removed *in vacuo*, yielding the product as a pale yellow solid.

Yield: 513.5 mg (0.680 mmol, 68%).

Elemental analysis: calcd: C 62.03, H 8.28, N 7.42; found: C 62.56, H 7.86, N 7.02.

bis(bis(trimethylsilyl)amido)(1,3-bis(1-naphthylmethyl)imidazolidin-2-ylidene) iron(II), **(BnNpMe)Fe[N(SiMe₃)₂]₂**

376.6 mg (1.00 mmol, 1.0 equivalent) of bis(bis(trimethylsilyl)amido)iron and 183.4 mg (1.00 mmol, 1.0 equivalent) of sodium bis(trimethylsilyl)amide were dissolved in 10 mL of toluene and stirred for 10 minutes. 435.0 mg (1.000 mmol, 1.0 equivalent) of 1,3-bis(1-naphthylmethyl)benzimidazolium chloride was added and the mixture was stirred for one hour at room temperature. All volatiles were removed *in vacuo*. The solid residue was washed with 1 mL of cold *n*-pentane and subsequently extracted with toluene. After filtration, the solvent was removed *in vacuo*, yielding the product as a pale yellow solid.

Yield: 558.1 mg (0.720 mmol, 72%).

Elemental analysis: calcd: C 63.53, H 7.54, N 7.23; found: C 63.62, H 7.24, N 7.07.

Hydrogenation was performed following the general method for kinetic examination in catalytic hydrogenation with **(SINpEt)Fe[(N(SiMe₃)₂)₂]** instead of **Fe[(N(SiMe₃)₂)₂]**.

Synthesis of starting material

α -(*n*-propyl)styrene

Synthesis following the procedure described by M. W. Justik, G. F. Koser; *Tetrahedron Lett.* **2004**, 45, 6159–6163



$C_{11}H_{14}$

146.23 g/mol

Appearance

colorless liquid

Yield

2.00 g, 8.20 mmol (55%)

TLC

R_f = 0.88 (SiO₂, *n*-pentane)

¹H-NMR

(300 MHz, CDCl₃) δ 7.50 – 7.39 (m, 2H), 7.42 – 7.23 (m, 3H), 5.31 (d, J = 1.7 Hz, 1H), 5.09 (q, J = 1.4 Hz, 1H), 2.52 (td, J = 7.8, 1.3 Hz, 2H), 1.52 (h, J = 7.4 Hz, 2H), 0.96 (t, J = 7.3 Hz, 3H).

¹³C-NMR

(75 MHz, CDCl₃) δ 148.52, 141.47, 128.25, 127.27, 126.16, 112.24, 37.48, 21.38, 13.83.

GC-MS

t_R = 5.87 min, (EI, 70 eV): m/z = 146 [M⁺], 131, 118, 103, 91, 77, 65, 51.

Analytical data were in full agreement with M. W. Justik, G. F. Koser, *Tetrahedron Lett.* **2004**, 45, 6159–6163.

α -(cyclohexyl)styrene

A flame-dried *Schlenk* flask was charged with methyltriphenylphosphonium bromide (21.3 mmol 7.74 g) in dry THF (40 mL). Sodium hydride (15.3 mmol, 612 mg, 60% in paraffine) was added in small portions. The suspension was stirred at room temperature for 2.5 h after which cyclohexylphenylketone (21.3 mmol, 4.00 g) in THF (10 mL) was added via syringe. The reaction mixture was stirred overnight, quenched with H₂O (20 mL) and extracted with Et₂O (3 × 20 mL). The combined organic layers were dried (Na₂SO₄), concentrated and subjected to silica gel flash chromatography (*n*-pentane).



$C_{14}H_{18}$

186.30 g/mol

Appearance

colorless liquid

Yield

1.80 g, 9.66 mmol (63%)

TLC	$R_f = 0.88$ (SiO ₂ , <i>n</i> -pentane)
¹H-NMR	(300 MHz, CDCl ₃) δ 7.41 – 7.18 (m, 5H), 5.14 (d, $J=1.3$, 1H), 5.02 (t, $J=1.4$, 1H), 2.55 – 2.33 (m, 1H), 1.94 – 1.64 (m, 5H), 1.44 – 1.12 (m, 5H).
¹³C-NMR	(75 MHz, CDCl ₃) δ 155.01, 142.97, 128.12, 126.99, 126.63, 110.34, 42.57, 32.72, 26.85, 26.46.
GC-MS	$t_R = 7.95$ min, (EI, 70 eV): $m/z = 186$ [M ⁺], 171, 143, 129, 118, 104, 91, 77, 67, 51.

Analytical data were in full agreement with A. L. Hansen, J.-P. Ebran, T. M. Gogsig, T. Skrydstrup, *J. Org. Chem.* **2007**, 72, 6464–6472.

α -(*tert*-butyl)styrene

A flame-dried *Schlenk* flask was charged with methyltriphenylphosphonium bromide (7.83 mmol 2.85 g) in dry THF (15 mL). Sodium hydride (5.63 mmol, 225 mg, 60% in paraffine) was added in small portions. The suspension was stirred at room temperature for 2.5 h after which *tert*-butylphenylketone (7.83 mmol, 1.27 g) in THF (10 mL) was added via syringe. The reaction mixture was stirred overnight, quenched with H₂O (10 mL) and extracted with Et₂O (3 \times 10 mL). The combined organic layers were dried (Na₂SO₄), concentrated and subjected to silica gel flash chromatography (*n*-pentane).



C₁₂H₁₆

160.26 g/mol

Appearance	colorless liquid
Yield	518 mg, 3.23 mmol (57%)
TLC	$R_f = 0.92$ (SiO ₂ , <i>n</i> -pentane)
¹H-NMR	(300 MHz, CDCl ₃) δ 7.31 – 7.24 (m, 3H), 7.19 – 7.11 (m, 2H), 5.18 (d, $J=1.7$, 1H), 4.78 (d, $J=1.7$, 1H), 1.13 (s, 9H).
¹³C-NMR	(75 MHz, CDCl ₃) δ 159.83, 143.48, 129.01, 127.27, 126.24, 111.50, 77.45, 77.03, 76.61, 36.13, 29.74, 29.66.
GC-MS	$t_R = 5.70$ min, (EI, 70 eV): $m/z = 160$ [M ⁺], 145, 128, 117, 104, 91, 77, 57, 51.

Analytical data were in full agreement with J. Stec, E. Thomas, S. Dixon, R. J. Whitby, *Chemistry* **2011**, 17, 4896–4904.

α -(*n*-propyl)ethylbenzeneC₁₁H₁₆

148.25 g/mol

¹H-NMR(300 MHz, CDCl₃) δ 7.35 – 7.27 (m, 2H), 7.24 – 7.15 (m, 3H), 2.71 (h, $J=7.0$, 1H), 1.63 – 1.51 (m, 2H), 1.30 – 1.17 (m, 5H), 0.89 (t, $J=7.3$, 3H).**¹³C-NMR**(75 MHz, CDCl₃) δ 147.95, 128.26, 127.01, 125.75, 40.73, 39.70, 22.33, 20.85, 14.18.**GC-MS** t_R = 5.55 min, (EI, 70 eV): m/z = 148 [M⁺], 105, 91, 77, 65, 51.

Analytical data were in full agreement with E. R. Lynch, E. B. McCall, *J. Chem. Soc.* **1960**, 1254.

 α -(cyclohexyl)ethylbenzeneC₁₄H₂₀

188.31 g/mol

¹H-NMR(300 MHz, CDCl₃) δ 7.32 – 7.25 (m, 2H), 7.22 – 7.12 (m, 3H), 2.44 (p, $J=7.2$, 1H), 1.95 – 1.69 (m, 2H), 1.70 – 1.55 (m, 2H), 1.51 – 1.32 (m, 2H), 1.24 (d, $J=7.0$, 3H), 1.22 – 1.02 (m, 3H), 1.02 – 0.90 (m, 1H), 0.89 – 0.76 (m, 1H).**¹³C-NMR**(75 MHz, CDCl₃) δ 147.13, 128.02, 127.72, 125.64, 45.97, 44.21, 31.50, 30.64, 26.58, 26.55, 18.86.**GC-MS** t_R = 7.82 min, (EI, 70 eV): m/z = 188 [M⁺], 105, 91, 77, 67, 55.

Analytical data were in full agreement with L. Anke, D. Reinhard, P. Weyerstahl, *Liebigs Ann. Chem.* **1981**, 1981, 591–602.

 α -(*tert*-butyl)ethylbenzeneC₁₂H₁₈

162.28 g/mol

¹H-NMR(300 MHz, CDCl₃) δ 7.30 – 7.23 (m, 2H), 7.22 – 7.13 (m, 3H), 2.56 (q, $J=7.2$, 1H), 1.26 (d, $J=7.2$, 3H), 0.87 (s, 9H).

^{13}C -NMR (75 MHz, CDCl_3) δ 145.24, 129.05, 127.42, 125.74, 77.45, 77.02, 76.60, 49.92, 33.69, 27.83, 15.83.

GC-MS t_{R} = 5.70 min, (EI, 70 eV): m/z = 162 [M^+], 147, 115, 105, 91, 77, 65, 57, 51.

Analytical data were in full agreement with S. Andersson, T. Drakenberg, *Org. Magn. Reson.* **1983**, 21, 730–744.

Determination of enantiomeric excess

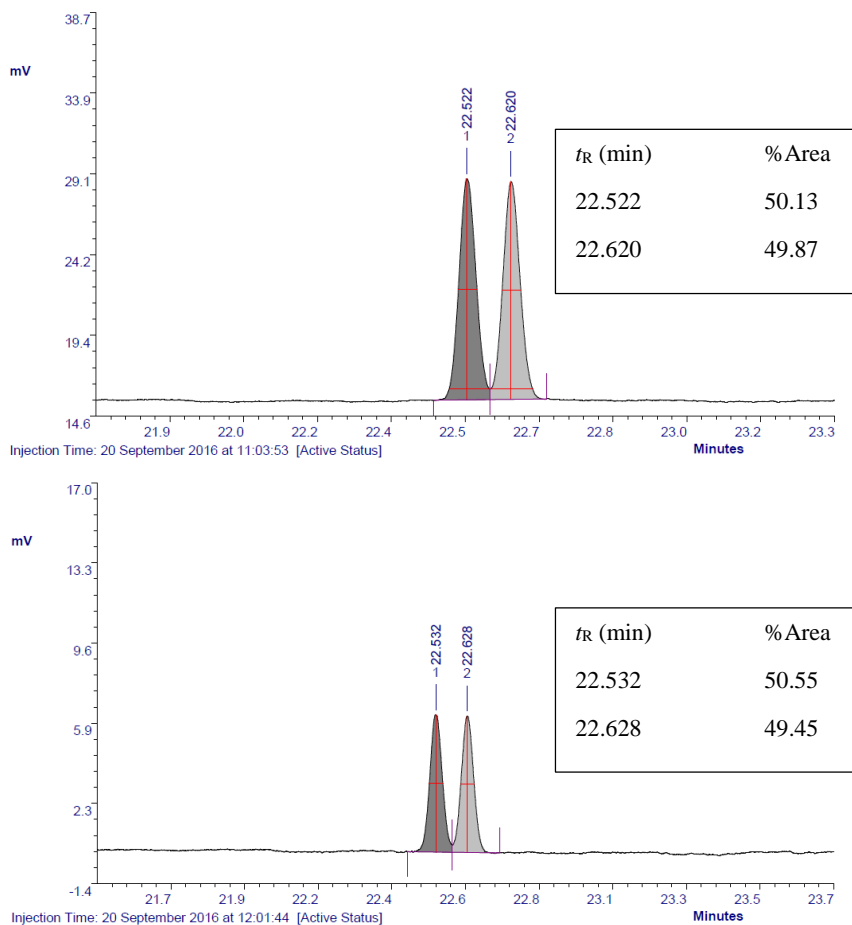


Figure 5-12. Chiral GC-FID chromatogram (5 °C per min) of α -(cyclohexyl)ethylbenzene synthesized by hydrogenation of α -(cyclohexyl)styrene with Pd/C (top) and (SINpMe)Fe[(N(SiMe₃)₂)₂]-DiBAIH (bottom).

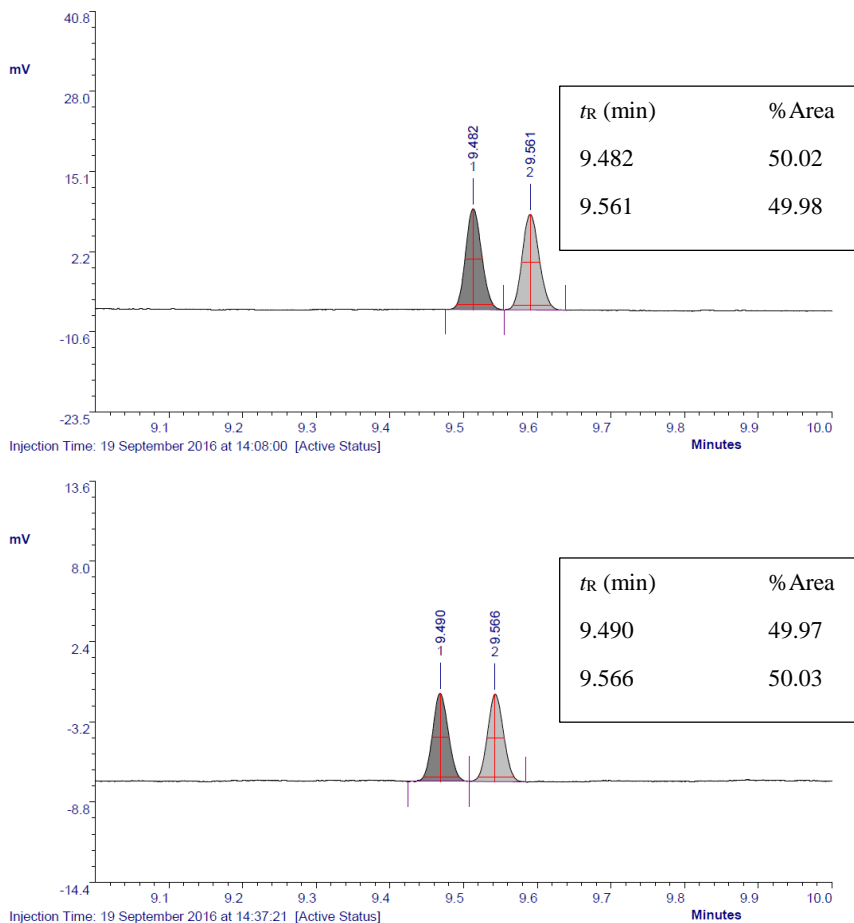


Figure 5-13. Chiral GC-FID chromatogram (10 °C per min) of α -(*tert*-butyl)ethylbenzene synthesized by hydrogenation of α -(*tert*-butyl)styrene with Pd/C (top) and (SINpM3e)Fe[(N(SiMe₃)₂)₂-DiBALH (bottom).

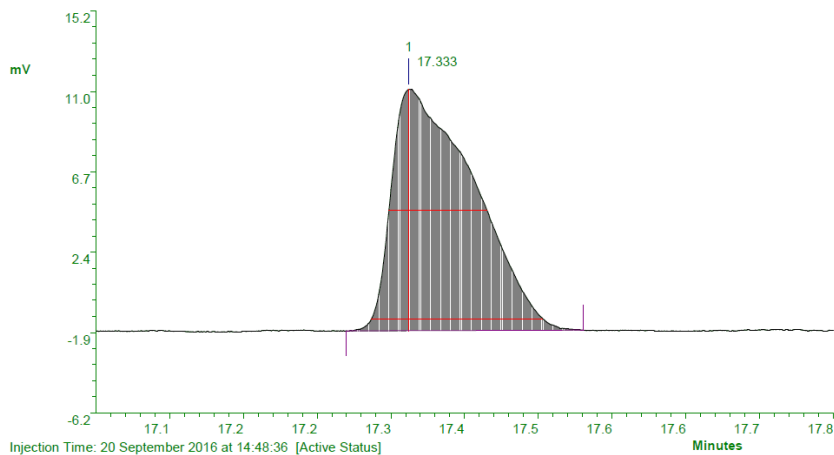


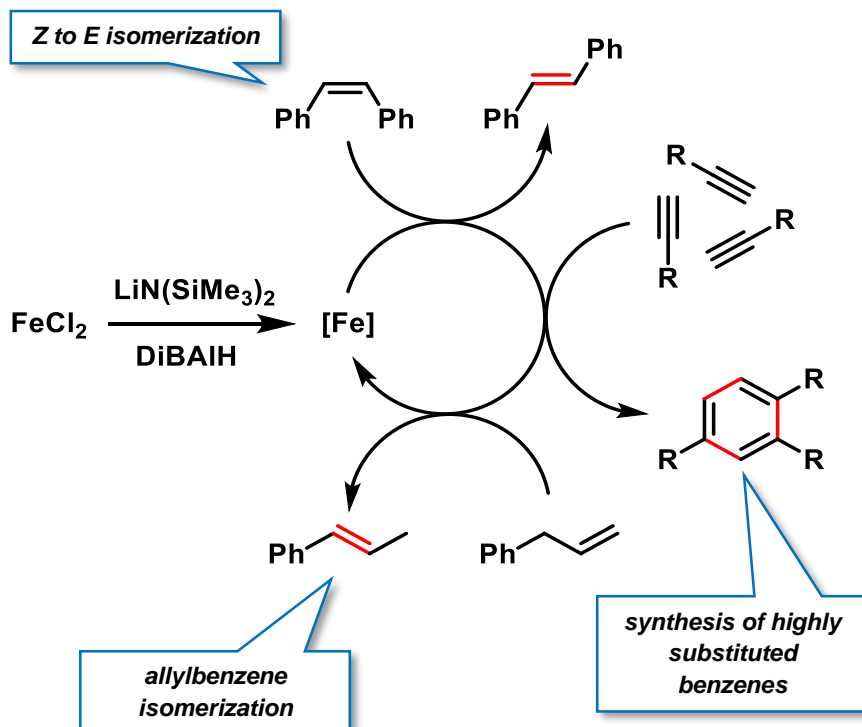
Figure 5-14. Chiral GC-FID chromatogram (3 °C per min) of α -(*n*-propyl)ethylbenzene synthesized by hydrogenation of α -(*tert*-butyl)styrene with Pd/C.

5.7 References

- [1] a) H. Bürger, U. Wannagat, *Monatsh. Chem.* **1963**, *94*, 1007–1012; b) H. Bürger, U. Wannagat, *Monatsh. Chem.* **1964**, *95*, 1099–1102; c) H. Bürger, W. Sawodny, U. Wannagat, *J. Organomet. Chem.* **1965**, *3*, 113–120.
- [2] R. A. Andersen, K. Faegri, J. C. Green, A. Haaland, M. F. Lappert, W. P. Leung, K. Rypdal, *Inorg. Chem.* **1988**, *27*, 1782–1786.
- [3] a) M. M. Olmstead, P. P. Power, S. C. Shoner, *Inorg. Chem.* **1991**, *30*, 2547–2551; b) P. P. Power, *Chem. Rev.* **2012**, *112*, 3482–3507.
- [4] L.-M. Lacroix, S. Lachaize, A. Falqui, T. Blon, J. Carrey, M. Respaud, F. Dumestre, C. Amiens, O. Margeat, B. Chaudret et al., *J. Appl. Phys.* **2008**, *103*, 07D521.
- [5] V. Kelsen, B. Wendt, S. Werkmeister, K. Junge, M. Beller, B. Chaudret, *Chem. Commun.* **2013**, *49*, 3416–3418.
- [6] a) F. Pelletier, D. Ciuculescu, J.-G. Mattei, P. Lecante, M.-J. Casanove, N. Yaacoub, J.-M. Greneche, C. Schmitz-Antoniak, C. Amiens, *Chemistry* **2013**, *19*, 6021–6026; b) A. Meffre, S. Lachaize, C. Gatel, M. Respaud, B. Chaudret, *J. Mater. Chem.* **2011**, *21*, 13464.
- [7] a) M. F. Sloan, A. S. Matlack, D. S. Breslow, *J. Am. Chem. Soc.* **1963**, *85*, 4014–4018; b) F. C. Loveless, D. H. Miller, U.S. patent 3,932,308, **1976**; c) S. J. Lapporte, U.S. Patent 3,205,278, **1965**.
- [8] a) D. Gärtner, A. Welther, B. R. Rad, R. Wolf, Jacobi von Wangelin, Axel, *Angew. Chem. Int. Ed.* **2014**, *53*, 3722–3726; b) R. Hudson, G. Hamasaka, T. Osako, Yamada, Yoichi M. A., C.-J. Li, Y. Uozumi, A. Moores, *Green Chem* **2013**, *15*, 2141–2148; c) D. J. Frank, L. Guiet, A. Kaslin, E. Murphy, S. P. Thomas, *RSC Adv* **2013**, *3*, 25698–25701; d) A. J. MacNair, M.-M. Tran, J. E. Nelson, G. U. Sloan, A. Ironmonger, S. P. Thomas, *Org. Biomol. Chem.* **2014**, *12*, 5082–5088; e) N. Guo, M.-Y. Hu, Y. Feng, S.-F. Zhu, *Org. Chem. Front.* **2015**, *2*, 692–696; f) T. N. Gieshoff, M. Villa, A. Welther, M. Plois, U. Chakraborty, R. Wolf, A. Jacobi von Wangelin, *Green Chem* **2015**, *17*, 1408–1413.
- [9] a) R. P. Yu, J. M. Darmon, J. M. Hoyt, G. W. Margulieux, Z. R. Turner, P. J. Chirik, *ACS Catal.* **2012**, *2*, 1760–1764; b) R. J. Trovitch, E. Lobkovsky, E. Bill, P. J. Chirik, *Organometallics* **2008**, *27*, 1470–1478.
- [10] EPA US Environmental Protection Agency, "Presidential Green Chemistry Challenge: 2014 Small Business Award. Farnesane: a Breakthrough Renewable Hydrocarbon for Use as Diesel and Jet Fuel", can be found under <https://www.epa.gov/greenchemistry/presidential-green-chemistry-challenge-2014-small-business-award>, **2016**.
- [11] R. H. Crabtree, *Chem. Rev.* **2012**, *112*, 1536–1554.
- [12] J. F. Sonnenberg, N. Coombs, P. A. Dube, R. H. Morris, *J. Am. Chem. Soc.* **2012**, *134*, 5893–5899.

- [13] D. R. Anton, R. H. Crabtree, *Organometallics* **1983**, 2, 855–859.
- [14] L. Huang, T. P. Ang, Z. Wang, J. Tan, J. Chen, P. K. Wong, *Inorg. Chem.* **2011**, 50, 2094–2111.
- [15] W. M. Alley, I. K. Hamdemir, K. A. Johnson, R. G. Finke, *Journal of Molecular Catalysis A: Chemical* **2010**, 315, 1–27.
- [16] J. Barrault, M. Blanchard, A. Derouault, M. Ksibi, M. I. Zaki, *J. Mol. Catal.* **1994**, 93, 289–304.
- [17] F. K. Schmidt, L. O. Nindakova, B. A. Shainyan, V. V. Saraev, N. N. Chipanina, V. A. Umanetz, *J. Mol. Catal. A: Chem.* **2005**, 235, 161–172.
- [18] a) J. Einhorn, C. Einhorn, F. Ratajczak, A. Durif, M.-T. Averbuch, J.-L. Pierre, *Tetrahedron Lett.* **1998**, 39, 2565–2568; b) C. Drost, P. B. Hitchcock, M. F. Lappert, *J. Chem. Soc., Dalton Trans.* **1996**, 3595–3601.
- [19] W. A. Herrmann, L. J. Goossen, C. Köcher, G. R. J. Artus, *Angew. Chem. Int. Ed. Engl.* **1996**, 35, 2805–2807.

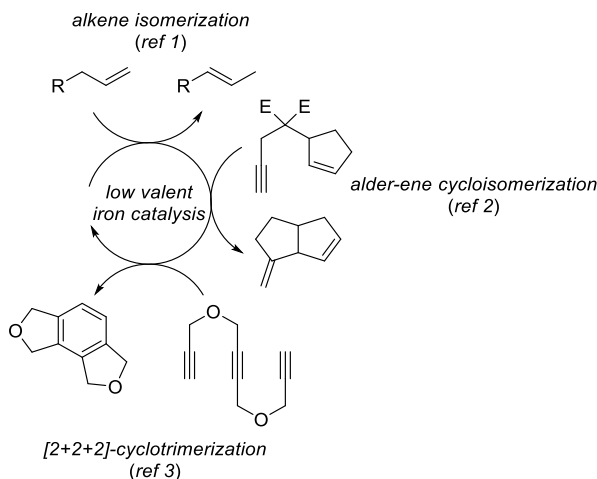
6 Iron-catalyzed isomerizations and cyclotrimerizations



The new catalyst system derived from the reaction of $\text{Fe}[\text{N}(\text{SiMe}_3)_2]_2$ with DiBAIH was additionally tested in redox-neutral transformations involving $\text{C}=\text{C}$ and $\text{C}\equiv\text{C}$ bond activation. *Z* to *E* alkene isomerization and allylbenzene isomerization were effectively catalyzed. Terminal alkynes were transformed to their [2+2+2]-cyclotrimerizations products.

6.1 Introduction

Besides hydrogenation reactions, low-valent iron species have been known to catalyze various additional transformations involving C=C and C≡C bond activation. A vast number of iron-catalyzed protocols have been reported including the redox-neutral isomerization of alkenes^[1], alder-ene cycloisomerization and cycloadditions^[2] as well as alkyne cyclotrimerizations^[3] (Scheme 6-1). Especially the latter transformations provide a useful tool to enrich complexity in molecules. In order to survey the scope of reactions catalyzed by Fe[N(SiMe₃)₂]₂-DiBAIH, isomerizations of alkenes and alkyne trimerization were briefly examined.



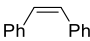
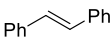
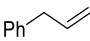
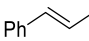
Scheme 6-1. Examples of low-valent iron catalyzed transformations.

6.2 Results and Discussion

Initially, *Z* to *E*- and allyl isomerization were studied under H₂-free conditions (Table 6-1). Excellent yield of (*E*)-stilbene was achieved after 18 h at room temperature. Isomerization of allylbenzene to the higher conjugated (*E*)- β -methylstyrene was observed in good yield after 18 h. Products of hydrogenation were detected in traces.

Isomerization of 1- and (*E*)-4-octene yielded a thermodynamic mixture of 2-,3- and 4-octenes in both cases (Table 6-2). Interestingly, activation of sterically hindered (*E*)-4-octene was possible as observed already under hydrogenation conditions. The unselective isomerization might limit the application of the catalyst system in selective terminal alkene isomerizations. Nevertheless, its high activity might provide a useful tool for the isomerization of sterically hindered alkenes.

Table 6-1. Isomerization of (*Z*)-stilbene and allylbenzene.

$ \begin{array}{c} \text{R}^1 \text{---} \text{CH}=\text{CH} \text{---} \text{R}^2 \\ \xrightarrow[\text{toluene, rt, 18 h}]{\begin{array}{c} 5 \text{ mol\% Fe[N(SiMe}_3)_2]_2 \\ 10 \text{ mol\% DiBAIH} \end{array}} \\ \text{R}^1 \text{---} \text{CH}=\text{CH} \text{---} \text{R}^2 \end{array} $			
Entry	Substrate	Product	Yield in % ^a
1			62 (68) ^b
			97 (97)
2			69 (71) ^b
			79 (79)

^a quantitative GC-FID vs. *n*-pentadecane as internal reference, conversion in % in parentheses; ^b after 2 h.

Table 6-2. Isomerization of 1- and (*E*)-4-octene.

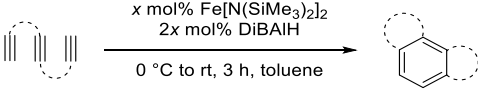
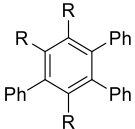
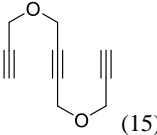
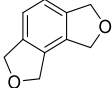
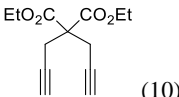
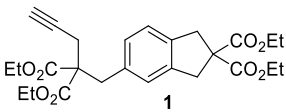
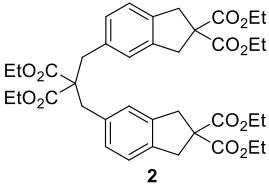
$ \begin{array}{c} \text{octene} \\ \xrightarrow[\text{toluene, rt, 18 h}]{\begin{array}{c} 5 \text{ mol\% Fe[N(SiMe}_3)_2]_2 \\ 10 \text{ mol\% DiBAIH} \end{array}} \\ \text{mixture of isomers} \end{array} $						
Entry	Substrate	Yield in % ^a				
		1-octene	(<i>E</i>)-2-octene	(<i>E</i>)-3-octene	(<i>E</i>)-4-octene	other isomers
1	1-octene	<1	29	43	16	13
2	(<i>E</i>)-4-octene	<1	27	41	20	12

^a determined by relative peak area ratios in GC-FID

While studying alkyne hydrogenations with Fe[N(SiMe₃)₂]₂-DiBAIH, the addition of terminal phenylacetylene to the catalyst solution resulted in an immediate exothermic polymerization reaction with minor trimerization products. In order to control the reaction in favor of a [2+2+2]-cyclotrimerization product, the addition of terminal alkynes was performed at 0 °C. Surprisingly, the reaction proceeded very selective, yielding >99% of 1,2,4-triphenylbenzene with only traces of the 1,3,5-isomer (Table 6-3) and outstands former protocols.^[4] Unfortunately, substrate scope was limited to terminal alkynes under mild reaction conditions (entries 2, 3). The synthesis of pyridines by addition of a mixture of phenylacetylene and benzonitrile was not successful, due to very fast and irreversible

formation of 1,2,4-triphenylbenzene. The reaction could be performed in an intramolecular fashion with moderate yield (entry 4). 1-Octyne polymerized with no formation of a [2+2+2]-cyclotrimerization product. Use of a di-yne yielded a mixture of dimerization product **1** and trimerization product **2**.

Table 6-3. Substrate scope of iron-catalyzed [2+2+2]-cycloisomerization.

					
Entry	Alkyne (x mol%)	R	Product	Yield in % ^b	
1	Ph—C≡C—R (5)	H		>99%	
2		Et		-	
3		Ph		- ^c	
4	 (15)			72	
5	 (10)		 1	28	
6			 2	58	

^a see chapter 6.4 for experimental details; ^b isolated yield; ^c 18 h, 80 °C.

6.3 Conclusion

The bimetallic Ziegler-type hydrogenation catalyst $\text{Fe}[\text{N}(\text{SiMe}_3)_2]_2\text{-DiBAIH}$ is active in the isomerization of alkenes. For allylbenzene, good conversion to its higher conjugated β -methyl styrene is observed. Octenes were isomerized to a thermodynamic mixture of 2-, 3- and 4-octenes. Terminal alkynes underwent [2+2+2]-cyclotrimerizations in a limited scope. Notably, high selectivity is observed in the cyclotrimerization of phenylacetylene.

6.4 Experimental

6.4.1 General

Analytical Thin-Layer Chromatography: TLC was performed using aluminium plates with silica gel and fluorescent indicator (*Merck*, 60, F254). Thin layer chromatography plates were visualized by exposure to ultraviolet light (366 or 254 nm) or by immersion in a staining solution of molybdatophosphoric acid in ethanol or potassium permanganate in water.

Column Chromatography: Flash column chromatography with silica gel 60 from *KMF* (0.040-0.063 mm). Mixtures of solvents used are noted in brackets.

Chemicals and Solvents: Solvents (THF, Et₂O, *n*-hexane, toluene) were distilled over sodium and benzophenone and stored over molecular sieves (4 Å). Solvents used for column chromatography were distilled under reduced pressure prior use (ethyl acetate). Fe[N(SiMe₃)₂]₂ was synthesized as described in chapter 5.6 DiBAIH was used as received from *SigmaAldrich* (1 M in toluene).

¹H- und ¹³C-NMR-Spectroscopy: Nuclear magnetic resonance spectra were recorded on a *Bruker Avance 300* (300 MHz) and *Bruker Avance 400* (400 MHz). ¹H-NMR: The following abbreviations are used to indicate multiplicities: s = singlet; d = doublet; t = triplet, q = quartet; m = multiplet, dd = doublet of doublet, dt = doublet of triplet, dq = doublet of quartet, ddt = doublet of doublet of quartet. Chemical shift δ is given in ppm to tetramethylsilane.

Fourier-Transformations-Infrared-Spectroscopy (FT-IR): Spectra were recorded on a *Varian Scimitar 1000 FT-IR* with ATR-device. All spectra were recorded at room temperature. Wave number is given in cm⁻¹. Bands are marked as s = strong, m = medium, w = weak and b = broad.

Gas chromatography with mass-selective detector (GC-MS): *Agilent 6890N* Network GC-System, mass detector 5975 MS. Column: HP-5MS (30m × 0.25 mm × 0.25 μm, 5% phenylmethylsiloxane, carrier gas: H₂. Standard heating procedure: 50 °C (2 min), 25 °C/min -> 300 °C (5 min)

High resolution mass spectrometry (HRMS): The spectra were recorded by the Central Analytics Lab at the Department of Chemistry, University of Regensburg, on a MAT SSQ 710 A from *Finnigan*.

6.4.2 General procedure for isomerization of alkenes

A 4 mL vial was charged with a solution of Fe[N(SiMe₃)₂]₂ in toluene (0.01 mmol, 0.2 mL, 50 mM) inside a glovebox. At room temperature, a solution of DiBAIH (0.2 mmol, 0.2 mL, 100 mM) was added dropwise (1 min) and the resulting black mixture

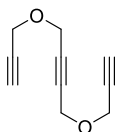
was stirred for 5 minutes. After addition of the alkene (0.2 mmol) and *n*-pentadecane (0.2 mmol) as internal reference, the reaction mixture was stirred under argon for 18 h. The reaction was quenched with an aqueous solution of NaHCO_3 (1 mL) and extracted with ethyl acetate (1×1 mL) and analyzed by GC-FID.

6.4.3 General procedure for [2+2+2]-cyclotrimerization of alkynes

A *Schlenk* flask was charged with a solution of $\text{Fe}[\text{N}(\text{SiMe}_3)_2]_2$ in toluene (0.09 mmol, 1.80 mL, 50 mM) inside a glovebox. At room temperature, a solution of DIBALH (0.18 mmol, 1.80 mL, 100 mM) was added dropwise (1 min) and the resulting black mixture was stirred for 5 minutes. After cooling the mixture to 0°C with the help of an ice bath, the alkyne (1.80 mmol/number of triple bond per substrate) was added and the reaction mixture was stirred at 0°C . After 1 h, the reaction mixture was allowed to warm to room temperature and stirred for additional 2 h. The reaction mixture was quenched with an aqueous solution of NaHCO_3 (5 mL) and extracted with ethyl acetate (3×15 mL). The combined organic layers were washed with brine (15 mL), dried over Na_2SO_4 , concentrated and subjected to silica gel flash chromatography (hexanes or hexanes/ethyl acetate).

6.4.4 Synthesis of starting material 1,4-bis(prop-2-yn-1-yloxy)but-2-yne

Synthesis following the procedure by R.G. Iafe, J. L. Kuo, D. G. Hochstatter, T. Saga, J. W. Turner, C. A. Merlic, *Org. Lett.* **2013**, *15*, 582-585.



$\text{C}_{10}\text{H}_{10}\text{O}_2$

162.19 g/mol

Appearance

yellowish liquid

Yield

3.16 g, 19.5 mmol (85%)

TLC

$R_f = 0.16$ (SiO_2 , hexanes/ethyl acetate = 19/1)

$^1\text{H-NMR}$

(300 MHz, CDCl_3) δ 4.31 (s, 4H), 4.26 (d, $J = 2.4$ Hz, 4H), 2.46 (t, $J = 2.4$ Hz, 2H).

$^{13}\text{C-NMR}$

(75 MHz, CDCl_3) δ 82.09, 78.78, 75.11, 56.73, 56.54.

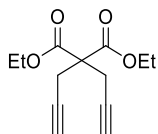
GC-MS

$t_R = 6.54$ min, (EI, 70 eV): $m/z = 162$ [M^+], 131, 103, 93, 77, 65, 53.

Analytical data were in full agreement with R.G. Iafe, J. L. Kuo, D. G. Hochstatter, T. Saga, J. W. Turner, C. A. Merlic, *Org. Lett.* **2013**, *15*, 582-585.

Diethyl 2,2-di(prop-2-yn-1-yl)malonate

A *Schlenk* flask was charged with sodium hydride (3.20 g, 80.0 mmol, 60% in paraffine) in dry THF (80 mL) and cooled to 0 °C. Diethyl malonate (6.41 g, 40.0 mmol) was added via syringe pump (0.2 mL/min). After complete addition, the reaction mixture was allowed to warm to room temperature and stirred for 2 h. The reaction mixture was cooled to 0 °C and propargylic bromide (14.87 g, 100 mmol, 80% in toluene) was added dropwise. The suspension was allowed to warm temperature and stirred overnight after which it was quenched with H₂O (15 mL). The reaction mixture was extracted with ethyl acetate (3 × 20 mL) and the combined organic layers were dried (Na₂SO₄), concentrated subjected to distillation under reduced pressure.

C₁₃H₁₆O₄

236.27 g/mol

Appearance

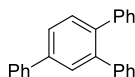
colorless liquid

Yield

8.92 g, 37.8 mmol (94%)

Boiling point91 °C at 10⁻¹ mbar**¹H-NMR**(300 MHz, CDCl₃) δ 4.23 (q, *J* = 7.1 Hz, 4H), 2.99 (d, *J* = 2.7 Hz, 4H), 2.03 (t, *J* = 2.7 Hz, 2H), 1.26 (t, *J* = 7.1 Hz, 6H).**¹³C-NMR**(75 MHz, CDCl₃) δ 168.60, 78.44, 71.68, 62.09, 56.25, 22.50, 14.03.**GC-MS***t*_R = 7.09 min, (EI, 70 eV): *m/z* = 197 [M-C₃H₃⁺], 162, 151, 133, 123, 105, 89, 77, 63, 51.

Analytical data were in full agreement with J. Aleman, V. del Solar, C. Navarro-Ranninger, *Chem. Commun.* **2010**, 46, 454–456.

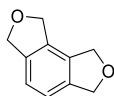
6.4.5 Products of [2+2+2]-cycloisomerization**1,2,4-Triphenylbenzene**C₂₄H₁₈

306.41 g/mol

$^1\text{H-NMR}$	(300 MHz, CDCl_3) δ 7.77–7.66 (m, 4H), 7.56 (d, $J = 7.7$ Hz, 1H), 7.50 (t, $J = 7.4$ Hz, 2H), 7.45–7.36 (m, 1H), 7.34–7.17 (m, 10H).
$^{13}\text{C-NMR}$	(75 MHz, CDCl_3) δ 141.54, 141.17, 141.04, 140.64, 140.43, 139.60, 131.18, 129.98, 129.94, 129.50, 128.90, 128.01, 127.98, 127.51, 127.21, 126.67, 126.60, 126.20.
GC-MS	$t_R = 12.52$ min, (EI, 70 eV): $m/z = 306$ [M^+], 289, 276, 228, 215, 202, 145, 77, 51.

Analytical data were in full agreement with M. Fernández, M. Ferré, A. Pla-Quintana, T. Parella, R. Pleixats, A. Roglans, *Eur. J. Org. Chem.* **2014**, 2014, 6242–6251.

1,3,6,8-Tetrahydro-2,7-dioxa-as-indacene



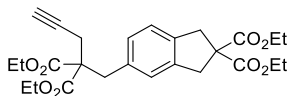
$\text{C}_{10}\text{H}_{10}\text{O}_2$

162.19 g/mol

$^1\text{H-NMR}$	(300 MHz, CDCl_3) δ 7.15 (s, 2H), 5.18–5.08 (m, 4H), 5.08–4.99 (m, 4H).
$^{13}\text{C-NMR}$	(75 MHz, CDCl_3) δ 138.69, 132.34, 119.91, 73.45, 72.23.
GC-MS	$t_R = 7.93$ min, (EI, 70 eV): $m/z = 162$ [M^+], 133, 104, 77, 63, 51.

Analytical data were in full agreement with M. Fernández, M. Ferré, A. Pla-Quintana, T. Parella, R. Pleixats, A. Roglans, *Eur. J. Org. Chem.* **2014**, 2014, 6242–6251.

Dimerization product 1



$\text{C}_{26}\text{H}_{32}\text{O}_8$

472.53 g/mol

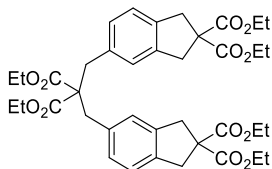
$^1\text{H-NMR}$	(300 MHz, CDCl_3) δ 7.11–7.06 (m, 1H), 7.01–6.93 (m, 2H), 4.23–4.16 (m, 8H), 3.54 (s, 4H), 3.34 (s, 2H), 2.66 (d, $J = 2.7$, 2H), 2.13 (dd, $J = 2.6$, 1H), 1.28–1.23 (m, 12H).
$^{13}\text{C-NMR}$	(75 MHz, CDCl_3) δ 171.64, 169.69, 167.11, 134.28, 133.71, 131.82, 128.64, 127.03, 125.62, 79.48, 72.15, 71.92, 61.74, 58.11, 40.19, 37.05, 29.81, 22.12, 14.07, 14.04.

GC-MS

$t_R = 13.12$ min, (EI, 70 eV): $m/z = 472$ [M^+], 427, 399, 353, 325, 295, 274, 251, 223, 201, 179, 153, 129.

HRMS

(EI, m/z): found 272.2090 [M^+] (calculated 272.2092).

Trimerization product 2


$C_{39}H_{48}O_{12}$

708.80 g/mol

 1H -NMR

(300 MHz, $CDCl_3$) δ 7.12–7.04 (m, 2H), 7.02–6.90 (m, 4H), 4.20 (q, $J=7.1$, 8H), 4.08 (q, $J=7.1$, 4H), 3.54 (s, 8H), 3.15 (s, 4H), 1.25 (t, $J=7.1$, 12H), 1.14 (t, $J=7.1$, 6H).

 ^{13}C -NMR

(75 MHz, $CDCl_3$) δ 171.64, 171.00, 140.01, 138.62, 135.06, 128.87, 125.94, 123.89, 61.71, 61.20, 60.45, 60.26, 40.40, 40.18, 38.98, 14.05, 13.91.

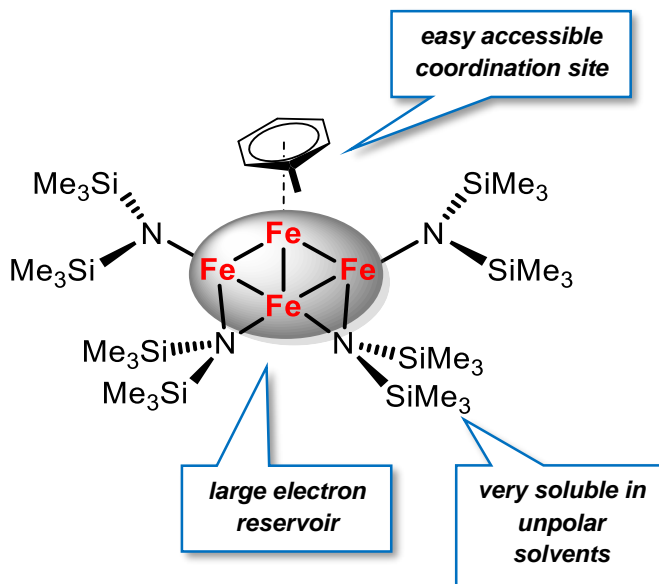
HRMS

(EI, m/z): found 709.3226 [$M+H^+$] (calculated 709.3219).

6.5 References

- [1] a) M. Mayer, A. Welther, A. Jacobi von Wangelin, *ChemCatChem* **2011**, 3, 1567–1571; b) E. N. Frankel, E. A. Emken, V. L. Davison, *J. Am. Oil Chem. Soc.* **1966**, 43, 307–311; c) P. A. Tooley, L. W. Arndt, M. Y. Darensbourg, *J. Am. Chem. Soc.* **1985**, 107, 2422–2427; d) M. R. Reddy, M. Periasamy, *J. Organomet. Chem.* **1995**, 491, 263–266; e) J. V. Crivello, S. Kong, *J. Org. Chem.* **1998**, 63, 6745–6748.
- [2] a) A. Fürstner, R. Martin, K. Majima, *J. Am. Chem. Soc.* **2005**, 127, 12236–12237; b) J. M. Takacs, Y.-C. Myoung, L. G. Anderson, *J. Org. Chem.* **1994**, 59, 6928–6942; c) J. M. Takacs, L. G. Anderson, *J. Am. Chem. Soc.* **1987**, 109, 2200–2202; d) M. W. Bouwkamp, A. C. Bowman, E. Lobkovsky, P. J. Chirik, *J. Am. Chem. Soc.* **2006**, 128, 13340–13341; e) A. Greco, A. Carbonaro, G. Dall'Asta, *J. Org. Chem.* **1970**, 35, 271–274.
- [3] a) N. Saino, D. Kogure, K. Kase, S. Okamoto, *J. Organomet. Chem.* **2006**, 691, 3129–3136; b) A. Fürstner, K. Majima, R. Martin, H. Krause, E. Kattnig, R. Goddard, C. W. Lehmann, *J. Am. Chem. Soc.* **2008**, 130, 1992–2004.
- [4] C. Breschi, L. Piparo, P. Pertici, A. Maria Caporusso, G. Vitulli, *J. Organomet. Chem.* **2000**, 607, 57–63.

7 Synthesis and characterization of a low-valent tetranuclear iron cluster^{i,ii}



A tetranuclear iron cluster was synthesized and characterized by ¹H-NMR and X-Ray crystallography. The unique structure combines key features like active site accessibility and high solubility for possible catalytic application. The large electron reservoir set up by four iron atoms in a mean formal oxidation state of +I could enable multielectron redox processes.

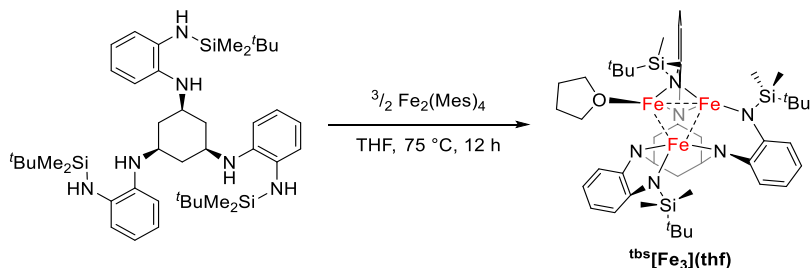
ⁱ Manuscript in preparation.

ⁱⁱ Authors contribution: U. Chakraborty, University Regensburg, improved complex synthesis and performed X-Ray structure determination.

7.1 Introduction

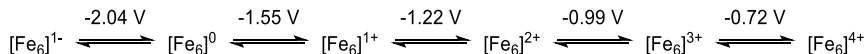
The synthesis of defined metal clusters is highly desirable, owing to their ability to perform stepwise multielectron redox process and mediate cooperative reaction chemistry. In nature, activation of small molecules by multielectron redox processes are catalyzed by polynuclear metalloenzymes. Examples involve cofactors in nitrogenases (FeMo, VFe, Fe-only) for 6 e^- N_2 reduction, hydrogenases (FeNi, Fe-only) for 2 e^- H_2 reduction or water oxidation catalyzed by photosystem II.^[1] Similarly, polynuclear reaction sites are found in heterogeneous catalysts, as in the Haber-Bosch process.^[2]

The synthesis of defined metal clusters is usually performed by the application of multidentate ligands to accommodate multiple transition metal ions as shown by Betley *et al.* In their publications, the group synthesized various defined iron clusters using hexamine ligands coordinating a $[\text{Fe}_3]$, $[\text{Fe}_6]$ or $[\text{Fe}_8]$ core. These clusters are usually synthesized by metathesis of Fe(II)-precursors with suitable amines. (Scheme 7-1).^{[4],[5]}



Scheme 7-1. Synthesis of tri-iron cluster $\text{tbs}[\text{Fe}_3](\text{thf})$ by Betley *et al.*

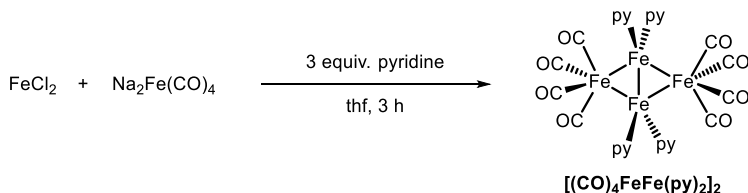
To verify the multielectron redox ability of these polynuclear clusters, Betley *et al.* used $\text{tbs}[\text{Fe}_3](\text{thf})$ for stoichiometric 2 e^- reduction of hydrazine to form ammonia and $\text{tbs}[\text{Fe}_3](\mu^3\text{-NH})$. Furthermore 4 e^- reduction of azobenzene was accomplished at 80°C demonstrating possible oxidation states up to $(\text{Fe}^{\text{IV}})(\text{Fe}^{\text{III}})_2$ within the $[\text{Fe}_3]$ core.^[4] Even more electron redox processes are achievable upon the use of a $[\text{Fe}_6]$ cluster, as verified by cyclic voltammetry indicating five fully reversible redox steps (Scheme 7-2).^[5]



Scheme 7-2. Reversible redox processes with $[\text{Fe}_6]$ cluster compound as reported by Betley. Redox potentials are given vs. ferrocene.

All synthesis for iron clusters reported by Betley and coworkers make use of iron in a +II oxidation state, which are used for reduction of small molecules. Low valent iron clusters, which may provide even more electron accessibility, would be of great interest for isolation and characterization. Most probably due to high tendency of low valent iron

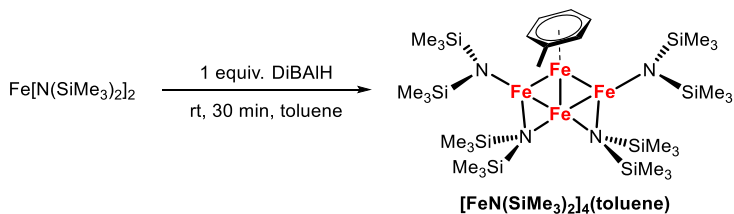
species to form nanoparticles, defined metal clusters of iron with direct Fe-Fe interaction in low oxidation states are scarcely known. The synthesis of a square planar $[\text{Fe}_4]$ cluster was reported in 1987 by Zanazzi and coworkers, where four iron atoms in oxidation state ± 0 form a plane and are coordinated by four pyridine and eight CO ligands (Scheme 7-3).^[6]



Scheme 7-3. Synthesis of tetra iron cluster $[(\text{CO})_4\text{FeFe(py)}_2]_2$ according to Zanazzi *et al.*

7.2 Results and Discussion

In the development of the hydrogenation catalyst derived from the reaction of $\text{Fe[N(SiMe}_3)_2]$ with two equivalents of DiAlH , crystallization of a black compound was observed in the reaction of $\text{Fe[N(SiMe}_3)_2]_2$ with one equivalent of DiAlH upon storage of the crude reaction mixture in toluene for ~ 2 months at -30°C . X-Ray structure determination revealed the formation of iron cluster $[\text{FeN(SiMe}_3)_2]_4(\text{toluene})$ (Scheme 7-4). Crystallization rate was drastically improved by prior drying of the reaction mixture by three cycles of freeze-pump-thaw to remove volatile aluminium-amide by-products. The powdered crude product was recrystallized in *n*-hexane to obtain $[\text{FeN(SiMe}_3)_2]_4(\text{toluene})$ in an overall 38% yield after storage for one day at -30°C . Interestingly, only traces of $[\text{FeN(SiMe}_3)_2]_4(\text{toluene})$ were observed in the crude $^1\text{H-NMR}$ spectrum upon use of two equivalents DiAlH . In addition to mechanistic experiments in chapter 5.3, the addition of an excess of DiAlH (>1 equivalents) presumably initiates further reduction and formation of Fe-nanoparticles.



Scheme 7-4. Synthesis of tetra iron cluster $[\text{FeN(SiMe}_3)_2]_4(\text{toluene})$.

The complex is very soluble in aliphatic organic solvents (*n*-hexane), important for possible catalytic application. No thermal decomposition was observed upon

determination of the melting point (123 °C). The toluene capping on one Fe atom might enable access of an active site by easy ligand exchange.

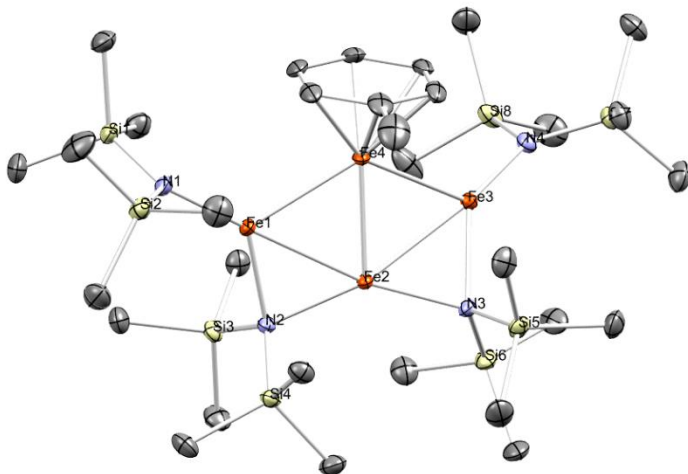


Figure 7-1. Crystallographic structure of $[\text{FeN}(\text{SiMe}_3)_2]_4(\text{toluene})$ visualized with software *Mercury*. Hydrogen atoms are omitted for clarity.

The structure consists of a slightly distorted planar tetra iron core with a torsion angle of 167° between the planes generated by (Fe2-Fe4-Fe3) and (Fe2-Fe4-Fe1). The outer core Fe-Fe bonds are in between 2.565 to 2.643 Å and are slightly longer than in the similar complex $[(\text{CO})_4\text{FeFe}(\text{py})_2]_2$ with bond lengths of 2.54 Å. The inner core Fe2-Fe4 bond length is short (2.474 Å) which is in the range as found in metallic iron (2.48 Å).^[7]

The bond angles of the triangles (Fe1-Fe4-Fe2) and (Fe2-Fe4-Fe3) are in the range of 56.6 to 63.2° setting up two nearly equilateral triangles.

Table 7-1. Selected bond lengths and angles in **[FeN(SiMe₃)₂]₄(toluene)**.

Bond	Bond lengths / Å	Bond	Bond angles in °
Fe3-Fe2	2.6003(3)	Fe2-Fe3-Fe4	56.632(8)
Fe3-Fe4	2.6152(3)	Fe3-Fe2-Fe1	120.741(10)
Fe2-Fe1	2.6425(3)	Fe4-Fe2-Fe3	61.988(8)
Fe2-Fe4	2.4739(3)	Fe4-Fe2-Fe1	60.072(8)
Fe1-Fe4	2.5652(3)	Fe4-Fe1-Fe2	56.702(8)
		Fe2-Fe4-Fe3	61.380(8)
		Fe2-Fe4-Fe1	63.226(8)
		Fe1-Fe4-Fe3	123.217(10)

The compound [FeN(SiMe₃)₂]₄(toluene) is paramagnetic, the magnetic moment determined in solution by Evans method ($\mu_{\text{eff}} = 2.0$) is consistent with one unpaired electron. The ¹H-NMR spectrum shows two broad singlets at -1.83 and -5.31 ppm which can be assigned to the bridging and non-bridging -N(SiMe₃)₂ ligands. The ¹H-NMR signals of coordinated toluene is most likely detected at 52.84, -12.06, -20.57 and -22.73 ppm.

Detailed characterization of the complex is currently at work by S. Demeshko, University Göttingen and will help determining unpaired electrons, as well as the possibility of multiple reversible redox processes by cyclic voltammetry.

7.3 Conclusion

A tetranuclear [Fe₄] cluster was synthesized by the reaction of Fe[N(SiMe₃)₂]₂ with one equivalent of DiBAIH. The new paramagnetic compound with one unpaired electron might be interesting for the activation of small molecules by multielectron processes since its structure meets key requirements. An active site might be accessible by toluene ligand exchange, the complex is highly soluble and most interestingly, the [Fe₄] core with a low valent Fe-center may act as an electron reservoir for chemical transformations.

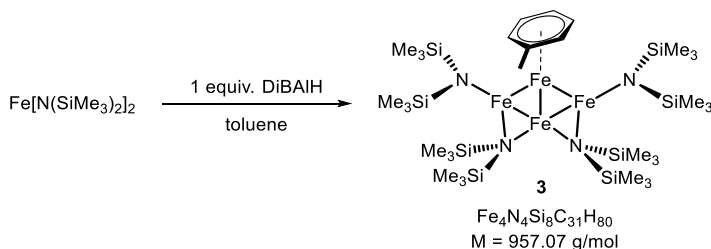
7.4 Experimental

7.4.1 General

Chemicals and Solvents: Solvents (THF, Et₂O, *n*-hexane, toluene) were distilled over sodium and benzophenone and stored over molecular sieves (4 Å). All manipulations were performed under purified argon inside a glovebox or using *Schlenk* techniques. Fe[N(SiMe₃)₂]₂ was synthesized as described in chapter 5.6. DiBAIH was used as received from *SigmaAldrich* (1 M in toluene).

¹H- und ¹³C-NMR-Spectroscopy: Nuclear magnetic resonance spectra were recorded on a *Bruker Avance 300* (300 MHz) and *Bruker Avance 400* (400 MHz). ¹H-NMR: The following abbreviations are used to indicate multiplicities: s = singlet; d = doublet; t = triplet, q = quartet; m = multiplet, dd = doublet of doublet, dt = doublet of triplet, dq = doublet of quartet, ddt = doublet of doublet of quartet. Chemical shift δ is given in ppm to tetramethylsilane.

7.4.2 Synthesis and characterization of [FeN(SiMe₃)₂]₄(toluene)



Scheme 7-5. Synthesis of [Fe₄]-cluster [FeN(SiMe₃)₂]₄(toluene)

A 10 mL flame-dried *Schlenk* flask was charged with Fe[N(SiMe₃)₂]₂ (190 mg, 0.50 mmol) in a mixture of *n*-hexane/toluene (4 mL, 3/1). A solution of DiBAIH in toluene (0.50 mmol, 1 M, 0.50 mL) was added at room temperature via syringe with immediate color change from green to brown-black. The reaction mixture was stirred at room temperature for 30 minutes, filtered through a P4 frit after which the solvent was removed completely under reduced pressure. The dark brown oily residue was powdered by 3 cycles freeze-pump-thaw and crystallized in *n*-hexane (0.3 mL) at -30 °C. After 24 h, dark crystalline compound **3** was obtained in 38% yield (46 mg, 0.048 mmol).

¹H-NMR (400 MHz, C₆D₆) δ 52.84 (bs), -1.83 (bs), -5.31 (bs), -12.06 (bs), -20.57 (bs), -22.73 (bs); effective magnetic moment (C₆D₆): μ_{eff} = 2.0 μ_B; melting point = 123 °C; elemental analysis calcd for Fe₄N₄Si₈C₃₁H₈₀ (957.07): C 38.90, H 8.43, N 5.85; found: C 38.05, H 8.19, N 5.87.

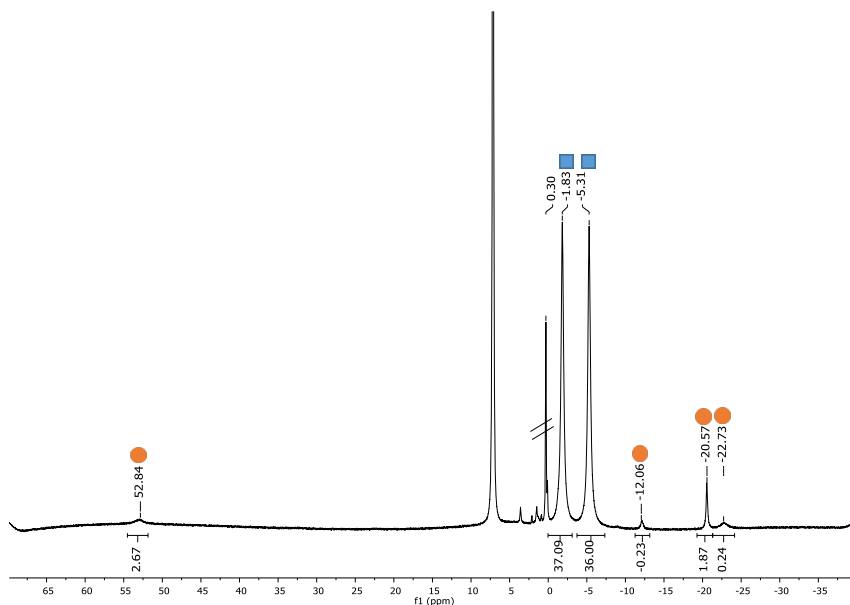


Figure 7-2.. ^1H -NMR of $[\text{FeN}(\text{SiMe}_3)_2]_4(\text{toluene})$ in C_6D_6 . Peak assignments: SiMe_3 (■), toluene (●).

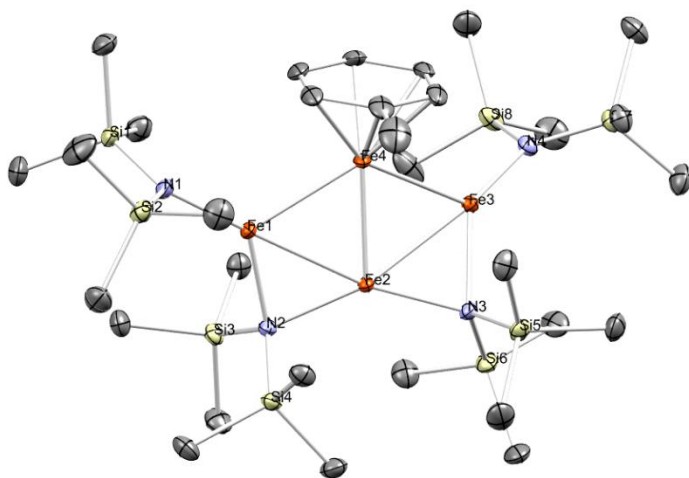
For X-Ray structure determination, a suitable crystal ($0.19 \times 0.16 \times 0.11$) mm^3 was selected and mounted on a MITIGEN holder with inert oil on a SuperNova, Single source at offset, Atlas diffractometer. The crystal was kept at $T = 123.00(10)$ K during data collection. Using **Olex2** (Dolomanov et al., 2009)ⁱ, the structure was solved in the space group $\text{P}2_1/\text{c}$ (# 14) by Direct Methods using the **ShelXT** (Sheldrick, 2015)ⁱⁱ structure solution program and refined by Least Squares using version 2014/7 of **ShelXL** (Sheldrick, 2015)ⁱⁱⁱ. All non-hydrogen atoms were refined anisotropically. Hydrogen atom positions were calculated geometrically and refined using the riding model. Data were measured using w scans scans of 1.0° per frame for 6.0 s using CuK α radiation (micro-focus sealed X-ray tube, n/a kV, n/a mA). The total number of runs and images was based on the strategy

ⁱ O.V. Dolomanov and L.J. Bourhis and R.J. Gildea and J.A.K. Howard and H. Puschmann, Olex2: A complete structure solution, refinement and analysis program, *J. Appl. Cryst.*, (2009), **42**, 339-341.

ⁱⁱ Sheldrick, G.M., Crystal structure refinement with ShelXL, *Acta Cryst.*, (2015), **C27**, 3-8.

ⁱⁱⁱ Sheldrick, G.M., ShelXT-Integrated space-group and crystal-structure determination, *Acta Cryst.*, (2015), **A71**, 3-8.

Crystal Data. $\text{C}_{31}\text{H}_{80}\text{Fe}_4\text{N}_4\text{S}_8$, $M_r = 957.11$, monoclinic, $\text{P2}_1/\text{c}$ (No. 14), $a = 18.59832(16)$ Å, $b = 14.75827(12)$ Å, $c = 18.28580(17)$ Å, $\beta = 96.4495(8)^\circ$, $\alpha = \gamma = 90^\circ$, $V = 4987.31(7)$ Å³, $T = 123.00(10)$ K, $Z = 4$, $Z' = 1$, $\mu(\text{CuK}\alpha) = 11.172$, 43076 reflections measured, 10425 unique ($R_{\text{int}} = 0.0307$) which were used in all calculations. The final wR_2 was 0.0650 (all data) and R_1 was 0.0262 ($I > 2(I)$).



220

7.5 References

- [1] a) S. M. Mayer, D. M. Lawson, C. A. Gormal, S. M. Roe, B. E. Smith, *J. Mol. Biol.* **1999**, 292, 871–891; b) O. Einsle, F. A. Tezcan, S. L. A. Andrade, B. Schmid, M. Yoshida, J. B. Howard, D. C. Rees, *Science* **2002**, 297, 1696–1700; c) K. N. Ferreira, T. M. Iverson, K. Maghlaoui, J. Barber, S. Iwata, *Science* **2004**, 303, 1831–1838; d) S. Shima, D. Chen, T. Xu, M. D. Wodrich, T. Fujishiro, K. M. Schultz, J. Kahnt, K. Ataka, X. Hu, *Nature Chem.* **2015**, 7, 995–1002; e) J. W. Peters, M. H. Stowell, S. M. Soltis, M. G. Finnegan, M. K. Johnson, D. C. Rees, *Biochemistry* **1997**, 36, 1181–1187.
- [2] F. Bozso, *J. Catal.* **1977**, 49, 18–41.
- [3] a) Q. Zhao, T. A. Betley, *Angew. Chem. Int. Ed.* **2011**, 50, 709–712; b) R. H. Sanchez, A. M. Willis, S.-L. Zheng, T. A. Betley, *Angew. Chem. Int. Ed.* **2015**, 54, 12009–12013.
- [4] Q. Zhao, T. D. Harris, T. A. Betley, *J. Am. Chem. Soc.* **2011**, 133, 8293–8306.
- [5] T. M. Powers, T. A. Betley, *J. Am. Chem. Soc.* **2013**, 135, 12289–12296.
- [6] a) C. Mealli, D. M. Proserpio, G. Fachinetti, T. Funaioli, G. Fochi, P. F. Zanazzi, *Inorg. Chem.* **1989**, 28, 1122–1127; b) G. Fachinetti, G. Fochi, T. Funaioli, P. F. Zanazzi, *J. Chem. Soc., Chem. Commun.* **1987**, 89.
- [7] F. A. Cotton (Ed.) *Multiple bonds between metal atoms*, Springer, New York, **2005**

8 Appendix

8.1 List of abbreviations

Ac	acetyl	MS	mass spectrometry
ATR	attenuated total reflection	[NaNaph]	sodium naphanelide
Bn	benzyl	NMR	nuclear magnetic resonance
Bu	butyl	Ph	phenyl
d	day	PS	polystyrene
dct	dibenzo[<i>a,e</i>]cyclooctatetraene	Pr	propyl
DiBAID	diisobutylaluminiumdeuteride	py	pyridine
DiBAIH	diisobutylaluminiumhydride	R_r	retention factor
ee	enantiomeric excess	rt	room temperature
ESI	electron spray ionization	SQUID	superconducting quantum interference device
Et	ethyl	TCD	thermal conductivity detector
FID	flame ionization	TEM	transmission electron microscopy
FT-IR	Fourier-Transform-Infrared spectroscopy	thf	tetrahydrofurane
GC	gas chromatography	TLC	thin layer chromatography
h	hour	TMS	trimethylsilyl
HR	high resolution	TOF	turnover frequency
IL	ionic liquid	WAXS	wide angle xray scattering
Me	methyl		
min	minute		

8.2 Summary

Aim of this thesis was the development of new iron-based catalyst systems for the hydrogenation of C=C and C≡C bonds.

In the introduction, recent advances in the development of molecular base metal catalysts and their application in the hydrogenation of alkenes and alkynes are presented. Key mechanistic steps are highlighted for the most important reports in this field.

In chapter 3, iron nanoparticles which were derived from the reduction of FeCl₃ with EtMgCl, were stabilized in ionic liquids and used for the hydrogenation of alkynes. The application of nitrile-functionalized ionic liquids or the addition of acetonitrile to the reaction mixture allowed the hydrogenation to proceed in a stereoselective fashion in favor of the formation of Z-alkenes in good selectivity. The stabilization of the catalyst in the polar ionic liquid allowed a simple separation from the unpolar product phase and its recycling.

In chapter 4, a simple catalyst system was developed based on the reduction of FeCl₃ with LiAlH₄. The bimetallic catalyst was used for the hydrogenation of various alkenes and alkynes at milder conditions. Mechanistic studies involving kinetic poisoning tests and spectroscopic analysis indicate the initial formation of a homogeneous catalyst which undergoes rapid agglomeration to form nanoparticles with less activity.

Chapter 5 is devoted to the development of a Ziegler-type hydrogenation catalyst, derived from the reaction of Fe[N(SiMe₃)₂]₂ with DiBAIH. In contrast to previous similar protocols, the hydrogenation of sterically hindered alkenes was possible at mild conditions. Mechanistic studies were performed to rationalize the reaction pathway of Fe[N(SiMe₃)₂]₂ with DiBAIH and to identify the catalytically active species.

The new catalyst system was briefly studied in alkene isomerizations and [2+2+2]-cyclootrimerizations (chapter 6). Some terminal alkynes were successfully transformed into their [2+2+2]-cyclootrimerizations products.

A tetranuclear iron cluster forms upon the reaction of Fe[N(SiMe₃)₂]₂ with one equivalent of DiBAIH (chapter 7). The nanocluster was isolated and characterized by ¹H-NMR, elemental analysis and X-ray crystallography. The unique structure provides key features which might enable the activation of small molecules by multiple redox processes. A large electron reservoir is set up by four iron atoms in a mean oxidation state of +I, additionally the nanocluster is highly soluble in unpolar solvents and presumably offers an easy accessible active site.

8.3 Zusammenfassung

Das Ziel der vorliegenden Arbeit war die Entwicklung von neuen Eisen-basierten Katalysatorsystemen für die Hydrierung von C=C und C≡C Bindungen.

Im Kapitel 2 sind jüngste Fortschritte in der Entwicklung von molekularen Eisen-, Kobalt- und Nickel-Katalysatoren und ihre Anwendung in der Hydrierung von Alkenen und Alkinen zusammengefasst. Mechanistische Schlüsselschritte in der Aktivierung von molekularem Wasserstoff sind hervorgehoben für die wichtigsten Arbeiten in diesem Bereich.

In Kapitel 3 wird beschrieben, wie Eisen-Nanopartikel aus der Reduktion von FeCl_3 mit EtMgCl in ionischen Flüssigkeiten stabilisiert und in der Hydrierung von Alkinen eingesetzt wurden. Die Verwendung von Nitril-funktionalisierten ionischen Flüssigkeiten oder die Zugabe von Acetonitril zur Reaktionsmischung erlaubt die stereoselektive Hydrierung von Alkinen zu Z-Alkenen in guter Selektivität. Die Stabilisierung des Katalysators in der polaren ionischen Flüssigkeit erlaubt die einfache Separierung von der unpolaren Produktphase, sowie dessen Rezyklierung.

In Kapitel 4 ist die Entwicklung eines einfachen Katalysatorsystems beschrieben, welches auf der Reduktion von FeCl_3 mit LiAlH_4 beruht. Der bimetallische Katalysator wurde in der Hydrierung von verschiedenen Alkenen und Alkinen unter milden Bedingungen eingesetzt. Mechanistische Studien, wie kinetische Vergiftungstests und spektroskopische Analysen weisen auf die Bildung eines homogenen Katalysators hin, welcher unter der Bildung weniger aktiven Nanopartikel schnell agglomeriert.

Kapitel 5 beschreibt die Entwicklung eines Ziegler-artigen Hydrierkatalysators, der aus der Reaktion von $\text{Fe}[\text{N}(\text{SiMe}_3)_2]_2$ mit DiBAIH gebildet wird. Im Gegensatz zu früheren ähnlichen Systemen erlaubt das bimetallische Katalysatorsystem die Hydrierung von sterisch anspruchsvollen Alkenen unter milden Bedingungen. Mechanistische Studien wurden durchgeführt, um den Reaktionspfad von $\text{Fe}[\text{N}(\text{SiMe}_3)_2]_2$ mit DiBAIH zu erklären, sowie die katalytisch aktive Spezies zu identifizieren.

Das neue Katalysatorsystem wurde in der Alken-Isomerisierung und in [2+2+2]-Cyclotrimerisierungen getestet (Kapitel 6). Einige terminale Alkine wurden erfolgreich in ihre [2+2+2]-Cyclotrimerisierungsprodukte überführt.

Ein vierkerniger Eisen-Cluster bildet sich in der Reaktion von $\text{Fe}[\text{N}(\text{SiMe}_3)_2]_2$ mit einem Äquivalent DiBAIH (Kapitel 7). Der Nanocluster wurde isoliert und durch ^1H -NMR, Elementaranalyse und Röntgenkristallographie charakterisiert. Die einzigartige Struktur besitzt Schlüsseleigenschaften, welche die Aktivierung von kleinen Molekülen durch multiple Redoxschritte erlauben könnten. Ein großes Elektronenreservoir ist aus vier Eisen-Atomen mit einer formalen gemittelten Oxidationsstufe von +I aufgebaut, des

Weiteren ist der Nanocluster sehr löslich in unpolaren Lösemitteln und besitzt eine vermutlich leicht austauschbare Koordinationsstelle.

8.4 Acknowledgements

Dieser Abschnitt ist den Menschen gewidmet, die mich in den letzten Jahren in jeglicher Weise unterstützt haben.

Vorneweg möchte ich mich bei Axel für das interessante Thema und die hervorragende Betreuung bedanken. Die Zeit in deiner Arbeitsgruppe hat mich natürlich einerseits wissenschaftlich als auch persönlich entwickelt und geprägt.

Der Evonik-Stiftung danke ich für das Vertrauen, welches sie mir durch die finanzielle Unterstützung entgegengebracht hat. Viel mehr danke ich für das große Engagement, welches wir Stipendiaten bei der Unterstützung für die Zeit während und nach der Promotion erfahren.

Prof. Göpferich, Prof. Garcia-Mancheño und Prof. Matysik danke ich für die Übernahme des Kommissionsvorsitzes, des Zweitgutachtens sowie des Drittprüfers.

Den Kollaborationspartnern aus Köln, Paderborn und Regensburg danke ich für die gute Zusammenarbeit und die Hilfe in wichtigen Fragestellungen.

Sämtlichen ehemaligen wie aktuellen Kollegen danke ich für die tolle Arbeitsatmosphäre, die guten theoretischen und methodischen Diskussionen und Anregungen. Insbesondere möchte ich hier meine Laborpartnerinnen Michaela Lutz und Veronika Scheidler erwähnen, die mir im Laboralltag mit Rat und Tat immer zur Seite standen. Den Tischpartnern Josef Schachtner, Dominik Gärtner, Efrain Reyes-Rodriguez, Matteo Villa, Michael Neumeier und Sebastian Sandl danke ich für die spannenden Runden. Wenn ihr den Tisch von unten gesehen habt, habt ihr auch die schlechten Labortage aufgehehlt. Allen Kollegen danke ich für die schöne Zeit abseits des Labors beim Grillen, Bier trinken, sowie die erfolgreiche ChemCup-Turnierbilanz.

Meiner Familie und Jana danke ich für die Geduld und die Unterstützung, mich auch in angespannten Zeiten zu tragen.

8.5 Curriculum Vitae

Personal Data

Name: Tim Nicolas Gieshoff
 Birth Data: October 27th, 1988 in Siegburg
 Nationality: German, French

Education

2013 – 2016 Doctoral Thesis in Organic Chemistry, in the group of Prof. Dr. Axel Jacobi von Wangelin
 “Iron-catalyzed Hydrogenation of Olefins”
 2011 – 2013 M.Sc. Chemistry, University Regensburg (1.4)
 Master Thesis: „Entwicklung Eisen-basierter Katalysatorsysteme und deren Aktivität in der Hydrierung von Olefinen“; (1.0)
 2008 – 2011 B.Sc. Chemistry, Goethe University Frankfurt/Main (1.2)
 Bachelor Thesis: „Synthese eines 2'-O-Guanidinoethyladenosin-Derivats für die Herstellung modifizierter siRNA gegen das Hepatitis B-Virus“; (1.0)
 1999 – 2008 Secondary school Gelnhausen graduation: allgemeine Hochschulreife

List of publications

- 1) “Iron-catalyzed hydrogenation of sterically hindered alkenes”, T. N. Gieshoff, A. Jacobi von Wangelin, *in preparation*.
- 2) “C=C Hydrogenations with iron group metals”, T. N. Gieshoff, A. Jacobi von Wangelin in “Non-Noble Metal Catalysis: Molecular Approaches and Reactions”, R. J. M. Klein Gebbink, M. Moret (eds.), Wiley-VCH, **2017**.
- 3) “Iron-catalyzed olefin hydrogenation at 1 bar H₂ with a FeCl₃–LiAlH₄ catalyst”; T. N. Gieshoff, M. Villa, A. Welther, M. Plois, U. Chakraborty, R. Wolf, A. Jacobi von Wangelin, *Green Chem.* **2015**, 17, 1408–1413.
- 4) “Stereoselective iron-catalyzed alkyne hydrogenation in ionic liquids”; T. N. Gieshoff, A. Welther, M. T. Kessler, M. H. G. Pechtl, A. Jacobi von Wangelin, *Chem. Commun.* **2014**, 50, 2261–2264.
- 5) “Olefin-Assisted Iron-Catalyzed Alkylation of Aryl Chlorides”; S. Güllak, T. N. Gieshoff, A. Jacobi von Wangelin, *Adv. Synth. Catal.* **2013**, 355, 2197–2202.

Scholarships

2013 – 2016 Scholarship, *Evonik-Stiftung*
 2011 – 2013 Scholarship, *Deutschlandstipendium*

Presentations (oral, poster)

- 1) *OrChem* **2016**, Weimar, poster
- 2) *GdCh-Wissenschaftsforum* **2015**, Dresden, poster
- 3) *International Symposium of Heterogeneous and Homogeneous Catalysis* 2015, Utrecht, poster
- 4) *Jahrestreffen der Katalytiker* **2014**, Weimar, poster and oral
- 5) *GdCh-Wissenschaftsforum* **2013**, Darmstadt, poster
- 6) *Jahrestreffen der Katalytiker* **2013**, Weimar, poster

8.6 Eidesstattliche Erklärung

- I. Ich erkläre hiermit an Eides statt, dass ich die vorliegende Arbeit ohne unzulässige Hilfe Dritter und ohne Benutzung anderer als der angegebenen Hilfsmittel angefertigt habe; die aus anderen Quellen direkt oder indirekt übernommenen Daten und Konzepte sind unter Angabe des Literaturzitats gekennzeichnet.
- II. Bei der Auswahl und Auswertung haben mir die in den jeweiligen Kapiteln aufgeführten Personen in der beschriebenen Art und Weise unentgeltlich geholfen.
- III. Weitere Personen waren an der inhaltlich-materiellen Herstellung der vorliegenden Arbeit nicht beteiligt. Insbesondere habe ich hierfür nicht die entgeltliche Hilfe eines Promotionsberaters oder anderer Personen in Anspruch genommen. Niemand hat von mir weder unmittelbar noch mittelbar geldwerte Leistungen für Arbeiten erhalten, die im Zusammenhang mit dem Inhalt der vorgelegten Dissertation stehen.
- IV. Die Arbeit wurde bisher weder im In- noch im Ausland in gleicher oder ähnlicher Form einer anderen Prüfungsbehörde vorgelegt.

Regensburg, den 08.11.2016